U.S. Department of Energy
1000 Independence Avenue, S.W.
Washington, D.C. 20585

Fiscal Year 2015: Fourth Quarter

Progress Report
Advanced Battery Materials Research (BMR) Program

Released December 2015
for the period of July – September 2015

Approved by

Tien Q. Duong, Advanced Battery Materials Research Program Manager
Vehicle Technologies Office, Energy Efficiency and Renewable Energy

TABLE OF CONTENTS

A Message from the Advanced Battery Materials Research Program Manager 1

Task 1 – Advanced Electrode Architectures 2

Task 1.1 – Physical, Chemical, and Electrochemical Failure Analysis of Electrodes and Cells (Vincent Battaglia, Lawrence Berkeley National Laboratory) 3

Task 1.2 – Electrode Architecture-Assembly of Battery Materials and Electrodes (Karim Zaghib, Hydro-Quebec). 5

Task 1.3 – Design and Scalable Assembly of High-Density, Low-Tortuosity Electrodes (Yet-Ming Chiang, Massachusetts Institute of Technology) 7

Task 1.4 – Hierarchical Assembly of Inorganic/Organic Hybrid Si Negative Electrodes (Gao Liu, Lawrence Berkeley National Laboratory) 9

Task 1.5 – Studies in Advanced Electrode Fabrication (Vincent Battaglia, Lawrence Berkeley National Laboratory) 12

Task 2 – Silicon Anode Research 14

Task 2.1 – Development of Silicon-Based High Capacity Anodes (Ji-Guang Zhang and Jun Liu, PNNL; Prashant Kumta, University of Pittsburgh; Jim Zheng, PSU) 16

Task 2.2 – Pre-Lithiation of Silicon Anode for High Energy Li Ion Batteries (Yi Cui, Stanford University) 19

Task 3 – High Energy Density Cathodes for Advanced Lithium-ion Batteries 22

Task 3.1 – Studies of High Capacity Cathodes for Advanced Lithium-ion Systems (Jagjit Nanda, Oak Ridge National Laboratory) 23

Task 3.2 – High Energy Density Lithium Battery (Stanley Whittingham, SUNY Binghamton) 26

Task 3.3 – Development of High-Energy Cathode Materials (Ji-Guang Zhang and Jie Xiao, Pacific Northwest National Laboratory) 28

Task 3.4 – *In situ* Solvothermal Synthesis of Novel High Capacity Cathodes (Patrick Looney and Feng Wang, Brookhaven National Laboratory) 30

Task 3.5 – Novel Cathode Materials and Processing Methods (Michael M. Thackeray and Jason R. Croy, Argonne National Laboratory) 33

Task 3.6 – High-capacity, High-voltage Cathode Materials for Lithium-ion Batteries (Arumugam Manthiram, University of Texas, Austin) 36

Task 3.7 – Lithium-bearing Mixed Polyanion (LBMP) Glasses as Cathode Materials (Jim Kiggans and Andrew Kercher, Oak Ridge National Laboratory) 39

Task 3.8 – Design of High Performance, High Energy Cathode Materials (Marca Doeff, Lawrence Berkeley National Laboratory) 41

Task 3.9 – Lithium Batteries with Higher Capacity and Voltage (John B. Goodenough, UT-Austin) 44

Task 3.10 – Exploiting Co and Ni Spinels in Structurally Integrated Composite Electrodes (Michael M. Thackeray and Jason R. Croy, Argonne National Laboratory) 47

Task 4 – Electrolytes for High-Voltage, High-Energy Lithium-ion Batteries....50

Task 4.1 – Fluorinated Electrolyte for 5-V Li-ion Chemistry (Zhengcheng Zhang, Argonne National Laboratory)....51

Task 4.2 – Daikin Advanced Lithium Ion Battery Technology – High Voltage Electric (Ron Hendershot, Joe Sunstrom, and Michael Gilmore, Daikin America)....53

Task 4.3 – Novel Non-Carbonate Based Electrolytes for Silicon Anodes (Dee Strand, Wildcat Discovery Technologies) 55

Task 5 – Diagnostics....57

Task 5.1 – Design and Synthesis of Advanced High-Energy Cathode Materials (Guoying Chen, Lawrence Berkeley National Laboratory) 58

Task 5.2 – Interfacial Processes – Diagnostics (Robert Kostecki, Lawrence Berkeley National Laboratory)....61

Task 5.3 – Advanced *in situ* Diagnostic Techniques for Battery Materials (Xiao-Qing Yang and Xiqian Yu, Brookhaven National Laboratory) 64

Task 5.4 – NMR and Pulse Field Gradient Studies of SEI and Electrode Structure (Clare Grey, Cambridge University) 67

Task 5.5 – Optimization of Ion Transport in High-Energy Composite Cathodes (Shirley Meng, UC San Diego) 69

Task 5.6 – Analysis of Film Formation Chemistry on Silicon Anodes by Advanced *In situ* and *Operando* Vibrational Spectroscopy (Gabor Somorjai, UC Berkeley, and Phil Ross, Lawrence Berkeley National Laboratory) 72

Task 5.7 – Microscopy Investigation on the Fading Mechanism of Electrode Materials (Chongmin Wang, Pacific Northwest National Laboratory)....75

Task 5.8 – Energy Storage Materials Research using DOE's User Facilities and Beyond (Michael M. Thackeray and Jason R. Croy, Argonne National Laboratory)....78

Task 6 – Modeling Advanced Electrode Materials 81

Task 6.1 – Electrode Materials Design and Failure Prediction (Venkat Srinivasan, Lawrence Berkeley National Laboratory) 82

Task 6.2 – Predicting and Understanding Novel Electrode Materials from First-Principles (Kristin Persson, Lawrence Berkeley National Laboratory) 84

Task 6.3 – First Principles Calculations of Existing and Novel Electrode Materials (Gerbrand Ceder, MIT)....86

Task 6.4 – First Principles Modeling of SEI Formation on Bare and Surface/Additive Modified Silicon Anode (Perla Balbuena, Texas A&M University) 88

Task 6.5 – A Combined Experimental and Modeling Approach for the Design of High Current Efficiency Si Electrodes (Xingcheng Xiao, General Motors, and Yue Qi, Michigan State University) 91

Task 6.6 – Predicting Microstructure and Performance for Optimal Cell Fabrication (Dean Wheeler and Brian Mazzeo, Brigham Young University) 94

Task 7 – Metallic Lithium and Solid Electrolytes 97

Task 7.1 – Mechanical Properties at the Protected Lithium Interface (Nancy Dudney, ORNL; Erik Herbert, MTU; and Jeff Sakamoto, UM) 99

Task 7.2 – Solid Electrolytes for Solid-State and Lithium-Sulfur Batteries (Jeff Sakamoto, University of Michigan) 102

Task 7.3 – Composite Electrolytes to Stabilize Metallic Lithium Anodes (Nancy Dudney and Sergiy Kalnaus, Oak Ridge National Laboratory) 105

Task 7.4 – Overcoming Interfacial Impedance in Solid-State Batteries (Eric Wachsman, University of Maryland, College Park) 107

Task 7.5 – Nanoscale Interfacial Engineering for Stable Lithium Metal Anodes (Yi Cui, Stanford University) 109

Task 7.6 – Lithium Dendrite Suppression for Lithium-Ion Batteries (Wu Xu and Ji-Guang Zhang, Pacific Northwest National Laboratory) 111

Task 8 – Lithium Sulfur Batteries 114

Task 8.1 – New Lamination and Doping Concepts for Enhanced Li – S Battery Performance (Prashant N. Kumta, University of Pittsburgh) 116

Task 8.2 – Simulations and X-ray Spectroscopy of Li-S Chemistry (Nitash Balsara, Lawrence Berkeley National Laboratory) 119

Task 8.3 – Novel Chemistry: Lithium Selenium and Selenium Sulfur Couple (Khalil Amine, Argonne National Laboratory) 122

Task 8.4 – Multi-Functional Cathode Additives (MFCA) for Li-S Battery Technology (Hong Gan, Brookhaven National Laboratory, and Co-PI Esther Takeuchi, Brookhaven National Laboratory and Stony Brook University) 124

Task 8.5 – Development of High-Energy Lithium-Sulfur Batteries (Jie Xiao and Jun Liu, Pacific Northwest National Laboratory) 127

Task 8.6 – Nanostructured Design of Sulfur Cathodes for High Energy Lithium-Sulfur Batteries (Yi Cui, Stanford University) 130

Task 8.7 – Addressing Internal “Shuttle” Effect: Electrolyte Design and Cathode Morphology Evolution in Li-S Batteries (Perla Balbuena, Texas A&M University) 132

Task 9 – Li-Air Batteries 135

Task 9.1 – Rechargeable Lithium-Air Batteries (Ji-Guang Zhang and Wu Xu, PNNL) 137

Task 9.2 – Efficient Rechargeable Li/O_2 Batteries Utilizing Stable Inorganic Molten Salt Electrolytes (Vincent Giordani, Liox) 140

Task 9.3 – Li-Air Batteries (Khalil Amine, ANL) 142

Task 9.4 – Overcome the Obstacles for the Rechargeable Li-air Batteries (Deyang Qu, University of Wisconsin – Milwaukee and Xiao-Qing Yang, Brookhaven National Laboratory) 145

Task 10 – Na-ion Batteries 148

Task 10.1 – Exploratory Studies of Novel Sodium-Ion Battery Systems (Xiao-Qing Yang and Xiqian Yu, Brookhaven National Laboratory) 149

LIST OF FIGURES

Figure 1. Capacity versus cycle number for full cells of MCMB/NCM with baseline electrolyte (left) and high-voltage electrolyte (right). 4

Figure 2. Energy versus cycle number for MCMB/NCM cells with baseline electrolyte (left) and high-voltage electrolyte (right). 4

Figure 3. Photo of anode electrode of nano-Si/PAA/C composite. 6

Figure 4. Cycle life of nano-Si/PAA/C composite with different loading levels: 2mils of ca.1.5 mg/cm^2, 3mils of ca. 2.0 mg/cm^2, 5mils of ca. 3.0 mg/cm^2. 6

Figure 5. Photos of anode slurry (a) nano-Si in H^2O, (b) nano-Si in H^2O with pH 4, and (c) of the electrodes: left electrode from slurry (a) and right electrode from slurry (b). 6

Figure 6. Discharge under repeated DST with 2C maximum discharge rate pulse for NCA electrode of 35 vol% porosity made by directional freezing and sintering. 8

Figure 7. (a) Chemical structure of PPyMAA conductive polymer binder. (b) A comparison of 0.3 g of high-tap-density nanoSi (left) and regular nanoSi produced by chemical vapor deposition (right). (c) Histograms of AFM rupture force distribution corresponding to pulling a single polymer chain from a glass surface. Averaged rupture forces for PPyMAA, PAA, PPy, and PVDF on glass substrate were 95±58, 99±54, 72±40 and 68±38 piconewton (pN), respectively, with mean rupture forces ± standard deviations and N= # of observed unbinding events. The pulling velocity is 1000 nm/s and dwell time is 0.5 seconds. (d) Charge (delithiation) capacities of high tap density Si electrodes at C/10 with different binders. 10

Figure 8. SEM of a cross-sectioned electrode. 13

Figure 9. EDS image showing the distribution of F across a cross-sectioned electrode. 13

Figure 10. (a) Porous Si anode with the areal capacity of ~2.5 mAh/cm^2 at a discharge current density of ~0.5 mA/cm^2 and a charge current density of ~0.75 mA/cm^2. (b) Porous Si-graphite composite anode with the areal capacity of ~2.8 mAh/cm^2 at a charge/discharge current density of 0.4 mA/cm^2. 17

Figure 11. Long term cycling of (a) Si flakes and (b) Si nanorods and (c) voltage vs. capacity plot of Si nanorods showing 13% first cycle irreversible loss. 17

Figure 12. (a) 1st cycle galvanostatic discharge/charge profiles of artificial-SEI coated Li_xSi NPs. (b) 1st cycle voltage profiles of Si Ps/coated Li_xSi composite (55:10 by weight) and Si NPs control cells (The capacity is based on the total mass of Si in the electrodes.). (c) 1st cycle voltage profiles of graphite/coated Li_xSi composite (85:5 by weight) and graphite control cells. (d) Cycling performance of graphite/coated Li_xSi composite and graphite control cells at C/20 for the first three cycles and C/5 for the following cycles. The purple line is the Coulombic efficiency of graphite/coated Li_xSi composite. 20

Figure 13. (a) The extraction capacity of artificial-SEI coated NPs exposed to dry air for varying periods of time. The inset shows the change of capacity as a function of exposure time. (b) The extraction capacity of artificial-SEI coated NPs exposed to air for 6 hours at different humidity levels. 20

Figure 14. First-cycle voltage profile during charge and discharge of a $Li_2Cu_{0.5}Ni_{0.5}O_2$ half cell for *in situ* Raman spectroscopy. (b) Raman spectra of $Li_2Cu_{0.5}Ni_{0.5}O_2$ cathode collected during galvanostatic charge and discharge. Spectra are shown every two hours during the first cycle. The Raman spectra of $LiNiO_2$ and $NaCuO_2$ are also shown for comparison. 24

Figure 15. Cycling behavior of a Sn_2Fe composite electrode at 0.2 mA/cm^2. The Sn/C/Ti weight ratio is 1/10/0.25. 27

Figure 16. The initial cycling behavior of the solid solution $Cu_{1-y}Fe_yF_2$ cathode, for y = 0.5. 27

Figure 17. (a) Voltage profiles vs. specific capacity, (b) voltage profiles vs. areal capacity, (c) cycling performance and (d) capacity retention of NMC electrodes with different areal capacity loadings. 29

Figure 18. SEM images of Li anodes after 300 cycles in cells using (a, c) 2 mAh cm^{-2} NMC counter electrode and (b, d) 4 mAh cm^{-2} NMC counter electrode in terms of (a, b) surface views and (c, d) cross-section views. 29

Figure 19. Electrochemical cycling performance of α-$CuVO_3$ in cells constructed with Li-polystyrene-b-poly(ethylene oxide) (SEO) polymer electrolyte (a), in comparison to that in the cells with general liquid (b). 31

Figure 20. Electrochemical properties of baseline and coated $_{0.25}Li_2MnO_3 \bullet {}_{0.75}LiMn_{0.375}Ni_{0.375}Co_{0.25}O_2$ electrodes with 6% target spinel: (a) Discharge capacity vs. cycle number (4.6-2.5V, 15mA/g), (b) dQ/dV plots, and (c) Discharge capacities at different current rates (15, 75, 150, 300, 1500mA/g, 4.6-2.5V) after first cycle activation at 4.6-2V (trickle charge 30 min). 34

Figure 21. XRD patterns of the samples prepared to substitute vanadium in pyrophosphate. 37

Figure 22. Scanning electron micrographs of $LiFe_{1-x}VxP_2O_7$ with x = 0.00, 0.025, 0.058, 0.116. 37

Figure 23: Combined vanadate/borate substitution improved the electrochemical performance of lithium copper metaphosphate glass. 40

Figure 24. Concentrations of elements in a spray pyrolyzed sample of NMC-442 as a function as depth from the surface, determined by a transmission x-ray microscopy experiment at the Stanford Synchrotron Radiation Lightsource. 42

Figure 25. Initial five charge/discharge voltage curves of $NaCrO_2$ with bare stainless steel anode current collector coated with various polymers. (a) PETT-FC, (b) PETT-EO, (c) PETT-Sulfone, and (d) PETT-Ester. 45

Figure 26: (a) XRD patterns and (b) initial voltage profiles of spinel $Li_{0.5}[Mn_{0.75}Ni_{0.25-x}Co_x]O_2$ products (x = 0, 0.125 and 0.25). 48

Figure 27. LiNMO/graphite cell with Li reservoir. 52

Figure 28. Capacity retention (a) and Coulombic efficiency (b) of LNMO/graphite cells. 52

Figure 29. Cycle life at 4.6 V Daikin fluorinated electrolytes (capacity – top; resistance –bottom). 54

Figure 30. Calendar life at 4.6 V of Daikin fluorinated electrolyte (capacity – top; resistance – bottom). 54

Figure 31. Gas volume change vs time for LMNO/graphite cell at 4.9 V. 54

Figure 32. Example results from solvent ratio study, including effect of salt. 56

Figure 33. Beneficial additives identified for use in carbonate formulations. 56

Figure 34. (a) First charge-discharge voltage profiles of the $Li_{1.2}Ni_{0.13}Mn_{0.54}Co_{0.13}O_2$ half cells, (b) rate capability of the crystal samples, (c) and (d) long-term cycling and capacity retention of the cells at a current density of 20 mA/g. 59

Figure 35. (a) Average charge and discharge voltages of the $Li_{1.2}Ni_{0.13}Mn_{0.54}Co_{0.13}O_2$ half cells, (b) comparison of the charge and discharge voltage gaps at cycle 5 and 85, and (c) Co L_3 peak ratio of the TEY XAS spectra, with a higher ratio corresponding to a lower oxidation state. 59

Figure 36. Near-field spectroscopic absorption of SiO_2 substrate through graphene membrane. 62

Figure 37. Comparison of UV ultrafast LIBS emission from Si (a) in liquid and (b) in air. 62

Figure 38. Rendering of the 3D structure of a selected $LiNi_{0.33}Mn_{1.34}Fe_{0.33}O_4$ particle is shown in panel (a) with the scale indicated in the axis and the color legend shown in the inset. Panels (c) through (g) are slices at different depth of the particle, showing that it is a solid piece with no internal pores and the density distribution is relatively homogeneous. The elemental concentration over the line path indicated in panel (e) is plotted in panel (b) (the blue, green, and red curves represent the concentration of Mn, Ni, and Fe, respectively), which is in good agreement with the elemental composition of the material. Panels (a) and (c) through (g) are reconstructed from nano-tomography data collected at 8380 eV (above the absorption k edges of all the three transition metal elements), while the data plotted in panel (b) is retrieved from the evaluation of the energy dependency of the absorption coefficient using a method known as Absorption Correlation Tomography. 65

Figure 39. Discharge-charge curves for Li-O_2 cells using mesoporous SP and TiC, and macroporous rGO electrodes, with capacities limited to 500 mAh/g (based on the mass of carbon or TiC) and a 0.25 M LiTFSI/DME electrolyte. For SP and rGO electrodes, 0.05 M LiI was added to the LiTFSI/DME electrolyte in a second set of electrodes (purple and red curves). All cells in were cycled at 0.02 mA/cm^2. The horizontal dashed line represents the position (2.96 V) of the thermodynamic voltage of a Li-O_2 cell. 68

Figure 40. Electrochemical charge/ discharge profile with corresponding lithium occupancy at different states of delithiation/ lithiation for (a) HLR and (b) LLR. 70

Figure 41. ADF-STEM images of the lithiated silicon nanoparticles cycled in EC/DEC at (a) 1 cycle and (b) 5 cycles. Electrodes cycled in EC/DEC/FEC at (c) 1 cycle and (d) 5 cycles. 70

Figure 42. Relative composition of the SEI after (a, b) first lithiation, (c, d) first delithiation, and (e, f) 100 cycles in the delithiated state. 70

Figure 43. The three reduction peaks at a Si(100)-H anode of the electrolyte (1.0 M $LiPF_6$ in EC : DEC, 1:2 v/v) are presented in this cyclic-voltagram. The reduction of DEC is around 1.5 V. The reduction of EC is about 0.5 V, and Li intercalation (lithiation) occurs around 0.10 V. Scan rate was 1mV/sec. 73

Figure 44. (a) The evolution of SFG signal under reaction conditions of crystalline silicon Si(100)-hydrogen terminated anode. The SFG spectra were taken at open circuit potential and after cyclic-voltammetry at: 1.1 V ↔ 0.8 V, 0.65 V ↔ 0.35 V and 0.1 V ↔ -0.05 V. To emphasize the evolution of the Si-ethoxy peaks, we divided the SFG spectra by their former potentials, as follows: SFG1.1 V ↔ 0.8 V / OCP (black), SFG0.65 V ↔ 0.35 V / SFG1.1 V ↔ 0.8 V (blue) and SFG-0.05 V ↔ 0.1 V / SFG0.65 V ↔ 0.35 V (red). (b) The SFG profiles of crystalline silicon oxide Si(100) anode after cycling between 0.5 V ↔ 2.0 V (blue) and -0.05 V ↔ 3.0 V (red). All CVs were repeated for 30 cycles at a scan rate of 1mV/sec. 74

Figure 45. SEM images of (a) pristine agglomerated particles, (b) and (c) TEM specimen prepared by FIB lift-out techniques from cycled electrode. (d-i) STEM-EDS mapping results from the boxed region in (c). The scale bars are 30 nm in (d-i). 76

Figure 46. (a) Voltage profiles of Li/$_{0.25}Li_2MnO_3 \bullet _{0.75}LiNi_{0.75}Mn_{0.125}Co_{0.125}O_2$ half-cells with a targeted 10% spinel component in the cathode, synthesized under different conditions; Black: annealed in air at 850°C; Blue: annealed in O_2 at 750°C; and Red: annealed in O_2 at 850°C. (b) and (c) STEM images of complex domain structures formed in cathode compositions when annealed in air at 850°C. 79

Figure 47. Simulation domain showing positive current collector, porous electrode, and lithium negative electrode. For clarity, porous matrix and separator are not shown. 83

Figure 48: Comparison of 3C discharge curves obtained by experiment, macroscale simulation, and microscale simulation 83

Figure 49. Structure of layered Li-excess material of (100) direction and Li-ion migration process between the transition metal layer and Li-layer. Li-ion has two paths in inter-layer migrations (a). Li-ion can be migrated from red octahedral site to blue octahedral site or vice versa (b). 85

Figure 50. Cycling performances of $Li_{1.25}Nb_{0.25}Mn_{0.5}O_2$ at 55°C (a) and room temperature (b). 87

Figure 51. XRD shows a pure disordered rocksalt phase; EELS spectra confirm that Mn and O are both redox active. 87

Figure 52. An example of a mesoscopic model to capture longer scale times and lengths. 89

Figure 53. Interfacial resistance (Rct) of samples under different lithiation (delithiation) stage. Higher LiF content (SEI1) leads to lower impedance. 92

Figure 54. Above: 2-D illustration of the topology of the designed SEI structure for optimized ionic conductivity. A: Li_2CO_3; B: LiF. Below: The increment of ionic conduction for different average grain size of Li_2CO_3 at various volumetric ratios 92

Figure 55. Schematic figure showing the defect reaction and defect distribution near the LiF Li_2CO_3 interface 92

Figure 56. Viscosity of slurry at different shear rates for pure carbon (green), and active sample (blue) from experiment (line), and simulation (symbols). In some cases error bars are smaller than symbol sizes. Lines are used for experiments due to the close spacing of the data. 95

Figure 57. Sample between Li contacts. 100

Figure 58. Cycling of Li through LLZO sample in both directions (left). Response of the impulse acoustic echo indicated as the wavespeed (right). 100

Figure 59. Critical current density as a function of the Li-LLZO interfacial resistance, which was controlled by the surface contamination. 103

Figure 60. EIS data for Li-LLZO-Li cells using the standard surface preparation (a) and the new surface treatment (b). 103

Figure 61. An example of the scalable, composite membranes produced with 50 vol.% Ohara glass particles dispersed in polymer electrolyte matrix. 106

Figure 62. Comparison of conductivity determined from impedance scans of composites and ceramic-free polymer electrolyte prepared by different slurries 106

Figure 63. Structured garnet surface; white shiny areas are garnet columns. 108

Figure 64. Impedance of cathode on smooth and structured garnet electrolyte interface. 108

Figure 65. PFPE-DMC synthesis procedure. 108

Figure 66. CV of two types of PFPE solvent in Li/PFPE+LiTFSI/Ti system (left, type 1; right, type 2). 108

Figure 67. Schematic of the fabrication of the Li-coated PI matrix. Electrospun PI was coated with a layer of ZnO via ALD to form core-shell PI-ZnO. The existence of ZnO coating renders the matrix "lithiophilic" such that molten Li can steadily infuse into the matrix. The final structure of the electrode is Li coated onto a porous, non-conducting polymeric matrix. 110

Figure 68. Electrochemical behaviors of the Li electrodes in EC/DEC electrolyte. (top) Cross-sectional SEM images of nanoporous lithium anode before and after complete lithium stripping. (bottom) Comparison of the cycling stability of the Li-coated PI matrix and the bare Li electrode at a current density of 1 mA/cm^2 with fixed capacity of 1mAh/cm^2. 110

Figure 69. Long-term cycling stability of Li||NMC-442 coin cells with 10 electrolytes at RT. 112

Figure 70. (a) Initial charge/discharge profiles at C/20 (1C = 1.5 mA cm^{-2}) and (b) long-term cycling performance of graphite||NCA full cells using electrolytes containing different amounts of PC at room temperature. (c) Rate capability at room temperature. (d) Long-term cycling stability (C/2 rate for charge and discharge) of graphite||NCA full cells using non-PC control and E20PC-Cs electrolytes at an elevated temperature of 60°C. 112

Figure 71. Morphology of sulfur-containing nanoporous CFMs and improvement in cycling stability as a result of the same. 117

Figure 72. Effect of doping on electronic conductivity of sulfur. 117

Figure 73. Sulfur K-edge XAS of discharging Li-S cell. 120

Figure 74. Spectral compositions determined using theoretical sulfur spectra. 120

Figure 75. Scanning electron microscopy images of (a) Ketjenblack carbon black, (b) multiwall carbon nanotube, and (c) ordered microporous carbon (OMC). The insert in Figure 75c is a transmission electron microscopy image showing micron channels (about 5 nm in diameter) in OMC to host Se_2S_5. 123

Figure 76. (a) Weight loss of a Se_2S_5/Ketjenblack-CNT composite during TGA analysis, confirming the proper loading of the active material in carbon matrix; and (b) charge/discharge capacity of cell using the prepared electrode using a carbonate-based electrolyte. 123

Figure 77. Charge/discharge capacity of a cell comprising Se_2S_5/ Ketjenblack-CNT. The electrolyte used was 1.0 M LiTFSI in DOL/TTE (1:1 by volume) with 0.1 M $LiNO_3$. 123

Figure 78. TEM of Nano-Fe_2O_3 precursor. 125

Figure 79. TEM of Nano-FeS_2. 125

Figure 80. Schematic of Li_2S core with TiS_2 shell. 125

Figure 81. (a) Continuous coating of sulfur electrodes with adjustable loading. The S/C composite was prepared according to patented approach reported earlier. (b) An example of double-side coated sulfur electrodes. (c) Assembled pouch cell using thick sulfur cathodes and prelithiated graphite anodes. (d) Cycling of the Li-ion sulfur prototype cell that will be used to evaluate the electrochemical properties of thick sulfur electrodes. 128

Figure 82. (a) Representative charge-discharge profiles of the composite electrodes at 0.1 C. (b) Specific capacity and the corresponding Coulombic efficiency of the composite electrodes upon prolonged 300 charge-discharge cycles at 0.5 C. 131

Figure 83. (a) Li_2S film thickness and coverage variation versus time. (b) SEM image of Li_2S nanoislands formation on carbon substrate from F.Y. Fan et al. *Advanced Materials*, 27 (2015): 5203-5209. (c) Snapshot of Li_2S nanoislands formation on carbon substrate from Coarse-Grained KMC simulation. 133

Figure 84. Cycling stability of electrolytes, LiTFSI-3DMSO (a, c) and LiTFSI-4DMSO (b, d), in Li-O_2 coin cells at two different capacity limitations at 1000 mAh g^{-1} (a, b) and 600 mAh g^{-1} (c, d). 138

Figure 85. (a) Voltage profiles of treated catalyst/carbon cloth air electrode in Li-O_2 coin cells at selected cycles. (b) Cycling stability of Li-O_2 coin cells with air electrodes of treated catalyst/carbon cloth, pristine catalyst/carbon cloth, and pure carbon cloth under full discharge/charge (2.0~4.5 V) cycling. 138

Figure 86. LSV/*in situ* gas analysis performed on Ir wire working electrode in LiOH-saturated (Li,K)NO_3 electrolyte at 150°C. v = 5 mV/s. 141

Figure 87. Li/O_2 cell galvanostatic cycling at 0.25 mA/cm^2 in $LiNO_3$-KNO_3 eutectic at 150°C. Left plot: nanoporous Au cathode. Right plot: Ni nanopowder cathode both under Ar and O_2 gas. 141

Figure 88. FT-IR spectra showing sensitivity of this method to carboxlylate groups (red curve) from TEGDME decomposition after cycling in a Li-O_2 cell. 143

Figure 89. The oxidation of B1, B2 and B3-O_2^{2-}. 146

Figure 90. HPLC-MS analysis for the stability of B2 (left) and B3 (right) after reacting with Li_2O and L_2O_2. 146

Figure 91. *Ex situ* Fourier transformed magnitude of Fe K-edge EXAFS spectra of the NaFe(1.63) electrode collected at different charge and discharge states. 150

LIST OF TABLES

Table 1. Preliminary experiments in fabricating thicker electrodes resulted in a final thickness that was approximately a third of the height of the doctor blade 13

Table 2. Elemental ratios and lattice parameters various spinel samples. 48

Table 3. Comparison of key properties between simulation and experiment, with 95% confidence intervals where repeated independent samples were collected. Volume fractions are for the solid state.. 95

Table 4. Bulk concentration and diffusion coefficient of LiOH and Li_2CO_3 in molten nitrate electrolyte $LiNO_3$-KNO_3 at 150°C. 141

Table 5. Examples of the synthesized B-compound (left) and their properties (right). 146

A MESSAGE FROM THE ADVANCED BATTERY MATERIALS RESEARCH PROGRAM MANAGER

The Advanced Battery Materials Research (BMR) Program focuses on identifying the fundamental chemical, electrochemical, and mechanical issues that impede battery usage in electric and hybrid-electric vehicles. In addition, research is directed toward identifying affordable electrode materials and electrolytes that are superior to those used in existing lithium ion batteries. BMR investigators come from a number of organizations, including national laboratories, universities, and industry. Together they work in ten topic areas: cell analysis, silicon anodes, advanced cathodes, liquid electrolytes, diagnostics, electrode modeling, metallic lithium and solid electrolytes, lithium sulfur batteries, lithium air batteries, and sodium ion batteries. This document summarizes the investigator's activities performed during the period from July 1, 2015, through September 30, 2015.

A few selected highlights from the BMR tasks are summarized below:

- University of Pittsburg (Kumta's Group) prepared silicon nano-flakes by high-energy mechanical milling. Subsequent chemical vapor deposition demonstrated a reversible capacity of ~ 1100 mAh/g Si in 100 cycles and a Coulombic efficiency of ~99.5% – 99.8%.
- Daikin (Hendershot and Sunstrom) showed that the performance limit for fluorinated electrolytes is between 4.5 and 4.6 V.
- Cambridge University (Grey's Group) discovered the use of a redox mediator (LiI) to cycle the lithium-oxygen cell with a high efficiency, a large capacity, and a very low over-potential.
- Massachusetts Institute of Technology (Ceder's Group) designed and prepared a new disordered material, $Li_{1.25}Nb_{0.25}Mn_{0.5}O_2$, that delivers a large initial discharge capacity of 287 mAh/g and energy density of 909 Wh/kg when operating at 55^{o}C. At room temperature, the cathode exhibited capacity of 200 mAh/g with reasonable cycling stability. The material was observed to undergo oxygen oxidation/reduction during cycling, providing a new path for discovery of lithium-ion cathodes.
- Pacific Northwest National Laboratory (Xu and Zhang) showed that stable cycling to 500 deep cycles could be achieved for graphite/NMC (nickel manganese cobalt) coin cells by adding $CsPF_6$ and PC to a $LiPF_6$-EC/EMC electrolyte solution.

The next BMR quarterly report will cover progress made during October through December 2015 and will be available March 2016.

Sincerely,

Tien Q. Duong

Manager, Advanced Battery Materials Research (BMR) Program

Energy Storage R&D

Office of Vehicle Technologies

Energy Efficiency and Renewable Energy

U.S. Department of Energy

TASK 1 – ADVANCED ELECTRODE ARCHITECTURES

Summary and Highlights

Energy density is a critical characterization parameter for batteries for electric vehicles, given the limited space for the battery and requirements for travel of more than 200 miles. The DOE targets are 500 Wh/L on a system basis and 750 Wh/L on a cell basis. Not only do the batteries have to have high energy density, they must also still deliver 1000 Wh/L for 30 seconds on the system level. To meet these requirements not only entails finding new, high energy density electrochemical couples, but also highly efficient electrode structures that minimize inactive material content, allow for expansion and contraction from one to several thousand cycles, and allow full access to the active materials by the electrolyte. In that vein, the DOE Vehicle Technologies Office VTO supports five projects in the BMR Program under Electrode Architectures: (1) Physical, Chemical, and Electrochemical Failure Analysis of Electrodes and Cells at LBNL, (2) Assembly of Battery Materials and Electrodes at Hydro-Quebec, (3) Design and Scalable Assembly of High-density, Low-tortuosity Electrodes at MIT, (4) Hierarchical Assembly of Inorganic/Organic Hybrid Si Negative Electrodes at LBNL, and (5) Studies in Advanced Electrode Fabrication at LBNL.

One of the more promising active materials for higher energy-density Li-ion batteries is Si used as the anode. It has a specific capacity of over 3500 mAh/g and an average voltage during delithiation of 0.4 V vs. the Li/Li+ electrode. This material suffers from two major problems associated with the 300% volume change the material experiences as it goes from a fully delithiated state to a fully lithiated one: (1) the volume change results in a change in exposed surface area to electrolyte during cycling that consumes electrolyte and results in a lithium imbalance between the cathode and anode, and (2) the volume change causes the particles to become electrically disconnected (which is further enhanced if particle fracturing also occurs) during cycling. Projects 2 and 4 in this task are focused on Si to make it a more robust electrode by finding better binders.

Another approach to higher energy density is to make the electrodes thicker. The problem with thicker electrodes is that the salt in the electrolyte has to travel a farther distance to meet the current needs of the entire electrode throughout the discharge. If the salt cannot reach the back of the electrode at the discharge rates required of batteries for automobiles, the battery is said to be running at its limiting current. If the diffusional path through the electrode is tortuous or the volume for electrolyte is too low, the limiting current is reduced. The other problem with thicker electrodes is that they tend to not cycle as well as thinner electrodes and thus reach the end-of-life condition sooner, delivering fewer cycles. Projects 1, 3, and 5 are focused on increasing the limiting current of thick electrodes while maintaining cyclability through the fabrication of less tortuous electrodes or of electrodes with less binder and more room for electrolyte.

If these projects are successful, they will result in a 25% increase in energy density as a result of replacing graphite with Si, and another 20% increase in energy density by moving from 2 mAh/cm^2 electrodes to 4 mAh/cm^2 electrodes. This would result in a net increase of 50% in energy density of the cell, and so a battery that once allowed a vehicle to travel only 200 miles may now allow travel of 300 miles.

The highlight for this quarter is that Karim Zagrib's Group (Hydro-Quebec) was able to improve the cyclability of a Si material through the use of a polyimide binder and by reducing the pH of the aqueous slurry down from 7.5 to 4.

Task 1.1 – Physical, Chemical, and Electrochemical Failure Analysis of Electrodes and Cells (Vincent Battaglia, Lawrence Berkeley National Laboratory)

Project Objective. This project investigates failure modes of targeted chemistries as defined by the BMR Program and its Focus Groups. The emphasis of this effort for 2015 will be on the High-Voltage and Si Anode Focus Groups. The objectives are to identify and quantify the chemical and physical aspects of cell cycling and aging that lead to reduced electrochemical performance. Specifically, research will focus on the effects on material stability as a result of increasing the cell voltage of Graphite/NCM (nickel cobalt Manganese cells from 4.2 V to 4.7 V. In addition, differences in performance between Graphite/NCM and Si/NCM will be investigated. Specifically, investigations into the differences in cell performance as a result of Coulombic inefficiencies and the effects of increased electrode loadings on cyclability will be carried out.

Project Impact. Success with understanding and improving the stability of NCM in the presence of electrolyte at voltages greater than 4.3 V vs. Li/Li+ will translate to an increase in capacity and voltage and hence a compounding improvement in energy density by as much as 45%. Improvement in the loading of anodes and cathodes from 2 to 5 mAh/cm^2 could result in larger fractions of active materials in cells and a projected increase in energy density by an additional 20%.

Out-year Goals. Provide a prescription of the physical and structural properties required to increase the accessible capacity of layered oxide materials. Demonstrate high loading cells with an increased energy density of 20% with no change in chemistry or operating parameters.

Collaborations. This project engages in collaborations with many BMR principal investigators.

Milestones

1. Measure and report the difference in capacity fade in mAh/h between LCO and high-voltage LCO at 4.3 V in mAh/h. (12/31/14 – Complete)
2. Identify and report the electrochemical phenomena responsible for the capacity fade of the LCO and HV-LCO cells at 4.3 V. (3/31/15 – Complete)
3. Measure and report the phenomena responsible for the capacity fade of a 3 mAh/cm^2 cell in mAh/h. (6/30/15 – Ongoing)
4. Measure and report the self-discharge rate of the baseline Li/S cell in mA/(g of S) and decide if this is an appropriate baseline design. (9/30/15)

Progress Report

Milestone 4. Measure and report the self-discharge rate of the baseline Li/S cell in mA/(g of S) and decide if this is an appropriate baseline design. (9/30/15)

As mentioned last quarter, interest in developing a standardized Li/S for the purposes of comparing technologies has waned; for FY 2016, our focus will be on fabricating thicker electrodes. Meanwhile, we are completing our investigations of materials tested to high voltage. Last quarter, the cycle life of NCM material cycled to 4.5 V *versus* a Li-metal counter electrode was shown for a baseline electrolyte and a "high-voltage" electrolyte. The performance in both electrolytes was good, with 2.5% loss of capacity for the baseline electrolyte after 100 cycles and 0.8% loss of capacity for the high-voltage electrolyte for the same number of cycles. With this preliminary result, the electrode and electrolytes were tested in full cells with MCMB (MesoCarbon MicroBeads) graphite as the counter electrode. After some break-in cycles, the cells were cycled at C/3 charge and C/2 discharge between 2.8 and 4.4 V. To accelerate fading mechanisms, the cells were tested at 55°C. The graphs in Figure 1 provide the capacity as a function of cycle number for the first 100 cycles or so. One can see that the data for the baseline electrolyte shows a 10.7% capacity fade after 100 cycles, whereas the full cell with the high-voltage electrolyte shows a 16.7% capacity loss after the same number of cycles. Thus, the improved performance gained in the half cell using high-voltage electrolyte was lost in the full cells. Inspection of the discharge energy of the cells at 55°C shows that the energy in the baseline electrolyte declines by 11%, indicating that the voltage is slightly improving with cycling. The energy of the cell with high voltage electrolyte declined by approximately 16%, indicating little impedance rise in this cell as well.

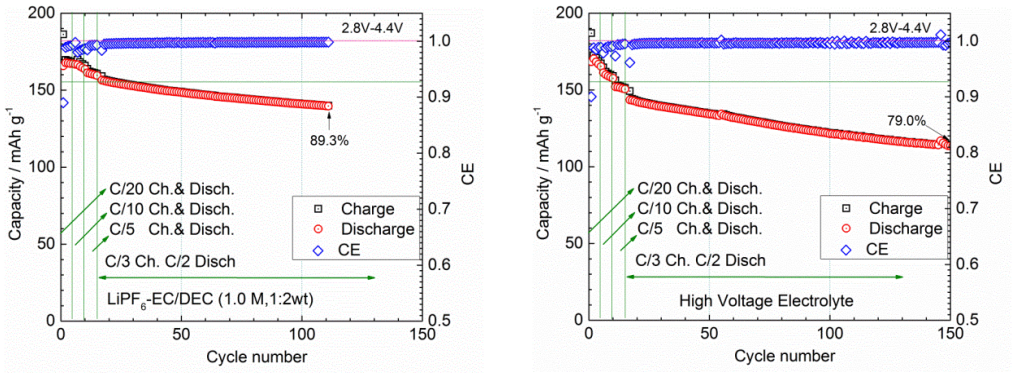

Figure 1. Capacity *versus* cycle number for full cells of MCMB/NCM with baseline electrolyte (left) and high-voltage electrolyte (right).

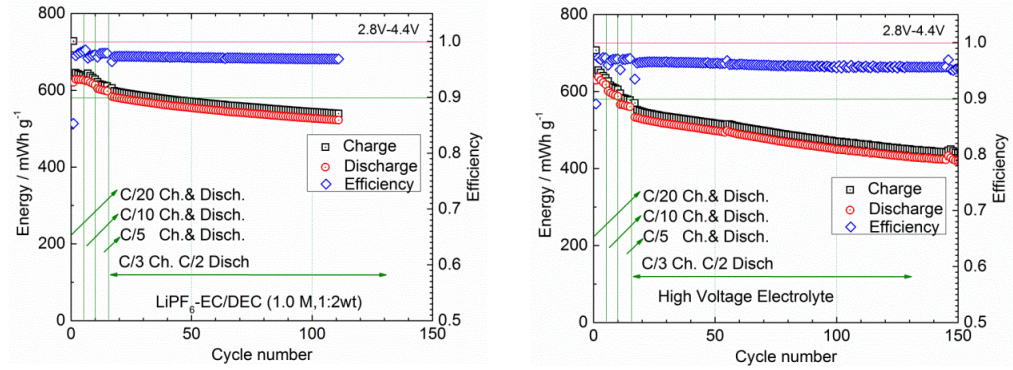

Figure 2. Energy versus cycle number for MCMB/NCM cells with baseline electrolyte (left) and high-voltage electrolyte (right).

Task 1.2 – Electrode Architecture-Assembly of Battery Materials and Electrodes (Karim Zaghib, Hydro-Quebec)

Project Objective. The project objective is to develop high-capacity, low-cost electrodes with good cycle stability and rate capability to replace graphite in Li-ion batteries.

The aim is to overcome the limit of electrochemical capacity (both gravimetric and volumetric) of conventional carbon anodes. This will be achieved by developing low-cost electrodes that utilize a high-capacity material such as silicon. Controlling the composition (that is, loading of the active material, ratio of binder and carbon additive) of the electrode will yield a more tolerant anode with acceptable volume change, useful cycle life, and low capacity fade. A high-energy, large-format, Li-ion cell will be produced using optimized Si-based anode and high-energy cathode electrodes.

Project Impact. Production of Si nano-powder using commercially scalable and affordable methods will justify replacing the graphite anode without jeopardizing the cost structure of conventional batteries. In addition, the energy density of cells is increased to > 250 Wh/kg by using a high content of Si (> 50%) with reasonable loading (2 mAh/cm^2). The results obtained in large-format cells (> 20Ah) will enable us to study the wide spectrum of electrochemical performance under actual vehicle operation conditions.

Out-Year Goals. Out-year goals include the following:

- Complete the optimization of the electrode composition by varying the carbon additive ratio and the type of carbon. In addition to *in situ* SEM analyses, *in situ* impedance spectroscopy will be employed to enhance the understanding of capacity fade of the Si-material. These analyses will clarify the mechanism leading to electrode failure and guide further improvement and design of the electrode architecture.
- Complete optimization of the method to synthesize Si-nano powder developed at HQ.
- As a final goal, the optimized Si-anode and high-energy cathode will be coated in the pilot line and then assembled in large-format cells (> 20Ah) using the new automatic stacking machine at Hydro-Quebec (HQ).

Collaborations. This project collaborates with BMR members: V. Battaglia and G. Liu from LBNL, C. Wong and Z. Jiguang from PNNL, and J. Goodenough from the University of Texas.

Milestones

1. Complete optimization of the nano-Si-anode formulation. (12/31/14 – Complete)
2. Complete optimization of the synthesis of nano-size Si developed at HQ. Go/No-Go decision: Terminate the Si synthesis effort if the capacity is less than 1200 mAh/g. (3/31/15 – Complete)
3. Produce and supply laminate films of Si-anode and LMNO-cathode (10 m) to BMR principal investigators. (6/30/15 – Complete)
4. Produce and supply large-format 20 Ah high-energy stacking cells (4) to BMR principal investigators. (9/30/15 – Complete)

Progress Report

During this quarter, Hydro-Quebec focused on increasing the loading level and cycle life of *nano*-Si anodes by improving the adhesion strength of the binder. To address these issues, the surface treatment of the *nano*-Si powder was investigated by using a spray drying technique. Polyacrylic acid (PAA) was used as a surface treatment material dissolved in NMP media. The performance of the anode has been found to be better when a surface treatment is applied to a composite of Si powder and carbon. By this method, secondary particles were formed and the loading was improved (Figure 3). Furthermore, *nano*-Si particles having the surface decorated with PAA material have shown suppression of gas evolution when an aqueous binder is used. However, the adhesion strength was poor and the capacity faded rapidly. This result led to a change to a nonaqueous binder with a polyimide base. A comparative cycle life test of an anode based on *nano*-Si/PAA/C with different loadings (1.5, 2.0, 3.0 mg/cm^2) is shown in Figure 4. It was noted that the adhesion strength of the anode was improved with the addition of the polyimide binder. The cycling performance at C/6 is clearly affected by the loading: with 1.5 mg/cm^2 the capacity fades by 22%, compared to 80% when the anode loading is doubled. Despite the change in binder, the anode performance suffers at higher loadings.

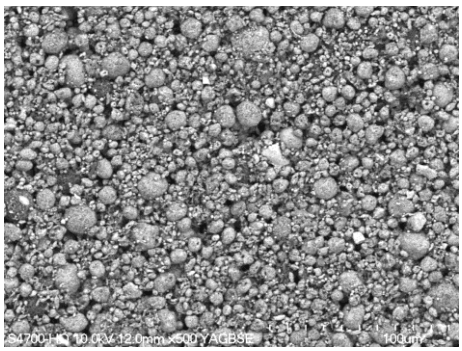

Figure 3. Photo of anode electrode of *nano*-Si/PAA/C composite.

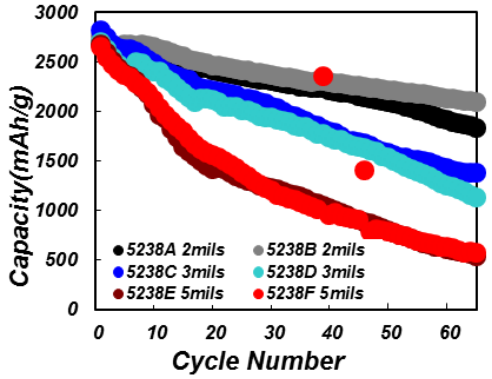

Figure 4. Cycle life of *nano*-Si/PAA/C composite with different loading levels: 2mils of *ca*.1.5 mg/cm^2, 3mils of *ca*. 2.0 mg/cm^2, 5mils of *ca*. 3.0 mg/cm^2.

The manufacturing processes, especially the mixing and coating, were varied to evaluate the possibility of using Si in large size batteries. In previous work, the gas generation during the mixing and coating process was reported to produce non-homogeneous coatings and made it difficult to control the exact loading level. In this quarterly, pH control of the Si-anode slurry was investigated. Using aqueous binder, the pH measured 7.5 with high gas generation. When the pH was reduced to 4 through the addition of acetic acid, the gas generation was suppressed (Figure 5a-b), the electrodes were more uniform, and loading was more easily controlled.

Figure 5. Photos of anode slurry (a) *nano*-Si in H_2O, (b) *nano*-Si in H_2O with pH 4, and (c) of the electrodes: left electrode from slurry (a) and right electrode from slurry (b).

Deliverable: Two large prismatic Li-ion cells of 49Ah: NCM/nano-Si were supplied as the third deliverable to LBNL for evaluation.

Task 1.3 – Design and Scalable Assembly of High-Density, Low-Tortuosity Electrodes (Yet- Ming Chiang, Massachusetts Institute of Technology)

Project Objective. The project objective is to develop scalable, high-density, low-tortuosity electrode designs and fabrication processes enabling increased cell-level energy density compared to conventional Li-ion technology, and to characterize and optimize the electronic and ionic transport properties of controlled porosity and tortuosity cathodes as well as densely-sintered reference samples. Success is measured by the area capacity (mAh/cm^2) that is realized at defined C-rates or current densities.

Project Impact. The high cost ($/kWh) and low energy density of current automotive lithium-ion technology is in part due to the need for thin electrodes and associated high inactive materials content. If successful, this project will enable use of electrodes based on known families of cathode and anode actives but with at least three times the areal capacity (mAh/cm^2) of current technology while satisfying the duty cycles of vehicle applications. This will be accomplished via new electrode architectures fabricated by scalable methods with higher active materials density and reduced inactive content; this will in turn enable higher energy density and lower-cost EV cells and packs.

Approach. Two techniques are used to fabricate thick, high density electrodes with low tortuosity porosity oriented normal to the electrode plane: (1) directional freezing of aqueous suspensions; and (2) magnetic alignment. Characterization includes measurement of single-phase material electronic and ionic transport using blocking and non-blocking electrodes with ac and dc techniques, electrokinetic measurements, and drive-cycle tests of electrodes using appropriate battery scaling factors for electric vehicles (EVs).

Out-Year Goals. The out-year goals are as follows:

- Identify anodes and fabrication approaches that enable full cells in which both electrodes have high area capacity under EV operating conditions. Anode approach will include identifying compounds amenable to same fabrication approach as cathode, or use of very high capacity anodes, such as stabilized lithium or Si-alloys that in conventional form can capacity-match the cathodes.
- Use data from best performing electrochemical couple in techno-economic modeling of EV cell and pack performance parameters.

Collaborations. Within BMR, this project collaborates with Antoni P. Tomsia (LBNL) in fabrication of low-tortuosity, high-density electrodes by directional freeze-casting, and with Gao Liu (LBNL) in evaluating Si anodes. Outside of BMR, the project collaborates with Randall Erb (Northeastern University) on magnetic alignment fabrication methods for low-tortuosity electrodes.

Milestones

1. Fabricate and test at least one anode compound in an electrode structure having at least a 10 mAh/cm^2 theoretical capacity. (12/31/14 – Complete)
2. Demonstrate at least 5 mAh/cm^2 capacity per unit area at 1C continuous cycling rate for at least one candidate anode. (3/31/15 – Complete)
3. Downselect at least one anode composition for follow-on work. Go/No-Go milestone: Demonstrate an electrode with at least 7.5 mAh/cm^2 that passes the USABC dynamic stress test (DST) with peak discharge C-rate of 2C. (6/30/15 – Complete)
4. Demonstrate an electrode with at least 10 mAh/cm^2 that passes the USABC dynamic stress test (DST) with peak discharge C-rate of 2C. (9/30/15 – Complete)

Progress Report

Milestone 4. Demonstrate an electrode with at least 10 mAh/cm^2 that passes the USABC dynamic stress test (DST) with peak discharge C-rate of 2C. (9/30/15).

During this program year, two methods have been explored for fabricating low-tortuosity electrodes with aligned, quasiperiodically spaced pore channels within a microporous matrix. Both a directional freezing and a magnetic alignment method have yielded improved area capacity under galvanostatic cycling tests. However, to more completely characterize performance under operating conditions appropriate to vehicle applications, the USABC dynamic stress test (DST) has been adopted. The DST is a power versus time profile in which the power in each step is specified as a percentage of the peak power of the battery pack, which is here converted to C-rates by taking the peak power of the pack to be at 2C rate, as would be the case, for example, for a 50 kWh EV pack delivering 100 kW peak power. The duration at the maximum charge rate of 1C and maximum discharge rate of 2C in the DST is 8s. By looping this test repeatedly, a fully charged cell is discharged until the lower cutoff voltage is reached during any one of the pulses. The area capacity of the electrode is thus determined under a model drive cycle. The milestone for this quarter is to reach area capacity of 10 mAh/cm^2 in an electrode under this protocol. This milestone was achieved for a sintered NCA electrode prepared by directional freezing of an NCA electrode (7.5°C/min cooling rate) and sintering at 840°C to reach 35 vol% porosity. As shown in Figure 6, a 160 μm thick electrode tested in a half-cell exhibited 11.5 mAh/cm^2 area capacity in this test, which is 91% of the theoretical capacity of 12.7 mAh/cm^2.

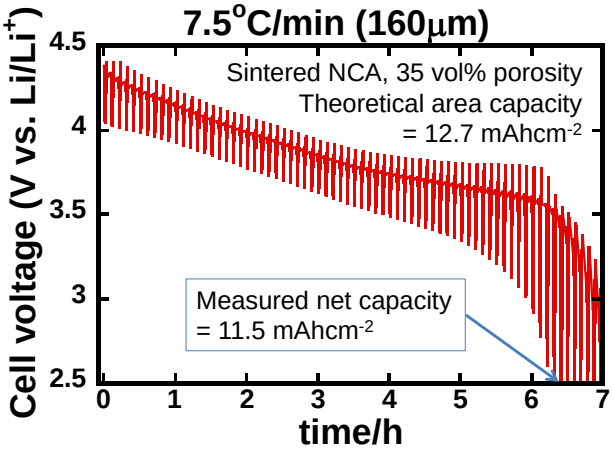

Figure 6. Discharge under repeated DST with 2C maximum discharge rate pulse for NCA electrode of 35 vol% porosity made by directional freezing and sintering.

In addition, progress was made in a new variant of the magnetic alignment approach, reported last quarter, in which emulsion droplets of magnetic fluid are induced to form chains under applied magnetic field. These chained droplets are removed by evaporation, leaving aligned pore arrays. Compared to the magnetic microrod alignment approach discussed in the previous quarterly report, the emulsion droplet chaining approach has several advantages. The chains that are formed span the entire thickness of the electrodes and therefore form pore channels that penetrate completely, rather than having a length determined by the length of the added rods. There exists a slight repulsion between chains of magnetic emulsion droplets, causing them to form quasiperiodic hexagonal arrays, a desired architecture. Finally, the volume fraction porosity, average diameter of the pore channels, and the spacing of the pore channels are all readily controlled through composition and process variables. These results will be discussed in detail in a future report.

Patents/Publications/Presentations

Publication

- Swamy, T., and Y.-M. Chiang. "Electrochemical Charge Transfer Reaction Kinetics at the Silicon-Liquid Electrolyte Interface." *J. Electrochem. Soc.*, 162, no. 3, (2015): A7129-A7134. doi: 10.114912.018153jes.

Task 1.4 – Hierarchical Assembly of Inorganic/Organic Hybrid Si Negative Electrodes (Gao Liu, Lawrence Berkeley National Laboratory)

Project Objective. This proposed work aims to enable Si as a high-capacity and long cycle-life material for negative electrode to address two of the barriers of Li-ion chemistry for EV and Plug-in Hybrid (PHEV) application: insufficient energy density and poor cycle life performance. The proposed work will combine material synthesis and composite particle formation with electrode design and engineering to develop high-capacity, long-life, and low-cost hierarchical Si-based electrode. State of the art Li-ion negative electrodes employ graphitic active materials with theoretical capacities of 372 mAh/g. Silicon, a naturally abundant material, possesses the highest capacity of all Li-ion anode materials. It has a theoretical capacity of 4200 mAh/g for full lithiation to the $Li_{22}Si_5$ phase. However, Si volume change disrupts the integrity of electrode and induces excessive side reactions, leading to fast capacity fade.

Project Impact. This work addresses the adverse effects of Si volume change and minimizes the side reactions to significantly improve capacity and lifetime to develop negative electrode with Li-ion storage capacity over 2000 mAh/g (electrode level capacity) and significantly improve the Coulombic efficiency to over 99.9%. The research and development activity will provide an in-depth understanding of the challenges associated with assembling large volume change materials into electrodes and will develop a practical hierarchical assembly approach to enable Si materials as negative electrodes in Li-ion batteries.

Out-Year Goals. There are three aspects of this proposed work: bulk assembly, surface stabilization, and Li enrichment; these are formulated into 10 tasks in a four-year period.

- Develop hierarchical electrode structure to maintain electrode mechanical stability and electrical conductivity. (bulk assembly)
- Form *in situ* compliant coating on Si and electrode surface to minimize Si surface reaction. (surface stabilization)
- Use prelithiation to compensate first cycle loss of the Si electrode. (Li enrichment)

The goal is to achieve a Si-based electrode at higher mass loading of Si that can be extensively cycled with minimum capacity loss at high Coulombic efficiency to qualify for vehicle application.

Collaborations. This project collaborates with the following: Vince Battaglia and Venkat Srinivasan of LBNL; Xingcheng Xiao of GM; Jason Zhang and Chongmin Wang of PNNL; Yi Cui of Stanford; and the Si-Anode Focus Group.

Milestones

1. Design and synthesize three more PEFM polymers with different ethylene oxide (EO) content to study the adhesion and swelling properties of binder to the Si electrode performance. (December 2013 – Complete**)**
2. Go/No-Go: Down select Si vs. Si alloy particles and particle sizes (nano vs. micro.) Criteria: Down select based on cycling results. (March 2014 – Complete)
3. Prepare one type of Si/conductive polymer composite particles and test its electrochemical performance. (June 2014 – On schedule)
4. Design and synthesize one type of vinylene carbonate (VC) derivative that is targeted to protect Si surface and test it with Si-based electrode. (September 2014 – Complete)

Progress Report

High-tap-density silicon nanomaterials are highly desirable as anodes for lithium ion batteries due to their small surface area and minimum first-cycle loss. However, this material poses formidable challenges to polymeric binder design. Binders rely on adhesion to the surface to sustain the drastic volume changes during cycling. The low porosities and small pore size associated with this material are also detrimental to lithium ion transport.

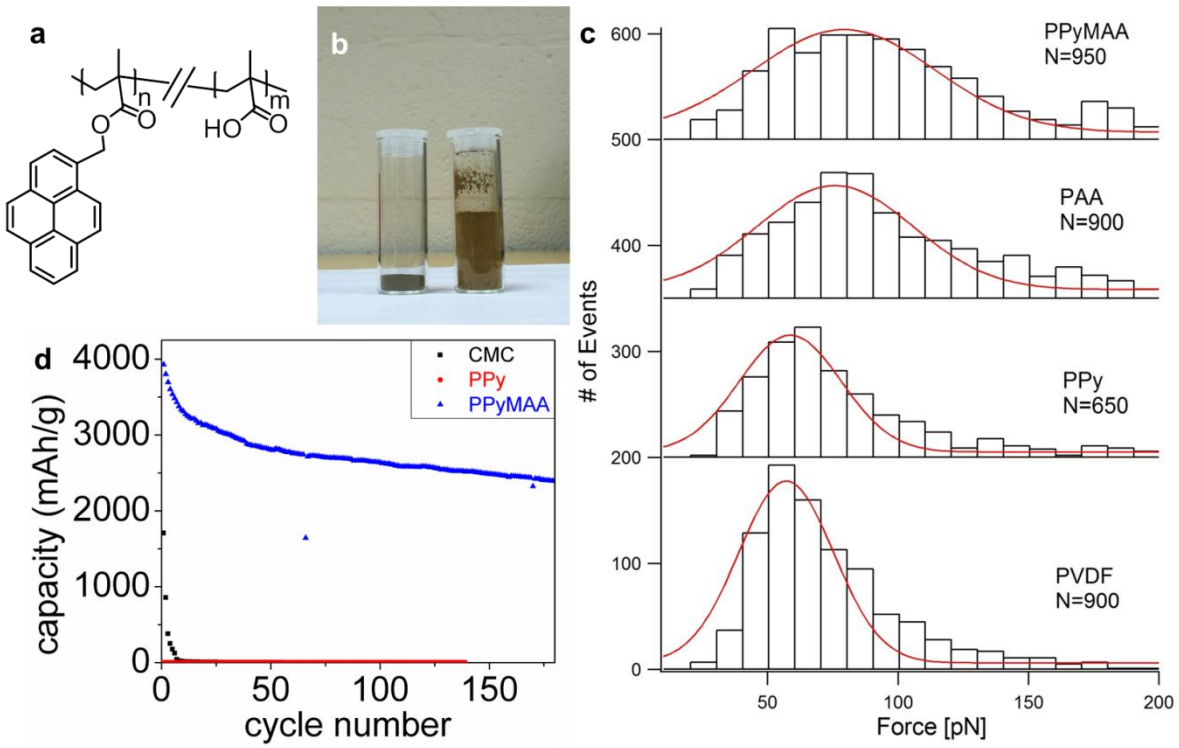

Figure 7. (a) Chemical structure of PPyMAA conductive polymer binder. (b) A comparison of 0.3 g of high-tap-density nanoSi (left) and regular nanoSi produced by chemical vapor deposition (right). (c) Histograms of AFM rupture force distribution corresponding to pulling a single polymer chain from a glass surface. Averaged rupture forces for PPyMAA, PAA, PPy, and PVDF on glass substrate were 95±58, 99±54, 72±40 and 68±38 piconewton (pN), respectively, with mean rupture forces ± standard deviations and N= # of observed unbinding events. The pulling velocity is 1000 nm/s and dwell time is 0.5 seconds. (d) Charge (delithiation) capacities of high tap density Si electrodes at C/10 with different binders.

This study introduces a new binder, poly(1-pyrenemethyl methacrylate-co-methacrylic acid) (PPyMAA), to be used for a high tap-density, nano-silicon electrode that will cycle in a stable manner with a first cycle efficiency of 82%—a value that is further improved to 87% when combined with graphite. Incorporating the MAA acid functionalities does not change the lowest unoccupied molecular orbital (LUMO) features nor lower the adhesion performance of the PPy homopolymer. Our single-molecule force microscopy measurement of PPyMAA reveals similar adhesion strength to the anode surface when compared with conventional polymer such as homo-polyacrylic acid (PAA), while possessing electronic conductivity. The combined conductivity and adhesion afforded by the MAA and pyrene copolymer results in good cycling performance for the high-tap-density Si.

Patents/Publications/Presentations

Publications

- Jia, Zhe, and Hui Zhao, Ying Bai, Ting Zhang, Amanda Siemens, Andrew Minor, and Gao Liu. "Solvent Processed Conductive Polymer with Single-walled Carbon Nanotube Composites." *Journal of Materials Research* (2015 – Accepted).
- Bai, Ying, and Xingzhen Zhou, Zhe Jia, Chuan Wu, Liwei Yang, Mizi Chen, Hui Zhao, Feng Wu, and Gao Liu. Understanding the Combined Effects of Microcrystal Growth and Band Gap Reduction for $Fe_{(1-x)}Ti_xF_3$ Nanocomposites as Cathode Materials for Lithium-ion Batteries. *Nano Energy* 17 (2015): 140-151.
- Zhao, Hui, and Fadi Asfour (co-first author), Yanbao Fu, Zhe Jia,Wen Yuan, Ying Bai, Min Ling, Heyi Hu, Gregory Baker, and Gao Liu. "Plasticized Polymer Composite Single-ion Conductors for Lithium Batteries." *ACS Applied Materials & Interfaces* 7 (2015): 19494-19499.
- Dai, Kehua, and Zhihui Wang (co-first author), Guo Ai, Hui Zhao, Wen Yuan, Xiangyun Song, Vincent Battaglia, Chengdong Sun, Kai Wu, and Gao Liu. "The Transformation of Graphite Electrode Materials in Lithium Ion Batteries after Cycling." *J. Power Sources* 298 (2015): 349-354.
- Zhao, Hui, and Zhe Jia (co-first author), Wen Yuan, Heyi Hu, Yanbao Fu, Gregory Baker, and Gao Liu. "Fumed Silica Based Single-ion Nanocomposite Electrolyte for Lithium Batteries." *ACS Applied Materials & Interfaces* 7 (2015): 19335-19341.
- Yan, Xiaodong, and Zhihui Wang, Min He, Zhaohui Hou, Ting Xia, Gao Liu, and Xiaobo Chen. "TiO_2 Nanomaterials as Anode Materials for Lithium-ion Rechargeable Batteries." *Energy Technology* 3 (2015): 801-814.

Task 1.5 – Studies in Advanced Electrode Fabrication (Vincent Battaglia, Lawrence Berkeley National Laboratory)

Project Objective. This project supports BMR principal investigators through the supply of electrode materials, laminates, and cells as defined by the BMR Focus Groups. The emphasis of the 2015 effort will be on the High-Voltage Focus Group, the Si-Anode Focus Group, and a nascent Li/S effort. The objectives are to screen sources of materials, define baseline chemistries, and benchmark performance of materials targeted to specific Focus Group topics. This provides a common chemistry and performance metrics that other BMR institutions can use as a benchmark for their own efforts on the subject. In addition, test configurations will be designed and built to identify and isolate problems associated with poor performance. Also, Li/S cells will be designed and tested.

Project Impact. Identification of baseline chemistries and availability of baseline laminates will allow a group of BMR principal investigators to work as a team. Such team work is considered crucial in the acceleration of the advancement of today's Li-ion and Li/S systems. Since all of the focus groups are dedicated to some aspect of increased energy density, all of this work will have an impact on this area.

Out-Year Goals. This framework of a common chemistry will accelerate advancements in energy density and should lead to baseline systems with an increased energy density of at least 40%. It should also provide a recipe for making electrodes of experimental materials that are of high enough performance to allow for critical down select—an important part of the process in advancing any technology.

Collaborations. This project collaborates with many BMR principal investigators.

Milestones

1. Identify and report the source of additional impedance of a symmetric cell. (12/31/14 – Complete)
2. Measure and report the gas composition of a symmetric cathode/cathode cell and an anode/anode cell. (3/31/15 – Complete)
3. Identify the first iteration of the baseline Li/S cell. (6/30/15)
4. Measure and report gas volume *versus* rate of side reaction at several upper voltage cut-off points. (9/30/15)

Progress Report

Milestone 4. Measure and report gas volume versus rate of side reaction at several upper voltage cut-off points. (9/30/15)

Bryan McCloskey, formerly at IBM, joined the LBNL Battery Research team at the beginning of the calendar year. He brings to the program, among other things, the capability of simultaneously measuring electrochemical performance and gas analysis (DEMS). Over the past nine months he has established this capability in his labs. Because of this, the measurement of gas volumes and gas composition has become of less importance for our group. We will work with Bryan in this area, providing electrodes of interest, but he will report on this activity in his quarterly reports.

That being said, we started some preliminary experiments in fabricating thicker electrodes. This will be the focus of our effort for FY 2016. The first activity was to cast electrodes using our standard formulation of 85% active material, 8% binder, and 7% Super P Li carbon additive to different thicknesses. The binder is Kureha 1100 PVDF (polyvinylidene fluoride). (In the future, PVDF binders from Arkema will be the center of our research: material is expected to arrive early October.) The active material is NCM from a major commercial supplier. The materials are combined with NMP to form a slurry. After an hour of mixing, the viscosity of the slurry was measured at 1810 cp at 6 RPM. The coating speed for casting the slurry was set at 60 cm/min (about 50 times slower than is found in industry). Table 1 provides a list of the doctor blade heights and the final thickness of the laminates once the electrodes had dried. One sees that the final thickness is approximately a third of the height of the doctor blade. (These are the measured heights before calendaring.) From this preliminary data it was discovered that electrodes cast at doctor blade heights of 600 microns and greater were difficult to handle as they easily delaminated from the aluminum current collector.

Table 1. Preliminary experiments in fabricating thicker electrodes resulted in a final thickness that was approximately a third of the height of the doctor blade.

Doctor blade gap (μm)	250	300	400	500	600	750
Laminate thickness (μm)	80	95	130	180	205	275

Once electrodes were cast they were taken to the Battery Program Scanning Electron Microscopy (SEM) for analysis. A method to section electrodes has been developed as can be seen in Figure 8. Energy dispersive spectroscopy (EDS) of the cross-section can also be taken as seen in Figure 9 to acquire chemical composition and distribution.

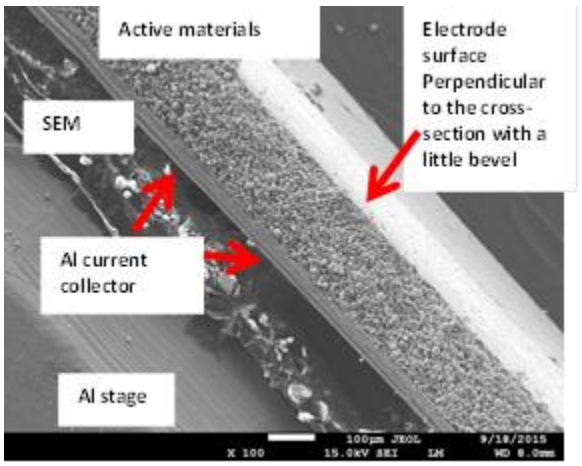

Figure 8. SEM of a cross-sectioned electrode.

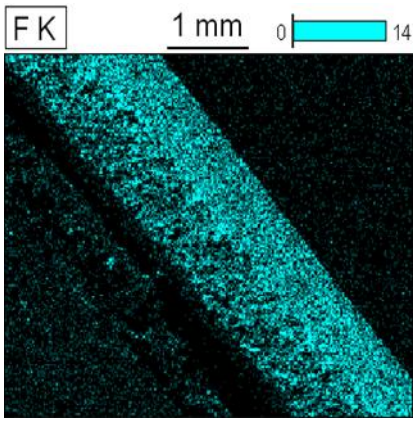

Figure 9. EDS image showing the distribution of F across a cross-sectioned electrode.

Task 2 – Silicone Anode Research

Summary and Highlights

Most Li-ion batteries used in the state-of-the-art electric vehicles (EVs) contain graphite as their anode material. Limited capacity of graphite (LiC_6, 372 mAh/g) is one of the barriers that prevent the long-range operation of EVs required by the EV Everywhere Grand Challenge proposed by the DOE Office of Energy Efficiency and Renewable Energy (EERE). In this regard, silicon (Si) is one of the most promising candidates as an alternative anode for Li-ion battery applications. Si is environmentally benign and ubiquitous. The theoretical specific capacity of silicon is 4212 mAh/g ($Li_{21}Si_5$), which is 10 times greater than the specific capacity of graphite. However, the high specific capacity of silicon is associated with large volume changes (more than 300 percent) when alloyed with lithium. These extreme volume changes can cause severe cracking and disintegration of the electrode and can lead to significant capacity loss.

Significant scientific research has been conducted to circumvent the deterioration of silicon-based anode materials during cycling. Various strategies, such as reduction of particle size, generation of active/inactive composites, fabrication of silicon-based thin films, use of alternative binders, and the synthesis of one-dimensional silicon nanostructures, have been implemented by a number of research groups. Fundamental mechanistic research also has been performed to better understand the electrochemical lithiation and delithiation processes during cycling in terms of crystal structure, phase transitions, morphological changes, and reaction kinetics. Although significant progress has been made on developing silicon-based anodes, many obstacles still prevent their practical application. Long-term cycling stability remains the foremost challenge for Si-based anode, especially for the high-loading electrode (> 3mAh/cm2) required for many practical applications. The cyclability of full cells using silicon-based anodes is also complicated by multiple factors, such as diffusion-induced stress and fracture, loss of electrical contact among silicon particles and between silicon and current collector, and the breakdown of solid-electrolyte interphase (SEI) layers during volume expansion/contraction processes. The design and engineering of a full cell with a silicon-based anode still needs to be optimized. Critical research remaining in this area includes, but is not limited to, the following:

- The effects of SEI formation and stability on the cyclability of silicon-based anodes need to be further investigated. Electrolytes and additives that can produce a stable SEI layer need to be developed.
- Low-cost manufacturing processes have to be found to produce nano-structured silicon with the desired properties.
- A better binder and a conductive matrix need to be developed. They should provide flexible but stable electrical contacts among silicon particles and between particles and the current collector under repeated volume changes during charge/ discharge processes.
- The performances of full cells using Si-based anode need to be investigated and optimized.

The main goal of Task 2 is to gain a fundamental understanding on the failure mechanism of Si-based anode and improve its long term stability, especially for thick electrode operated at full cell conditions. The Stanford group will address the problem of large first cycle loss in Si-based anode by novel prelithiation approaches. Two approaches will be investigated in this study: (1) developing facile and practical methods to increase first-cycle Coulombic efficiency of Si anodes, and (2) synthesizing fully lithiated Si to pair with high capacity lithium-free cathode materials. The PNNL/UP/FSU team will explore new electrode structures using nano Si and SiO_x to enable high-capacity and low-cost Si-based anodes with good cycle stability and rate capability. Nanocomposites of silicon lithium oxide will be prepared by novel *in situ* chemical reduction methods to reduce the first cycle loss. Mechanical and electrochemical stability of the SEI layer formed on the surface of Si particles will be investigated by electrochemical evaluation and *in situ/ex situ* microscopic analysis. Success of this project will accelerate large-scale application of Si based anode and improve the energy density of Li-ion batteries to meet the goal of EV Everywhere.

The highlights for this quarter include the following:

- **Kumta (Pittsburgh).** Si nano-flake prepared by high energy mechanical milling and subsequent chemical vapor deposition (CVD) demonstrates a reversible capacity of ~ 1100 mAh/g Si in 100 cycles and a Coulombic efficiency of ~99.5% – 99.8 %.
- **Cui (Stanford).** Developed artificial SEI-protected Li_xSi nanoparticles as prelithiation additives that are stable in the air with 10% relative humidity.

Task 2.1 – Development of Silicon-Based High Capacity Anodes (Ji-Guang Zhang/Jun Liu, PNNL; Prashant Kumta, Univ. of Pittsburgh; Jim Zheng, PSU)

Project Objective. The objective of this project is to develop high-capacity and low-cost Si-based anodes with good cycle stability and rate capability to replace graphite in Li-ion batteries. Nanocomposites of silicon and Li-ion conducting lithium oxide will be prepared by novel *in situ* chemical reduction methods to solve the problems associated with large first cycle irreversible capacity loss, while achieving acceptable Coulombic efficiencies. Large irreversible capacity loss in the first cycle will also be minimized by pre-doping Li into the anode using stabilized lithium metal powder or additional sacrificial Li electrode. The optimized materials will be used as the baseline for both thick electrode fabrication and studies to advance our fundamental understanding of the degradation mechanism of Si-based anodes. The electrode structures will be modified to enable high utilization of thick electrode. Mechanical and electrochemical stability of the SEI layer will be investigated by electrochemical method, simulation, and *in situ* microscopic analysis to guide their further improvement.

Project Impact. Si-based anodes have much larger specific capacities compared with conventional graphite anodes. However, the cyclability of Si-based anodes is limited because of the large volume expansion characteristic of these anodes. This work will develop a low-cost approach to extend the cycle life of high-capacity, Si-based anodes. The success of this work will further increase the energy density of Li-ion batteries and accelerate market acceptance of electrical vehicles (EV), especially for the plug-in hybrid electrical vehicles (PHEV) required by the EV Everywhere Grand Challenge proposed by the DOE Office of Energy Efficiency and Renewable Energy (EERE).

Out-Year Goals. The main goal of the proposed work is to enable Li-ion batteries with a specific energy of >200 Wh/kg (in cell level for PHEVs), 5000 deep-discharge cycles, 15-year calendar life, improved abuse tolerance, and less than 20% capacity fade over a 10-year period.

Collaborations. We will continue to collaborate with the following battery groups on anode development:

- Dr. Karim Zaghib, Hydro-Quebec; preparation of nano-Si
- Prof. Michael Sailor, UCSD; preparation of porous Si
- Prof. David Ji, Oregon State University; preparation of porous Si by thermite reactions

Milestones

1. Identify the stability window of solid-electrolyte interphase (SEI) formed on Si-based anode. (12/31/2014 – Complete)
2. Optimize the synthesis conditions of the rigid-skeleton supported Si composite. (3/31/2015 – Complete)
3. Demonstrate the operation of full cell using Si anode and selected cathode with >80% capacity retention over 100 cycles. (6/30/2015 – Complete)
4. Achieve >80% capacity retention over 200 cycles of thick electrodes (~3 mAh/cm2) through optimization of the Si electrode structure and binder. (9/30/2015 – Complete)

Progress Report

Porous Si from electrochemical etching has good cycling stability at high loading. Figure 10a shows an electrode of porous Si with the areal capacity of 2.5 mAh/cm2 at 0.5 mA/cm^2 discharge and 0.75 mA/cm^2 charge. It is cycled between 5 mV and 1 V. The specific capacity is ~700 mAh/g based on full electrode. The capacity retention is 76% after 200 cycles. Porous Si/graphite composite electrode was also developed to further improve the cycling stability. Figure 10b shows a thick electrode of porous Si/graphite composite electrode with the areal capacity of ~3.2 mAh/cm^2 at 0.06 mA/cm2 charge/discharge current density. The areal capacity is ~2.8 mAh/cm^2 at 0.4 mA/cm^2 charge/discharge. The capacity retention is 90% after 200 cycles. The specific capacity is ~450 mAh/g based on full anode. Further optimization of the performance is being investigated.

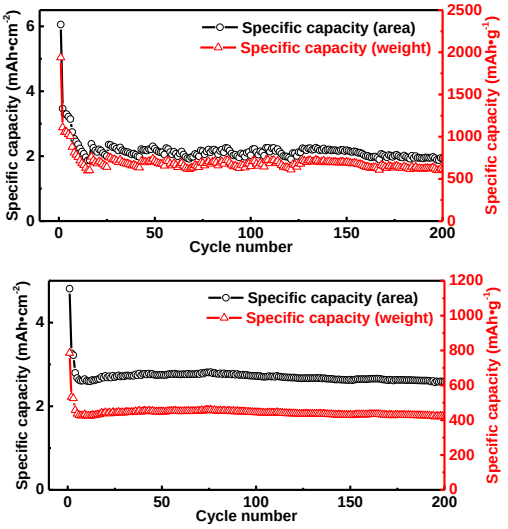

Figure 10. (a) Porous Si anode with the areal capacity of ~2.5 mAh/cm^2 at a discharge current density of ~0.5 mA/cm^2 and a charge current density of ~0.75 mA/cm^2. (b) Porous Si-graphite composite anode with the areal capacity of ~2.8 mAh/cm^2 at a charge/discharge current density of 0.4 mA/cm^2.

During this period, two other types of nano-Si have been developed by a low-cost abundant water soluble template based approach using high-energy mechanical milling followed by low-pressure chemical vapor deposition to develop the Si nanostructures. The template has been ball milled by mechanical milling for 2h and 20h to reduce the size of the particles and coating it with silicon by thermal decomposition of Si precursors. After washing the template, the Si obtained from the 2h milled template showed nanoflakes morphology of thickness ~50-100nm, while the Si obtained from the 20h milled template showed a mixture of nanorods and nanoparticles. The Si nanorods show an initial discharge and charge capacity of ~2930 mAh/g and ~2475 mAh/g, while the Si nanoflakes display similar capacities of ~2780 mAh/g and ~2200 mAh/g. The long-term cycling of the nanoflakes and nanorods (Figure 11) exhibit reversible capacity of ~1050 mAh/g and ~1125 mAh/g by the end of 100 cycles, respectively, with a Coulombic efficiency of ~99.5% – 99.8%. Studies are on-going to understand the morphology and further improve cycling response.

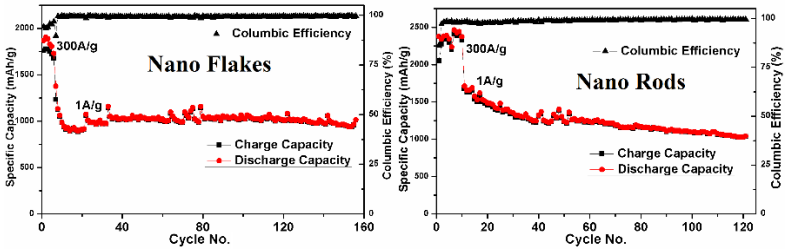

Figure 11. Long term cycling of (a) Si flakes and (b) Si nanorods and (c) voltage vs. capacity plot of Si nanorods showing 13% first cycle irreversible loss.

The IR voltage drop from the anode and cathode of Li-ion capacitors (LIC) during charge and discharge was studied. At high SLMP (stabilized lithium metal powder) loadings, small IR voltage drops were obtained for both low and high cell voltages. Four three-electrode LIC test cells with no, low, medium, and high SLMP loadings on anode were assembled and tested. The SLMP loadings were 0, 1.4, 2.06, and 2.6 mg, which will be referred as no, low, medium, and high loading, respectively. The potentials of both anode and cathode reduced with increasing SLMP loading. Because more SLMP loading was applied to the anode, the intercalation of more Li into anode leads to a lower potential. It can also be seen that the IR drop from anode was greater than that from cathode; particularly, large values of IR drops were obtained from anodes with no and low SLMP loadings. Overall IR drops from cells were 0.25 – 0.27 V for medium-high SLMP loadings, 0.59 V for low SLPM loading, and as high as 1 V for no SLMP loading; For no and low SLMP loading on the anode, the IR drop of at the cell voltage of 2 V was greater than that at 4 V. Therefore, the experimental results clearly showed that the SLMP loading to the anode in LICs not only determined the potential of the anode and the cyclability, but also determined the IR drop as well as maximum power of the LIC cells.

Patents/Publications/Presentations

Publications

- Epur, Rigved, and Madhumati Ramanathan, Moni K. Datta, Dae Ho Hong, Prashanth H. Jampani, Bharat Gattu, and Prashant N. Kumta. "Scribable Multi-walled Carbon Nanotube-silicon Nanocomposites: A Viable Lithium-ion Battery System." *Nanoscale* 7 (2015): 3504 – 3510.
- Luo, Langli, and Peng Zhao, Hui Yang, Borui Liu, Ji-Guang Zhang, Yi Cui, Guihua Yu, Sulin Zhang, and Chong-Min Wang. "Surface Coating Constraint Induced Self-Discharging of Silicon Nanoparticles as Anodes for Lithium Ion Batteries." *Nano Letters*, DOI: 10.1021/acs.nanolett.5b03047.
- Epur, Rigved, and Prashanth H. Jampani, Moni K. Datta, Dae Ho Hong, Bharat Gattu, and Prashant N. Kumta. "A Simple and Scalable Approach to Hollow Silicon Nanotube (h-SiNT) Anode Architectures of Superior Electrochemical Stability and Reversible Capacity." *J. Mater. Chem. A* 3 (2015): 11117 – 11129.
- Luo, Langli, and Hui Yang, Pengfei Yan, Jonathan J. Travis, Younghee Lee, Nian Liu, Daniela Molina Piper, Se-Hee Lee, Peng Zhao, Steven M. George, Ji-Guang Zhang, Yi Cui, Sulin Zhang, Chunmei Ban, and Chong-Min Wang. "Surface-Coating Regulated Lithiation Kinetics and Degradation in Silicon Nanowires for Lithium Ion Battery." *ACS Nano* 9 (2015): 5559−5566.
- Gattu, B., and P. Jampani, P.P. Patel, M.K. Datta, and P.N. Kumta. "High Performing Hollow Silicon Nanotube Anodes for Lithium Ion Batteries." 227th ECS Meeting, Chicago (May 2015).
- Cao, W.J., and M. Greenleaf, Y.X. Li, D. Adams, M. Hagen, T. Doung, and J.P. Zheng. "The Effect of Lithium Loadings on Anode to the Voltage Drop during Charge and Discharge of Li-ion Capacitors." *J. Power Sources* 280 (2015): 600.

Task 2.2 – Pre-Lithiation of Silicon Anode for High Energy Li Ion Batteries (Yi Cui, Stanford University)

Project Objective. Prelithiation of high-capacity electrode materials such as Si is an important means to enable those materials in high-energy batteries. This study pursues two main directions: (1) developing facile and practical methods to increase first-cycle Coulombic efficiency of Si anodes, and (2) synthesizing fully lithiated Si to pair with high-capacity, lithium-free cathode materials.

Project Impact. The first-cycle Coulombic efficiency of anode materials will be increased dramatically via prelithiation. Prelithiation of high capacity electrode materials will enable those materials in next-generation high-energy-density lithium ion batteries. This project's success will make high-energy-density lithium ion batteries for electric vehicles.

Out-Year Goals. Compounds containing a large quantity of Li will be synthesized for pre-storing Li ions inside batteries. First-cycle Coulombic efficiency (1st CE) will be improved and optimized (over 95%) by prelithiating anode materials with the synthesized Li-rich compounds.

Collaborations. This project works with the following collaborators: (1) BMR program principal investigators, (2) Stanford Linear Accelerator Center (SLAC): *in situ* x-ray, Dr. Michael Toney, and (3) Stanford: mechanics, Prof. Nix.

Milestones

1. Prelithiate anode materials by direct contact of Li metal foil to anodes. (January 2014 – Complete)
2. Synthesize Li_xSi nanoparticles with high capacity (>1000 mAh/g Si). (July 2014 – Complete)
3. Prelithiate anode materials with dry-air-stable Li_xSi-Li_2O core-shell nanoparticles. (April 2015 – Complete)
4. Synthesize artificial-SEI (solid-electrolyte interphase) protected Li_xSi NPs. (June 2015 – Complete)
5. Synthesize Li_xSi nanoparticles with high capacity (>2000 mAh/g Si). (July 2015 – Complete)
6. Artificial-SEI protected Li_xSi NPs show negligible capacity decay in dry air after 5 days and maintain a high capacity of 1600 mAh/g in humid air (~10% relative humidity). (September 2015 – Complete)

Progress Report

To evaluate the electrochemical performance of artificial-SEI coated Li_xSi NPs, coated Li_xSi NPs were first lithiated to 0.01 V and then delithiated to 1 V, exhibiting a high prelithiation capacity of 2100 mAh/g as shown in Figure 12a. Figure 12b-c demonstrate artificial-SEI coated Li_xSi NPs can be mixed with anode materials during slurry processing and serve as an excellent prelithiation reagent for both Si NPs and commercial graphite. The incorporation of a small amount of coated Li_xSi (graphite/coated Li_xSi = 85:5 by weight) improves the 1st cycle CE from 87.4% to 99.2%. Due to its small size, the added Li_xSi NPs are expected to be embedded in the interstices of graphite microparticles. Since Li_xSi is already in its expanded state, sufficient space has been created during electrode fabrication. The Li_xSi NPs will not squeeze each other during cycling. Accordingly, with the introduction of coated Li_xSi (Figure 12d), graphite anodes exhibit consistent higher capacity and good cycling at C/20 for the first three cycles and C/5 for the following cycles. To evaluate the dry air stability, coated Li_xSi NPs were stored in a dry room (dew point = −50ºC) for different days. After in dry air for five days, the coated Li_xSi NPs still exhibit a high capacity of 1921 mAh/g, which is only an 8% decay from the initial capacity (Figure 13a). In addition, the capacity decay in dry air is much slower for coated NPs than pristine NPs, confirming that the artificial-SEI coating slows down the NPs' side reaction rate in dry air. To further explore the stability in humid air, coated Li_xSi NPs were stored in air with different humidity levels for 6 hours. After exposure to humid air with 10% RH, the coated Li_xSi NPs still exhibit a high extraction capacity of 1604 mAh/g, as shown in Figure 13b. For humidity levels higher than 20% RH, the Li extraction capacity shows a large drop after the 6 h storage period. However, this humidity level is higher than battery electrode fabrication conditions in industry.

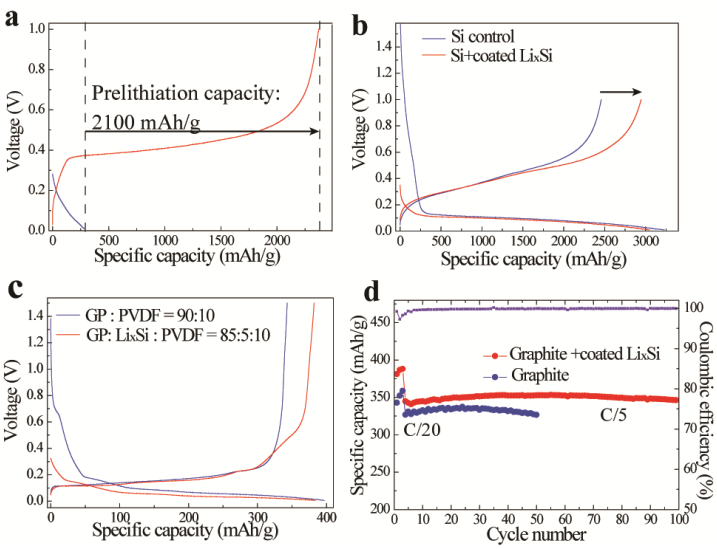

Figure 12. (a) 1st cycle galvanostatic discharge/charge profiles of artificial-SEI coated Li_xSi NPs. (b) 1st cycle voltage profiles of Si Ps/coated Li_xSi composite (55:10 by weight) and Si NPs control cells. (The capacity is based on the total mass of Si in the electrodes.) (c) 1st cycle voltage profiles of graphite/coated Li_xSi composite (85:5 by weight) and graphite control cells. (d) Cycling performance of graphite/coated Li_xSi composite and graphite control cells at C/20 for the first three cycles and C/5 for the following cycles. The purple line is the Coulombic efficiency of graphite/coated Li_xSi composite.

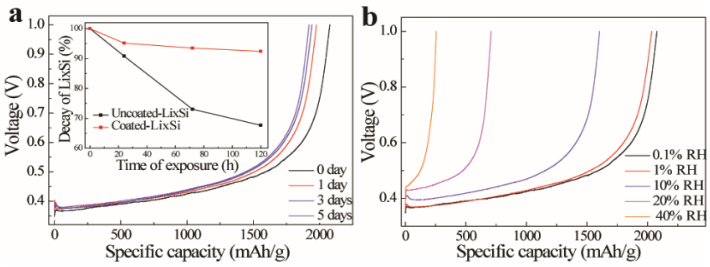

Figure 13. (a) The extraction capacity of artificial-SEI coated NPs exposed to dry air for varying periods of time. The inset shows the change of capacity as a function of exposure time. (b) The extraction capacity of artificial-SEI coated NPs exposed to air for 6 hours at different humidity levels.

Patents/Publications/Presentations

Patent

- Patent application: S14-109| Dry-air-stable Li_xSi–Li_2O core–shell nanoparticles as high-capacity prelithiation reagents.

Publications

- Zhao, J., et al. "Dry-air-stable Lithium Silicide–lithium Oxide Core–shell Nanoparticles as High-capacity Prelithiation Reagents." *Nat. Commun*. 5, no. 5088 (2014).
- Zhao, J., et al. "Artificial Solid Electrolyte Interphase-Protected Li_xSi Nanoparticles: An Efficient and Stable Prelithiation Reagent for Lithium-Ion Batteries." *J. Am. Chem. Soc*. 137 (2015).

Presentation

- 2015 MRS Spring Meeting and Exhibit (2015 – Poster presentation).

TASK 3 – HIGH ENERGY DENSITY CATHODES FOR ADVANCED LITHIUM-ION BATTERIES

Summary and Highlights

Developing high energy density, low-cost, thermally stable, and environmentally safe electrode materials is a key enabler for advanced batteries for transportation. High energy density is synonymous with reducing cost per unit weight or volume. Currently, one major technical barrier toward developing high energy density lithium-ion batteries (LiBs) is the lack of robust, high-capacity cathodes. As an example, the most commonly used anode material for LiBs is graphitic carbon, which has a specific capacity of 372 mAh/g, while even the most advanced cathodes like lithium nickel manganese cobalt oxide (NMC) has a maximum capacity of ~180 mAh/g. This indicates an immediate need to develop high capacity (and voltage) intercalation type cathodes that have stable reversible capacities of 300 mAh/g and beyond. High volumetric density is also critical for transportation applications. Alternative high capacity cathode chemistries such as those based on conversion mechanisms, Li-S, or metal air chemistries still have fundamental issues that must be addressed before integration into cells for automotive use. Successful demonstration of high energy cathodes will enable high energy cells that meet or exceed the DOE cell level targets of 400 Wh/kg and 600 Wh/L with a system level cost target of $125/kWh.

During the last decade, many high-voltage cathode chemistries have been developed under the BATT (now BMR) program, including Li-rich NMC and Ni-Mn spinels. Current efforts are directed toward new syntheses and modifications to improve stability (both bulk and interfacial) under high-voltage cycling condition (> 4.6 V) for Li-rich NMC [Nanda, ORNL; Zhang & Jie, PNNL; Thackeray and Croy, ANL; Marca Doeff, LBNL]. Three other subtasks are directed toward synthesis and structural stabilization of high capacity, multivalent, polyanionic cathodes, both in crystalline and amorphous phases [Manthiram, UT-Austin; Looney and Wang, BNL; Whittingham, SUNY-Binghamton; and Kercher-Kiggans, ORNL]. Approaches also include aliovalent or isovalent doping to stabilize cathode structures during delithiation, as well as surface coatings to improve interfacial stability. John Goodenough's group at UT-Austin is developing novel separators to enable lithium metal anodes and high capacity cathodes in a flow cell.

The highlights for this quarter are as follows:

- **Task 3.1.** $Li_2Cu_{1-x}Ni_xO_2$ solid solution cathodes show stability till 3.9 V; oxygen loss begins thereafter, contributing to the capacity but increasing capacity fade.
- **Task 3.2.** $Cu_{1-y}Fe_yF_2$ conversion cathode showed capacity ~ 290 mAh/g for 10 cycles exceeding the Go/No-Go milestone.
- **Task 3.3.** NMC electrodes showed good cycling stability even with the capacity loading up to ~ 4.0 mAh cm^{-2}, exhibiting capacity retention higher than 90% after 100 cycles.
- **Task 3.4.** Collaboration between Balsara group at LBNL and BNL team demonstrated novel high-capacity cathode (α-$CuVO_3$) with extraordinary cycling stability for solid-state batteries showing capacity above 230 mAh/g and 98% retention over 50 cycles.
- **Task 3.5.** Stabilizing Li-rich NMC with a Co-based spinel component with capacity ~200 mAh/g.
- **Task 3.6.** Aliovalent doping in $Li_2M_{1-3/2x}V_x\square_{x/2}P_2O_7$ by low-temperature synthesis approaches did not yield the target capacity (> 110 mAh/g). [Go/No-Go]
- **Task 3.7.** 10% borate substitution in $LiCu(PBV)_3$ and $Li_2Cu(PBV)_4$ glass cathodes improves the 1st cycle reversibility, and reduces voltage hysteresis.
- **Task 3.8.** Full-field transmission X-ray microscopy (TXM) on spray pyrolized NMC-442 show lower Ni concentration in the surface than bulk compared to standard co-precipitation process.
- **Task 3.9.** Probed the electrochemical stability of alkali metal deposition on polymer coated stainless steel current collectors using a $NaCrO_2$ cathode.
- **Task 3.10.** Synthesis and structural characterization of LT- $Li[Mn_{1.5}Ni_{0.5-2x}Co_{2x}]O_4$; x = 0, 0.125 to stabilize spinel in layered TM oxides.

Task 3.1 – Studies of High Capacity Cathodes for Advanced Lithium-ion Systems (Jagjit Nanda, Oak Ridge National Laboratory)

Project Objective. The overall project goal is to develop high energy density lithium-ion electrodes for electric vehicles (EV) and plug-in hybrid EV (PHEV) applications that meet and/or exceed the DOE energy density and life cycle targets as from the USDRIVE/USABC roadmap. Specifically, this project aims to address and mitigate the technical barriers associated with high-voltage cathode compositions such as lithium-manganese rich NMC (LMR-NMC) and $Li_2M^IM^{II}O_2$, where M^I and M^{II} are transition metals that do not include Mn or Co. Major emphasis is placed on developing new materials modifications (including synthetic approaches) for high-voltage cathodes that will mitigate issues such as: (i) voltage fade associated with LMR-NMC composition that leads to loss of energy over the cycle life; (ii) transition metal dissolution that leads to capacity and power fade; (iii) thermal and structural stability under the operating SOC range; and (iv) voltage hysteresis associated with multivalent transition metal compositions. Another enabling feature of the project is utilizing (and developing) various advanced characterization and diagnostic methods at the electrode and/or cell level for studying cell and/or electrode degradation under abuse conditions. The techniques include electrochemical impedance spectroscopy, Micro-Raman, aberration corrected electron microscopy combined with EELS, x-ray photoelectron spectroscopy, ICP-AES, Fluorescence, and x-ray and Neutron diffraction.

Project Impact. The project has both short-term and long-term deliverables directed toward the DOE Vehicle Technologies Office (VTO) Energy Storage 2015 and 2022 goals. Specifically, we are working on advanced electrode couples that have cell-level energy density targets of 400 Wh/kg and 600 Wh/l for 5000 cycles. Increasing the energy density per unit mass or volume ultimately reduces the cost of battery packs consistent with the DOE 2022 EV Everywhere goal of $125/kWh.

Out-Year Goals. The project is directed toward developing high-capacity cathodes for advanced lithium-ion batteries. The goal is to develop new cathode materials that have high capacity, are based on low-cost materials, and meet the DOE road map in terms of safety and cycle life. Two kinds of high-energy cathode materials are being studied. Over the last few years, the principal investigator has worked on improving cycle life and mitigating energy losses of high-voltage, Li-rich composite cathodes (referred to as LMR-NMC) in collaboration with the voltage fade team at ANL. Efforts also include surface modification of LMR-NMC cathode materials to improve their electrochemical performance under high-cycling (> 4.5 V). The tasks involve collaborating with researchers at the Stanford Synchrotron Research Lightsource (SSRL) and Advanced Photon Source at LBNL to understand local changes in morphology and microstructure under *in situ* and *ex-situ* conditions.

Collaborations. This project collaborates with Johanna Nelson, SSRL, Stanford Linear Accelerator Center: x-ray imaging and XANES; Guoying Chen, LBNL: *in situ* XAS and XRD; Feng Wang, BNL: x-ray synchrotron spectroscopy and microscopy; and Bryant Polzin, ANL: CAMP Facility for electrode fabrication.

Milestones

1. Investigation of surface reactivity, vacancy disorder, and interfacial kinetics of LMR-NMC composite cathodes to mitigate voltage fade and transition metal ™ dissolution to achieve DOE cell level EV goals of 400 WH/kg and 600 Wh/L for 5000 cycles. (Complete)
2. Stabilize structure and electrochemical performance of high-capacity $Li_2Cu_xNi_{1-x}O_2$ cathodes to achieve capacity between 250-300 mAh/g for > 50 charge-discharge cycles at C/3 rate. (Complete)
3. Undertake *in situ and ex-situ* x-ray synchrotron and spectroscopic studies to correlate changes in local structure, surface chemistry, and morphology of cycled high energy density electrodes (LMR- NMC and 5V Mn-Ni spinel) and compare the changes with pristine or uncycled electrodes. (Complete)
4. Investigate the role of Ni in stabilizing the structure of $Li_2Cu_xNi_{1-x}O_2$ and identify the role of oxygen reactivity from gas generation experiments. (09/30/15 – Complete) [Smart Milestone]

Progress Report

Last quarter, we reported *in situ* X-ray absorption studies on $Li_2Cu_{0.5}Ni_{0.5}O_2$ to identify the respective Cu and Ni redox processes that either contribute to the reversible capacity or result in irreversible loss. This quarter we report two important results related to stability of this chemistry, (i) *in situ* Raman studies to monitor first cycle irreversible structural transformation and (ii) gas evolution studies to estimate the oxygen release when $Li_2Cu_{0.5}Ni_{0.5}O_2$ is cycled above 3.9 V. Figure 14 shows how the Raman spectra evolve during the first charge-discharge cycle. Clearly, the structure changes significantly with the removal of even a small amount of lithium. For opaque, conductive samples Raman spectroscopy is surface sensitive (skin depth <100 nm). It is, therefore, possible that the dramatic structural changes initially occur at the surface and do not reflect the particle bulk. For comparison, the Raman spectra of $LiNiO_2$ and $NaCuO_2$ are also shown in Figure 14. $NaCuO_2$ is isostructural with $LiCuO_2$, but can be prepared in high purity using conventional solid-state reactions. After delithiation, the Raman spectrum of $Li_2Cu_{0.5}Ni_{0.5}O_2$ closely resembles that of other close-packed layered oxides such as $LiNiO_2$ and $LiNi_{1-y}Co_yO_2$. The spectra bear little resemblance to the monoclinic $NaCuO_2$ phase. These results are consistent with earlier work from Imanishi, et al. [*Solid State Ionics*, 2006], which showed using x-ray diffraction (XRD) that during cycling $Li_2Cu_{0.5}Ni_{0.5}O_2$ transforms from the orthorhombic phase into a close-packed layered structure and not the C2/m monoclinic phase. Further, we undertook quantitative measurements of gas generation in $Li_2Cu_{0.5}Ni_{0.5}O_2$ pouch cells. Charging the cell from the OCP to 3.9 V did not yield any measurable amount of gas. However, significant amounts of gas were generated when the cell was charged above 3.9 V. In fact, we observed that after each charging step above 3.9 V, the open circuit potential (OCP) of the cell relaxed to ~ 3.9 V. We compared the total capacity that was extracted from the cell during charging steps between 3.9 V and 4.3 V with the capacity that can be attributed to gas evolution (not shown here). The capacity due to gas evolution was calculated assuming that all of the evolved gas is O_2. This assumption is reasonable, since the carbonate electrolyte is known to be quite stable within this voltage range. Also, no measurable quantity of gas was evolved in a control cell resting at OCP (2.4 V) for a period of one month. Our analysis shows that virtually all of the capacity extracted from $Li_2Cu_{0.5}Ni_{0.5}O_2$ above 3.9 V is due to oxygen evolution. However, if the voltage window is limited to avoid oxygen release, the higher voltage redox reactions at 3.9 V (oxidation) and 3.6 V (reduction) are also eliminated.

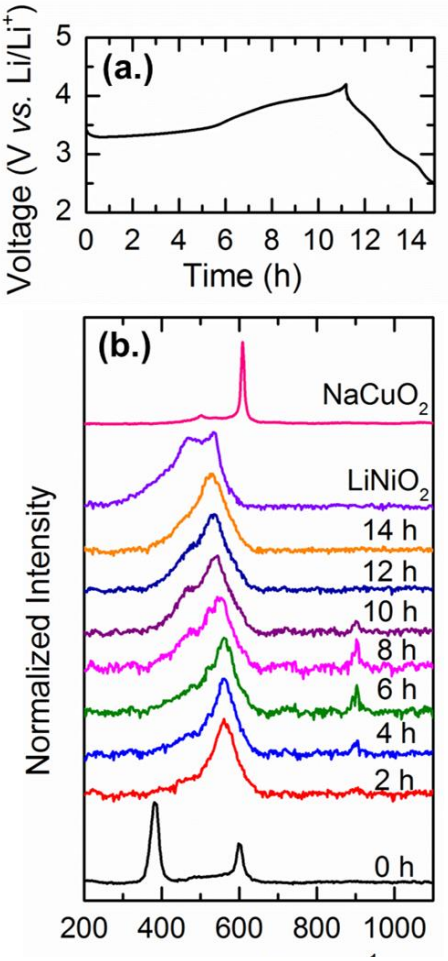

Figure 14. First-cycle voltage profile during charge and discharge of a $Li_2Cu_{0.5}Ni_{0.5}O_2$ half cell for *in situ* Raman spectroscopy. (b) Raman spectra of $Li_2Cu_{0.5}Ni_{0.5}O_2$ cathode collected during galvanostatic charge and discharge. Spectra are shown every two hours during the first cycle. The Raman spectra of $LiNiO_2$ and $NaCuO_2$ are also shown for comparison.

Patents/Publications/Presentations

Publications

- Ruther, R., and H. Zhou, C. Dhital, K. Saravanan, A.K. Kercher, G. Chen, A. Huq, Frank M. Delnick, and J. Nanda. "Synthesis, Structure, and Electrochemical Performance of High Capacity $Li_2Cu_{0.5}Ni_{0.5}O_2$ Cathodes." *Chem. Mater.* 227 (2015): 6746-6754.
- Pannala, S., and J.A. Turner, S. Allu, W.R. Elwasif, S. Kalnaus, S. Simunovic, A. Kumar, J.J. Billings, H. Wang, and J. Nanda. "Multiscale Modeling and Characterization for Performance and Safety of Lithium-Ion Batteries." *J. Appl. Phys.* 118 (2015): 072017.
- Stershic, A.J., and S. Simunovic and J. Nanda. "Modeling the Evolution of Lithium-Ion Particle Contact Distributions Using a Fabric Tensor Approach." *J. Power Sources* 297 (2015): 540.
- Ruther, R., and H. Dixit, A. Pezesheki, R. Sacci, V. Cooper, J. Nanda, and G. Veith. "Correlating Local Structure with Electrochemical Activity in Li_2MnO_3." *J. Phys. Chem. C* 119 (2015): 18022-18029.

Task 3.2 – High Energy Density Lithium Battery (Stanley Whittingham, SUNY Binghamton)

Project Objective. The project objective is to develop the anode and cathode materials for high-energy density cells for use in plug-in hybrid electric vehicles (PHEVs) and in electric vehicles (EV) that offer substantially enhanced performance over current batteries used in PHEVs and with reduced cost. Specifically, the primary objectives are to:

- Increase the volumetric capacity of the anode by a factor of 1.5 over today's carbons
  - Using a SnFeC composite conversion reaction anode
- Increase the capacity of the cathode
  - Using a high-capacity conversion reaction cathode, CuF_2, and/or
  - Using a high-capacity 2 Li intercalation reaction cathode, $VOPO_4$
- Enable cells with an energy density exceeding 1 kWh/liter

Project Impact. The volumetric energy density of today's lithium-ion batteries is limited primarily by the low volumetric capacity of the carbon anode. If the volume of the anode could be cut in half, and the capacity of the cathode to over 200 Ah/kg, then the cell energy density can be increased by over 50% to approach 1 kWh/liter (actual cell). This will increase the driving range of vehicles.

Moreover, smaller cells using lower cost manufacturing will lower the cost of tomorrow's batteries.

Out-Year Goals. The long-term stretch goal of this project is to enable cells with an energy density of 1 kWh/liter. This will be accomplished by replacing both the present carbon used in Li-ion batteries with anodes that approach double the volumetric capacity of carbon, and the present intercalation cathodes with materials that significantly exceed 200 Ah/kg. By the end of this project, it is anticipated that cells will be available that can exceed the volumetric energy density of today's Li-ion batteries by 50%.

Collaborations. The Advanced Photon Source (Argonne National Laboratory) and when available the National Synchrotron Light Source II (Brookhaven National Laboratory) will be used to determine the phases formed in both *ex-situ* and *operando* electrochemical cells. University of Colorado, Boulder, will provide some of the electrolytes to be used.

Milestones

1. Demonstrate synthesis and complete characterization of CuF_2. (December 2014 – Complete)
2. Determine discharge product of CuF_2. (March 2015 – Complete)
3. Begin cyclability testing of CuF_2. (June 2015 – Complete)
4. Demonstrate more than 100 cycles on Sn_2Fe at 1.5 times the volumetric energy density of carbon. (September 2015 – Complete)
5. *Go/No-Go*: Demonstrate cyclability of CuF_2. Criteria: Capacity of 200 mAh/g over 10 cycles. (September 2015 – Accomplished)

Progress Report

The goal of this project is to synthesize tin-based anodes that have 1.5 times the volumetric capacity of the present carbons, and conversion and intercalation cathodes with capacities over 200 Ah/kg.

The major effort this quarter was to demonstrate the cyclability of Sn_2Fe and CuF_2-based electrodes.

Milestone 4: Demonstrate more than 100 cycles on Sn_2Fe at 1.5 times the volumetric energy density of carbon. This milestone is complete. The extended cyclability of the Sn_2Fe anode composite with carbon is under way, with over 100 cycles achieved. The tap density of this composite was determined to be around 1.8 g/cc, much higher than that of graphitic carbon, which does not exceed 1 g/cc. The calculated actual density of this anode composite is 2.77 g/cc, based on the products in the lithiated electrode. Lithiated carbon, C_6Li, on the same basis is 0.75 g/cc and delivers theoretical capacities of 340 mAh/g and 747 mAh/cc. As Figure 15 shows, the Sn_2Fe electrode has a capacity after 100 cycles of around 500 mAh/g, which translates into a volumetric capacity of 1.38 Ah/cc. This is more than 1.5 times that of graphitic carbon.

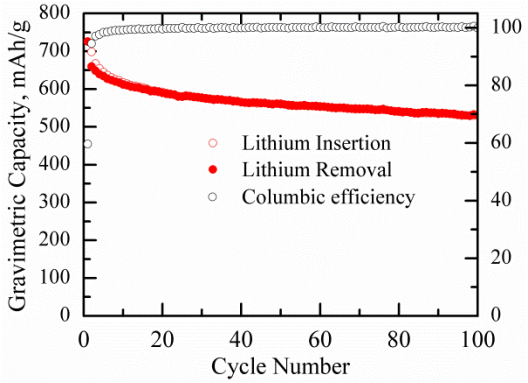

Figure 15. Cycling behavior of a Sn_2Fe composite electrode at 0.2 mA/cm^2. The Sn/C/Ti weight ratio is 1/10/0.25.

Go/No-Go Milestone 5: Demonstrate cyclability of CuF_2; Criteria – Capacity of 200 mAh/g over 10 cycles. A major effort is focused on the solid solution $Cu_{1-y}Fe_yF_2$ composite with carbon. The cycling behavior is showing promising results, as indicated in Figure 16; after 10 cycles, the capacity is 290 mAh/g, exceeding the Go/No-Go target of 200 mAh/g.

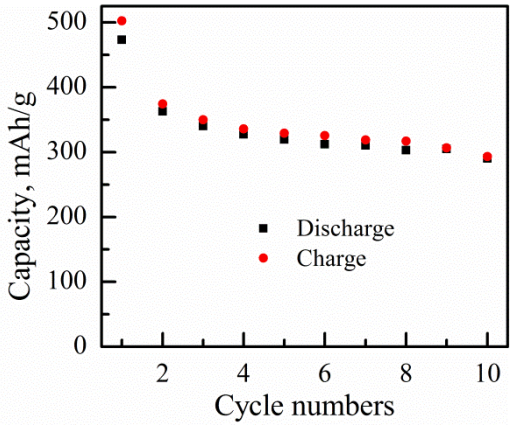

Figure 16. The initial cycling behavior of the solid solution $Cu_{1-y}Fe_yF_2$ cathode, for y = 0.5.

Task 3.3 – Development of High-Energy Cathode Materials (Ji-Guang Zhang and Jie Xiao, Pacific Northwest National Laboratory)

Project Objective. The objective of this project is to develop high-energy, low-cost, cathode materials with long cycle life. Based on the knowledge gathered in FY 2014 on the failure mechanism of Li-Mn-rich (LMR) cathode, synthesis modification will be pursued to improve distribution of different transition metal cations at the atomic level. Leveraging with PNNL's advanced characterization capabilities, the effects from synthesis alteration and the surface treatment will be monitored and correlated to the electrochemical properties of LMR to guide the rational design of LMR. Extension of the cutoff voltage on traditional layered $LiNi_1/3Mn_1/3Co_{1/3}O_2$ (NMC) will be also investigated to increase the usable energy density from NMC while maintaining structural integrity and long lifespan.

Project Impact. Although state-of-the-art cathode materials such as LMR layered composites have very high energy densities, their voltage fade and long-term cycling stability still need to be further improved. In this work, we will investigate the fundamental fading mechanism of LMR cathodes and develop new approaches to reduce the energy loss of these high-energy cathode materials. The success of this work will increase the energy density of Li-ion batteries and accelerate market acceptance of electric vehicles (EV), especially for plug-in hybrid electric vehicles (PHEV) required by the EV Everywhere Grand Challenge proposed by the DOE/EERE.

Out-Year Goals. The long-term goal of the proposed work is to enable Li-ion batteries with a specific energy of > 96 Wh/kg (for PHEVs), 5000 deep-discharge cycles, 15-year calendar life, improved abuse tolerance, and less than 20% capacity fade over a 10-year period.

Collaborations. This project engages with the following collaborators:

- Dr. Bryant Polzin (ANL)- LMR electrode supply
- Dr. X.Q. Yang (BNL) – *in situ* x-ray diffraction (XRD) characterization during cycling
- Dr. Karim Zaghib (Hydro-Quebec) − material synthesis
- Dr. Kang Xu (ARL) − new electrolyte

Milestones

1. Investigate the transition metal migration pathway in LMR during cycling. (12/31/14 – Complete)
2. Identify appropriate synthesis step to enhance the homogenous cation distribution in the lattice and demonstrate 200 stable cycling with less than 10% energy loss. (3/31/15 – Complete)
3. Develop the surface treatment approaches to improve the stability of high-energy cathode at high-voltage conditions. (6/30/2015 – Complete)
4. Demonstrate high-voltage operation of modified NCM with 180 mAh/g capacity and less than 20% capacity fade for 100 cycling. (9/30/2015 – Complete)

Progress Report

This quarter, $LiNi_{1/3}Mn_{1/3}Co_{1/3}O_2$ (NMC) cathode with different areal capacity loading has been systematically investigated at a high charge cutoff voltage of 4.5 V. The NMC electrodes with capacity loading ranging from ~1.5 to ~4.0 mAh cm^{-2} (Figure 17a) delivered similar specific capacity of ca. 185 mAh g^{-1} during the formation cycles at C/10 (Figure 17a). The NMC electrodes showed good cycling stability even with the capacity loading up to ~4.0 mAh cm^{-2}, exhibiting capacity retention higher than 90% after 100 cycles (Figure 17c-d).

During further cycling to 300 cycles, an obvious difference was observed for NMC electrodes with different capacity loadings. The electrode with moderately high capacity loading (~2.0 mAh cm^{-2}) still cycled well and retained ca. 90% of its initial discharge capacity, indicating a decent structural stability of NMC electrode during cycling at charge cutoff 4.5 V. However, further increase of the electrode loading resulted in an accelerated capacity fading, as reflected by the considerably lower capacity retention of 75.8% and 9.8% for electrodes with ~3.0 and ~4.0 mAh cm^{-2} areal capacity after 300 cycles, respectively. Based on the good cycling stability of NMC with low-to-moderate loadings, it is inferred that the fast capacity decay of higher loading electrodes could be ascribed to the poor stability of lithium metal anode.

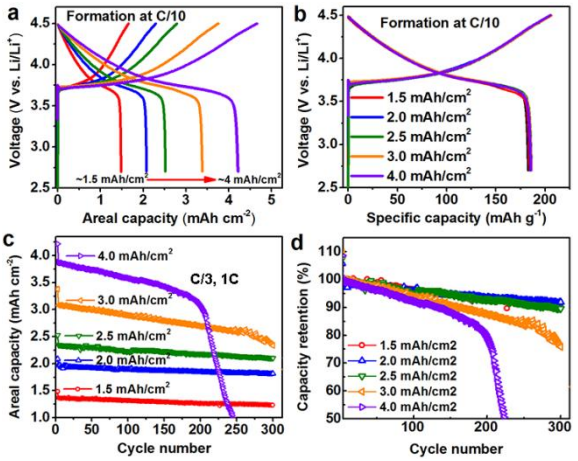

Figure 17. (a) Voltage profiles vs. specific capacity, (b) voltage profiles vs. areal capacity, (c) cycling performance and (d) capacity retention of NMC electrodes with different areal capacity loadings.

After cycling, the lithium metal anodes were retrieved and their morphologies were characterized using scanning electron microscopy (SEM) and compared in Figure 18. With moderate loading (~2.0 mAh cm^{-2}) NMC cathode, the initial structure of lithium metal anode was still well maintained although its surface was covered by a solid-electrolyte interphase (SEI) layer, which protected the bulk lithium from parasitic reactions with the electrolyte (Figure 18a, c). Using ~4.0 mAh cm^{-2} NMC cathode, twice amount of lithium was deposited and stripped in each cycle, which significantly increased the parasitic side reactions between the newly deposited lithium (charge process), the freshly exposed lithium (discharge process), and the electrolyte. The end result was the formation of serious cracks and porous/loose lithium after cycling (Figure 18b, d), leading to rapid increase of cell resistance and eventual cell failure. These findings highlighted that the influences from the degradation of lithium metal anode should be carefully considered during evaluation of the high energy density cathode materials with high electrode loading in lithium half cells.

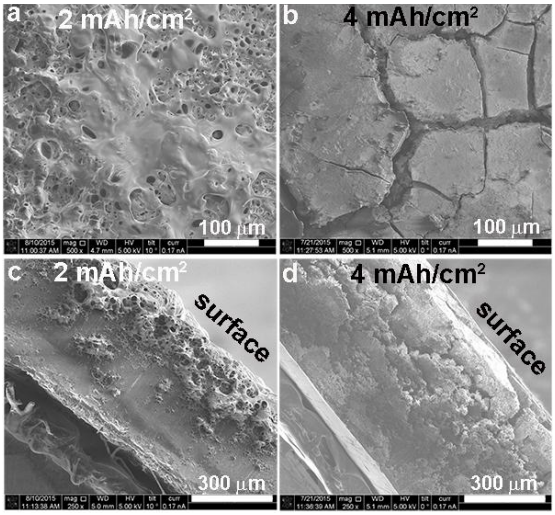

Figure 18. SEM images of Li anodes after 300 cycles in cells using (a, c) 2 mAh cm^{-2} NMC counter electrode and (b, d) 4 mAh cm^{-2} NMC counter electrode in terms of (a, b) surface views and (c, d) cross-section views.

Patents/Publications/Presentations

Publication

- Shi, Wei, and Jianming Zheng, Jie Xiao, Xilin Chen, Bryant J. Polzin, and Ji-Guang Zhang. "The Effect of Entropy and Enthalpy Changes on the Thermal Behavior of Li-Mn-rich Layered Composite Cathode Materials." Submitted to *Advanced Functional Materials*.

Task 3.4 – *In situ* Solvothermal Synthesis of Novel High Capacity Cathodes (Patrick Looney and Feng Wang, Brookhaven National Laboratory)

Project Objective. Develop low-cost cathode materials that offer high energy density (≥660 Wh/kg) and electrochemical properties (cycle life, power density, safety) consistent with USABC goals.

Project Impact. Present-day Li-ion batteries are incapable of meeting the 40-mile, all-electric range within the weight and volume constraints established for plug-in hybrid electric vehicles (PHEVs) by the DOE and USABC. Higher energy density cathodes are needed for Li-ion batteries to be widely commercialized for PHEV applications. This effort will focus on increasing energy density (while maintaining the other performance characteristics of current cathodes) using synthesis methods that have the potential to lower cost. The primary deliverable for this project is a reversible cathode with an energy density of about 660 Wh/kg or higher.

Out-Year Goals. In FY15, we will continue work on *in situ* solvothermal synthesis, structural and electrochemical characterization of V-based (fluoro)phosphates and other high-capacity cathodes. We will also work on technique development for *in situ* synthesis. Out-year goals include:

- Determining the reaction pathway during ion-exchange of $Li(Na)VPO_5F_x$
- Optimizing the ion-exchange procedures to maximize the Li-exchange content in $Li(Na)VPO_5F_x$
- Characterizing the structure of the intermediate and final exchanged products of $Li(Na)VPO_5F_x$ and their electrochemical properties
- Identifying at least one cathode material, with reversible specific capacity higher than 200 mAh/g under moderate cycling conditions
- Developing new *in situ* reactors that may be applied for different types of synthesis methods (beyond solvothermal) in making phase-pure cathodes
- Building new capabilities for simultaneous *in situ* measurements of multiple synthesis reactions in the newly built beamlines at NSLS II

Collaborations. This project engages with the following collaborators: (1) Jianming Bai, Lijun Wu, and Yimei Zhu of BNL; (2) Peter Khalifha of Stony Brook University; (3) Kirsuk Kang of Seoul National University; (4) Nitash Balsara and Wei Tong of LBNL; (5) Jagjit Nanda of ORNL; (6) Arumugam Manthiram of University of Texas at Austin; (6) Brett Lucht of University of Rhode Island; (7) Zaghib Karim of Hydro-Quebec; and (8) Jason Graetz of HRL Laboratories.

Milestones

1. Determine the reaction pathways and phase evolution during hydrothermal ion exchange synthesis of $Li(Na)VPO_5F_x$ cathodes via *in situ* studies. (12/01/14 – Complete)
2. Optimize ion exchange synthesis for preparing $Li(Na)VPO_5F_x$ with maximized Li content, and characterize its structural and electrochemical properties. (3/01/15 – Complete)
3. Develop new reactor design to enable high-throughput synthesis of phase-pure cathode materials. (6/01/15 – Complete)
4. Obtain good cycling stability of one high-capacity cathode in a prototype cell with specific capacity higher than 200 mAh/g. No-Go if 80% capacity retention after 50 cycles cannot be achieved. (9/01/15 – Complete)

Progress Report

In previous quarters, synthesis procedures were developed for preparing different phases of Cu-based vanadium oxides. Among them the α phase (α-$CuVO_3$) is particularly interesting for its unique 3D framework that enables high reversible capacity, 350 mAh/g; among the highest reversible capacity for any Cu-based vanadium oxide. A provisional patent was recently filed for the synthesis and optimization of $CuVO_3$ for potential application as a high-capacity cathode. However, Cu dissolution has been one long-standing issue for Cu-based vanadium oxides when they are cycled in liquid electrolyte and limits their practical application. Working with the Balsara group at LBNL, we tested the cycling stability of α-$CuVO_3$ in the cells constructed with Li-polystyrene-*b*-poly(ethylene oxide) (SEO) polymer. The cells were fabricated and tested by Dr. Didier Revaux. The capacity of α-$CuVO_3$ in the Li-SEO cells was measured to be *above 230 mAh/g at a rate of C/20, with only 2% decay over 50 cycles; an extraordinary cycling stability.* Some of the results are reported this quarter.

Figure 19 shows representative results from cycling tests of α-$CuVO_3$ in Li-SEO cells, in comparison to that in the cells with general liquid electrolyte. Due to the use of SEO electrolyte, α-$CuVO_3$ electrode shows 98% capacity retention in the first 50 cycles at a rate of C/20, followed with a gradual decay, to ~90% of the initial value (237 mAh/g) after 90 cycles. While cycling in liquid electrolyte, α-$CuVO_3$ exhibits a capacity retention of 85% for 20 cycles, and only 50% after 100 cycles (not shown here), largely due to Cu dissolution.

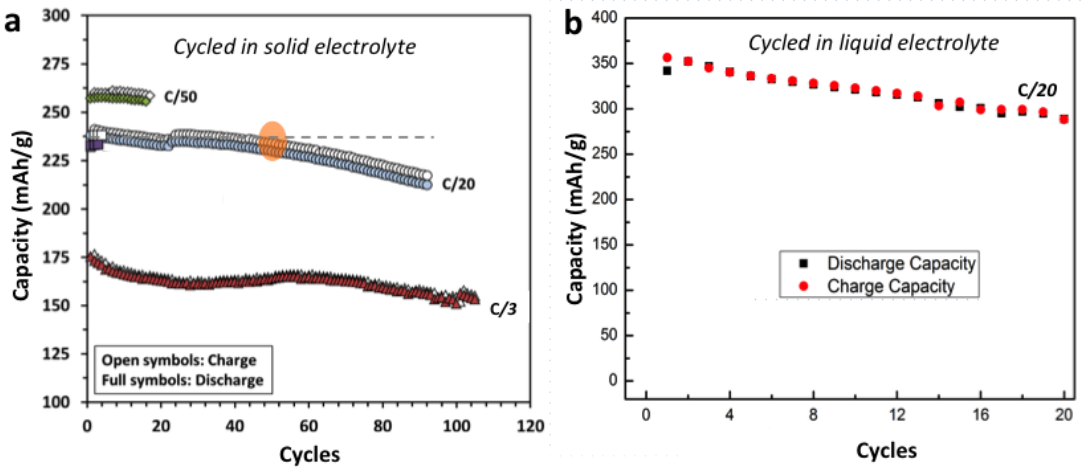

Figure 19. Electrochemical cycling performance of α-$CuVO_3$ in cells constructed with Li-polystyrene-b-poly(ethylene oxide) (SEO) polymer electrolyte (a), in comparison to that in the cells with general liquid (b).

Higher capacity was obtained in α-$CuVO_3$ electrodes at lower rates, up to 248.6 mAh/g at C/50, with almost no decay over 20 cycles (Figure 19a). The cell was also tested at higher rates, such as C/3, giving a capacity 175 mAh/g with high retention (87% over 100 cycles). Overall, excellent cycling stability of α-$CuVO_3$ in Li-SEO cells was observed during the early cycling stage, independently of the C-rate; only after prolonged cycling did capacity fade become obvious. Such an observation is similar to that of $LiFePO_4$ cathodes in a similarly configured Li-SEO cell (as reported by Balsara group; *J. Electrochem. Soc.*, 2015, *162*, A1301); in that study, the capacity fade was attributed to the delamination of the Li/SEO interface. Given the high capacity and extraordinary cycling stability in Li-SEO cells, *α*-$CuVO_3$ may be an appealing cathode for solid-state batteries.

All Milestones for FY 2015 have been completed, and progress for this project has exceeded the expected status (as listed in the out-year goals) for this fiscal year.

Patents/Publications/Presentations

Patent

- **Wang, F.**, and X. Wang, J. Graetz, and P. Khalifah. Nanostructured copper vanadium oxides as high-capacity cathodes for lithium ion batteries; U.S. provisional patent (filed).

Publications

- Kim, S.W., and N. Pereira, N.A. Chernova, F. Omenya, P. Gao, M.S. Whittingham, G.G. Amatucci, D. Su, and **F. Wang**. "Structure Stabilization by Mixed Anions in Oxyfluoride Cathodes for High-Energy Lithium Batteries." *ACS Nano* (pending).
- Wang, L., and J. Bai, P. Gao, X. Wang, J.P. Looney, and **F. Wang**. "Structure Tracking Aided Design and Synthesis of $Li_3V_2(PO_4)_3$ Nanocrystals as High-Power Cathodes for Lithium Ion Batteries." *Chem. Mater*. 27 (2015): 5712.

Presentation

- 228th ECS meeting, Phoenix (October 11-15, 2015): "*In Situ* solvothermal synthesis of High-Energy Cathodes for Lithium-Ion Batteries"; J. Bai, L. Wang, and F. Wang.

Task 3.5 – Novel Cathode Materials and Processing Methods (Michael M. Thackeray and Jason R. Croy, Argonne National Laboratory)

Project Objective. The goal of this project is to develop low-cost, high-energy and high-power Mn-oxide-based cathodes for lithium-ion batteries that will meet the performance requirements of plug-in electric vehicles (PHEV) and electric vehicles (EVs). Improving the design, composition and performance of advanced electrodes with stable architectures and surfaces, facilitated by an atomic-scale understanding of electrochemical and degradation processes, is a key objective of this work.

Project Impact. Standard lithium-ion battery technologies are currently unable to meet the demands of next-generation PHEV and EV vehicles. Battery developers and scientists alike will take advantage of the knowledge generated from this project, both applied and fundamental, to further advance the field. In particular, it is expected that this knowledge will enable progress toward meeting the DOE goals for 40-mile, all-electric range PHEVs.

Approach. Exploit the concept and optimize the performance of structurally integrated "composite" electrode structures with a prime focus on "layered-layered-spinel" materials. Alternative processing routes will be investigated; the Argonne National Laboratory comprehensive characterization facilities will be used to explore novel surface and bulk structures by both *in situ* and *ex-situ* techniques in the pursuit of advancing the properties of state-of-the-art cathode materials. A theoretical component will complement the experimental work of this project.

Out-Year Goals. The project out-year goals include the following:

- Identify high-capacity ('layered-layered' and 'layered-spinel') composite electrode structures and compositions that are stable to electrochemical cycling at high potentials (~4.5 V).
- Identify and characterize surface chemistries and architectures that allow fast Li-ion transport and mitigate or eliminate transition-metal dissolution.
- Use complementary theoretical approaches to further the understanding of electrode structures and electrochemical processes to accelerate progress of materials development.
- Scale-up, evaluate, and verify promising cathode materials using Argonne National Laboratory scale-up and cell fabrication facilities.

Collaborators. This project has engaged with the following collaborators: Joong Sun Park, Bryan Yonemoto, Roy Benedek (CSE), Mali Balasubramanian (APS), YoungHo Shin, and Gregory Krumdick (ES).

Milestones

1. Optimize the capacity and cycling stability of composite cathode structures with a low (~10%) Li_2MnO_3 content. Target capacity = 190-200 mAh/g (baseline electrode). (September 2015 – Complete)
2. Scale up the most promising materials to 1 kg batch size at the Argonne Materials Engineering Research Facility (MERF). (April 2015 – Complete)
3. Synthesize and characterize unique surface architectures that enable >200 mAh/g at a >1C rate with complementary theoretical studies of surface structures. (September 2015 – Complete)
4. Optimize capacity and cycling stability of composite cathode structures with a medium (~20%) Li_2MnO_3 content. Target capacity = 200-220 mAh/g (advanced electrode). (September 2015 – In Progress)

Progress Report

As part of the objective to scale up promising materials to a 1 kg batch size at Argonne's Materials Engineering Research Facility (MERF), lithium- and manganese-rich "layered-layered-spinel" (LLS) composite electrode structures containing a small amount of spinel (6% – 15%) were synthesized and evaluated. A targeted spinel content in the LLS structure was calculated by reducing the lithium content by an appropriate amount in the "layered-layered" (LL) $0.25Li_2MnO_3 \bullet 0.75LiMn_{0.375}Ni_{0.375}Co_{0.25}O_2$ composition (as described in: Long, B.R., and J.R. Croy, J.S. Park, J. Wen, D.J. Miller, and M.M. Thackeray, *J. Electrochem. Soc.* 161, no. 14 (2014): A2160-A2167.) Pre-pilot scales of carbonate and hydroxide precursors were synthesized by co-precipitation methods, and thereafter reacted with either Li_2CO_3 or LiOH, respectively, at 900°C. The secondary particles of the resulting LLS electrode powder were approximately 10 µm in diameter; the tap density was 1.8 g/cc. When cycled in lithium half cells between 4.6 and 2.5 V at 15 mA/g, discharge capacities of 205-210 mAh/g were obtained (Figure 20a).

A representative d*Q*/d*V* plot of the electrochemical profile of the cell at the 15th cycle (black line) is shown in Figure 20b. This 'baseline' LLS cell showed stable and symmetric redox behavior at ~3.7 V during charge and discharge, with little voltage fade that is typical of pristine "layered-layered" electrodes when continuously charged to 4.6 V. The increased cycling stability is attributed to a more stable oxygen array (little oxygen loss) and the suppression of transition metal migration when cells are charged to 4.45 V.

To suppress the surface reactivity between charged LLS electrodes and the electrolyte at high charging potentials, which lowers the rate of lithium diffusion at the electrode/electrolyte interface and increases cell impedance, protective coatings were applied to the surface of the electrode particles. Three different coatings were applied: (1) 'AlW_xF_y'(by ALD), (2) Li_3PO_4, and (3) Ni-substituted $Li_{2.9}Ni_{0.05}PO_4$, as described in earlier BMR/BATT reports. All three coatings resulted in superior electrode capacity relative to the baseline LLS electrode and similar charge discharge/charge behavior, as shown in the capacity vs. cycle number plots (Figure 20a) and dQ/dV plots (Figure 20b) of coated electrodes, respectively. Furthermore, a significant improvement in rate performance was delivered by the Li_3PO_4- and Ni-substituted $Li_{2.9}Ni_{0.05}PO_4$ coated electrodes relative to the baseline electrode, particularly for current rates of 300 mA/g and higher, with a capacity of 120 mAh/g being delivered by both phosphate-coated electrodes at a current rate of 1.5 A/g (~7C) (Figure 20c). Full (Li-ion) cells containing LLS electrodes with aliovalent-doped Li_3PO_4 coatings (defect structures) are being evaluated with a view to increasing the rate capability and reducing transition metal dissolution of the electrodes.

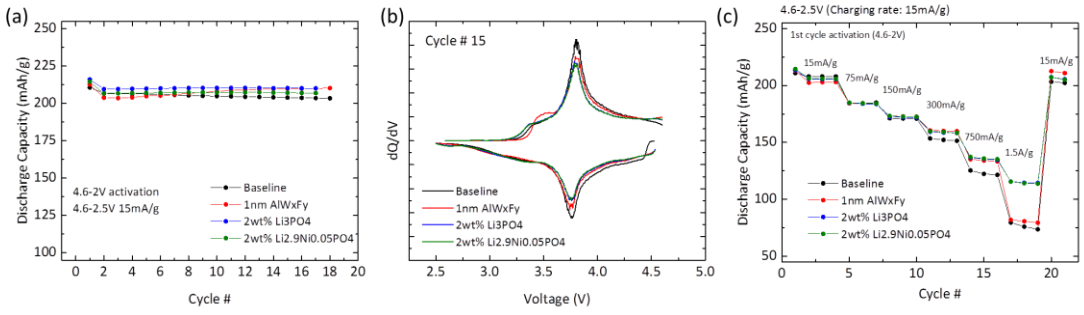

Figure 20. Electrochemical properties of baseline and coated $0.25Li_2MnO_3 \bullet 0.75LiMn_{0.375}Ni_{0.375}Co_{0.25}O_2$ electrodes with 6% target spinel: (a) Discharge capacity vs. cycle number (4.6-2.5V, 15mA/g), (b) d*Q*/d*V* plots, and (c) Discharge capacities at different current rates (15, 75, 150, 300, 1500mA/g, 4.6-2.5V) after first cycle activation at 4.6-2V (trickle charge 30 min).

Patents/Publications/Presentations

Publications

- Thackeray, M.M., and J.R. Croy, E. Lee, J.S. Park, B.R. Long, O. Kahvecioglu Feridun, Y. Shin, G.K. Krumdick, J.G. Wen, D.J. Miller, J. Wu, Q. Li, and V. Dravid. "Addressing the Instability of High Capacity Lithium Battery Cathodes." ECS Conference on Electrochemical Energy Conversion and Storage with SOFC-XIV, Glasgow, Scotland (July 27-30, 2015 – Invited).
- Croy, J.R., and K.G. Gallagher, M. Balasubramanian, J.S. Park, B.R. Long, and M.M. Thackeray. "High Energy Lithium-Ion Research and Development at Argonne National Laboratory." International Academy of Electrochemical Energy Science and Technology, Vancouver, Canada, (August 16-22, 2015 – Invited).

Presentation

- Analytical Chemistry Seminar Series, University of Illinois at Urbana-Champaign (September 4, 2015 – Invited): "Energy Storage: Challenges and Opportunities in an Evolving Lithium Economy"; M.M. Thackeray.

Task 3.6 – High-capacity, High-voltage Cathode Materials for Lithium-ion Batteries (Arumugam Manthiram, University of Texas, Austin)

Project Objective. A significant increase in capacity and/or operating voltage is needed to make the lithium-ion technology viable for vehicle applications. This project addresses this issue by focusing on the design and development of cathode materials based on polyanions that have the possibility for reversibly inserting/extracting more than one lithium ion per transition-metal ion and/or operating above 4.3 V. Specifically, high-capacity and/or high-voltage lithium transition-metal phosphate, silicate, and carbonophosphate cathodes are investigated. The major issue with the phosphate and silicate cathodes is the poor electronic and ionic transport, which limits the practical capacity, energy density, and power density. To overcome these difficulties, novel microwave-assisted solvothermal, microwave-assisted hydrothermal, and template-assisted synthesis approaches are pursued to realize controlled morphology with smaller particle size and to integrate conductive additives like graphene in a single synthesis step.

Project Impact. The critical requirements for the widespread adoption of lithium-ion batteries for vehicle applications are high energy, high power, long cycle life, low cost, and acceptable safety. The currently available cathode materials do not adequately fulfill these requirements. The polyanion cathodes with the novel synthesis approaches pursued in this project have the potential to significantly increase the energy and power. More importantly, the covalently bonded polyanion groups can offer excellent thermal stability and enhanced safety. The microwave-assisted synthesis approaches pursued also lower the manufacturing cost of the cathodes through a significant reduction in reaction time and temperature.

Out-Year Goals. The overall goal is to enhance the electrochemical performances of high- capacity, high-voltage polyanion cathode systems and to develop a fundamental understanding of their structure-composition-performance relationships. Specifically, the project is focused on enhancing the electrochemical performance of systems such as $LiMPO_4$, $Li_2MP_2O_7$, $LiYMSiO_4$, $Li_3V_2(PO_4)_3$, $Li_9V_3(P_2O_7)_3(PO_4)_2$, $Li_3M(CO_3)(PO_4)$, and their solid solutions with M = Mn, Fe, Co, Ni, and VO. Advanced structural, chemical, surface, and electrochemical characterizations of the materials synthesized by novel approaches are anticipated to provide in-depth understanding of the factors that control the electrochemical properties of the polyanion cathodes. For example, the possible segregation of certain cations to the surface in solid solution cathodes consisting of multiple transition-metal ions as well as the role of conductive graphene integrated into the polyanion cathodes can help design better-performing cathodes.

Milestones

1. Demonstrate the synthesis of $LiVOPO_4$ nanoparticles with > 200 mAh/g capacity by employing ordered macroporous carbon as a hard-template. (December 2014 – Complete)
2. Demonstrate aliovalent doping with Ti^{4+} in $LiM_{1-2x}Ti_x\square_xPO_4$ with enhanced electrochemical properties by the microwave-assisted solvothermal synthesis. (March 2015 –Complete)
3. Demonstrate the synthesis of α- and/or β-$LiVOPO_4$/graphene nanocomposites with > 200 mAh/g capacity by the microwave-assisted process. (June 2015 – Complete)
4. *Go/No-Go*: Demonstrate the extraction of more than one lithium (> 110 mAh/g) through aliovalent doping in $Li_2M_{1-3/2x}V_x\square_{x/2}P_2O_7$ by low-temperature synthesis approaches. (September 2015 – Complete)

Progress Report

Our previous work on aliovalent vanadium substitution in $LiMPO_4$ (M = Co,Mn) demonstrated enhanced electrochemical performance due to increased electronic and ionic transport. This quarter, we attempted to extend this strategy to aliovalently dope $Li_2FeP_2O_7$ with low-temperature synthesis methods. $Li_2FeP_2O_7$ was successfully synthesized with a known solid-state method that required calcination at 600°C. Attempts at substituting vanadium for iron with various vanadium precursors, including vanadium pentoxide and vanadium(III) acetylacetonate, resulted in the formation of an $LiVP_2O_7$ impurity, as shown by the x-ray diffraction (XRD) data in Figure 21. Therefore, alternate lower-temperature methods to synthesize $Li_2FeP_2O_7$ were investigated. Microwave-assisted solvothermal (MW-ST) methods using PO_4^{-3} precursors all failed to form $P_2O_7^{-4}$, indicating that the formation of $P_2O_7^{-4}$ is not possible by the MW-ST method at low temperatures (< 300 °C). The MW-ST method with pyrophosphoric acid and anhydrous precursors resulted in $Li_4P_2O_7$ rather than $Li_xFeP_2O_7$. Therefore, a two-step method was devised where $NH_4Fe(HPO_4)_2$ was produced via a microwave-assisted hydrothermal (MW-HT) method at 180°C and subsequently calcined with 1 equivalent of LiOH to form $LiFeP_2O_7$, shown in Figure 21. Unfortunately, attempts at producing $Li_2FeP_2O_7$ by calcination with 2 equivalents of LiOH resulted in $LiFePO_4$ and Li_3PO_4 impurities. $LiFeP_2O_7$ was further investigated because it has been shown to form $Li_2FeP_2O_7$ via electrochemical lithiation, and the low- temperature synthesis route could enable investigation of effects of vanadium substitution.

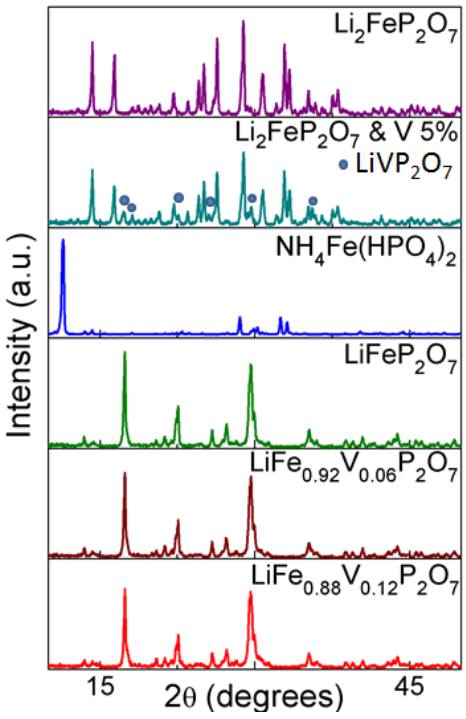

Figure 21. XRD patterns of the samples prepared to substitute vanadium in pyrophosphate.

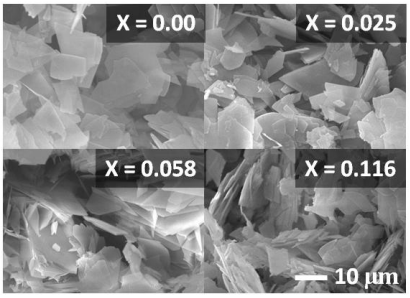

Figure 22. Scanning electron micrographs of $LiFe_{1-x}V_xP_2O_7$ with x = 0.00, 0.025, 0.058, 0.116.

Several samples of $NH_4Fe_{1-x}V_xP_2O_7$ were produced with x = 0.00, 0.025, 0.058, 0.116, as verified by inductively coupled plasma – optical emission spectroscopy (ICP-OES), and subsequently calcined with LiOH to form $LiFe_{1-x}V_xP_2O_7$, as shown by the XRD data in Figure 22. This novel two-step method produced $LiFeP_2O_7$ at ~ 450°C, which is lower than that in previously reported methods. Unfortunately, the substitution of vanadium could not be conclusively determined by the XRD patterns owing to both $LiFeP_2O_7$ and $LiVP_2O_7$ being isostructural and having nearly identical unit cell parameters. The produced particles have thin plate morphology with planar dimensions greater than 10 μm. Initial electrochemical characterization was carried out with ethylene carbonate/dimethyl carbonate electrolyte and a lithium anode. The cathodes were made from a 70: 20: 10 composite of $LiFe_{1-x}V_xP_2O_7$, carbon black, and polytetrafluoroethylene. The iron-only sample delivered a first cycle discharge capacity of 32 mAh/g when cycled at C/20, while the x = 0.11 sample delivered 42 mAh/g and had much lower polarization. The target of demonstrating capacity > 110 mAh/g was not achieved. Further optimization of the cathode construction and ball milling of the active material could lead to better electrochemical performance.

Patents/Publications/Presentations

Publications

- Kreder III, K.J., and G. Assat, and A. Manthiram. "Microwave-assisted Solvothermal Synthesis of Three Polymorphs of $LiCoPO_4$ and Their Electrochemical Properties." *Chemistry of Materials* 27 (2015): 5543-5549.
- He, G., and C.A. Bridges, and A. Manthiram. "Crystal Chemistry of Electrochemically and Chemically Lithiated Layered α_I-$LiVOPO_4$." *Chemistry of Materials* (2015). DOI: 10.1021/acs.chemmater.5b02609.
- Assat, G., and A. Manthiram. "Rapid Microwave-assisted Solvothermal Synthesis of Non-olivine Cmcm Polymorphs of $LiMPO_4$ (M = Mn, Fe, Co, and Ni) at Low Temperature and Pressure." Ch*emistry of Materials* (2015). DOI: 10.1021/acs.inorgchem.5b01787.
- Knight, J.C., and A. Manthiram. "Effect of Nickel Oxidation State on the Structural and Electrochemical Characteristics of Lithium-rich Layered Oxide Cathodes." *Journal of Materials Chemistry A* (2015). DOI: 10.1039/C5TA05703E.

Presentations

- Hanyang University, Seoul, South Korea (May 19, 2015 – Invited): "High Energy Density Rechargeable Batteries"; A. Manthiram.
- Institute of Chemistry, Beijing, China (June 1, 2015 – Invited): "Next Generation Rechargeable Battery Chemistries"; A. Manthiram.

Task 3.7 – Lithium-bearing Mixed Polyanion (LBMP) Glasses as Cathode Materials (Jim Kiggans and Andrew Kercher, Oak Ridge National Laboratory)

Project Objective. Develop mixed polyanion (MP) glasses as potential cathode materials for lithium ion batteries with superior performance to lithium iron phosphate for use in electric vehicle applications. Modify MP glass compositions to provide higher electrical conductivities, specific capacities, and specific energies than similar crystalline polyanionic materials. Test MP glasses in coin cells for electrochemical performance and cyclability. The final goal is to develop MP glass compositions for cathodes with specific energies up to near 1,000 Wh/kg.

Project Impact. The projected performance of MP glass cathode materials addresses the Vehicle Technologies Office (VTO) Multi-Year Plan goals of higher energy densities, excellent cycle life, and low cost. MP glasses offer the potential of exceptional cathode energy density up to 1,000 Wh/kg, excellent cycle life from a rigid polyanionic framework, and low-cost, conventional glass processing.

Out-Year Goals. MP glass development will focus on compositions with expected multi-valent intercalation reactions within a desirable voltage window and/or expected high-energy glass-state conversion reactions.

Polyanion substitution will be further adjusted to improve glass properties to potentially enable multi-valent intercalation reactions and to improve the discharge voltage and cyclability of glass-state conversion reactions. Cathode processing of the most promising mixed polyanion glasses will be refined to obtain desired cycling and rate performance. These optimized glasses will be disseminated to BMR collaborators for further electrochemical testing and validation.

Collaborations. No collaborations this quarter.

Milestones

1. Perform electron microscopy on mixed polyanion glass cathodes at key states of charge. (December 2014 – Completed 12/04/14)
2. Produce and electrochemically test MP glasses designed to have enhanced ionic diffusivity. (March 2015 – Completed 3/31/15)
3. Produce and electrochemically test an MP glass designed to have enhanced ionic diffusivity and theoretically capable of a multi-valent intercalation reaction. (June 2015 – Completed 6/30/15)
4. Determine the polyanion substitution effect on a series of non-phosphate glasses. (September 2015 – Completed 9/30/15)

Progress Report

Tailoring the polyanion content of lithium copper phosphate glasses has demonstrated strong effects on their electrochemical behavior (Figure 23). In a phosphate glass, vanadate improves electrical conductivity while borate increases the free volume. Vanadate-substituted (50%) lithium copper metaphosphate glass ($LiCu(PV)_3$) had a high capacity conversion reaction with a large voltage hysteresis and a large first cycle irreversible loss. Increasing the lithium and polyanion content had negligible effect on the electrochemical performance ($Li_2Cu(PV)_4$). However, the additional substitution of 10% borate [$LiCu(PBV)_3$ and $Li_2Cu(PBV)_4$] promoted nearly complete first-cycle reversibility, a reduction in voltage hysteresis, and limited intercalation capacity. Ongoing studies seek to utilize combined vanadate/borate substitution to improve electrochemical performance in other glass systems.

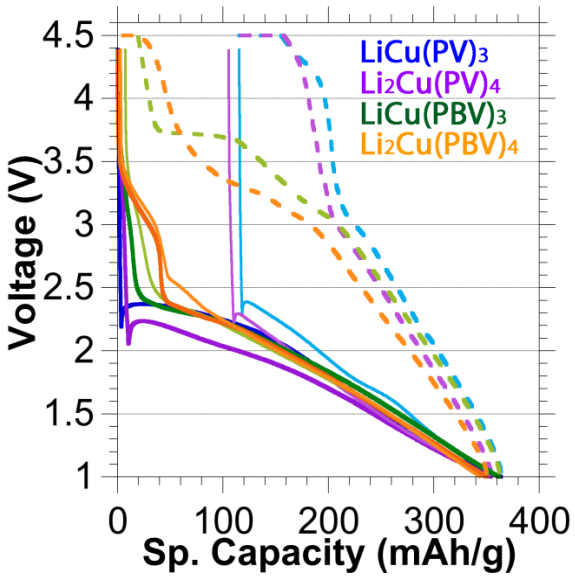

Figure 23: Combined vanadate/borate substitution improved the electrochemical performance of lithium copper metaphosphate glass.

Research has focused on polyanion substitution of phosphate glasses, but polyanion substitution may have different effects on the electrochemical performance of non-phosphate glasses. Initial work has been performed on borate glasses. Lithium copper borate glass cathodes demonstrated a high-capacity conversion reaction that cycled poorly, similar to copper metaphosphate and copper borophosphate glass cathodes. Manganese-bearing glasses theoretically can undergo Mn^{3+}-Mn^{2+} or even Mn^{4+}-Mn^{2+} intercalation reactions in a useful voltage window (< 4.8 V) and might be expected to undergo a Mn^{3+}-Mn^{0+} conversion reaction. Previously, lithium manganese phosphate glasses with vanadate substitution have demonstrated no significant electrochemical activity of the Mn cation. Similarly, lithium manganese borate glasses with 0%, 15%, and 30% vanadate substitution showed negligible capacity. Further research will determine whether polyanion substitution can enable high-capacity electrochemical reactions in other theoretically promising borate glasses.

Task 3.8 – Design of High Performance, High Energy Cathode Materials (Marca Doeff, Lawrence Berkeley National Laboratory)

Project Objective. The objective of the project is to develop high-energy, high-performance cathode materials including composites and coated powders, using spray pyrolysis and other synthesis techniques. The emphasis is on high-voltage systems including NMCs designed for higher voltage operation. Experiments are directed toward optimizing the synthesis, improving cycle life, and understanding the behavior of NMCs subjected to high-voltage cycling. Particle size and morphology are controlled during spray pyrolysis synthesis by varying residence time, temperature, precursors and other synthetic parameters. By exploiting differences in precursor reactivity, coated materials can be produced, and composites can be prepared by post-processing techniques such as infiltration. These approaches are expected to improve cycling due to reduced side reactions with electrolytes.

Project Impact. To increase the energy density of Li ion batteries, cathode materials with higher voltages and/or higher capacities are required, but safety and cycle life cannot be compromised. In the short term, the most promising materials are based on NMCs modified to undergo high-voltage cycling that do not require formation cycles or undergo structural transformations during cycling. Spray pyrolysis synthesis results in high quality materials that can be coated (solid particles) or used as the basis for composites (hollow particles) designed to withstand high-voltage cycling.

Out-Year Goals. The objective is to design high-capacity NMC cathodes that can withstand high-voltage cycling without bulk structural transformation. Materials will be synthesized by a simple, low-cost spray pyrolysis method, which has potential for commercialization. This technique produces phase-pure, unagglomerated powders and allows for excellent control over particle morphologies, sizes, and distributions. Coated materials will also be produced in either one or two simple steps by exploiting differing precursor reactivities during the spray pyrolysis procedure, or by first preparing hollow spheres of an electroactive material, infiltrating the spheres with precursors of a second phase (for example, high voltage spinel), and subsequent thermal treatment. The final result is expected to be a high energy density cathode material with good safety and cycling characteristics suitable for use in vehicular applications, which can be made by a low-cost process that is easily scalable.

Collaborations. Transmission x-ray microscopy (TXM) has been used this quarter to characterize NMC materials, with work done in collaboration with Yijin Liu (Stanford Synchrotron Radiation Lightsource – SSRL). Synchrotron and computational efforts continued in collaboration with Professor M. Asta (UCB); Dr. Dennis Nordlund, Dr. Yijin Liu, Dr. Tsu-Chien Weng, and Dr. Dimosthenis Sokaras (SSRL). Atomic layer deposition was performed in collaboration with Dr. Chunmei Ban (NREL). The transmission electron microscopy (TEM) effort continued in collaboration with Dr. Huolin Xin (BNL). We are also collaborating with Professor Shirley Meng (UCSD), Dr. Chunmei Ban (NREL), and Dr. Wei Tong (LBNL) on soft x-ray absorption spectroscopy (XAS) and x-ray Raman characterization of materials.

Milestones

1. Complete synchrotron x-ray Raman experiments on representative NMC samples. (12/31/14 – Experiments and analysis completed; Paper in preparation)
2. Finish survey of composites made with spray pyrolyzed NMC hollow particles. (3/31/15 – Postponed due to equipment and space issues)
3. *Go/no go decision*: Feasibility of coating processes using spray pyrolysis methods or molecular layer deposition. (6/30/15 – On Track)
4. Select best-performing coated or composite material based on capacities and high-voltage cycling results. (9/30/15 – High Ni-content NMCs Selected)

Progress Report

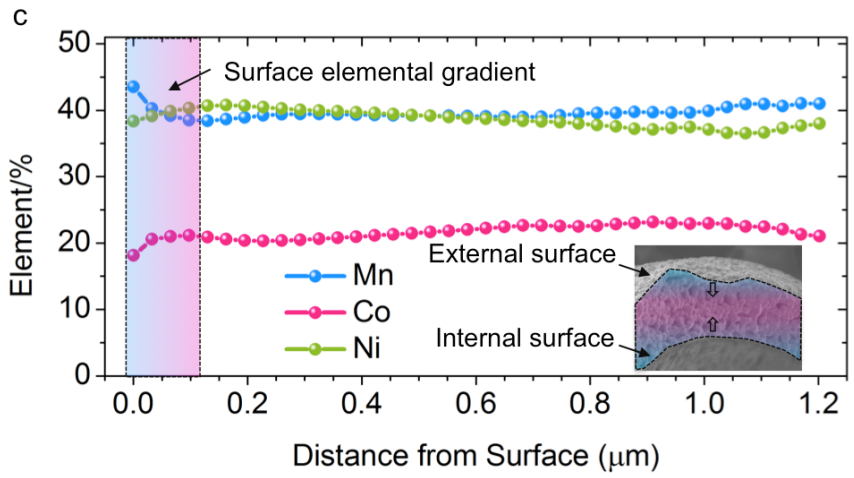

Figure 24. Concentrations of elements in a spray pyrolyzed sample of NMC-442 as a function as depth from the surface, determined by a transmission x-ray microscopy experiment at the Stanford Synchrotron Radiation Lightsource.

Analysis of data from full-field TXM to elucidate the elemental distribution in a spray pyrolyzed NMC-442 powder as a function of distance from the surface was carried out on data obtained last quarter (Figure 24). This showed that the sample is Ni-poor on the surface compared to the bulk, on the secondary particle size level. Scanning transmission electron microscopy/electron energy loss spectroscopy (STEM/EELS) experiments show a similar deficiency of Ni on the surfaces of the nanometric primary particles that make up the secondary particles. In contrast, samples made by traditional co-precipitation processes show no evidence of a compositional gradient, as determined by TXM experiments. The lower concentration of Ni on the surfaces of the co-precipitated NMC-442 particles is thought to be responsible for the reduced degree of surface reconstruction observed in cycled samples, compared to the co-precipitated materials cycled under the same regime. This, in turn, is believed to be the source of the improved high-voltage cycling seen in the spray-pyrolyzed NMC-442 materials compared to the conventionally prepared compounds. These results have been summarized in a paper that will be published in the journal *Nature Energy*; this is the first paper to have been accepted by this new journal.

This is the final quarter for this project. A new project directed towards applying insights obtained on our study of NMC materials with matched Ni and Mn contents will be directed toward materials with higher Ni contents. To this end, NMC-523 and -622 samples have been made by spray pyrolysis and co-precipitation and are being tested.

Patents/Publications/Presentations

Publications

- Rettenwander, D., and A. Welzl, L. Cheng, J. Fleig, M. Musso, E. Suard, M.M. Doeff, G.J. Redhammer, and G. Amthauer. "Synthesis, Crystal Chemistry, and Electrochemical Properties of $Li_{7-2x}La_3Zr_{2-x}Mo_xO_{12}$ (x=0.1-0.4): Stabilization of the Cubic Garnet Polymorph via Substitution of Zr^{4+} by Mo^{6+}." *Inorg. Chem*. (2015). DOI:10.1021/acs.inorgchem.5b01895
- Hou, H., and L. Cheng, T. Richardson, G. Chen, M. Doeff, R. Zheng, R. Russo, and V. Zorba. "Three-Dimensional Elemental Imaging of Li-ion Solid-State Electrolytes Using fs-Laser Induced Breakdown Spectroscopy (LIBS)." *J. Anal. Atomic Spectroscopy* 30 (2015): 2295.
- Wolff-Goodrich, S., and F. Lin, I. Markus, D. Nordlund, H. Xin, M. Asta, and M.M. Doeff. "Tailoring the Surface Properties of $LiNi_{0.4}Mn_{0.4}Co_{0.2}O_2$ by Titanium Substitution for Improved High Voltage Cycling Performance." *Phys. Chem. Chem. Phys*. 17 (2015): 21778.
- He, K., and F. Lin, Y. Zhu, X. Yu, J. Li, R. Lin, D. Nordlund, T.-C. Weng, R. Ryan, X.-Q. Yang, M. Doeff, E. Stach, Y. Mo, H. Xin, and D. Su. "Sodiation Kinetics of Metal Oxide Conversion Electrodes: A Comparative Study with Lithiation." *Nano Lett*. (2015): DOI: 10.1021/ acs.nanolett.5b01709.
- Cheng, Lei, and Hao Wu, Angelique Jarry, Wei Chen, Yifan Ye, Junfa Zhu, Robert Kostecki, Kristin Persson, Jinghua Guo, Miquel Salmeron, Guoying Chen, and Marca Doeff. "Interrelationships among Grain Size, Surface Composition, Air Stability, and Interfacial Resistance of Al-substituted $Li_7La_3Zr_2O_{12}$ Solid Electrolytes." *ACS Applied Mater. & Interfaces* 7 (2015): 17649.
- He, Kai, and Huolin L. Xin, Kejie Zhao, Xiqian Yu, Dennis Nordlund, Tsu-Chien Weng, Jing Li, Yi Jiang, Christopher A. Cadigan, Ryan M. Richards, Marca M. Doeff, Xiao-Qing Yang, Eric A. Stach, Ju Li, Feng Lin, and Dong Su. "Transitions from Near-Surface to Interior Redox upon Lithiation in Conversion Electrode Materials." *Nano Lett.* 15 , 1437 (2015).
- Iturrondobeitia, Amaia, and Aintzane Goñi, Izaskun Gil De Muro, Luis Lezama, Chunjoong Kim, Marca Doeff, Jordi Cabana, and Teofilo Rojo. "High Voltage Cathode Materials for Lithium Ion Batteries: Freeze-dried $LiMn_{0.8}Fe_{0.1}M_{0.1}PO_4$/C (M=Fe, Co, Ni, Cu) Nanocomposites." *Inorg. Chem.* 54 (2015): 2671.

Task 3.9 – Lithium Batteries with Higher Capacity and Voltage (John B. Goodenough, UT – Austin)

Project Objective. The objectives of this project are to increase cell energy density for a given cathode and to allow low-cost rechargeable batteries with cathodes other than insertion compounds.

Project Impact. A solid Na^+ or Li^+-electrolyte separator would permit use of a Li^0 anode, thus maximizing energy density for a given cathode, and liquid flow-through and air cathodes of high capacity as well as high-voltage solid cathodes given two liquid electrolytes having different windows.

Out-Year Goals. The out-year goals are to increase cell energy density for a given cathode and to allow low-cost, high-capacity rechargeable batteries with cathodes other than insertion compounds.

Collaborations. This project collaborates with A. Manthiram at UT Austin and with Karim Zaghib at Hydro-Quebec.

Milestones

1. Fabricate oxide/polymer composite membrane as a separator in an alkali-ion (Li+, Na+) battery and optimization of pore size, oxide loading, and thickness for blocking anode dendrites with fast alkali- ion transport. (3/31/15 –Complete)
2. Investigate membranes that can block a customized soluble redox couple in a flow-through cathode. (6/30/15 – Complete)
3. Evaluate Li-ion and Na-ion cells with a metallic Li or Na anode, oxide/polymer membrane as separator, and a flow-through liquid cathode. (9/30/15 – Complete).
4. Measure performance of cells with a metallic Li or Na anode, oxide/polymer composite membrane as separator, and an insertion compound as cathode. (12/31/15 – Complete)

Progress Report

Development of a discharged cell with a bare current collector anode can further increase energy density of a cell. Alkali metal deposition on a metallic current collector was characterized with $NaCrO_2$ cathode and a stainless-steel current collector as anode. To enhance the mechanical integrity and electrical contact between the deposited alkali metal and current collector, stainless steel was coated with various Li+-conducting polymers: PETT-FC, PETT-EO, PETT-Sulfone, and PETT-Ester where PETT is a tetrathiol crosslinker, and structures of FC, EO, Sulfone, and Ester can be found in Figure 25. For coin cell tests, 1M $NaClO_4$ in EC/DEC (1/1) was used as electrolyte.

Galvanostatic charge/discharge cycling data are shown in Figure 25. The electrochemical performance is disappointing, but several important points were identified in this study. First, with the presence of a liquid electrolyte, there is a voltage plateau at ~2 V vs. Na/Na+ in all the cells, which corresponds to the formation of the solid-electrolyte interphase (SEI) layer. The extent of the plateau directly affects initial Coulombic efficiency: for example, PETT-EO and PETT-Sulfone have less SEI formation and higher Coulombic efficiencies (> 50%) while PETT-FC and PETT-Ester have more pronounced plateaus and lower efficiencies (< 40%). Second, cycle performance is poor regardless of the different polymers. The liquid electrolyte reacts with fresh sodium dendrites in each cycle, which robs reversible working ions indefinitely. The formation of Na dendrites with a liquid electrolyte is prone to rob working ions irreversibly. Therefore, to use a liquid electrolyte, the current collector should have a surface layer that can promote wetting of the current-collector surface by an electrodeposited alkali metal. However, unfortunately it cannot guarantee stable long-term cycle life if the dendrite problems are still present. An alternative method is to use a dry solid electrolyte membrane that can eliminate SEI layer formation and block dendrite penetration.

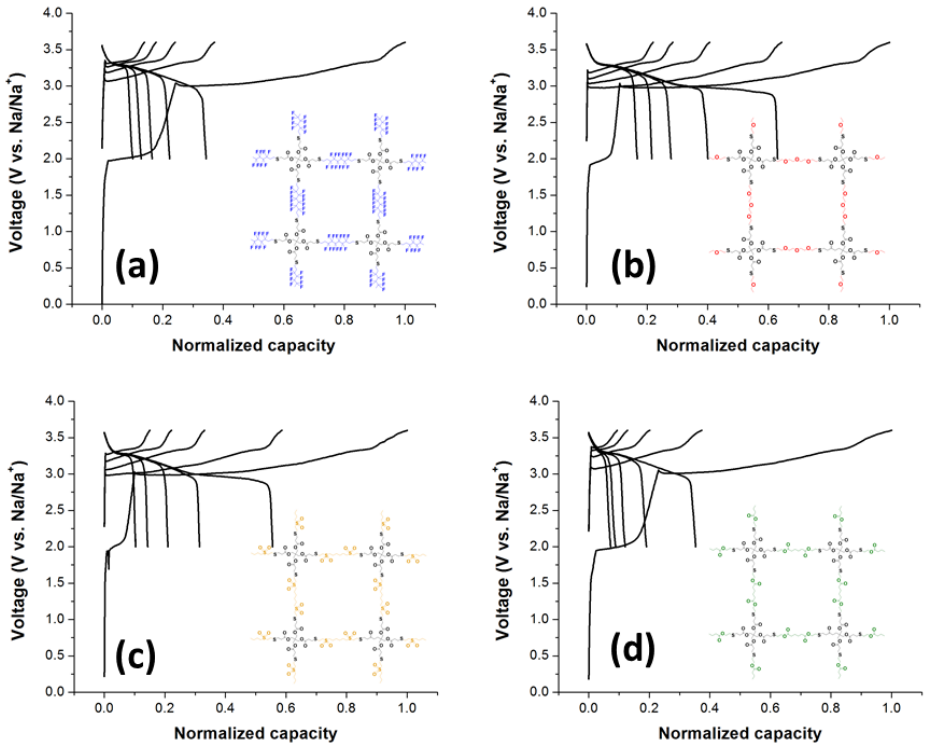

Figure 25. Initial five charge/discharge voltage curves of $NaCrO_2$ with bare stainless steel anode current collector coated with various polymers. (a) PETT-FC, (b) PETT-EO, (c) PETT-Sulfone, and (d) PETT-Ester.

Patents/Publications/Presentations

Publication

- Park, K., and J.H. Cho, J.H. Jang, B.C. Yu, A.T. De La Hoz, K.M. Miller, C.J. Ellison, and J.B. Goodenough. "Trapping Lithium Polysulfides by Forming Lithium Bonds in Polymer Electrolytes for a Li-S Battery." *Energy Environ. Sci.* 8 (2015): 2389-2395.

Task 3.10 – Exploiting Co and Ni Spinels in Structurally Integrated Composite Electrodes (Michael M. Thackeray and Jason R. Croy, Argonne National Laboratory)

Project Objective. This is a new project, the goal of which is to stabilize high capacity, composite 'layered-layered' electrode structures with lithium-cobalt-oxide and lithium-nickel-oxide spinel components (referred to as LCO-S and LNO-S, respectively), or solid solutions thereof (LCNO-S), which can accommodate lithium at approximately 3.5 V vs. metallic lithium. This approach and the motivation to use LCO-S and LNO-S spinel components, about which relatively little is known, is novel.

Project Impact. State-of-the-art lithium-ion batteries are currently unable to satisfy the performance goals for plug-in hybrid electric vehicles (PHEV) and electric vehicles (EV). If successful, this project will impact the advance of energy storage for electrified transportation as well as other applications, such as portable electronic devices and the electrical grid.

Approach. Focus on the design and synthesis of new spinel compositions and structures that operate above 3 V and below 4 V and to determine their structural and electrochemical properties through advanced characterization. This information will subsequently be used to select the most promising spinel materials for integration as stabilizers into high-capacity composite electrode structures.

Out-Year Goals. The electrochemical capacity of most high-potential lithium-metal oxide insertion electrodes is generally severely compromised by their structural instability and surface reactivity with the electrolyte at low lithium loadings (that is, at highly charged states). Although some progress has been made by cation substitution and structural modification, the practical capacity of these electrodes is still restricted to approximately 160-170 mAh/g. This project proposes a new structural and compositional approach with the goal of producing electrode materials that can provide 200-220 mAh/g without significant structural or voltage decay for 500 cycles. If successful, the materials processing technology will be transferred to the Argonne Materials Engineering and Research Facility (MERF) for scale up and further evaluation.

Collaborations. This project collaborates with Eungje Lee, Joong Sun Park (ANL), Mali Balasubramanian (ANL), and V. Dravid and C. Wolverton (Northwestern University).

Milestones

1. Synthesize and optimize LCO-S, LNO-S and LCNO-S spinel compositions and structures and determine their structural and electrochemical properties. (September 2015 – Complete)
2. Devise synthesis techniques to embed the most promising spinel compositions into layered structures. (September 2015 – Complete)
3. Determine the impact of embedding LCO-S or LNO-S components on the electrochemical properties and cycling stability of composite 'layered-spinel' or 'layered-layered-spinel' structures. (September 2015 – Complete)
4. Use complementary theoretical approaches to further the understanding of the structural and electrochemical properties of LCO-S, LNO-S and LCNO-S electrodes and protective surface layers. (September 2015 – In Progress)

Progress Report

Previous reports have shown that lithiated spinels, such as LT-$Li_2[Co_{2-x}Ni_x]O_4$, prepared at low-temperature, typically 400°C, gradually transform to a layered structure as the synthesis temperature is increased to 800°C. Samples prepared at an intermediate temperature, for example between 600°C and 700°C, have structural and electrochemical properties that differ from pure spinel or layered materials. These Co- and Ni-based spinel materials are of particular interest as potential stabilizers for high-capacity 'layered-layered' cathode structures that are prone to voltage fade during electrochemical cycling. A key objective of this study is to evaluate the electrochemical properties of the most appropriate spinel compositions for 'layered-layered-spinel' NMC electrode structures. This report compares the structural and electrochemical properties of baseline $LiM_{2-z}Co_zO_4$ (M = Mn and Ni) spinel materials.

A series of stoichiometric spinel $Li_{0.5}[Mn_{0.75}Ni_{0.25-x}Co_x]O_2$ (that is, $Li[Mn_{1.5}Ni_{0.5-2x}Co_{2x}]O_4$; x = 0, 0.125 and 0.25) samples was prepared by thoroughly mixing lithium carbonate and transition metal oxalate precursors in a mortar and calcining the powder at 750°C for 1 h in air. In addition, a $Li[Mn_{1.5}Ni_{0.5-2x}Co_{2x}]O_4$ spinel sample with x=0.125 was prepared by chemically-delithiating one Li from a $0.5Li_2MnO_3 \bullet 0.5LiMn_{0.5}Ni_{0.25}Co_{0.25}O_2$ 'layered-layered' precursor structure (or $Li_{1.5}Mn_{0.75}Ni_{0.125}Co_{0.125}O_{2.25}$) and calcining the $Li_{0.5}Mn_{0.75}Ni_{0.125}Co_{0.125}O_{2+\delta}$ product at 750°C for 12 h to induce the layered-to-spinel transition. The target compositions and elemental (AAS) analysis data for the various products are provided in Table 2.

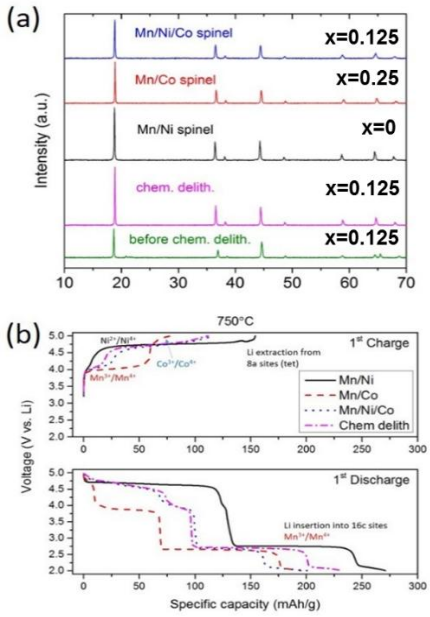

Figure 26: (a) XRD patterns and (b) initial voltage profiles of spinel $Li_{0.5}[Mn_{0.75}Ni_{0.25-x}Co_x]O_2$ products (x = 0, 0.125 and 0.25).

The X-ray diffraction patterns of the samples are shown in Figure 26. All $Li_{0.5}[Mn_{0.75}Ni_{0.25-x}Co_x]O_2$ samples were single phase, irrespective of the method of synthesis. The lattice parameter, a, decreases with increasing Co content (Table 2). Of particular note is that chemical delithiation and subsequent calcination of the 'layered-layered' $0.5Li_2MnO_3 \bullet 0.5LiMn0_{.5}Ni_{0.25}Co_{0.25}O_2$ structure results in a single phase spinel product with an a lattice parameter value (8.158 Å) close to that of the spinel product made by solid state synthesis (8.148 Å); it highlights the opportunity for synthesizing composite 'layered-layered-spinel' structures with a low spinel content by slightly reducing the lithium content in 'layered-layered' compositions. These two spinel products (x=0.125) exhibit similar electrochemical profiles (Figure 26b). Figure 26b also highlights the differences in electrochemical behavior of the well known high-voltage spinel $Li[Mn_{1.5}Ni_{0.5}]O_4$ (x=0) and $Li[Mn_{1.5}Co_{0.5}]O_4$ (x=0.25): the Mn/Ni spinel exhibits a voltage plateau at 4.7 V corresponding to a Ni(II)/Ni(IV) redox reaction, whereas the Mn/Co spinel exhibits a voltage plateau at ~4.0 V, consistent with a Mn(III)/Mn(IV) couple. The Mn/Ni/Co spinel electrode (x=0.125) exhibits intermediate behavior, the sloping voltage response at ~4.7 V suggesting that Co(III) perturbs the ordering of Mn(IV) and Ni(II), and induces more single-phase insertion behavior than two-phase behavior.

Table 2: Elemental ratios and lattice parameters various spinel samples.

Sample	Target composition	Li	Mn	Ni	Co	*a* (Å)
Mn/Ni spinel (x = 0)	$Li_{0.5}Mn_{0.75}Ni_{0.25}O_2$	0.53	0.75	0.29	-	8.172
Mn/Ni/Co spinel (x = 0.125)	$Li_{0.5}Mn_{0.75}Ni_{0.125}Co_{0.125}O_2$	0.54	0.75	0.14	0.14	8.158
Mn/Co spinel (x = 0.25)	$Li_{0.5}Mn_{0.75}Co_{0.25}O_2$	0.51	0.75	-	0.29	8.134
Layered-layered	$Li_{1.5}Mn_{0.75}Ni_{0.125}Co_{0.125}O_2$	1.62	0.75	0.15	0.15	N/A
Chem. delith. (spinel) (x ≈ 0.125)	$Li_{0.5}Mn_{0.75}Ni_{0.125}Co_{0.125}O_2$	0.57	0.75	0.14	0.14	8.148

Patents/Publications/Presentations

Patent Application

- Thackeray, M.M., and J.R. Croy, and B.R. Long. *Lithium Metal Oxide Electrodes for Lithium Batteries*, U.S. Pat. Appl. 20150180031, 25 June 2015.

Presentation

- Lee, Eungje, and Jason Croy, Joong Sun Park, Christopher Johnson, and Michael Thackeray. "Low-Temperature Prepared Lithium-Cobalt-Nickel-Oxide Spinels." Electrochemical Society Meeting, Phoenix (October 11 – 15, 2015).

TASK 4 – ELECTROLYTES FOR HIGH-VOLTAGE, HIGH-ENERGY LITHIUM-ION BATTERIES

Summary and Highlights

The current lithium-ion electrolyte technology is based on $LiPF_6$ solutions in organic carbonate mixtures with one or more functional additives. Lithium-ion battery chemistries with energy density of 175~250 Wh/Kg are the most promising choice. To further increase the energy density, the most efficient way is to raise either the voltage and/or the capacity of the positive materials. Several high energy materials including high-capacity composite cathode $xLi_2MnO_3 \bullet (1\text{-}x)LiMO_2$ and high-voltage cathode materials such as $LiNi_{0.5}Mn_{1.5}O_4$ (4.8 V) and $LiCoPO_4$ (5.1 V) have been developed. However, their increased operating voltage during activation and charging poses great challenges to the conventional electrolytes, whose organic carbonate-based components tend to oxidatively decompose at the threshold beyond 4.5 V *vs.* Li^+/Li.

Other candidate positive materials for PHEV application that have potential of providing high capacity are the layered Ni-rich NCM materials. When charged to a voltage higher than 4.5 V, they can deliver a much higher capacity. For example, $LiNi_{0.8}Co_{0.1}Mn_{0.1}O_2$ (NCM 811) only utilizes 50% of its theoretical capacity of 275 mAh/g when operating in a voltage window of 4.2 V-3.0 V. Operating voltage higher than 4.4 V would significantly increase the capacity to 220 mAh/g; however, the cell cycle life becomes significantly shortened mainly due to the interfacial reactivity of the charged cathode with the conventional electrolyte. The oxidative voltage instability of the conventional electrolyte essentially prevents the practicality to access the extra capacities of these materials.

To address the above challenges, new electrolytes that have substantial high-voltage tolerance at high temperature with improved safety are needed urgently. Organic compounds with low HOMO (highest occupied molecular orbital) energy level are suitable candidates for high-voltage application. An alternative approach to address the electrolyte challenges is to mitigate the surface reactivity of high-voltage cathodes by developing cathode passivating additives. Like the indispensable role of solid-electrolyte interphase (SEI) on the carbonaceous anodes, cathode electrolyte interphase (CEI) formation additives could kinetically suppress the thermodynamic reaction of the delithiated cathode and electrolyte, thus significantly improving the cycle life and calendar life of the high energy density lithium-ion battery.

An ideal electrolyte for high-voltage, high-energy cathodes also requires high compatibility with anode materials (graphite or silicon). New anode SEI formation additives tailored for the new high-voltage electrolyte are equally critical for the high-energy lithium-ion battery system. Such an electrolyte should have the following properties: high stability against 4.5-5.0 V charging state, particularly with cathodes exhibiting high surface oxygen activity; high compatibility with a strongly reducing anode under high-voltage charging; high Li salt solubility (>1.0 M) and ionic conductivity (> $6x10^{-3}$ S/cm @ room temperature); and non-flammability (no flash point) for improved safety and excellent low-temperature performance (-30°C).

The highlights from this quarter include the following:

- Preliminary Auger measurements showed film formation at the cathode surface when fluorether solvent is used. The film contains significant concentrations of fluorine, which cannot be accounted for only by residual PF_6 ions.
- Additional experiments are now underway to determine the bonding nature of this film. The performance limit for the Daikin fluorinated electrolyte now appears to be between 4.5 and 4.6 V.

Task 4.1 – Fluorinated Electrolyte for 5-V Li-ion Chemistry (Zhengcheng Zhang, Argonne National Laboratory)

Project Objective. The objective of this project is to develop a new advanced electrolyte system with outstanding stability at high voltage and high temperature and improved safety characteristic for an electrochemical couple consisting of the high-voltage $LiNi_{0.5}Mn_{1.5}O_4$ (LNMO) cathode and graphite anode. The specific objectives of this proposal are the design, synthesis, and evaluation of (1) non-flammable, high-voltage solvents to render intrinsic voltage and thermal stability in the entire electrochemical window of the high-voltage cathode materials, and (2) electrolyte additives to enhance the formation of a compact and robust solid electrolyte interphase (SEI) on the surface of the high-voltage cathode. A third objective is to gain fundamental understanding of the interaction between electrolyte and high-voltage electrode materials, the dependence of SEI functionality on electrolyte composition, and the effect of high temperature on the full Li-ion cells using the advanced electrolyte system.

Project Impact. This innovative fluorinated electrolyte is intrinsically more stable in electrochemical oxidation due to the fluorine substitution; therefore, it would be also applicable to cathode chemistries based on transmission metal ™ oxides other than LNMO. The results of this project can be further applied to a wide spectrum of high-energy battery systems oriented for PHEVs that operate at high potentials, such as $LiMPO_4$ (M=Co, Ni, Mn), or battery systems that require a high-voltage activation process, such as the high-capacity Li-Mn-rich $_xLi_2MnO_3 \cdot (1\text{-}x)Li[Ni_xMn_yCo_z]O_2$. This electrolyte innovation will push the U.S. supply base of batteries and battery materials past the technological and cost advantages of foreign competitors, thereby increasing economic value to the USA. ANL's new fluorinated electrolyte material will enable the demand for more plug-in hybrid electric vehicles (PHEVs) and electric vehicles (EVs), which directly transforms to greatly reduced gasoline consumption and pollutant emissions.

Out-Year Goals. The goal of this project is to deliver a new fluorinated electrolyte system with outstanding stability at high voltage and high temperature with improved safety characteristic for an electrochemical couple consisting of 5-V Ni-Mn spinel LiNi0.5Mn1.5O4 (LNMO) cathode and graphite anode. The specific objectives of this proposal are the design, synthesis, and evaluation of (1) non-flammable high voltage fluorinated solvents to attain intrinsic voltage stability in the entire electrochemical window of the high-voltage cathode material and (2) effective electrolyte additives that form a compact and robust SEI on the surfaces of the high voltage cathode and graphitic anode.

Collaborations. This project collaborates with Dr. Kang Xu, U.S. Army Research Laboratory; Dr. Xiao-Qing Yang, BNL; Dr. Brett Lucht, University of Rhode Island; and Dr. Andrew Jansen and Dr. Gregory Krumdick, ANL.

Milestones

1. Complete theoretical calculation of electrolyte solvents; Validate electrochemical properties of available fluorinated solvents by cyclic voltammetry and leakage current experiment. (March 2014 – Complete)
2. Synthesize and characterize the Gen-1 electrolyte. (June 2014 – Complete)
3. Evaluate the LNMO/graphite cell performance of Gen-1 F-electrolyte. (September 2014 – Complete)
4. Design and build interim cells and baseline pouch cells. (January 2015 – Complete)
5. Synthesize and evaluate Gen-2 F-electrolyte based on TF-PC. (March 2015 –Complete)
6. Develop optimized F-electrolyte containing multinary F-solvents. (June 2015 – Complete)
7. Design and build final cells. (September 2015 – Complete)

Progress Report

To further enhance the cycling performance of the LNMO/graphite cell, especially at 55°C, we examined the effect of an active lithium reservoir introduced by the placement of a lithium foil (Figure 27b), SLMP (stabilized lithium metal powder from FMC) (Figure 27c), or electrochemically prelithiated graphite anode (Figure 27d) before assembling the LNMO/graphite cell with fluorinated electrolyte. Figure 28a shows the capacity retention profiles of the cell, with lithium foil cycled at C/3 rate with a cut-off voltage of 3.5 V – 4.9 V at 55°C. The specific capacity of 120 mAh g^{-1} with a Coulombic efficiency of > 99.5% (Figure 28b) was maintained even after 100 cycles at 55°C with no capacity loss, which has never been achieved before. Figure 28a also provides the capacity retention profiles of LNMO/graphite cells using HVE electrolyte and Gen 2 electrolyte without lithium foil for comparison. The slight fluctuation in capacity retention of the new cell suggests that the lithium compensation might have been on and off during the cycling process because of poor contact of the Li metal and the electrolyte, possibly due to the location where the lithium was incorporated. Post analysis of the disassembled cell indicated that the Li metal was not completely consumed, which means the cycle life of the cell could be extended further.

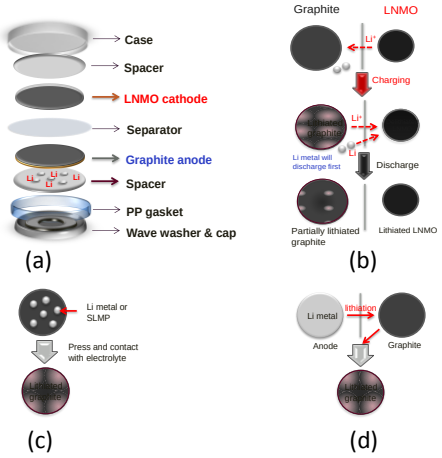

Figure 27. LiNMO/graphite cell with Li reservoir.

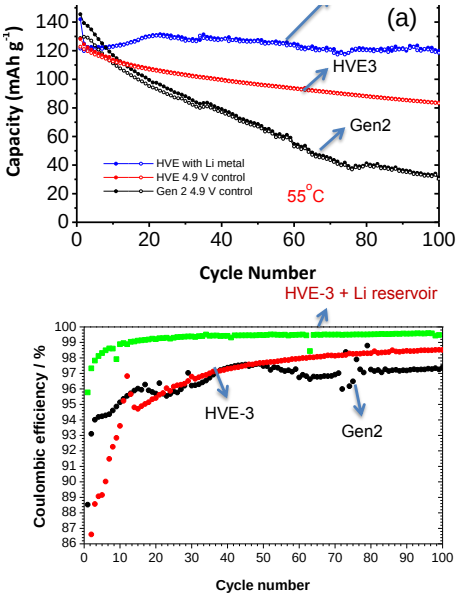

Figure 28. Capacity retention (a) and Coulombic efficiency (b) of LNMO/graphite cells.

The voltage profile of LNMO/graphite cells with the Li reservoir strongly resembles that of the LNMO/Li cells instead of LNMO/graphite cells, indicating that at the end of discharge the graphite anode is not fully delithiated and that the potential remains low. Nevertheless, this data indicates that the introduction of the auxiliary lithium in the LNMO/graphite cell (Figure 27b) can compensate for the active lithium loss caused by electrolyte decomposition on the LNMO cathode, thus enhancing cell performance.

While the lithium reservoir can also be used in cells with the conventional carbonate electrolytes, our data indicates that it is not a practical solution since the severe oxidative decomposition of the electrolyte on LNMO cathode would lead to faster consumption of the extra lithium, and the cell dies quickly. To investigate the effect of the oxidative stability of electrolyte on the performance of the LNMO/graphite cell with lithium reservoir, we carried out the same experiment as described above with Gen 2 electrolyte. As predicted, the improvement of the Gen 2 cell is not as good as the HVE-3 cell; the added lithium was fully consumed in 70 cycles upon disassembling the cell, indicating that even with the aid of lithium compensation, a more stable electrolyte is still indispensable for high-voltage cells at high temperature.

To further demonstrate the concept that Li compensation is not limited to the delivery method illustrated in Figure 27b, experiments with other methods were also examined using Gen 2 electrolyte. All results provide clear evidence that both methods showed performance improvement over the pristine cells. In addition, we found that adding extra lithium does not have significant impact on the rate capability of the electrolyte; the rate performance is similar to cells without lithium reservoir.

Task 4.2 – Daikin Advanced Lithium Ion Battery Technology – High-Voltage Electrolyte (R. Hendershot/J. Sunstrom/Michael Gilmore, Daikin America)

Project Objective. The project objective is to develop a stable (300 – 1000 cycles), high-voltage (at 4.6 V), and safe (self-extinguishing) formulated electrolyte.

- Exploratory Development (Budget Period #1 – October 1, 2013 to January 31, 2015)
  - Identify promising electrolyte compositions for high-voltage (4.6 V) electrolytes via the initial experimental screening and testing of selected compositions
- Advanced Development (Budget Period #2 – February 1, 2015 to September 31, 2015)
  - Detailed studies and testing of the selected high-voltage electrolyte formulations and the fabrication of final demonstration cells

Project Impact. Fluorinated small molecules offer the advantage of low viscosity along with high chemical stability due to the strength of the C-F bond. Due to this bond strength, Daikin fluorochemical materials are among the most electrochemical stable materials that still have the needed performance attributes for a practical electrolyte. Such an electrolyte will allow routine operating voltages to be increased to 4.6 V. This technological advance would allow significant cost reduction by reducing the number of cells needed in a particular application and/or allow for greater driving range in PHEV applications.

Out-Year Goals. This project has clearly defined goals for both temperature and voltage performance, which are consistent with the deliverables of this proposal. Those goals are to deliver an electrolyte capable of 300 – 1000 cycles at 3.2 V – 4.6 V at nominal rate with stable performance. An additional goal is to have improved high temperature (> 60°C) performance. An additional safety goal is to have this electrolyte be self-extinguishing.

Collaborations. Daikin is continuing a limited testing agreement with Coulometrics. Surface studies that may include Auger spectroscopy, x-ray photoelectron spectroscopy, and TOF-SIMS mass spectrometry have been contracted to Materials Research Laboratory in Struthers, Ohio.

Milestones

Budget Period #1 – Oct. 1, 2013 to Jan. 31, 2015

1. Complete identification of promising electrolyte formulations. Experimental design completed with consistent data sufficient to build models. Promising electrolyte formulations are identified that are suitable for high-voltage battery testing. (Complete)
2. Successful fabrication of 10 interim cells and delivery of cells to a DOE laboratory (to be specified). (Final report received from ANL. Interim cells did not complete tests.)
3. Electrochemical and battery cycle tests are completed, and promising results demonstrate stable performance at 4.6 V. (Ongoing)

Progress Report

The technical approach to achieve the milestones is based on an iterative plan following a sound scientific method, also sometimes referred to as a Plan-Do-Check-Act (PDCA) cycle, which has been described in detail in previous reports.

Status. The final test report for the preliminary cells submitted in February has been issued from Argonne. The cells were 1 Ah NMC-111/graphite cells filled with best guess optimal electrolyte 1.2 $LiPF_6$ FEC/EMC/F-solvent (2:6:2) + 1% additive A. The cycle life testing data is shown in Figure 29. The capacity and resistance as a function of cycle number are shown in the top and bottom panels, respectively. The cells completed 80 cycles down to an 80% capacity retention cutoff at 4.6 V that was most likely due to high resistance change between 50 and 100 cycles. Cells were shut off at RPT (Reference Performance Test) 3 (150 cycles).

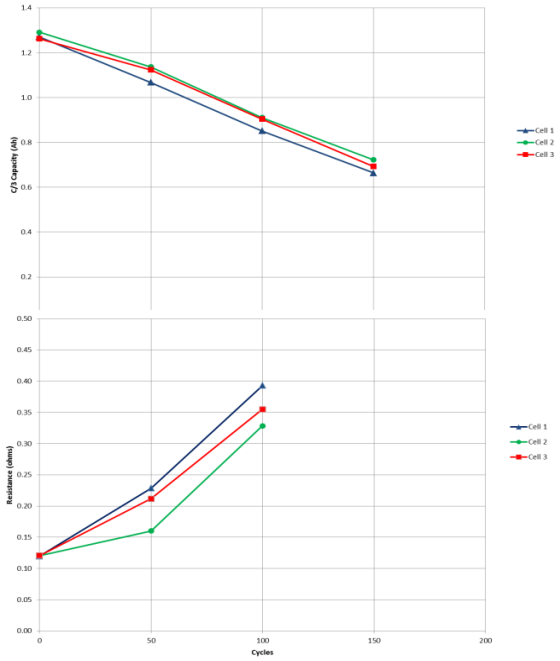

Figure 29. Cycle life at 4.6 V Daikin fluorinated electrolytes (capacity – top; resistance –bottom).

The calendar life test is shown in Figure 30. The calendar life did not finish RPT6. The drop in capacity in the 10th week is again consistent with a large resistance increase. No post mortem has yet been conducted on these cells.

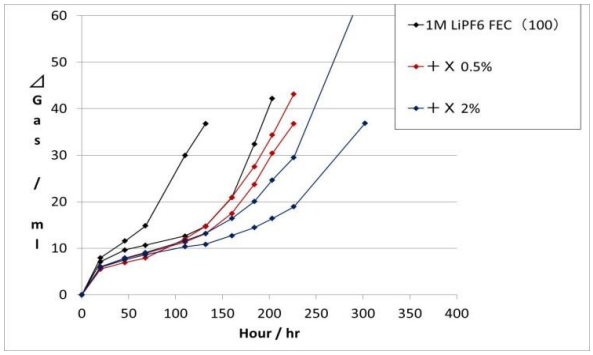

Figure 30. Calendar life at 4.6 V of Daikin fluorinated electrolyte (capacity – top; resistance – bottom).

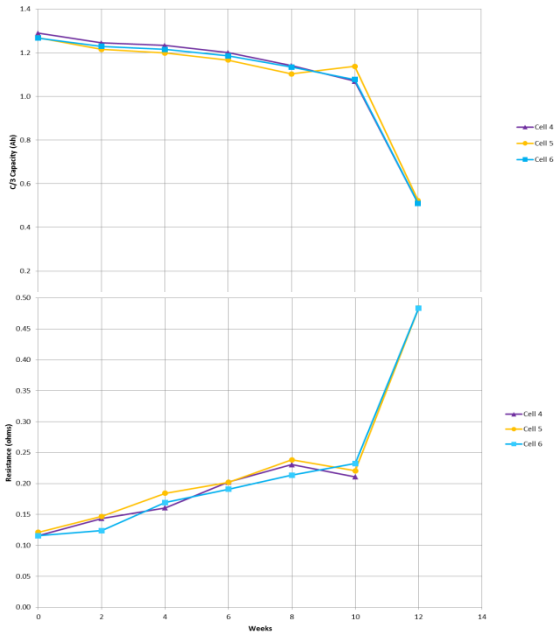

Figure 31. Gas volume change vs time for LMNO/graphite cell at 4.9 V.

Additional work this quarter focused on evaluating new gassing additives developed at Daikin Industries Laboratory. These additives are focused on protecting the cathode from the FEC, which is a primary source of gas. Figure 31 shows an example of an additive of this type. The figure shows the gas volume vs. time for an LMNO/graphite cell run held at 4.9 V. The additive is effective in reducing gassing and is being considered for next generation electrolyte.

Task 4.3 – Novel Non-Carbonate Based Electrolytes for Silicon Anodes (Dee Strand, Wildcat Discovery Technologies)

Project Objective. The objective of this project is to develop non-carbonate electrolytes that form a stable solid-electrolyte interphase (SEI) on silicon alloy anodes, enabling substantial improvements in energy density and cost relative to current lithium ion batteries (LiBs). These improvements are vital for mass market adoption of electric vehicles. At present, commercial vehicle batteries employ cells based on $LiMO_2$ (M = Mn, Ni, Co), $LiMn_2O_4$, and/or $LiFePO_4$ coupled with graphite anodes. Next generation cathode candidates include materials with higher specific capacity or higher operating voltage, with a goal of improving overall cell energy density. However, to achieve substantial increases in cell energy density, a higher energy density anode material is also required. Silicon anodes demonstrate very high specific capacities, with a theoretical limit of 4200 mAh/g and state-of-the-art electrodes exhibiting capacities greater than 1000 mAh/g. While these types of anodes can help achieve target energy densities, their current cycle life is inadequate for automotive applications. In graphite anodes, carbonate electrolyte formulations reductively decompose during the first-cycle lithiation, forming a passivation layer that allows lithium transport, yet is electrically insulating to prevent further reduction of bulk electrolyte. However, the volumetric changes in silicon upon cycling are substantially larger than graphite, requiring a much more mechanically robust SEI film.

Project Impact. Silicon alloy anodes enable substantial improvements in energy density and cost relative to current lithium ion batteries. These improvements are vital for mass market adoption of electric vehicles, which would significantly reduce CO_2 emissions as well as eliminate U.S. dependence on energy imports.

Out-Year Goals. Development of non-carbonate electrolyte formulations that:

- form stable SEIs on 3M silicon alloy anode, enabling Coulombic efficiency > 99.9% and cycle life > 500 cycles (80% capacity) with NMC cathodes;
- have comparable ionic conductivity to carbonate formulations, enabling high power at room temperature and low temperature;
- are oxidatively stable to 4.6V, enabling the use of high energy NMC cathodes in the future; and
- do not increase cell costs over today's carbonate formulations.

Collaborations. Wildcat is working with 3M on this project. To date, 3M is supplying the silicon alloy anode films and NMC cathode films for use in Wildcat cells.

Milestones

1. Assemble materials, establish baseline performance with 3M materials. (December 2013 – Complete)
2. Develop initial additive package using non-SEI forming solvent. (March 2014 – Complete)
3. Screen initial solvents with initial additive package. (June 2014 –Complete)
4. Design/build interim cells for DOE (September 2014 –Complete)
5. Improve performance with noncarbonate solvents and new SEI additives (March 2015 – On Track; continuous to end of project)
6. Optimize formulations (August 2015 –On Track; continuous to end of project)
7. Design/build final cells for DOE (March 2016, due to no-cost extension)

Progress Report

We continue to focus on optimizing the promising solvent formulations found in previous phases; this extends from the last quarterly report, and is the longest phase of the project as cycle times are increased. This includes optimization of (1) salt content and concentration, (2) solvent combinations and ratios, and (3) additive type, concentrations, and combinations. Wildcat is systematically screening these variables to identify formulations with target cycle life, as well as promising leads to hit other key metrics.

Last quarter we reported results on the salt optimization screen, including binary combinations of salt. This quarter we completed experimental designs where we studied the effect of solvent ratios and the use of ternary combinations of solvents. We also began studies to establish the baseline performance of our best formulations at higher voltage.

After optimization of salts, we designed experiments to look at different combinations and ratios of the novel solvents previously identified. This included multiple approaches such as changing the ratio of the high dielectric to low viscosity solvent and investigating ternary solvents systems. From this effort, a number of promising systems were identified for further investigation. Figure 32 shows example results for a subset of the experiments in the design.

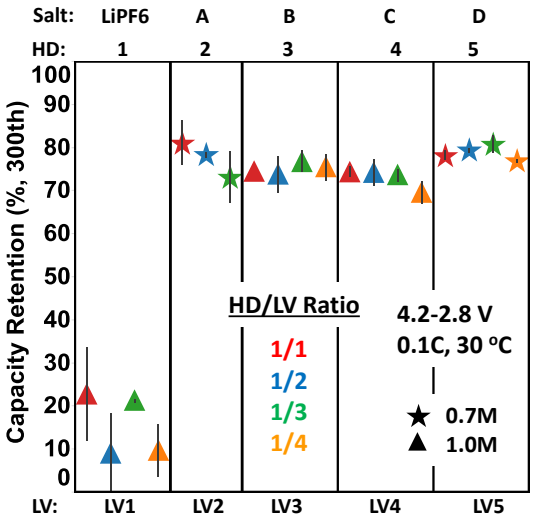

Figure 32. Example results from solvent ratio study, including effect of salt.

In parallel to these studies, we have designed and assembled cells to follow up on and optimize electrolyte additives that were identified very early in this project. This also includes additional work on EC-containing formulations, as several additive categories showed benefit in the presence of EC. Results for a subset of the new additive screen are shown in Figure 33, where each color represents a different additive category. One category of additives (green) was similar in performance to the addition of FEC, and will be expanded on in future experimental designs.

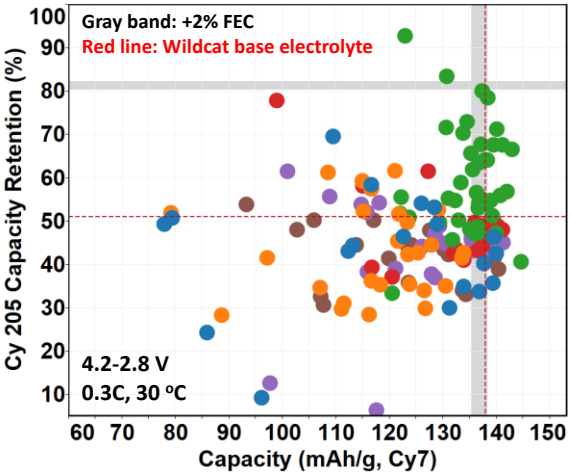

Figure 33. Beneficial additives identified for use in carbonate formulations.

We have also started testing electrolyte formulations at voltage higher than 4.2 V, which was used for all studies to date. The most promising formulations were tested at 4.35 V, 4.45 V, and 4.55 V. Results at the highest voltage (4.55 V) presented last quarter indicate that high-voltage solutions are possible. We are extending this work by introducing high-voltage additives, with cells now being tested.

TASK 5 – DIAGNOSTICS

Summary and Highlights

To meet the goals of the DOE Vehicle Technologies Office (VTO) Multi-Year Program Plan and develop lower-cost, abuse-tolerant batteries with higher energy density, higher power, better low-temperature operation and longer lifetimes suitable for the next-generation of hybrid electric vehicles (HEVs), plug-in hybrid electric vehicles (PHEVs), and electric vehicles (EVs), there is a strong need to identify and understand structure-property-electrochemical performance relationships in materials, life-limiting and performance-limiting processes, and various failure modes to guide battery development activities and scale-up efforts. In the pursuit of batteries with high energy density, high cell operating voltages and demanding cycling requirements lead to unprecedented chemical and mechanical instabilities in cell components. Successful implementation of newer materials such as Si anode and high voltage cathodes also requires better understanding of fundamental processes, especially those at the solid/electrolyte interface of both anode and cathode.

Task 5 takes on these challenges by combining model system, *ex situ*, *in situ* and *operando* approaches with an array of the start-of-the-art analytical and computational tools. Four subtasks are tackling the chemical processes and reactions at the electrode/electrolyte interface. Researchers at LBNL use *in situ* and *ex situ* vibrational spectroscopy, far- and near-field scanning probe spectroscopy and laser-induced breakdown spectroscopy (LIBS) to understand the composition, structure, and formation/degradation mechanisms of the solid electrolyte interphase (SEI) at Si anode and high-voltage cathodes. UCSD combines scanning transmission electron microscopy (STEM)/electron energy loss spectroscopy (EELS), x-ray photoelectron spectroscopy (XPS) and *ab initio* computation for surface and interface characterization and identification of instability causes at both electrodes. At Cambridge, nuclear magnetic resonance (NMR) is being used to identify major SEI components, their spatial proximity, and how they change with cycling. Subtasks at BNL and PNNL focus on the understanding of fading mechanisms in electrode materials, with the help of synchrotron based x-ray techniques (diffraction and hard/soft x-ray absorption) at BNL and high-resolution transmission electron microscopy (HRTEM) and spectroscopy techniques at PNNL. At LBNL, model systems of electrode materials with well-defined physical attributes are being developed and used for advanced diagnostic and mechanistic studies at both bulk and single-crystal levels. These controlled studies remove the ambiguity in correlating material's physical properties and reaction mechanisms to its performance and stability, which is critical for further optimization. The final subtask takes advantage of the user facilities at ANL that bring together x-ray and neutron diffraction, x-ray absorption, emission and scattering, HRTEM, Raman spectroscopy and theory to look into the structural, electrochemical, and chemical mechanisms in the complex electrode/electrolyte systems. The diagnostics team not only produces a wealth of knowledge that is key to developing next-generation batteries, it also advances analytical techniques and instrumentation that have a far-reaching effect on material and device development in a range of fields.

The highlights for this quarter are as follows:

- Grey's group discovered the use of a redox mediator (LiI) to cycle the Li-oxygen cell with a high efficiency, large capacity and a very low over-potential.
- Meng's group demonstrated the use of *operando* neutron diffraction to quantify Li site occupancy and probe lithium migration dynamics in Li transition-metal oxide cathodes during charge and discharge.

Task 5.1 – Design and Synthesis of Advanced High-Energy Cathode Materials (Guoying Chen, Lawrence Berkeley National Laboratory)

Project Objective. The successful development of next-generation electrode materials requires particle-level knowledge of the relationships between materials' specific physical properties and reaction mechanisms to their performance and stability. This single-crystal-based project was developed specifically for this purpose, and it has the following objectives: (1) obtain new insights into electrode materials by utilizing state-of-the-art analytical techniques that are mostly inapplicable on conventional, aggregated secondary particles, (2) gain fundamental understanding on structural, chemical, and morphological instabilities during Li extraction/insertion and prolonged cycling, (3) establish and control the interfacial chemistry between the cathode and electrolyte at high-operating voltages, (4) determine transport limitations at both particle and electrode levels, and (5) develop next-generation electrode materials based on rational design as opposed to more conventional empirical approaches.

Project Impact. This project will reveal performance-limiting physical properties, phase-transition mechanisms, parasitic reactions, and transport processes based on the advanced diagnostic studies on well-formed single crystals. The findings will establish rational, non-empirical design methods that will improve the commercial viability of next-generation $Li_{1+x}M_{1-x}O_2$ (M = Mn, Ni and Co) and spinel $LiNixMn_{2-x}O_4$ cathode materials.

Approach. Prepare crystal samples of Li-rich layered oxides and high-voltage Ni/Mn spinels with well-defined physical attributes. Perform advanced diagnostic and mechanistic studies at both bulk and single-crystal levels. Global properties and performance of the samples will be established from the bulk analyses, while the single-crystal based studies will utilize time- and spatial-resolved analytical techniques to probe material's redox transformation and failure mechanisms.

Out-Year Goals. This project aims to determine performance and stability limiting fundamental properties and processes in high-energy cathode materials and to outline mitigating approaches. Improved electrode materials will be designed and synthesized.

Collaborations. This project has collaborated with Drs. E. Crumlin and P. Ross (LBNL); Drs. Y. Liu and D. Nordlund (Stanford Synchrotron Radiation Lightsource); Prof. C. Grey (Cambridge); Dr. C. Wang (PNNL); and Dr. J. Nanda (ORNL).

Milestones

1. Characterize Ni/Mn spinel solid solutions and determine the impact of phase transformation and phase boundary on rate capability. (December 2014 – Complete)
2. Complete the investigation on crystal-plane specific reactivity between Li-rich layered oxides and the electrolyte. Determine morphology effect in side reactions. (March 2015 – Complete)
3. Develop new techniques to characterize reactions and processes at the cathode-electrolyte interface. Evaluate the effect of surface compositions and modifications on side reactions and interface stability (June 2015 – Complete)
4. *Go/No-Go*: Continue the approach of using synthesis conditions to vary surface composition if significant structural and performance differences are observed. (September 2015 – Delayed to January 2016)

Progress Report

Last quarter, complementary depth-profiling core-level spectroscopies, namely X-ray absorption spectroscopy (XAS) and electron energy loss spectroscopy (EELS), as well as aberration corrected scanning transmission electron microscopy (STEM) were used to investigate particle surface termination, transition metal (TM) redox activities, and surface crystal structural transformation on well-formed $Li_{1.2}Mn_{0.13}Mn_{0.54}Co_{0.13}O_2$ crystal samples with six distinct morphologies (plate, needle, S-Poly, L-Poly, box and octahedron). A morphology-dependent thin layer of defective spinel with reduced TMs was found on the native crystal surfaces, with the least on the plate and L-Poly samples and the most on the S-Poly and box samples. Cycling-induced TM reduction follows a similar trend, with L-Poly and box being the most and least stable samples, respectively. This quarter, the electrochemical performance of the crystal samples was evaluated by half-cell cycling of the composite electrodes, consisting of the oxide crystals (80 wt%), a carbon additive (10 wt%), and a PVdF binder (10 wt%), in a 1 M $LiPF_6$ in EC-DEC (1:1) electrolyte. Figure 34a compares the first-cycle voltage profiles of the cells charged and discharged between 2.5 V and 4.8 V at a current density of 10 mA/g. An activation plateau around 4.5 V was observed on all samples, although the actual plateau length varied significantly. The smaller sized S-Poly sample was most activated, while the least activation was observed on the box and L-Poly samples. Except the box sample, the profile of the slope region between 3.8 V and 4.5 V appears similar. The plate crystals delivered the highest capacities among the micron-sized samples, and the box had a much lower capacity, which indicated an effect of particle morphology as well as a coupled relationship between the level of first-charge activation and discharge capacity. The effects of particle morphology and surface properties were further demonstrated on the rate capability comparison in Figure 34b. S-Poly crystals consistently outperformed other samples at all rates tested, suggesting the dominating effect of particle size in kinetic behavior. Long-term cycling is compared in the plots for discharge capacity (Figure 34c) and capacity retention (Figure 34d), where the superior cycling stability of L-Poly sample is clearly shown. Figure 35 compares the changes in average charge and discharge voltages along cycling. A gradual decrease in the discharge voltage, commonly known as the voltage decay phenomenon in these Li- and Mn-rich oxides, is observed on all samples (Figure 35a). The L-Poly sample experienced a much smaller voltage gap (265 mV at cycle 5) and slowest gap increase during the cycling (165 mV increase from cycle 5 to 85, Figure 35b). The trends in both voltage depression and capacity retention are consistent with that of cycling-induced TM reduction previously determined by soft XAS studies (Figure 35c). The study demonstrates the correlation in TM reduction and oxide stabilities, and the critical role of particle surface engineering in minimizing cycling-induced structural changes, voltage decay and hysteresis in this class of high-capacity cathode materials.

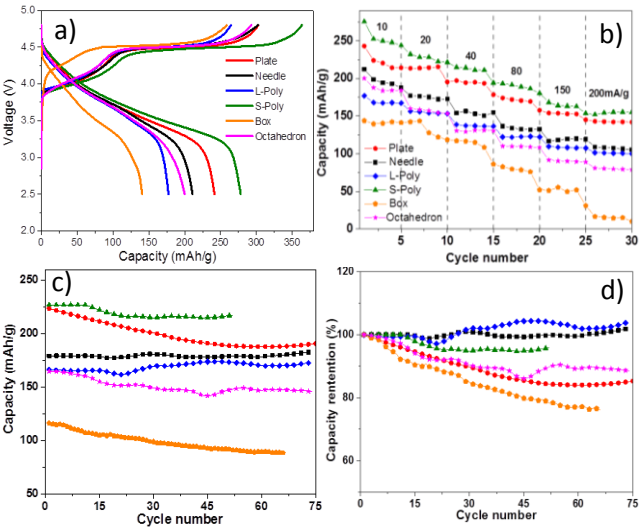

Figure 34. (a) First charge-discharge voltage profiles of the $Li_{1.2}Ni_{0.13}Mn_{0.54}Co_{0.13}O_2$ half cells, (b) rate capability of the crystal samples, (c) and (d) long-term cycling and capacity retention of the cells at a current density of 20 mA/g.

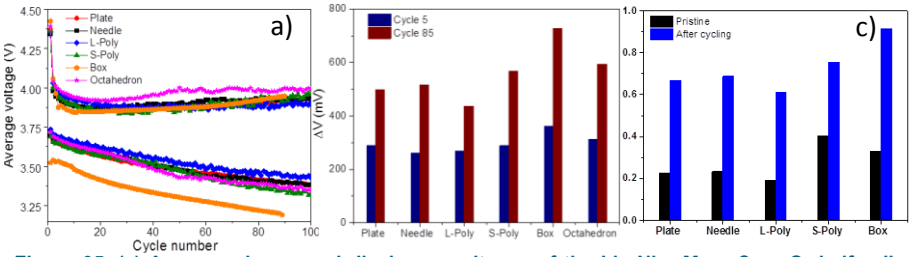

Figure 35. (a) Average charge and discharge voltages of the $Li_{1.2}Ni_{0.13}Mn_{0.54}Co_{0.13}O_2$ half cells, (b) comparison of the charge and discharge voltage gaps at cycle 5 and 85, and (c) Co L_3 peak ratio of the TEY XAS spectra, with a higher ratio corresponding to a lower oxidation state.

Patents/Publications/Presentations

Publications

- Shukla, A.K., and Q. Ramasse, C. Ophus, H. Duncan, and G. Chen. "Unraveling Structural Ambiguities in Li and Mn Rich Transition Metal Oxides." *Nature Communications*, in press (2015).
- Kuppan, S., and H. Duncan and G. Chen. "Controlling Side Reactions and Self-discharge in High-voltage Spinel Cathodes: Critical Role of Surface Crystallographic Facets." *Physical Chemistry Chemical Physics* 17 (2015): 26471.
- Ruther, R., and H. Zhou, C. Dhital, S. Kuppan, A. Kercher, G. Chen, A. Huq, F. Delnick, and J. Nanda. "Synthesis, Structure, and Electrochemical Performance of High Capacity $Li_2Cu_{0.5}Ni_{0.5}O_2$ Cathodes." *Chemistry of Materials* 27, no. 19 (2015): 6746.
- Hou, H., and L. Cheng, T. Richardson, G. Chen, M.M. Doeff, R. Zheng, R. Russo, and V. Zorba. "Three-Dimensional Elemental Imaging of Li-ion Solid-State Electrolytes Using fs-Laser Induced Breakdown Spectroscopy (LIBS)." *Journal of Analytical Atomic Spectrometry* 30 (2015): 2295.

.

Task 5.2 – Interfacial Processes – Diagnostics (Robert Kostecki, Lawrence Berkeley National Laboratory)

Project Objective. The main objective of this task is to obtain detailed insight into the dynamic behavior of molecules, atoms, and electrons at electrode/electrolyte interfaces of intermetallic anodes (Si) and high voltage Ni/Mn-based materials at a spatial resolution that corresponds to the size of basic chemical or structural building blocks. The aim of these studies is to unveil the structure and reactivity at hidden or buried interfaces and interphases that determine battery performance and failure modes. To accomplish these goals, novel far- and near-field optical multifunctional probes must be developed and deployed *in situ*. The work constitutes an integral part of the concerted effort within the BMR Program, and it attempts to establish clear connections between diagnostics, theory/modelling, materials synthesis, and cell development efforts.

Project Impact. This project provides better understanding of the underlying principles that govern the function and operation of battery materials, interfaces, and interphases, which is inextricably linked with successful implementation of high energy density materials such as Si and high-voltage cathodes in Li-ion cells for plug-in hybrid electric vehicles (PHEVs) and electric vehicles (EVs). This task involves development and application of novel innovative experimental methodologies to study the basic function and mechanism of operation of materials, composite electrodes, and Li-ion battery systems for PHEV and EV applications.

Approach. Design and employ novel and sophisticated *in situ* analytical methods to address key problems of the BMR baseline chemistries. Experimental strategies combine imaging with spectroscopy aimed at probing electrodes at an atom, molecular, or nanoparticulate level to unveil structure and reactivity at hidden or buried interfaces and determine electrode performance and failure modes in baseline Li_xSi-anodes and high-voltage LMNO cathodes. The proposed methodologies include *in situ* and *ex-situ* Raman, Fourier transform infrared spectroscopy (FTIR) and laser-induced breakdown spectroscopy (LIBS) far- and near-field spectroscopy/microscopy, scanning probe microscopy (SPM), spectroscopic ellipsometry, electron microscopy (SEM, HRTEM), and standard electrochemical techniques and model single particle and/or monocrystal model electrodes to probe and characterize bulk and surface processes in Si anodes, and high-energy cathodes.

Out-Year Goals. The main goal is to gain insight into the mechanism of surface phenomena on thin-film and monocrystal Sn and Si intermetallic anodes and evaluate their impact on the electrode long-term electrochemical behavior. Comprehensive fundamental study of the early stages of solid-electrolyte interphase (SEI) layer formation on polycrystalline and single crystal face Sn and Si electrodes will be carried out. *In situ* and *ex situ* far- and near-field scanning probe spectroscopy and LIBS will be employed to detect and monitor surface phenomena at the intermetallic anodes and high-voltage (> 4.3V) model and composite cathodes.

Collaborations. This project collaborates with Vincent Battaglia, Ban Chunmei, Vassilia Zorba, Bryan D. McCloskey, and Miguel Salmeron.

Milestones

1. Determine the mechanism of formation of the metal complexes species that are produced at high-energy Li-ion cathodes. (December 2014 –Complete)
2. Resolve SEI layer chemistry of coated Si single crystal and thin film anodes (collaboration with Chunmei Ban). (March 2015 –Complete)
3. Determine the mechanism of SEI layer poisoning by Ni and Mn coordination compounds (collaboration with Bryan D. McCloskey). (June 2015 – Complete)
4. *Go/No-Go*: Demonstrate feasibility of *in situ* near-field and LIBS techniques at Li-ion electrodes (collaboration with Vassilia Zorba). Criteria: Stop development of near-field and LIBS techniques, if the experiments fail to deliver adequate sensitivity. (September 2015 – Complete)

Progress Report

This quarter, we continued to develop the capability to perform *in situ* near-field infrared (IR) studies on Li-ion electrodes. After switching focus from developing a traditional liquid cell due to technical infeasibility as previously reported, we focused on development of graphene electrodes for a trans-membrane near-field IR characterization of the growing solid-electrolyte interphase (SEI) on a model electrode. This allows *in situ* capability while maintaining a completely sealed cell, avoiding numerous issues associated with liquid immersion. To demonstrate feasibility of this technique, we prepared a sample consisting of chemical vapor deposition (CVD) graphene on an SiO_2 substrate. The sample was characterized by near-field IR spectroscopy using the Advanced Light Source Synchrotron (ALSS) beamline 5.4.1.

The results of this characterization are shown in Figure 36. The spectrum shows a characteristic Si-O phonon absorption band in the 1050 cm^{-1} range. This shows that the near-field IR contrast can be resolved through graphene, which is a known Li-ion electrode, demonstrating the feasibility of this approach to *in situ* characterization and completing Milestone 4. We have recently developed and fabricated, in cooperation with the Salmeron group at the LBNL Molecular Foundry, an *in situ* cell using graphene held up by a perforated membrane as a negative electrode. This cell, in combination with the near-field technique demonstrated above, will allow full *in situ* near-field IR characterization of the growing SEI layer on a graphite-like electrode. Experiments using this cell have begun.

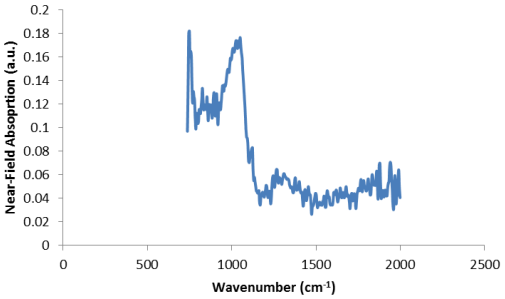

Figure 36. Near-field spectroscopic absorption of SiO_2 substrate through graphene membrane.

To pursue *in situ* LIBS (laser-induced breakdown spectroscopy) for the analysis of SEI layers formed in complex organic carbonate-based electrolytes, we followed two distinct strategies. These strategies address two individual issues that currently limit *in situ* depth-resolved analysis: sensitivity and specificity. In the previous period, we demonstrated that double femtosecond pulse configuration (scheme where collinear fs-laser pulses are temporally separated by hundreds of nanosecond to microseconds), can provide improved sensitivity though the formation of a rarified atmosphere by the first pulse in the form of cavitation bubbles, exposing the SEI surface directly to the second pulse. Very significant enhancements in sensitivity were observed in organic carbonate-based electrolytes.

The second challenge was to de-convolute information originating from the electrolyte and SEI. This period, we addressed this issue by implementing an ultraviolet femtosecond laser excitation, and highly sensitive gated spectrometer/intensified charge-coupled device (ICCD) detection, to study the optical emission characteristics of pre-cycled SEIs and other samples like Si. The samples were submerged in surrogate liquids (such as organic solvents or water) with focus on improving specificity while maintaining high depth resolution. Under ideal conditions, the ultrafast LIBS lines detected in liquids should be very similar to that in air. Figure 37 shows the time-resolved emission spectra of Si in the 240-300 nm spectral ranges, where the most prominent Si_I lines are clearly resolved in (a) liquid and (b) air. We concluded that LIBS has potential to address and elucidate the complex mechanisms leading to the SEI layer formation *in situ.*

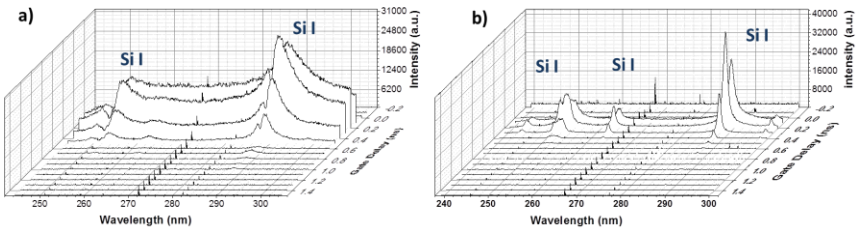

Figure 37. Comparison of UV ultrafast LIBS emission from Si (a) in liquid and (b) in air.

.

Patents/Publications/Presentations

Publication

- Ayache, M., and D. Jang, J. Syzdek, and R. Kostecki. "Near-Field IR Nanoscale Imaging of the Solid Electrolyte Interphase on a HOPG Electrode." *Journal of the Electrochemical Society* 162.13 (2015): A7078-A7082.

Presentations

- Westfälische Wilhelms-Universität, Summer Seminar, MEET Batterieforschungszentrum, Muenster, Germany (August 13, 2015): "Challenges and Opportunities in Battery Characterization"; R. Kostecki.
- *LiBD-7 2015* – "Electrode Materials," Arcachon, France (June 21 – 26, 2015): "The Mechanism of Mn and Ni Dissolution at the $Li_xNi_{0.5}Mn_{1.5}O_{4-\delta}$ / Organic Carbonate Electrolyte Interface"; Angélique Jarry, Sébastien Gottis, Young-Sang Yu, Josep Roque-Rosell, Chunjoong Kim, Jordi Cabana, John Kerr, and Robert Kostecki.

Task 5.3 – Advanced *in situ* Diagnostic Techniques for Battery Materials (Xiao-Qing Yang and Xiqian Yu, Brookhaven National Laboratory)

Project Objective. The primary objective of this project is to develop new advanced *in situ* material characterization techniques and to apply these techniques to support the development of new cathode and anode materials for the next generation of lithium-ion batteries (LiBs) for plug-in hybrid electric vehicles (PHEV). To meet the challenges of powering the PHEV, LiBs with high energy and power density, low cost, good abuse tolerance, and long calendar and cycle life must be developed.

Project Impact. The Multi Year Program Plan (MYPP) of the DOE Vehicle Technologies Office (VTO) describes the goals for battery: "Specifically, lower-cost, abuse-tolerant batteries with higher energy density, higher power, better low-temperature operation, and longer lifetimes are needed for the development of the next-generation of HEVs, PHEVs, and EVs." The knowledge gained from diagnostic studies through this project will help U.S. industries develop new materials and processes for new generation LiBs in the effort to reach these VTO goals.

Approach. This project will use the combined synchrotron based *in situ* x-ray techniques (x-ray diffraction, and hard and soft x-ray absorption) with other imaging and spectroscopic tools such as high-resolution transmission electron microscopy (HRTEM) and mass spectroscopy (MS) to study the mechanisms governing the performance of electrode materials and provide guidance for new material and new technology development regarding Li-ion battery systems.

Out-Year Goals. For the high-voltage spinel $LiMn_{1.5}Ni_{0.5}O_4$, the high-voltage charge and discharge cycling is a serious challenge for the electrolyte oxidation decomposition. Studies on improvement of thermal stability are important for better safety characteristics. For high energy density $Li(NiMnCo)O_2$ composite materials, the problem of poor rate capability during charge and discharge and performance degradation during charge-discharge cycling are issues to be addressed.

Collaborations. The BNL team will work closely with material synthesis groups at ANL (Drs. Thackeray and Amine) for the high-energy composite; at UT Austin for the high-voltage spinel; and at PNNL for the Si-based anode materials. Such interaction between the diagnostic team at BNL and synthesis groups of these other BMR members will catalyze innovative design and synthesis of advanced cathode and anode materials. We will also collaborate with industrial partners at General Motor, Duracell, and Johnson Controls to obtain feedback information from battery end users.

Milestones

1. Complete the thermal stability studies of a series of blended $LiMn_2O_4$ (LMO) -$LiNi_{1/3}Co_{1/3}Mn_{1/3}O_2$ (NCM) cathode materials with different weight ratios using *in situ* time-resolved x-ray diffraction (XRD) and mass spectroscopy techniques in the temperature range of 25°C to 580°C. (December 2014 – Complete)

2. Complete the *in situ* XRD studies of the structural evolution of $Li_{2-x}MoO_3$ ($0 \leq x \leq 2$) high energy density cathode material during charge-discharge cycling between 2.0 V and 4.8 V. (March 2015 – Complete)

3. Complete the x-ray absorption near edge structure (XANES) and extended x-ray absorption fine structure (EXAFS) studies at Mo K-edge of Li_2MoO_3 at different charge-discharge states. (June 2015 – Complete)

4. Complete the preliminary studies of elemental distribution of Fe substituted high-voltage spinel cathode materials using transmission x-ray microscopy (TXM). (September 2015 – Complete)

Progress Report

This quarter, the fourth milestone for FY 2015 has been completed.

BNL focused on the studies of elemental distribution of Fe substituted high-voltage spinel cathode materials using transmission x-ray microscopy (TXM). To study the elemental distribution of the three transition metal elements across the sample particles, we also performed nondestructive transmission x-ray microscopic (TXM) investigations. In Figure 38, the three-dimensional tomographic results (collected at 8380 eV, above the k edges of all the three transition metal elements: Mn, Fe, and Ni) of a ~10-micron-sized particle (Figure 38a) and several selected slices through different depth (Figures 38c-g) are shown. The three dimensional density distributions within this solid particle are homogeneous. By tuning the x-ray energy, we studied the energy dependency of each single voxel within this volume, and quantitatively retrieved the elemental concentration as indicated in Figure 38b, in which the elemental concentration over the line path highlighted in Figure 38e is plotted. The relative concentration of Mn, Fe, and Ni, shown in Figure 38b, is in good agreement with the expected elemental composition as designed. These results clearly demonstrate that the new material synthesized has a good degree of homogeneity in the structure and chemical distribution with designed composition.

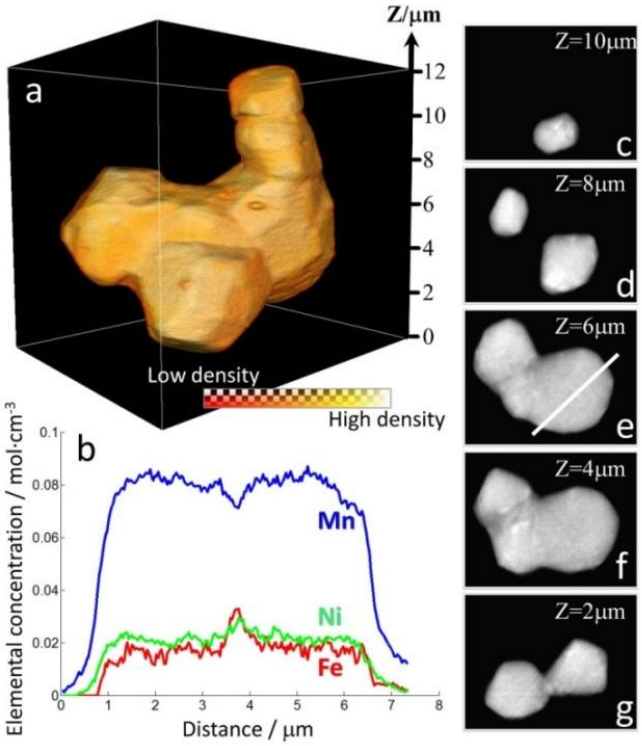

Figure 38. Rendering of the 3D structure of a selected $LiNi_{0.33}Mn_{1.34}Fe_{0.33}O_4$ particle is shown in panel (a) with the scale indicated in the axis and the color legend shown in the inset. Panels (c) through (g) are slices at different depth of the particle, showing that it is a solid piece with no internal pores and the density distribution is relatively homogeneous. The elemental concentration over the line path indicated in panel (e) is plotted in panel (b) (the blue, green, and red curves represent the concentration of Mn, Ni, and Fe, respectively), which is in good agreement with the elemental composition of the material. Panels (a) and (c) through (g) are reconstructed from nano-tomography data collected at 8380 eV (above the absorption k edges of all the three transition metal elements), while the data plotted in panel (b) is retrieved from the evaluation of the energy dependency of the absorption coefficient using a method known as Absorption Correlation Tomography.

Patents/Publications/Presentations

Publications

1. Lyu, Y., and N. Zhao, E. Hu, R. Xiao, X. Yu, L. Gu, X.Q. Yang, and H. Li. "Probing Reversible Multi-electron Transfer and Structure Evolution of $Li_{1.2}Cr_{0.4}Mn_{0.4}O_2$ Cathode Material for Li-ion Batteries in a Voltage Range of 1.0-4.8 V." *Chem. Mater.* 27 (July 2015): 5238.

2. He, Kai, and Feng Lin, Yizhou Zhu, Xiqian Yu, Jing Li, Ruoqian Lin, Dennis Nordlund, Tsu-Chien Weng, Ryan M. Richards, Xiao-Qing Yang, Marca M. Doeff, Eric A. Stach, Yifei Mo, Huolin Xin, and Dong Su*. "Sodiation Kinetics of Metal Oxide Conversion Electrodes: A Comparative Study with Lithiation." *Nano Lett.* 15, no. 9 (August 2015): 5755 – 5763.

3. Xiao, L., and J. Xiao, X. Yu, P. Yan, J. Zheng, M. Engelhard, P. Bhattacharya, C. Wang, X.-Q. Yang, and J.-G. Zhang. "Effects of Structural Defects on the Electrochemical Activation of Li_2MnO_3." *Nano Energy* 16 (September 2015): 143.

Task 5.4 – NMR and Pulse Field Gradient Studies of SEI and Electrode Structure (Clare Grey, Cambridge University)

Project Objective. The formation of a stable solid-electrode interphase (SEI) is critical to the long-term performance of a battery, since the continued growth of the SEI on cycling/aging results in capacity fade (due to Li consumption) and reduced rate performance due to increased interfacial resistance. Although arguably a (largely) solved problem with graphitic anodes/lower voltage cathodes, this is not the case for newer, much higher capacity anodes such as silicon, which suffer from large volume expansions on lithiation, and for cathodes operating above 4.3 V. Thus it is essential to identify how to design a stable SEI. The objectives are to identify major SEI components, and their spatial proximity, and how they change with cycling. SEI formation on Si vs. graphite and high-voltage cathodes will be contrasted. Li+ diffusivity in particles and composite electrodes will be correlated with rate. The SEI study will be complemented by investigations of local structural changes of high-voltage/high-capacity electrodes on cycling.

Project Impact. The first impact of this project will be an improved, molecular based understanding of the surface passivation (SEI) layers that form on electrode materials, which are critical to the operation of the battery. Second, we will provide direct evidence for how additives to the electrolyte modify the SEI. Third, we will provide insight to guide and optimize the design of more stable SEIs on electrodes beyond $LiCoO_2$/graphite.

Out-Year Goals. The goals of this project are to identify the major components of the SEI as a function of state of charge and cycle number different forms of silicon. We will determine how the surface oxide coating affects the SEI structure and establish how the SEI on Si differs from that on graphite and high-voltage cathodes. We will determine how the additives that have been shown to improve SEI stability affect the SEI structure and explore the effect of different additives that react directly with exposed fresh silicon surfaces on SEI structure. Via this program, we will develop new nuclear magnetic resonance (NMR)-based methods for identifying different components in the SEI and their spatial proximities within the SEI, which will be broadly applicable to the study of SEI formation on a much wider range of electrodes. These studies will be complemented by studies of electrode bulk and surface structure to develop a fuller model with which to describe how these electrodes function.

Collaborations. This project collaborates with B. Lucht (Rhode Island); E. McCord, W. Holstein (DuPont); J . Cabana, (UIC); G. Chen, K. Persson (LBNL); S. Whittingham (Binghamton U); P. Bruce (St. Andrews U), R. Seshadri, A. Van der Ven (UCSB), S. Hoffman, A. Morris (Cambridge), N. Brandon (Imperial College), and P. Shearing (University College London).

Milestones

1. Complete initial Si SEI work and submit for publication. Complete 4V spinel work (*in situ* NMR) and submit for publication. (12/31/14 – Complete; paper published in *Angewandte*)
2. Identify differences in Si SEI after one and multiple cycles. (Complete**)**
3. Identify major organic components on the SEIs formed on high surface area carbons by NMR. (Ongoing)
4. Complete initial carbon-SEI interfacial studies. (Complete) *Go/No-Go*: Determine whether NMR has the sensitivity to probe organics on the cathode side in paramagnetic systems. (Delayed – Need to collect more data)

Progress Report

Using Redox Mediators to Cycle Li-oxygen Batteries via LiOH Formation and Decomposition

The commercial use of a lithium-air battery faces many challenges, such as its unrealized high capacity, poor cycling capability and rate performance, low round-trip efficiency, and sensitivity to the presence of H_2O and CO_2. Our recent work (*Science*, October 2015) has shown that we can use the redox mediator LiI to cycle a cell with high efficiency, large capacity and a very low overpotential. Figure 39 shows the electrochemical results for Li-O_2 batteries prepared with a Li metal anode, 0.25 M lithium bis (trifluoromethyl) sulfonylimide (LiTFSI)/dimethoxyethane (DME) electrolyte with and without 0.05 M LiI additive. Hierarchically macroporous reduced graphene oxide (rGO) electrodes were used due to their low mass/large pore volumes, and were compared to mesoporous SP carbon and mesoporous titanium carbide (TiC) electrodes. All these electrodes show good electrochemical stability within a voltage window of 2.4 – 3.5 V in a LiTFSI/DME electrolyte and can be used to reversibly cycle LiI ($I_3^- + 2e^- \leftrightarrow 3I^-$). In the absence of LiI, cells using either mesoporous TiC or macroporous rGO showed much smaller overpotentials during charge, in comparison to that obtained with the SP electrodes. Addition of the redox mediator to the SP electrode, however, led to a noticeable drop in the overpotential over that seen with SP only. The charge voltage profile is not, however, flat, but gradually increases on charging. When LiI is used with rGO electrodes, a flat process is observed at 2.95 V. The discharge overpotential for rGO-based Li-oxygen cells also decreases by 0.15 V (arrows in Figure 39), from 2.6 (SP/TiC) to 2.75 V (rGO, regardless of the use of LiI). Overall, the voltage gap becomes only 0.2 V (indicated by arrows), representing an energy efficiency of 93.2%.

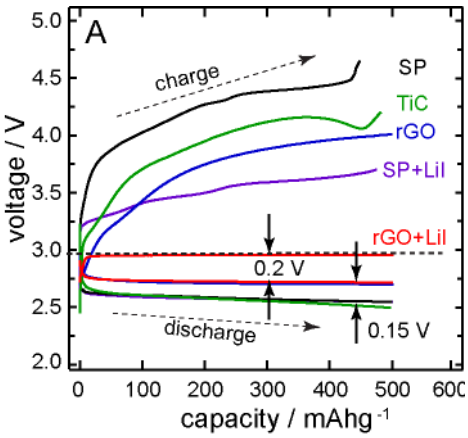

Figure 39. Discharge-charge curves for Li-O_2 cells using mesoporous SP and TiC, and macroporous rGO electrodes, with capacities limited to 500 mAh/g (based on the mass of carbon or TiC) and a 0.25 M LiTFSI/DME electrolyte. For SP and rGO electrodes, 0.05 M LiI was added to the LiTFSI/DME electrolyte in a second set of electrodes (purple and red curves). All cells in were cycled at 0.02 mA/cm². The horizontal dashed line represents the position (2.96 V) of the thermodynamic voltage of a Li-O_2 cell.

LiOH is the only observed crystalline discharge product for LiI/rGO electrodes (x-ray and nuclear magnetic resonance results), the LiOH being removed after a full charge. Without added LiI, Li_2O_2 is the predominant discharge product. A series of experiments performed with deuterated DME and D_2O reveals that trace water impurities are the source of protons in these cells. Cells cycled in the presence of 45,000 ppm of water or with wet air show no deterioration in performance. Optical and SEM images show that the electrode surface is completely covered by micron sized LiOH agglomerates, following discharge. When limiting the specific capacity to 1000, 5000 and 8000 mAh/g_c, the cells show no capacity fade with little increase in voltage polarization after 2000, 300 and 100 cycles, respectively. When cycled at 1 A/g_c, the voltage gap is ~0.2 V; at higher rates the gaps widen to 0.7 V at 8 A/g_c. Although a certain level of scattering in the total capacity is observed, likely due to variations in the electrode structure, the cell capacity is typically 25,000 – 40,000 mAh/g_c (i.e. 2.5 – 4.0 mAh) for an rGO electrode of 0.1 mg and 200 μm thick. This corresponds to a specific energy of approximately 5800 Wh/kg. Mechanistic studies are ongoing.

Task 5.5 – Optimization of Ion Transport in High-Energy Composite Cathodes (Shirley Meng, UC – San Diego)

Project Objective. This project aims to probe and control the atomic-level kinetic processes that govern the performance limitations (rate capability and voltage stability) in a class of high-energy composite electrodes. A systematic study with powerful suite of analytical tools [including atomic resolution scanning transmission electron microscopy (a-STEM) and Electron energy loss spectroscopy (EELS), X-ray photoelectron spectroscopy (XPS) and first principles (FP) computation] will be used to pin down the mechanism and determine the optimum bulk compositions and surface characteristics for high rate and long life. Moreover, it will help the synthesis efforts to produce materials at large scale with consistently good performance. It is also aimed to extend the suite of surface-sensitive tools to diagnose the silicon anodes types.

Project Impact. If successful, this research will provide a major breakthrough in commercial applications of the class of high energy density cathode material for lithium ion batteries. Additionally, it will provide in-depth understanding of the role of surface modifications and bulk substitution in the high-voltage composite materials. The diagnostic tools developed here can also be leveraged to study a wide variety of cathode and anode materials for rechargeable batteries.

Approach. Unique approach that combines STEM/EELS, XPS, and *ab initio* computation as quantities diagnostic tools for surface and interface characterization and to enable quick identification of causes of surface instability (or stability) in various electrode materials including both high-voltage cathodes and low-voltage anodes.

Out-Year Goals. The goal is to control and optimize Li-ion transport, transition metal (TM) migration, and oxygen activity in the high-energy composite cathodes and to optimize electrode/electrolyte interface in silicon anodes so that their power performance and cycle life can be significantly improved.

Collaborations. This project engages in collaborations with the following:

- Michael Sailor (UCSD) – Porous silicon and carbonization of silicon based anodes
- Keith Stevenson (UT Austin) – XPS and Time-of-Flight Secondary Ion Mass Spectrometry (TOF-SIMS)
- Nancy Dudney and Juchuan Li (Oak Ridge National Lab) – Silicon thin film fabrication
- Chunmei Ban (National Renewable Energy Laboratory) – Molecular layer deposition
- Envia Systems – Materials supplies, high Li-rich and low-Li-rich
- Zhaoping Liu and Yonggao Xia [Ningbo Institute of Materials Technology and Engineering (NIMTE), Chinese Academy of Sciences]

Milestones

1. Identify at least two high-voltage cathode materials that deliver 200mAh/g reversible capacity when charged to high voltages. (12/31/14 – Complete)
2. Obtain the optimum surface coating and substitution compositions in lithium rich layered oxides when charged up to 4.8V (or 5.0 V). (3/31/15 –Complete)
3. Identify the appropriate SEI characteristics and microstructure for improving first-cycle irreversible capacity of silicon anode. (Improve to 85-95%; 9/30/15 – Complete)
4. Identify the mechanisms of ALD and MLD coated silicon anode for their improved chemical stability upon long cycling. (12/30/15 – On Track)
5. Identify the path-specific lithium dynamics in lithium rich layered oxides. Compare high Li-rich (HLR), $Li_{1.193}$ material, and low Li-rich (LLR), $Li_{1.079}$ material. (12/30/15 – On Track)

Progress Report

***Operando* neutron diffraction observation of path-specific lithium dynamic.** Operando neutron diffraction was used to investigate and quantify the lithium migration dynamics of various transition metal cathodes upon battery cycling. In particular, high Li-rich $Li_{1.193}Ni_{0.154}Co_{0.106}Mn_{0.547}O_2$ (HLR) and low Li-rich $Li_{1.079}Ni_{0.251}Co_{0.262}Mn_{0.408}O_2$ (LLR) that exhibit different degrees of oxygen activation at high voltage were examined. Based on the $R\bar{3}m$ layered structure, two different lithium sites exist within the Li-rich layered oxide cathode. Most of the lithium ions are located in the lithium layer, while the excess lithium ions are located in transition metal (TM) layer. Figure 40 demonstrates the lithium dynamics from HLR and LLR cathodes. First, the extraction of lithium in the slope region is largely dominated by its migration within the lithium layer. In region 2, the lithium migration within the lithium layer decreases, and the migration from the TM layer occurs. Upon discharge, lithium ions from the TM layer are largely irreversible. After the first cycle, the lithium content in HLR and LLR TM layer irreversibly decreased from its open circuit voltage to 29% and 33%, respectively. These results shed light into the lithium migration behavior and demonstrate the unique capabilities that one can observe light elements in bulk under *operando* neutron diffraction.

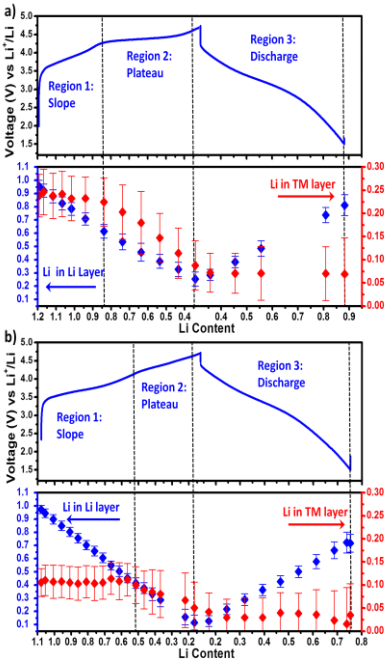

Figure 40. Electrochemical charge/ discharge profile with corresponding lithium occupancy at different states of delithiation/ lithiation for (a) HLR and (b) LLR.

Visualization and chemical composition the SEI on silicon. Herein, a-STEM/EELS and XPS were used to directly decipher the effect fluoethylene electrolyte additive on the solid-electrolyte interphase (SEI). Given that lithiated silicon and the SEI are extremely sensitive, the electron dose and spatial resolution were optimized. Figure 41 shows the annular dark-field (ADF) STEM images of lithiated silicon nanoparticles cycled with EC/DEC and EC/DEC/FEC electrolyte at cycle 1 and 5. The electrode cycled in EDEC/FEC are covered by a dense and uniform SEI layer; however, the electrode cycled with EC/DEC forms a porous uneven SEI. More importantly, a-STEM/EELS is a local technique that focuses on single particles; therefore, XPS analysis was conducted in order to analyze a larger sample area. Figure 42 demonstrates the chemical evolution throughout electrochemical cycling for electrodes cycled with EC/DEC and EC/DEC/FEC. In the first lithiation, the electrode cycled in EC/DEC has a higher atomic percentage of RCO, ROCO, and Li_X than its counterpart. Here, Li_X corresponds to alkyl lithium, inorganic lithium oxide, and lithium phosphor-oxy-fluoride compounds. After 100 cycles, the electrode cycled in EC/DEC contained higher amount of carbonate species (CO_3) and less LiF. On the other hand, the electrode cycled in EC/DEC/FEC contained fewer carbonate species and more LiF. These results correlate well with the a-STEM/EELS results.

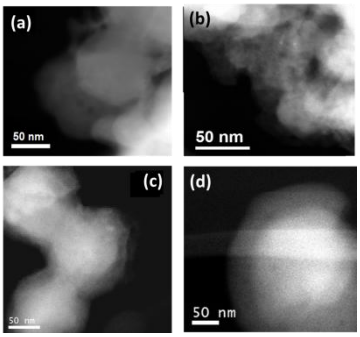

Figure 41. ADF-STEM images of the lithiated silicon nanoparticles cycled in EC/DEC at (a) 1 cycle and (b) 5 cycles. Electrodes cycled in EC/DEC/FEC at (c) 1 cycle and (d) 5 cycles.

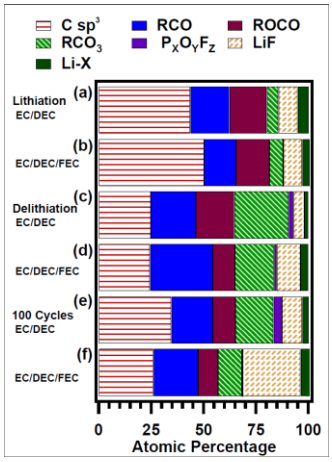

Figure 42. Relative composition of the SEI after (a, b) first lithiation, (c, d) first delithiation, and (e, f) 100 cycles in the delithiated state.

Patents/Publications/Presentations

Publication

- Liu, H.D., and Y. Chen, S. Hy, K. An, S. Venkatachalam, D. Qian, M. Zhang, and Y.S. Meng. "*Operando* Lithium Dynamics in the Li-Rich Layered Oxide Cathode Material via Neutron Diffraction." (to be submitted)

Presentations

- 228th Electrochemical Society Meeting, Symposium A02, Phoenix (August 2015 – Invited): "Probing Interface Stability and Oxygen Activities in Li Rich Mn Rich Layered Oxides"; Shirley Meng.
- Joint NSRC Workshop, ORNL (June 2015 – Poster): "STEM Characterization for Oxygen Activities in Li-rich Layered Oxides for High Energy Li-ion Batteries"; Minghao Zhang, Bao Qiu, Danna Qian, Haodong Liu, and Ying Shirley Meng.
- Microscopy and Microanalysis, Portland, Oregon (August 2015 – Poster): "Comprehensive insights into the SEI layer formation of Silicon anode using STEM/EELS"; M. Sina, J. Alvarado, H. Shobukawa, and Y.S. Meng.

Task 5.6 – Analysis of Film Formation Chemistry on Silicon Anodes by Advanced *In situ* and *Operando* Vibrational Spectroscopy
(Gabor Somorjai, UC – Berkeley; Phil Ross, Lawrence Berkeley National Laboratory)

Project Objective. Understand the composition, structure, and formation/degradation mechanisms of the solid-electrolyte interphase (SEI) on the surfaces of Si anodes during charge/discharge cycles by applying advanced *in situ* vibrational spectroscopies. Determine how the properties of the SEI contribute to failure of Si anodes in Li-ion batteries in vehicular applications. Use this understanding to develop electrolyte additives and/or surface modification methods to improve Si anode capacity loss and cycling behavior.

Project Impact. A high-capacity alternative to graphitic carbon anodes is Si, which stores 3.75 Li per Si versus 1 Li per 6 C yielding a theoretical capacity of 4008 mAh/g versus 372 mAh/g for C. But Si anodes suffer from large first cycle irreversible capacity loss and continued parasitic capacity loss upon cycling leading to battery failure. Electrolyte additives and/or surface modification developed from new understanding of failure modes will be applied to reduce irreversible capacity loss, and to improve long-term stability and cyclability of Si anodes for vehicular applications.

Approach. Model Si anode materials including single crystals, e-beam deposited polycrystalline films, and nanostructures are studied using baseline electrolyte and promising electrolyte variations. A combination of *in situ* and *operando* Fourier Transform Infrared (FTIR), Sum Frequency Generation (SFG), and UV-Raman vibrational spectroscopies are used to directly monitor the composition and structure of electrolyte reduction compounds formed on the Si anodes. Pre-natal and post-mortem chemical composition is identified using x-ray photoelectron spectroscopy. The Si films and nanostructures are imaged using scanning electron microscopies.

Out-Year Goals. Extend the study of interfacial processes with advanced vibrational spectroscopies to high-voltage oxide cathode materials. The particular oxide to study will be chosen based on materials of interest at that time and availability of the material in a form suitable for these studies (for example, sufficiently large crystals or sufficiently smooth/reflective thin films). The effect of electrolyte composition, electrolyte additives, and surface coatings will be determined, and new strategies for improving cycle life will be developed.

Collaborations. The project did not engage in collaboration this period.

Milestones

1. Determine the reduction products of the electrolyte additive FEC on a characteristic Si electrode and relate composition to the function in cycling. (December 2014 – Complete)
2. Determine the role of $–O_x$ and –OR (R = H, CH_3, C_2H_5, etc.) surface functional groups on baseline electrolyte reduction chemistry. (March 2015 – Completed)
3. Determine role of the Si surface morphology (for example, roughness) on the SEI formation structure and cycling properties. (June 2015 – Complete)
4. *Go/No-Go*: Feasibility of surface functionalization to improve SEI structure and properties. Criteria: Functionalize a model Si anode surface, and determine how SEI formation is changed. (September 2015 – Complete)

Progress Report

This quarter, we studied a common electrolyte, 1.0 M $LiPF_6$: ethylene carbonate (EC): diethyl carbonate (DEC), reduction products on crystalline silicon (Si) electrodes in a lithium (Li) half-cell system under reaction conditions. We employed sum frequency generation vibrational spectroscopy (SFG-VS) with interface sensitivity to probe the molecular composition of the solid-electrolyte interphase (SEI) surface species under various applied potentials where electrolyte reduction is expected. We found that in Si(100)-hydrogen terminated, a Si-ethoxy ($Si\text{-}OC_2H_5$) surface intermediate forms due to DEC decomposition. Other main products are lithium ethyl-dicarbonate (LiEDC) and poly-EC that are common SEI components in both oxide and hydrogen terminated crystalline Si.

Our results suggest that the SEI surface composition varies depending on the termination of Si surface, that is, the acidity of the Si surface. We provide the evidence of specific chemical composition of the SEI on the anodes *surface* under reaction conditions. This supports an electrochemical electrolyte reduction mechanism in which the reduction of DEC molecule to an ethoxy moiety plays a key role.

We took the SFG-VS spectra under working conditions at three potential ranges. The voltagram shown in Figure 43 was taken with a Si(100) hydrogen terminated surface, and has three reduction peaks at ~ 1.5 V, ~ 0.5 V, and ~ 0.10 V that are consistent with values reported in the literature.

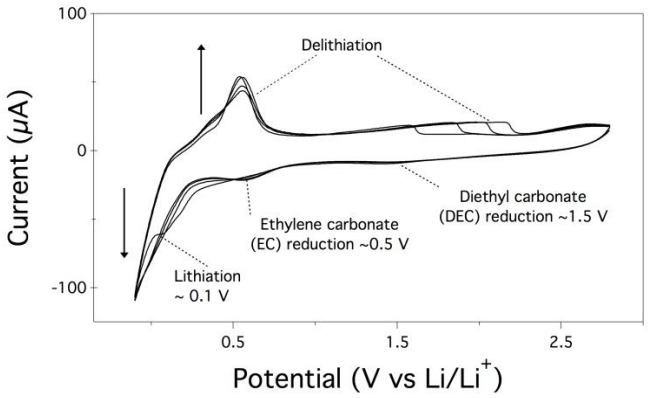

Figure 43. The three reduction peaks at a Si(100)-H anode of the electrolyte (1.0 M LiPF6 in EC : DEC, 1:2 v/v) are presented in this cyclic-voltagram. The reduction of DEC is around 1.5 V. The reduction of EC is about 0.5 V, and Li intercalation (lithiation) occurs around 0.10 V. Scan rate was 1mV/sec.

In Figure 44a, Si(100)-H electrode, we show the divided SFG spectrum after applying a 30 cycle cyclic-voltammetry potential near 1 V by the SFG in OCP. Dividing the SFG spectra emphasizes the appearance of ethoxy group vibrational peaks (black line). The SFG from the Si/SEI is interfered with the SFG generated from the Si substrate. We assume that if an intermediate specie ethoxy radical $^{\bullet}OCH_2CH_3$ (or anion, $^{-}OCH_2CH_3$) is formed near the Si anode surface it will react with Si-H to produce a $Si\text{-}OCH_2CH_3$ bond. This reaction cannot take place if a passivating oxide layer is present. In Figure 44a, we assigned the SFG peaks corresponding to Si-ethoxy bonds and SFG signals relating to the various SEI components as follows: 2875 cm^{-1} ($s\text{-}CH_3$), 2895 cm^{-1} ($s\text{-}OCH_2$), and at 2975 and 3000 cm^{-1} (both $as\text{-}OCH_2$).

After a 30 cycle cyclic voltammetry (CV) at ~ 0.5 V (blue line), we observed peaks appearing at 2845 cm^{-1} ($s\text{-}CH_2$), 2895 cm^{-1} ($s\text{-}OCH_2$), 2920 cm^{-1} ($as\text{-}CH_2$) and 2985 cm^{-1} ($as\text{-}OCH_2$). These reduction reactions are attributed to the beginning of the SEI formation. The SFG spectra taken after 30 CV between 0.1 V and -0.05 V (red line) show increasing peaks at 2850 cm^{-1}, and 2960 cm^{-1}, presumably due to the formation of LiEDC and poly-EC. The peaks broaden due to surface deterioration after lithiation.

In the case of Si(100) oxide we did not observe any change at ~ 1 V, therefore, we extended the CV potential range. In Figure 44b, we compare the SFG spectra of crystalline Si(100) oxide surface before and after lithiation. We preformed a potential sweep in the range of 0.5 V to 2.0V (blue profile) and between -0.05 V to 3.0 V. Each CV had 30 cycles and the rate was 1mV/sec. The SFG profile of the first potential range (blue) has some SEI features but none that are related to a Si-O to Si-OC_2H_5 substitution reaction. After lithiation (red) prominent peaks appear and we assign them accordingly: 2817 cm^{-1} (s-CH_2), 2848 cm^{-1} (s-CH_3), 2895 and 2908 cm^{-1} (both as-CH_2), 2960 cm^{-1} (as-CH_3), 2985 and 3022 cm^{-1} (both as-OCH_2).

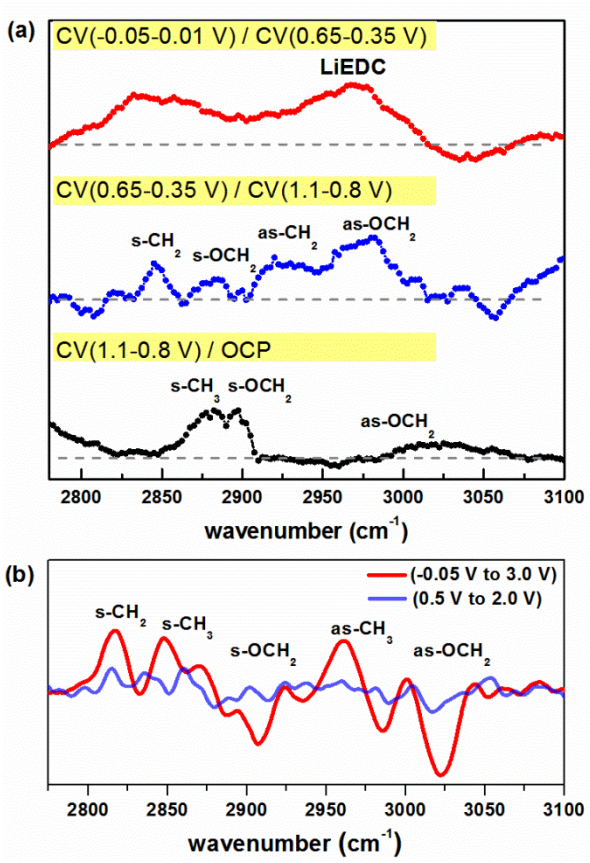

Figure 44. (a) The evolution of SFG signal under reaction conditions of crystalline silicon Si(100)-hydrogen terminated anode. The SFG spectra were taken at open circuit potential and after cyclic-voltammetry at: 1.1 V ↔ 0.8 V, 0.65 V ↔ 0.35 V and 0.1 V ↔ -0.05 V. To emphasize the evolution of the Si-ethoxy peaks, we divided the SFG spectra by their former potentials, as follows: SFG1.1 V ↔ 0.8 V / OCP (black), SFG0.65 V ↔ 0.35 V / SFG1.1 V ↔ 0.8 V (blue) and SFG-0.05 V ↔ 0.1 V / SFG0.65 V ↔ 0.35 V (red). (b) The SFG profiles of crystalline silicon oxide Si(100) anode after cycling between 0.5 V ↔ 2.0 V (blue) and -0.05 V ↔ 3.0 V (red). All CVs were repeated for 30 cycles at a scan rate of 1mV/sec.

In conclusion, we have observed that the Si hydrogen terminated layer has been changed to Si-ethoxy (Si-OCH_2CH_3) at ~ 1.0 V in the presence of 1.0 M $LiPF_6$ in EC: DEC. The role of each electrolyte component (EC and DEC) was investigated separately. This substitution reaction at ~1.0 V did not take place when we changed the electrolyte to 1.0 M $LiPF_6$ in EC or when the Si(100)-O_x was used as the anode material. When we further reduced the potential to ~ 0.5 V only poly-EC and LiEDC formation was observed. Further *in operando* spectroelectrochemical (SFG-VS) experiments of EC at reduction potentials of ~ 1.0 V and ~ 0.5 V suggests that it has been possibly reduced to poly-EC but no Si-ethoxy termination was detected.

Future SFG-VS experiments in the C=O carbonyl stretch range are planned, as well as determining the role of Si surface morphology (for example, roughness) on the SEI formation structure and cycling properties. In 2016 we will apply the same successful methodology in researching the cathode material spinel $LiMn_{1.5}Ni_{0.5}O_4$ (LMNO) and its variants.

Patents/Publications/Presentations

Publication

- Horowitz, Yonatan, and Hui-Ling Han, Philip N. Ross, and Gabor A. Somorjai. "Potentiodynamic Analysis of Electrolyte Reactions with Silicon Electrodes Using Sum Frequency Generation Vibrational Spectroscopy Study." Submitted to *J. Am. Chem. Soc.*

Task 5.7 – Microscopy Investigation on the Fading Mechanism of Electrode Materials (Chongmin Wang, Pacific Northwest National Laboratory)

Project Objective. The objective of this work is to use *ex-situ*, *in situ*, and *operando* high-resolution transmission electron microscopy (TEM) and spectroscopy to probe the fading mechanism of electrode materials. The focus of the work will be on using *in situ* TEM under real battery operating conditions to probe the structural evolution of electrodes and interfaces between the electrode and electrolyte and correlate this structural and chemical evolution with battery performance. The following three questions will be addressed:

- How do the structure and chemistry of electrode materials evolve at a dimension ranging from atomic-scale to meso-scale during the charge and discharge cycles?
- What is the correlation of the structural and chemical change to the fading and failure of lithium (Li)-ion batteries?
- How does the interface evolve between the electrode and the electrolyte and their dependence on the chemistry of electrolytes?

Project Impact. Most previous microscopic investigations on solid-electrolyte interphase (SEI) layer formation and morphology evolution on electrodes are either *ex situ* studies or used low-vapor-pressure electrolytes so they cannot reveal the details of the dynamic information under practical conditions. We have developed new *operando* characterization tools to characterize SEI formation and electrode/electrolyte interaction using practical electrolyte that are critical for making new breakthroughs in this field. The success of this work will increase the energy density of Li-ion batteries and accelerate market acceptance of electrical vehicles (EV), especially for plug-in hybrid electrical vehicles (PHEV) required by the EV Everywhere Grand Challenge proposed by the DOE Office of Energy Efficiency and Renewable Energy (EERE).

Approach. Extend and enhance the unique *ex situ* and *in situ* TEM methods for probing the structure of Li-ion batteries, especially for developing a biasing liquid electrochemical cell that uses a real electrolyte in a nano-battery configuration. Use various microscopic techniques, including *ex situ*, *in situ*, and especially the *operando* TEM system, to study the fading mechanism of electrode materials in batteries. This project will be closely integrated with other research and development efforts on high-capacity cathode and anode projects in the BMR Program to 1) discover the origins of voltage and capacity fading in high-capacity layered cathodes and 2) provide guidance for overcoming barriers to long cycle stability of silicon (Si)-based anode materials.

Out-year goals: The out-year goals are as follows:

- Extended the *in situ* TEM capability for energy storage technology beyond Li ions, such as Li-S, Li-air, Li-metal, sodium ions, and multi-valence ions.
- Multi-scale (that is, ranging from atomic-scale to meso-scale) *in situ* TEM investigation of failure mechanisms for energy-storage materials and devices (both cathode and anode).
- Integration of the *in situ* TEM capability with other microscopy and spectroscopy methods to study energy-storage materials, such as *in situ* SEM, *in situ* SIMS, and *in situ* x-ray diffraction.
- Atomic-level *in situ* TEM and scanning transmission electron microscopy (STEM) imaging to help develop a fundamental understanding of electrochemical energy-storage processes and kinetics of both cathodes and anode.

Collaborations: We are collaborating with the following principal investigators: Dr. Chunmei Ban (NREL); Dr. Gao Liu (LBNL); Dr. Khalil Amine (ANL); Professor Yi Cui (Stanford); Dr. Jason Zhang (PNNL); Dr. Jun Liu (PNNL); Dr. Guoying Chen (LBNL); and Dr. Xingcheng Xiao (GM).

Milestones

1. Establish the methodology that enables reliably positioning a nanowire on the chip to assembly the closed liquid cell. Complete the *in situ* TEM study of the behavior of native oxide layer during lithiation and delithiation. (12/31/2014 – Complete)
2. Complete quantitative measurement of coating layer and SEI layer thickness as a function of cycle number on a Si anode in a liquid cell with a practical electrolyte. (03/31/2015 – Complete)
3. Complete the *operando* TEM study of cathode materials with/without coating layer and the SEI layer formation. (9/30/2015 – Complete)

Progress Report

The recent work reveals that cycling of the layer structured cathodes at a high cut-off voltage leads to the formation of a P-rich SEI layer on their surface, indicating decomposition of Li-salt ($LiPF_6$). A systematic investigation indicates such cathode/Li-salt side reaction shows strong dependence on structure of the cathode, operating voltage and temperature. These findings provide valuable insights on the complex interface between the high-voltage cathode and the electrolyte, indicating the feasibility of solid-electrolyte interphase (SEI) engineering to mitigate the capacity and voltage fading of battery. For rechargeable lithium ion battery, SEI layer has been perceived to play critical role for the stable operation of the batteries. However, the structure and chemical composition of SEI layer and its spatial distribution and dependence on the battery operating condition remain unclear. The structure and chemistry of SEI layer on high voltage cathodes have been explored by using (STEM energy dispersive spectroscopy) to investigate the chemical composition and elemental spatial distribution with high resolution of SEI layer formed on the very surface of cathodes that were cycled at a high cut-off voltage (4.7 V) in this work. As typically illustrated in Figure 45, it was found that a significant amount of phosphorus (P) appears in the cathode SEI layer in addition to other well-known elements, such as C, O and F. Such P-rich SEI layer presents direct evidence of side reactions between cathodes and $LiPF_6$ containing electrolyte. Further studies show that these side reactions can be significantly aggravated at elevated temperature (60°C) but reduced by cycling within a low cut-off voltage (4.2V vs Li/Li^+,) window.

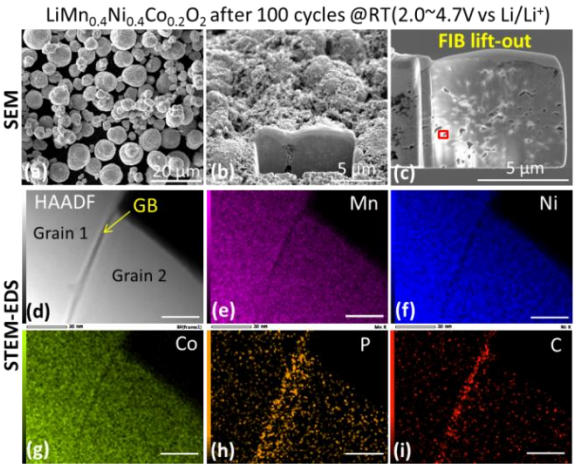

Figure 45. SEM images of (a) pristine agglomerated particles, (b) and (c) TEM specimen prepared by FIB lift-out techniques from cycled electrode. (d-i) STEM-EDS mapping results from the boxed region in (c). The scale bars are 30 nm in (d-i).

Interestingly, high cut-off voltage does not always result in a P-rich SEI layer. When $LiMn_{1.5}Ni_{0.5}O_4$ spinel cathode was cycled between 3.0 V and 5.0V vs Li/Li^+ for 45 cycles, no appreciable P signal can be identified on the surface of cathode. This likely indicates that spinel type lithium transition metal oxide cathode has negligible side reaction with Li salt during battery cycling and its surface chemistry is significantly different from the layered lithium transition metal oxides, which seems to support the previous reports that high voltage spinels exhibit high surface stability. Therefore, the extent of the cathode side reaction also closely related to the cathode materials used, indicating that structure and composition of cathode material also play an important role in the electrolyte decomposition. It can be generally concluded that P enrichment is a general characteristic for the SEI layer of various high voltage layered cathodes, which is attributed to side reactions between cathode and Li-salt. The results also demonstrate that Li-salt decomposition increases with increasing temperature. Based on the P content observed on the SEI layers formed in the six cathodes, the

electrolyte experiences decreasing stability in the following order: $LiMn_{1.5}Ni_{0.5}O_4$ > NCM424 > NCA > NC-LMR ≈ 20N-LMR > Li_2MnO_3. The results indicate that side reactions between electrolyte and cathodes are strongly dependent on cathode structure and chemical composition. These findings can further our understanding in the composition of SEI and provide valuable knowledge regarding the SEI formation mechanism which, in turn is very helpful for future development of lithium-ion batteries.

Patents/Publications/Presentations

Publication

- Yan, Pengfei, and Jianming Zheng, Dongping Lu, Yi Wei, Jiaxin Zheng, Zhiguo Wang, Saravanan Kuppan, Jianguo Yu, Langli Luo, Danny Edwards, Matthew Olszta, Khalil Amine, Jun Liu, Jie Xiao, Feng Pan, Guoying Chen, Ji-Guang Zhang, and Chong-Min Wang. "Atomic-Resolution Visualization of Distinctive Chemical Mixing Behavior of Ni, Co, and Mn with Li in Layered Lithium Transition-Metal Oxide Cathode Materials." *Chem. Mater*. 27 (2015): 5393−5401.

Presentations

- Microscopy and Microanalysis, Portland, Oregon (August 2015): "Charge Discharge Cycling Induced Structure and Chemical Evolution of Li_2MnO_3 Cathode for Li ion Batteries"; Pengfei Yan, Jianming Zheng, Ji-Guang Zhang, and Chong-Min Wang.
- Microscopy and Microanalysis, Portland, Oregon (August 2015): "Structural and Chemical Evolution of Li and Mn Rich Layered Oxide Cathode and Correlation with Capacity and Voltage Fading"; Chong-Min Wang, Pengfei Yan, and Ji-Guang Zhang.

Task 5.8 – Energy Storage Materials Research Using DOE's User Facilities and Beyond (Michael M. Thackeray and Jason R. Croy, Argonne National Laboratory)

Project Objective. The primary objective of this project is to explore the fundamental, atomic-scale processes that are most relevant to the challenges of next-generation, energy-storage technologies. A deeper understanding of these systems will rely on novel and challenging experiments that are only possible through unique facilities and resources. The goal of this project is to capitalize on a broad range of facilities to advance the field through cutting-edge science, collaborations, and multi-disciplinary efforts.

Project Impact. This project is being implemented to capitalize on and exploit DOE's user facilities and other accessible national and international facilities (including skilled and trained personnel) in order to produce knowledge to advance energy-storage technologies. Specifically, furthering the understanding of structure-electrochemical property relationships and degradation mechanisms will contribute significantly to meeting the near-to-long term goals of electric vehicle (EV) and plug-in hybrid electric vehicle (PHEV) battery technologies.

Approach. A wide array of unique capabilities including x-ray and neutron diffraction, x-ray absorption, emission and scattering, high-resolution transmission electron microscopy, Raman spectroscopy, and theory will be brought together to focus on challenging experimental problems. Combined, these resources promise an unparalleled look into the structural, electrochemical, and chemical mechanisms at play in novel, complex electrode/electrolyte systems being explored at Argonne National Laboratory.

Out-Year Goals. The out-year goals are as follows:

- Gain new, fundamental insights into complex structures and degradation mechanisms of composite cathode materials from novel, probing experiments carried out at user facilities and beyond.
- Investigate structure-property relationships that will provide insight into the design of improved cathode materials.
- Use the knowledge and understanding gained from this project to develop and scale up advanced cathode materials in practical lithium-ion prototype cells,

Collaborators. This project engages in collaboration with Joong Sun Park, as well as Chongmin Wang and Pangfei Yan of PNNL.

Milestones

1. Evaluation of lithium-ion battery electrodes using DOE User Facilities at Argonne (Advanced Photon Source, Electron Microscopy Center, and Argonne Leadership Computing Facility) and facilities elsewhere, for example., neutron spallation sources at Spallation Neutron Source (Oak Ridge). Other facilities include the neutron facility ISIS, Rutherford Laboratory (UK), and the NUANCE characterization center (Northwestern University) and PNNL's Environmental Molecular Sciences Laboratory (EMSL). (September 2015 – In Progress, see text)

2. Evaluation of Li_2MnO_3 end member and composite $Li_2MnO_3 \bullet (1\text{-}x)LiMO_2$ (M = Mn, Ni, Co) structures by combined neutron/x-ray diffraction. (September 2015 – In Progress)

3. Evaluation of transition metal migration in lithium-metal-oxide insertion electrodes. (September 2015 – In Progress)

4. Analysis, interpretation, and dissemination of collected data for publication and presentation. (September 2015 – In Progress)

Progress Report

Recent electrochemical results on 'layered-layered-spinel' (LLS) $y[xLi_2MnO_3 \bullet (1-x)LiMO_2] \bullet (1-y)LiM_2O_4$ (for example, M = Mn, Ni, Co) cathode materials have revealed the possibility of obtaining capacities of ~200 mAh/g or more with stable cycling, even with compositions that are relatively rich in manganese. The major challenge associated with the further development of these materials is the ability to systematically control both the elemental and structural compositions within the cathode particles. Current work is focused on identifying optimized end-member 'layered-layered' (LL) $xLi_2MnO_3 \bullet (1-x)LiMO_2$ materials as well as spinel LiM_2O_4 compositions that, when structurally integrated, may lead to stable bulk structures and "customized" voltage profiles well-suited for high-capacity cycling. Understanding and characterizing the effects of synthesis conditions on the elemental distribution and structural architecture is critical for designing optimized cathode materials to realize the full potential of these complex systems.

Figure 46a shows the first-charge voltage profiles of three lithium half-cells with 'layered-layered-spinel' cathodes, with a targeted 10% spinel content, that were derived from a lithium deficient, Ni-rich $0.25Li_2MnO_3 \bullet 0.75LiNi_{0.75}Mn_{0.125}Co_{0.125}O_2$ (LL) precursor. The cathodes were synthesized under different conditions. Depending on the annealing temperature and atmosphere (750 – 850°C, O_2 or air), the first-cycle activation plateaus are clearly not the same (circled), revealing differences in the structural arrangements and compositions, as well as the electrochemical properties of the cathode materials. Figure 46b-c shows scanning transmission electron microscopy (STEM) images, obtained at PNNL's Environmental Molecular Sciences Laboratory (EMSL), of cathode particles when annealed in air at 850°C. Interestingly, the STEM images reveal multi-domain structures within single, well-crystallized particles interspersed with complex, disordered and rock salt-like domains. These images, combined with previous TEM data, illustrate an important inherent property of these complex materials. Although long-range techniques like X-ray diffraction often show typical signatures of well-layered materials, local environments, as can only be revealed by powerful techniques such as STEM, are quite often much more complex. These complex, local environments can significantly alter the macroscopic and electrochemical behavior of composite electrode structures. While nominally denoted as $y[xLi_2MnO_3 \bullet (1-x)LiMO_2] \bullet (1-y)LiM_2O_4$ (relative to a Li_2MnO_3-$LiMO_2$-LiM_2O_4 phase diagram), it is probable that the cation distribution leads to localized and incoherent structures with intermediate layered/spinel character. Nevertheless, electrochemical results show unequivocally that the reducing the lithium content slightly in high capacity 'layered-layered' electrode structures provides important benefits to cathode performance. Efforts are being continued to exploit the wide phase space of 'layered-layered-spinel' cathode materials, which is largely unexplored, to further our understanding of this class of cathode materials.

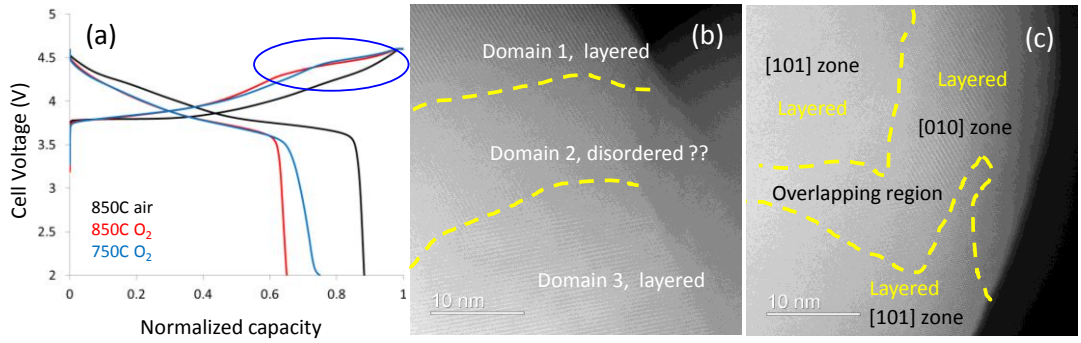

Figure 46. (a) Voltage profiles of Li/$0.25Li_2MnO_3 \bullet 0.75LiNi_{0.75}Mn_{0.125}Co_{0.125}O_2$ half-cells with a targeted 10% spinel component in the cathode, synthesized under different conditions; Black: annealed in air at 850°C; Blue: annealed in O_2 at 750°C; and Red: annealed in O_2 at 850°C. (b) and (c) STEM images of complex domain structures formed in cathode compositions when annealed in air at 850°C.

Patents/Publications/Presentations

Publications

- Thackeray, M.M., and J.R. Croy, E. Lee, J.S. Park, B.R. Long, O. Kahvecioglu Feridun, Y. Shin, G.K. Krumdick, J.G. Wen, D.J. Miller, J. Wu, Q. Li, and V. Dravid. "Addressing the Instability of High Capacity Lithium Battery Cathodes." ECS Conference on Electrochemical Energy Conversion and Storage with SOFC-XIV, Glasgow, Scotland (July 27-30, 2015 – Invited).
- Croy, Jason R., and K. Gallagher, M. Balasubramanian, J.S. Park, B.R. Long, and M.M. Thackeray. "High Energy Lithium-Ion Research and Development at Argonne National Laboratory." IAOEES-EEST Vancouver, Canada (August 16-22, 2015 – Invited).

Lecture

- Croy, Jason R., and Joong Sun Park, Kevin G. Gallagher, Brandon R. Long, Michael M. Thackeray, Mahalingam Balasubramanian, Fulya Dogan, Matthew Suchomel, Dean Miller, and Jianguo Wen. "High-Energy, Composite, Lithium-Ion Cathodes." Argonne Outloud Public Lecture Series, Lemont, Illinois, (September 2015 – Invited).

TASK 6 – MODELING ADVANCED ELECTRODE MATERIALS

Summary and Highlights

Achieving the performance, life, and cost targets outlined in the EV Everywhere Grand Challenge will require moving to next generation chemistries, such as higher capacity Li-ion intercalation cathodes, silicon and other alloy-based anodes, lithium metal anode, and sulfur cathodes. However, numerous problems plague the development of these systems, from material level challenges in ensuring reversibility to electrode level issues in accommodating volume changes, to cell-level challenges in preventing cross talk between the electrodes. In this task, a mathematical perspective is applied to these challenges in order to provide an understanding of the underlying phenomenon and to suggest solutions that can be implemented by the material synthesis and electrode architecture groups.

The effort spans multiple length sales from *ab initio* methods to continuum-scale techniques. Models are combined with experiments, and extensive collaborations are established with experimental groups to ensure that the predictions match reality. Efforts are also focused on obtaining the parameters needed for the models, either from lower length scale methods or from experiments. Projects also emphasize pushing the boundaries of the modeling techniques used to ensure that the task stays at the cutting edge.

In the area of intercalation cathodes, the effort is focused on understanding the working principles of the high Ni layered materials with an aim of understanding structural changes and the associated changes in transport properties. In addition, focus is paid to the assembling of porous electrodes with particles to predict the conduction behavior and developing tools to measure electronic conduction. In this quarter, the lithium diffusion process in the excess-lithium material was studied. The results suggest that the insertion of a lithium results on fluctuations away from the minimum configuration in the nearest 4 to 6 neighbors. In the area of new disordered materials, the project has discovered a new disordered material, $Li_{1.25}Nb_{0.25}Mn_{0.}5O_2$. As synthesized this material delivers a large initial discharge capacity of 287 mAh/g. Finally, to understand how cathodes are assembled, the dynamic packing model (DPP) was compared to experimental process parameters. The following properties were compared: slurry viscosity, elasticity of the dried film, shrinkage ratio during drying, volume fraction of phases, slurry and dried film densities, and microstructure of cross sections.

In the area of silicon anodes, the effort is in trying to understand the interfacial instability and suggest ways to improve the cyclability of the system. In addition, effort is focused on designing artificial solid-electrolyte interphase (SEI) layers that can accommodate the volume change, and in understanding the ideal properties for a binder to accommodate the volume change without delamination. A mesoscale model was developed for SEI growth with input from the first principles analysis on the rate of reaction. Work also continued on understanding the nature of the SEI and the conduction through it.

In the area of sulfur cathodes, the focus is on developing better models for the chemistry with the aim of describing the precipitation reactions accurately. Efforts are focused on performing the necessary experiments to obtain a physical picture of the phase transformations in the system and in measuring the relevant thermodynamic, transport, and kinetic properties. In addition, changes in the morphology of the electrode are described and tested experimentally. Work continued this quarter to understand the impact of film resistance on performance.

Finally, microstructure models are an area of focus to ensure that the predictions move away from average techniques to more sophisticated descriptions of processes inside electrodes. Efforts are focused on understanding conduction within the electrode and on incorporating the intricate physics of the various processes in the battery electrode. These efforts are combined with tomography information as input into the models. This quarter, a comparison was made between the "Newman" model (where the parameters are averaged) and the microstructure model (which includes tomographic information). The two models were compared to rate data on the NMC cathode, and clear differences are seen in the two approaches. Work is underway to understand these differences.

Task 6.1 – Electrode Materials Design and Failure Prediction (Venkat Srinivasan, Lawrence Berkeley National Laboratory)

Project Objective: The goal of this project is to use continuum-level mathematical models along with controlled experiments on model cells to (i) understand the performance and failure models associated with next-generation battery materials, and (ii) design battery materials and electrodes to alleviate these challenges. The research will focus on the Li-S battery chemistry and on microscale modeling of electrodes. Initial work on the Li-S system will develop a mathematical model for the chemistry along with obtaining the necessary experimental data, using a single ion conductor (SIC) as a protective layer to prevent polysulfide migration to the Li anode. The initial work on microscale modeling will use the well-understood $Li(NiMnCo)_{1/3}O_2$ (NMC) electrode to establish a baseline for modeling next-generation electrodes.

Project Impact: Li-S cells promise to increase the energy density and decrease the cost of batteries compared to the state of the art. If the performance and cycling challenges can be alleviated, these systems hold the promise for meeting the EV Everywhere Grand Challenge targets.

Out-Year Goals: At the end of this project, a mathematical model will be developed that can address the power and cycling performance of next-generation battery systems. The present focus is on microscale modeling of electrodes and Li-S cells, although the project will adapt to newer systems, if appropriate. The models will serve as a guide for better design of materials, such as in the kinetics and solubility needed to decrease the morphological changes in sulfur cells and increase the power performance.

Collaborations: This project did not engage in collaborative activity during this quarter.

Milestones

1. Develop a model of a Li-S cell incorporating concentration solution framework. (12/31/14 – Complete)
2. Develop a custom Li-S electrochemical cell with small (~200 μm) catholyte layer incorporating a SIC. (Due 3/31/15) Stop custom cell development if unable to prevent SIC damage during cell assembly. **Status: Go**
3. Use custom cell to perform rate experiments. If unsuccessful in developing custom cell, develop cell without SIC and measure shuttle current. (6/30/15 – Complete)
4. Compare microscale and macroscale simulation results and experimental data to determine the importance of microstructural detail. (9/30/15 – Complete)

Progress Report

Comparison of microscale and macroscale simulation results. A volume reconstruction obtained from our previous x-ray microtomography experiments on NMC electrodes was transformed into surface meshes by first labeling each voxel in the reconstruction as either active material or porous matrix using an intensity threshold selected to match the volume fractions used in our group's earlier work in macroscale simulations of NMC electrodes. While one might instead identify three phases (active material, conductive matrix, and pore), only two phases were used in the simulations because the simulation package did not allow the creation of a porous matrix region in which the solid phase is electrically conductive. The choice to identify two phases was made to ensure that the active material surface exposed to electrolyte solution was sufficiently large, as opposed to being largely surrounded by a nonporous conductive phase that is not permeable to electrolyte solution. The surface meshes generated from the voxel data were imported into the simulation package, repaired as needed, and transformed into simulation domains. These microstructure-derived domains were interfaced with each other and with additional domains with simple shapes representing a positive current collector, a separator, and a lithium negative electrode (Figure 47).

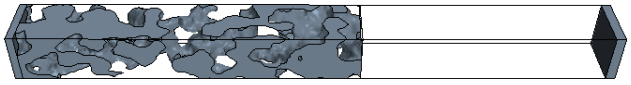

Figure 47. Simulation domain showing positive current collector, porous electrode, and lithium negative electrode. For clarity, porous matrix and separator are not shown.

A constant-current simulation involving an electrochemical reaction, electrical current, and mass transport was constructed and executed. Where applicable, simulation parameters were chosen for consistency with earlier macroscale simulations performed by our research group. The simulated cell potential for a 3C discharge is plotted with experimental and macroscale model results as a function of specific capacity in Figure 48. The cell potential from the microscale simulation is seen to be somewhat higher than that observed experimentally and predicted by the macroscale simulation, but the capacity is closer to that obtained experimentally than from the latter. No parameters were adjusted to improve agreement. The discrepancy between microscale and macroscale simulation results primarily reflects the difference between solving spatially-averaged equations (involving concepts such as tortuosity) on a geometrically simple domain and solving continuum equations on a spatially detailed domain. This completes the fourth quarter milestone.

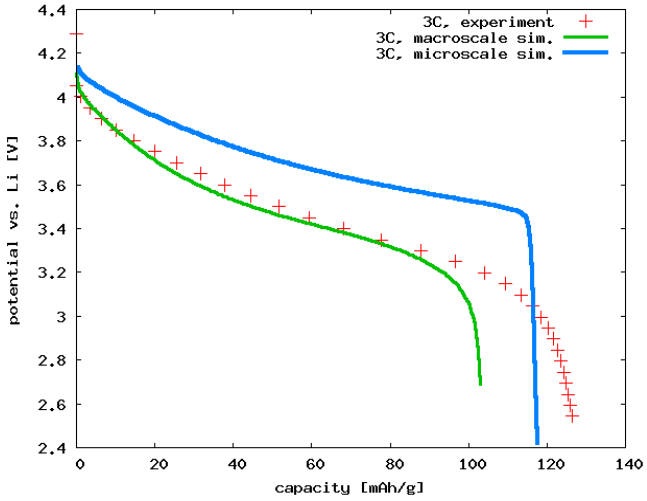

Figure 48: Comparison of 3C discharge curves obtained by experiment, macroscale simulation, and microscale simulation

Task 6.2 – Predicting and Understanding Novel Electrode Materials from First-Principles (Kristin Persson, Lawrence Berkeley National Laboratory)

Project Objective. The project aim is to model and predict novel electrode materials from first-principles focusing on (1) understanding the atomistic interactions behind the behavior and performance of the high-capacity lithium excess and related composite cathode materials, and (2) predicting new materials using the recently developed Materials Project high-throughput computational capabilities at LBNL. More materials and new capabilities will be added to the Materials Project Lithium Battery Explorer App (www.materialsproject.org/apps/battery_explorer/).

Project Impact. The project will result in a profound understanding of the atomistic mechanisms underlying the behavior and performance of the Li-excess as well as related composite cathode materials. The models of the composite materials will result in prediction of voltage profiles and structural stability—the ultimate goal being to suggest improvements based on the fundamental understanding that will increase the life and safety of these materials. The Materials Project aspect of the work will result in improved data and electrode properties being calculated to aid predictions of new materials for target chemistries relevant for ongoing BMR experimental research.

Out-Year Goals. During year 1-2, the bulk phase diagram will be established , including bulk defect phases in layered Li_2MnO_3, layered $LiMO_2$ (M = Co, Ni, and Mn) and $LiMn_2O_4$ spinel to map out the stable defect intermediate phases as a function of possible transition metal rearrangements. Modeling of defect materials (mainly Li_2MnO_3) under stress/strain will be undertaken to simulate effect of composite nano-domains. The composite voltage profiles as function of structural change and Li content will be obtained. In years two to four, the project will focus on obtaining Li activation barriers for the most favorable TM migration paths as a function of Li content as well as electronic density of states (DOS) as a function of Li content for the most stable defect structures identified in years one to two. Furthermore, stable crystal facets of the layered and spinel phases will be explored, as a function of O_2 release from surface and oxygen chemical potential. Within the Materials Project, hundreds of novel Li intercalation materials will be calculated and made available.

Collaborations. This project engages in collaboration with Gerbrand Ceder (MIT), Clare Grey (U Cambridge, UK), Mike Thackeray (ANL), and Guoying Chen (LBNL).

Milestones

1. Mn mobilities as a function of Li content in layered Li_xMnO_3 and related defect spinel and layered phases. (3/31/15 – Complete)
2. Surface facets calculated and validated for Li_2MnO_3. (3/31/15 – Delayed)
3. Calculate stable crystal facets. Determine whether facet stabilization is possible through morphology tuning. (6/30/15 – Delayed)
4. *Go/No-Go*: Stop this approach if facet stabilization cannot be achieved. (6/30/15 – Delayed)
5. Li mobilities as a function of Li content in layered Li_xMnO_3 and related defect spinel and layered phases. (9/30/15 – Complete)

Progress Report

We have continued to elucidate lithium-ion diffusion mechanisms of Li-excess layered materials using first-principle calculation methods. We have investigated Li-ion extraction mechanisms between the transition metal (TM)-layer and Li–layer in high Li content region. The migration energy barriers calculated with Nudged Elastic Band (NEB) method based on first principles density functional theory. Two symmetrical octahedral sites exist in the TM-layer (4g and 2b). Here, 4g sites are occupied by Manganese (Mn) and 2b sites are occupied by Li. Meanwhile, the Li-layer has two stable octahedral sites (4h and 2c). Therefore, inter-layer Li-ion migration can be presented with two migration paths that migrate from 4h site to 2b site (Figure 49a; dashed double side arrow) and from 2c site to 2b sites (Figure 49a; solid double side arrow).

We investigated in detail the migration path from the 2b site in TM-layer to the 4h site in the Li-layer. Our calculations indicate that the migration energy barriers of inter-layer and intra-layer Li diffusion are similar to each other. The kinetically resolved migration energy barrier (ΔE^{KRA}) is 640 meV which is comparable to average ΔE^{KRA} of intra-layer (690 meV). Figure 49b shows the mechanism of inter-layer Li-ion migration. Here, red and blue rectangles represent the stable octahedral sites which correspond to 2b site and 4h site, respectively. The yellow triangles in Figure 49b represent the tetrahedral sites between the two stable octahedral sites. Those two octahedral sites and tetrahedral sites are illustrated at the bottom part of Figure 49b. The mobile Li-ion is initially located at one of the octahedral sites, and then migrates to another octahedral site through a saddle point tetrahedral site (reverse triangle).

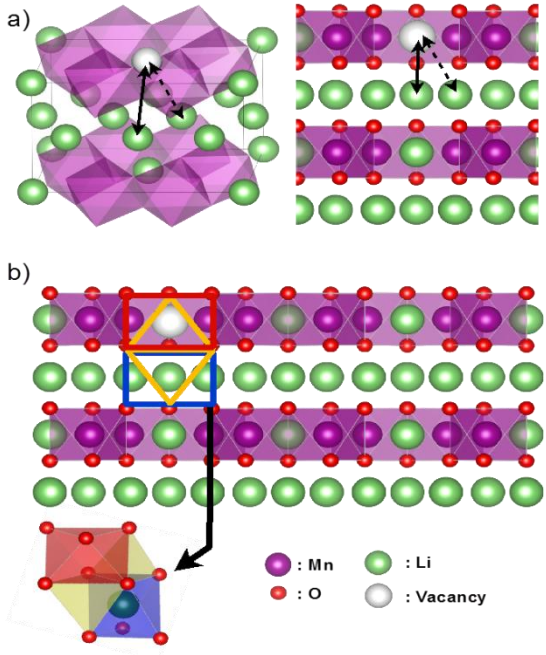

Figure 49. Structure of layered Li-excess material of (100) direction and Li-ion migration process between the transition metal layer and Li-layer. Li-ion has two paths in inter-layer migrations (a). Li-ion can be migrated from red octahedral site to blue octahedral site or vice versa (b).

Importantly, we find that neighboring Li-ions close to the migration path are significantly influenced by the mobile Li-ion. When a mobile Li-ion moves into or out from the Li-layer, 4 out of 6 first nearest neighbors fluctuate away from their local minimum configurations. These first nearest neighbor fluctuations were also observed in intra-layer Li-ion migrations in various Li-configurations. On the other hand, the Mn atoms in the TM-layer were not significantly influenced by Li migration.

Task 6.3 – First Principles Calculations of Existing and Novel Electrode Materials (Gerbrand Ceder, MIT)

Project Objective. Identify the structure of layered cathodes that leads to high capacity. Clarify the role of the initial structure as well as structural changes upon first charge and discharge. Give insight into the role of Li-excess and develop methods to predict ion migration in layered cathodes upon cycling and during overcharge. Develop predictive modeling of oxygen charge transfer and oxygen loss. Give insight into the factors that control the capacity and rate of Na-intercalation electrodes, as well as Na-vacancy ordering. Develop very high capacity layered cathodes with high structural stability (>250 mAh/g).

Project Impact. The project will lead to insight in how Li excess materials work and ultimately to higher capacity cathode materials for Li-ion batteries. The project will help in the design of high-capacity cathode materials that are tolerant to transition metal migration.

Out-Year Goals. Higher capacity Li-ion cathode materials, and novel chemistries for higher energy density storage devices. Guide the field in the search for higher energy density Li-ion materials.

Collaborations. This project collaborates with K. Persson at LBNL and C. Grey at Cambridge U.

Milestones

1. Demonstrate capability to accurately predict oxygen redox activity in cathode materials by comparing calculations to spectroscopic data. (12/31/14) **Completed**
2. Develop model for effect of Li-excess in Li(Li,Ni,Sb)O_2. **Completed**
3. Develop model for Na-vacancy ordering in Na-intercalation compounds (March 31). **Completed**
4. Identify at least one other disordered material with high reversible capacity. **Completed**

Progress Report

Layered Li-excess cathode materials can deliver very high capacities from 250 up to 300 mAh g^{-1}, which has been attributed to the additional charge compensation mechanism activated by Li-excess through either the oxidation of O_2- to O- or the release of O_2 followed by cation densification. Recently, the design space for Li-excess materials was broadened to rocksalts with partial or complete cation disorder through the understanding that more than 10% Li-excess creates a percolation network of 0-TM (transition metal) channels through which Li can diffuse. This opens the possibility to explore and find more candidate disordered materials with good electrochemical performances.

We designed and prepared a new disordered material, $Li_{1.25}Nb_{0.25}Mn0.5O_2$. As synthesized this material is a pure disordered rocksalt phase. It delivers a large initial discharge capacity of 287 mAh/g^{-1} and energy density of 909 Wh kg^{-1} in the first cycle.

Electron energy loss spectroscopy (EELS) results confirm that Mn and O are both redox active. In the first cycle, Mn is oxidized from 3+ to 4+ upon first charge, and reduced slightly below 3+ after the first discharge. In the oxygen K-edge spectra, an increase of the pre-edge intensity is observed beyond 145 mAh g^{-1} Li extraction. This pre-edge is caused by the transition of O 1s electrons to unoccupied 2p orbitals, and therefore indicates the contribution of an oxygen 2p hole, or oxygen oxidation to providing a substantial part of capacity. After the first cycle, the O K-edge largely returns to the pristine state, which suggests a reversible O redox reaction in the first electrochemical cycle. These results clarify that the $Li_{1.25}Nb_{0.25}Mn_{0.5}O_2$ material operates reversibly by means of oxygen oxidation and reduction.

We demonstrated a disordered rocksalt with high electrochemical capacity provided in a large part by reversible oxygen redox in the solid state. Together with our previous work on understanding Li transport in Li-excess and disordered materials, we believe that this is an important new direction to create high capacity cathode materials.

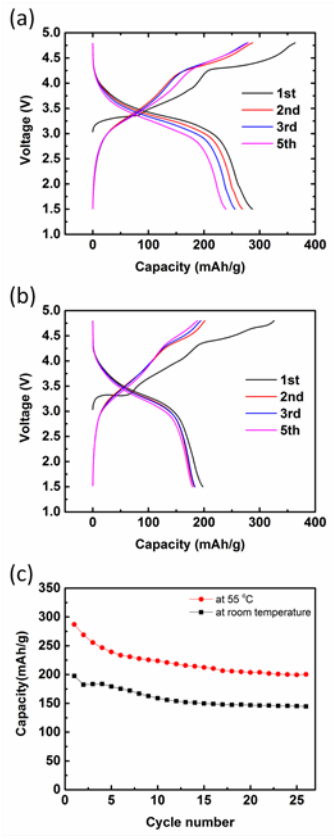

Figure 50. Cycling performances of $Li_{1.25}Nb_{0.25}Mn_{0.5}O_2$ at 55°C (a) and room temperature (b).

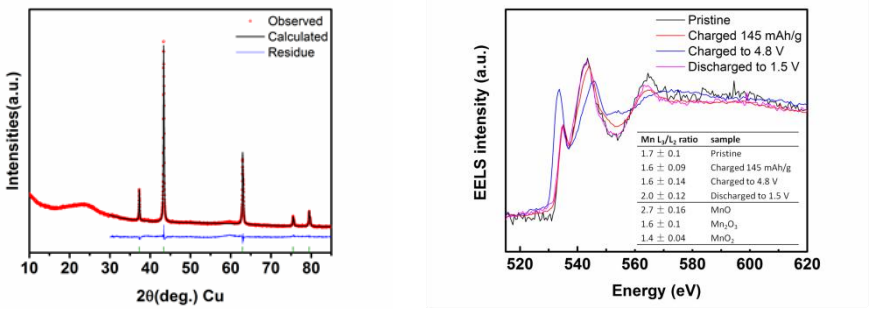

Figure 51. X-ray diffraction shows a pure disordered rocksalt phase; EELS spectra confirm that Mn and O are both redox active.

.

Task 6.4 – First Principles Modeling of SEI Formation on Bare and Surface/Additive Modified Silicon Anode (Perla Balbuena, Texas A&M University)

Project Objective. This project aims to develop fundamental understanding of the molecular processes that lead to the formation of a solid-electrolyte interphase (SEI) layer due to electrolyte decomposition on Si anodes, and to use such new knowledge in a rational selection of additives and/or coatings. The focus is on SEI layer formation and evolution during cycling and subsequent effects on capacity fade through two concatenated problems: (1) SEI layers formed on lithiated Si surfaces, and (2) SEI layers formed on coated surfaces. Key issues being addressed include the dynamic evolution of the system and electron transfer through solid-liquid interfaces.

Project Impact. Finding the correspondence between electrolyte molecular properties and SEI formation mechanism, structure, and properties will allow the identification of new/improved additives. Studies of SEI layer formation on modified surfaces will allow the identification of effective coatings able to overcome the intrinsic deficiencies of SEI layers on bare surfaces.

Approach. Investigating the SEI layer formed on modified Si surfaces involves analysis of the interfacial structure and properties of specific coating(s) deposited over the Si anode surface, characterization of the corresponding surface properties before and after lithiation, especially how such modified surfaces may interact with electrolyte systems (solvent/salt/additive), and what SEI layer structure, composition, and properties may result from such interaction. This study will allow identification of effective additives and coatings able to overcome the intrinsic deficiencies of SEI layers on bare surfaces. Once the SEI layer is formed on bare or modified surfaces, it is exposed to cycling effects that influence its overall structure (including the anode) and the chemical and mechanical stability.

Out-Year Goals. Elucidating SEI nucleation and electron transfer mechanisms leading to growth processes using a molecular level approach will help establish their relationship with capacity fading, which will lead to revisiting additive and/or coating design.

Collaborations. Work with Chunmei Ban (NREL) consists in modeling the deposition-reaction of Alucon coating on Si surfaces and their reactivity. Work with B. Lucht (U Rhode Island) relates to finding the best additives for optimum SEI formation on Si anodes. Reduction of solvents and additives on Si surfaces were studied in collaboration with K. Leung and S. Rempe (SNL). Collaborated with Prof. Jorge Seminario on electron transfer reactions and Dr. Partha Mukherjee on development of a multi-scale model to describe SEI growth on Si anodes (Texas A&M University – TAMU).

Milestones

1. Identification of lithiation and SEI formation mechanisms through Alucon coatings on Si surfaces. (Q1 – Complete)
2. Clarify role of additives (VC, FEC) vs. electrolyte without additive on SEI properties. (Q2 – Complete)
3. Characterization of SEI mosaic formation from building blocks. (Q3 – Complete)
4. *Go/No-Go*: Prediction of irreversible capacity loss and electron transfer mechanisms through the SEI layer. (Q4 – Complete)

Progress Report

A mesoscopic model to capture longer scale times and lengths. The model was developed in two stages: (1) a first-principles analysis of aggregation of lithium ethylene dicarbonate (Li_2EDC) over bare and coated Si surfaces was performed that provided information about adsorption and aggregation growth rates, and (2) the above discussed electron transfer analysis was confirmed. An example is shown in Figure 52.

On the basis of rates provided by the first principles analysis (Figure 52, top), a mesoscopic model was formulated in collaboration with Professor Mukherjee (TAMU). The microscopic events are: EC molecular adsorption, EC reduction, EC configuration transition, and Li_2EDC formation. The computational domain was divided into identical cubic cells. Initially all the kinetic rates were taken as constant. On this basis, a linear mean growth was found as a function of time. Further analyses showed that thickness δ growth rate significantly depends on EC reduction rate k2 (see Figure 52, center). The effects of EC adsorption rate were also determined. It was found that for very low adsorption rates, the SEI growth is determined by the adsorption rate, whereas higher adsorption rates do not affect SEI thickness growth. In a second stage, a SEI thickness dependent reduction rate was introduced. This reflects the effect of decreased electron concentration as the SEI thickness grows (Figure 52, bottom). The effect of increase of electron transport resistance on reduction of SEI growth thickness was quantified. Further refinements are in progress.

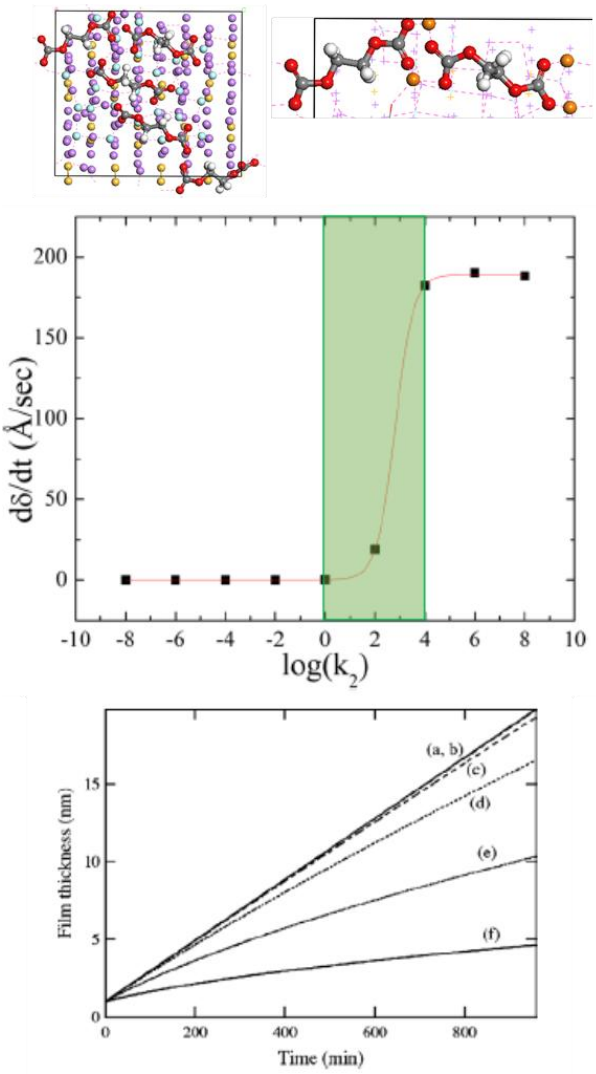

Figure 52. An example of a mesoscopic model to capture longer scale times and lengths.

Stability of SEI products. This group recently introduced the important concept of thermodynamic stability of SEI products (Balbuena et al., DOE-AMR meeting, June 2015). Within this theme, Sandia's main effort (Leung) focused on the examination of SEI formation and evolution on Li_xSi surfaces with varying Li content ("x"). Particular emphasis was put on elucidating the stability of Li_xSi-SEI interfaces, using model systems [lithium carbonate (Li_2CO_3) and lithium ethylene dicarbonate (Li_2EDC)]. This work was performed in collaboration with the Balbuena group and formed the core of an invited presentation at the Electrochemical Society Fall Meeting. The coupled mechanical-chemical response of SEI and electrolyte on Li_xSi surfaces due to the lateral expansion and contraction of Si as it inserts/de-inserts lithium was also examined. The instantaneous electronic (that is, the electronic) voltage was monitored and correlated with SEI formation.

Free energy studies of electrolyte solvation. The solvation free energy of Li ion in EC and PC using the classical force field is in progress (Rempe, et al.), as well as electronic structure methods coupled with continuum solvation models. By decomposing the free energy into components, new insights are gained about the relative importance of local chemical interactions, packing contributions, and the distant solvation environment.

Patents/Publications/Presentations

Publications

- Perez-Beltrán, S., and G.E. Ramirez-Caballero, and P.B. Balbuena. "First Principles Calculations of Lithiation of a Hydroxylated Surface of Amorphous Silicon Dioxide." *J. Phys. Chem. C* 119 (2015): 16424-16431.
- Ma, Y., and J.M. Martinez de la Hoz, I. Angarita, J.M. Berrio-Sanchez, L. Benitez, J.M. Seminario, S.-B. Son, S.-H. Lee, S.M. George, C.M. Ban, and P.B. Balbuena. "Structure and Reactivity of Alucone-Coated Films on Si and Li_xSi_y Surfaces." *ACS Appl. Mater. Inter*. 7 (2015): 11948-11955.
- Martinez de la Hoz, J.M., and F.A. Soto and P.B. Balbuena. "Effect of the Electrolyte Composition on SEI Reactions at Si Anodes of Li-ion Batteries." *J. Phys. Chem. C* 119 (2015): 7060-7068. DOI: 10.1021/acs.jpcc.5b01228.
- Soto, F.A., and Y. Ma, J.M. Martinez de la Hoz, J.M. Seminario, and P.B. Balbuena. "Formation and Growth Mechanisms of Solid-Electrolyte Interphase Layers in Rechargeable Batteries." *Chemistry of Materials*, under review.

Task 6.5 – A Combined Experimental and Modeling Approach for the Design of High Current Efficiency Si Electrodes
(Xingcheng Xiao, General Motors; Yue Qi, Michigan State University)

Project Objective. The use of high-capacity, Si-based electrode has been hampered by its mechanical degradation due to the large volume expansion/contraction during cycling. Nanostructured Si can effectively avoid Si cracking/fracture. Unfortunately, the high surface to volume ratio in nanostructures leads to unacceptable amount of solid-electrolyte interphase (SEI) formation and growth, thereby low current/Coulombic efficiency and short life. Based on mechanics models we demonstrate that the artificial SEI coating can be mechanically stable despite the volume change in Si, if the material properties, thickness of the SEI, and the size/shape of Si are optimized. Therefore, the objective of this project is to develop an integrated modeling and experimental approach to understand, design, and make coated Si anode structures with high current efficiency and stability.

Project Impact. The validated model will ultimately be used to guide the synthesis of surface coatings and the optimization of Si size/geometry that can mitigate SEI breakdown. The optimized structures will eventually enable a negative electrode with a 10x improvement in capacity (compared to graphite) while providing a >99.99% Coulombic efficiency, which could significantly improve the energy/power density of current lithium-ion battery.

Out-Year Goals. The out-year goal is to develop a well validated mechanics model that directly import material properties either measured from experiments or computed from atomic simulations. The predicted SEI induced stress evolution and other critical phenomena will be validated against *in situ* experiments in a simplified thin-film system. This comparison will also allow fundamental understanding of the mechanical and chemical stability of artificial SEI in electrochemical environments and the correlation between the Coulombic efficiency and the dynamic process of SEI evolution. Thus, the size and geometry of coated Si nanostructures can be optimized to mitigate SEI breakdown, thus providing high current efficiency.

Collaborations. This project engages in collaboration with LBNL, PNNL, and NREL.

Milestones

1. Identify SEI failure mode by using combined *in situ* electrochemical experiments and modeling techniques developed in 2014. (12/31/14 – Complete)
2. Reveal detailed SEI failure mode by using MD simulations with ReaxFF for Li-Si-Al-O-C system to model the deformation of SEI on a Si as it undergoes large strain. (3/31/15 – Complete)
3. Correlate and determine the desirable material properties for stable SEI, by applying the continuum model and experimental nanomechanics. Establish the material property design methodology for stabilizing SEI on Si. (6/30/15 – Complete)
4. *Go/No-Go*: Determine whether to select oxide, fluoridated, or carbon artificial SEI chemistry based on comparisons of their mechanical stability and transport properties. (9/30/15 – Complete; Identified the desirable SEI component)

Progress Report

Identified the desirable SEI components that can facilitate charge transfer. The inorganic components formed in SEI , including lithium carbonate (Li_2CO_3) and lithium fluoride (LiF), play a critical role in providing both mechanical and chemical protection, as well as facilitating lithium ion transport. Although Li_2CO_3 and LiF have relatively low ionic conductivity, we found, surprisingly, that the interface between Li_2CO_3 and LiF can facilitate space charge accumulation, which significantly improves lithium transport and reduces electron conduction (Figure 53). We found that, in the ionic space charge region of Li_2CO_3 near the LiF/ Li_2CO_3 interface, Li ion interstitial is accumulated but the electron is depleted. This demonstrates a possibility that, by engineering a mixture of LiF and Li_2CO_3 in an artificial SEI, the ionic conduction can be enhanced and the electron leakage through the SEI can be reduced, thus enhancing the durability and performance of electrodes. The synergetic effect of the two inorganic components leads to high current efficiency and long cycle stability.

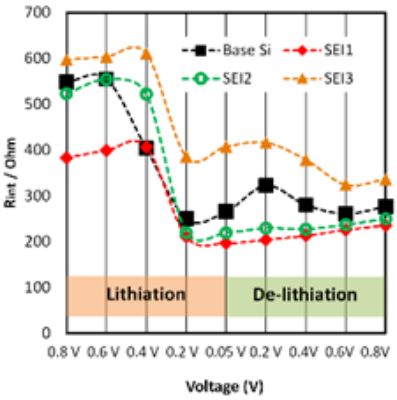

Figure 53. Interfacial resistance (Rct) of samples under different lithiation (delithiation) stage. Higher LiF content (SEI1) leads to lower impedance.

Design of multi-component solid electrolyte interphase with high ionic conductivity. Based on our thermodynamic data from DFT calculations and space charge model, we studied the effect of grain size and volumetric ratio on the total ionic conductivity. We chose a coating structure of LiF/Li_2CO_3, as shown in Figure 54 (top), with the LiF/ Li_2CO_3 interface parallel to the transport direction of ions. Theoretically, this structure presents an upper limit of the ionic conduction through a two-component mixture. As shown in Figure 54 (bottom), the ionic conductivity through Li_2CO_3 grain increases by decreasing the grain size. This is because the interfacial effect that causes the accumulation of ionic carrier (Figure 55) becomes more dominant when reducing the grain size. In addition, ionic conductivity is promoted dramatically at low volumetric ratio [RV=V(Li_2CO_3)/V(LiF)] with increasing RV and is saturated when RV is larger than 20. Thus, our results predict that the optimized ionic conduction can be achieved by reducing the grain size of Li_2CO_3 and introducing enough LiF into the artificial SEI.

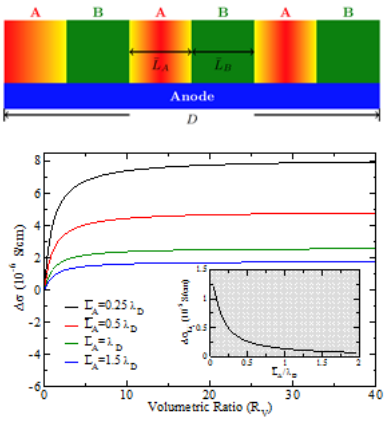

Figure 54. Above: 2-D illustration of the topology of the designed SEI structure for optimized ionic conductivity. A: Li_2CO_3; B: LiF. Below: The increment of ionic conduction for different average grain size of Li_2CO_3 at various volumetric ratios.

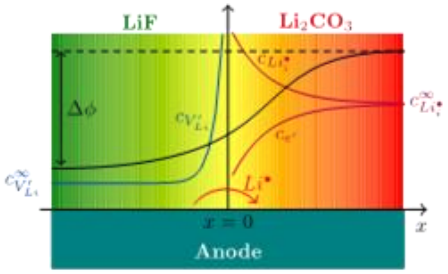

Figure 55. Schematic figure showing the defect reaction and defect distribution near the LiF Li_2CO_3 interface.

Patents/Publications/Presentations

Publications

- Verbrugge, Mark W., and Daniel R. Baker, Xingcheng Xiao, Qinglin Zhang, and Yang-Tse Cheng. "Experimental and Theoretical Characterization of Electrode Materials that Undergo Large Volume Changes and Application to the Lithium-Silicon System." *J. Phys. Chem. C* 119 (2015): 5341−5349.
- Pan, Jie, and Qingling, Zhang, Juchuan Li, M.J. Beck, Xingcheng Xiao, and Yangtse Cheng. "Effects of stress on lithium transport in amorphous silicon electrodes for lithium-ion batteries." *Nano Energy* 13 (2015): 192-199.

Presentation

- Symposium on "Hybrid Organic-Inorganic Materials for Alternative Energy - Materials for Batteries and Fuel Cells" at Materials Science and Technology (MS&T), Columbus, Ohio (October 4-8, 2015; Invited): "Studies of Hybrid Materials for Lithium Ion Batteries"; Yang-Tse Cheng.

Task 6.6 – Predicting Microstructure and Performance for Optimal Cell Fabrication (Dean Wheeler and Brian Mazzeo, Brigham Young University)

Project Objective. This work uses microstructural modeling coupled with extensive experimental validation and diagnostics to understand and optimize fabrication processes for composite particle-based electrodes. The first main outcome will be revolutionary methods to assess electronic and ionic conductivities of porous electrodes attached to current collectors, including heterogeneities and anisotropic effects. The second main outcome is a particle-dynamics model parameterized with fundamental physical properties that can predict electrode morphology and transport pathways resulting from particular fabrication steps. These two outcomes will enable the third, which is an understanding of the effects of processing conditions on microscopic and macroscopic properties of electrodes.

Project Impact. This work will result in new diagnostic tools for rapidly and conveniently interrogating electronic and ionic pathways in porous electrodes. A new mesoscale 3D microstructure prediction model, validated by experimental structures and electrode-performance metrics, will be developed. The model will enable virtual exploration of process improvements that currently can only be explored empirically.

Out-Year Goals. This project was initiated April 2013 and concludes March 2017. Goals by fiscal year are as follows.

- 2013: Fabricate first-generation micro-four-line probe, and complete associated computer model.
- 2014: Assess conductivity variability in electrodes; characterize microstructures of multiple electrodes.
- 2015: Fabricate first-gen ionic conductivity probe, N-line probe, and dynamic particle packing (DPP) model.
- 2016: Fabricate second-gen N-line probe and DPP model; assess effect of processing variables.
- 2017: Use conductivity predictions in full electrochemical model; evaluate effect of innovative processing conditions.

Collaborations. Bryant Polzin (ANL) and Karim Zaghib (Hydro-Quebec) provided battery materials. Transfer of our technology to A123 to improve their electrode production process took place in FY 2015. Collaborations continue with Simon Thiele (IMTEK, University of Freiburg) and Mårten Behm (KTH, Sweden).

Milestones

1. Develop localized ionic conductivity probe and demonstrate method by testing two candidate electrode materials. (December 2014 – Complete)
2. Use dynamic particle-packing (DPP) model to predict electrode morphology of Toda 523 material. (March 2014 – Complete)
3. Develop fabrication process of micro-N-line probe and demonstrate method by testing two candidate electrode materials (June 2015 – Complete)
4. *Go/No-Go*: Discontinue DPP model if predictions are not suitable match to real electrode materials (September 2015 – Complete; Go criterion met)

Progress Report

Milestone 4 (Go criterion met)

The fourth milestone of FY 2015 was to determine if the DPP model was fulfilling its purpose and development should be continued. This was determined by comparing the model predictions with real electrodes, namely Toda NCM-523 cathodes supplied by Argonne National Laboratory, to see if they were a suitable match. The following properties were compared between the model and experiment: slurry viscosity, elasticity of the dried film, shrinkage ratio during drying, volume fraction of phases, slurry and dried film densities, and microstructure of cross sections. Simulation results were in substantial agreement with experiment, showing that the simulations reasonably reproduce the relevant physics of particle arrangement during fabrication. For instance, Figure 56 shows the satisfactory agreement between the viscosity of the simulation vs. experiment. Similarly, Table 3 shows satisfactory agreement with respect to other physical parameters. Therefore, the DPP model will continue to be developed in FY 2016. It is anticipated that it will become a powerful platform for predicting the effects of fabrications steps on the evolution of the particle microstructure and will accelerate efforts to optimize electrodes.

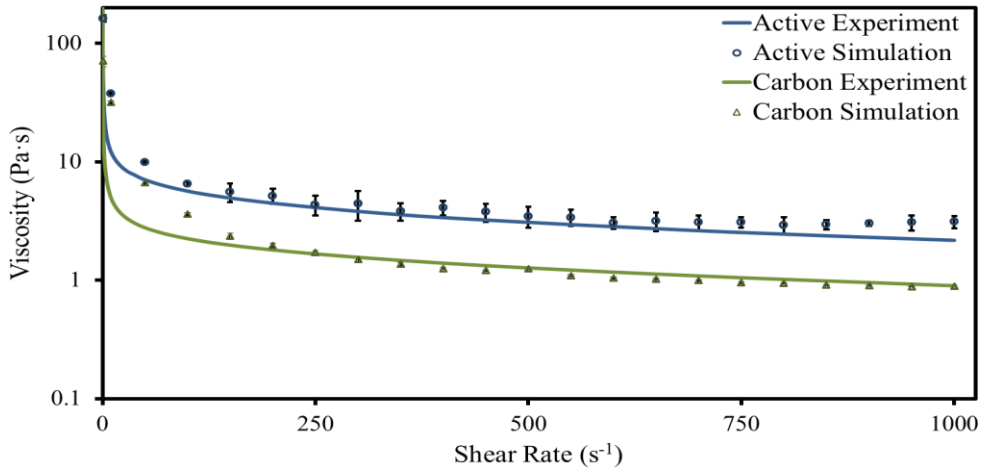

Figure 56. Viscosity of slurry at different shear rates for pure carbon (green), and active sample (blue) from experiment (line), and simulation (symbols). In some cases error bars are smaller than symbol sizes. Lines are used for experiments due to the close spacing of the data.

Table 3. Comparison of key properties between simulation and experiment, with 95% confidence intervals where repeated independent samples were collected. Volume fractions are for the solid state.

	Carbon Simulation	Carbon Experiment	Active Simulation	Active Experiment
Elasticity (MPa)	9.55 ± 0.15	9.32 ± 0.25	11.10 ± 0.73	11.32 ± 0.17
Shrinkage ratio	8.11 ± 0.04	8.70 ± 0.59	2.67 ± 0.05	3.29 ± 0.08
Liq dens (g cm^{-3})	1.027 ± 0.000	1.03	1.66 ± 0.00	1.65
Solid dens (g cm^{-3})	0.681 ± 0.004	0.696 ± 0.028	2.070 ± 0.037	2.029 ± 0.043
Active vol fraction	–	–	0.41 ± 0.03	0.45
CBD vol fraction	0.90	0.89	0.40 ± 0.01	0.36
Macro-pore vol frac	0.10	0.11	0.19 ± 0.04	0.19

Patents/Publications/Presentations

Publications

- Vierrath, L. Zielke, and R. Moroni, A. Mondon, D.R. Wheeler, R. Zengerle, and S. Thiele. "Morphology of Nanoporous Carbon-binder Domains in Li-ion Batteries - A FIB-SEM Study." *Electrochem. Comm.* 60 (2015): 176 –179.
- Lanterman, B.J., and A.A. Riet, N.S. Gates, J.D. Flygare, A.D. Cutler, J.E. Vogel, D.R. Wheeler, and B.A. Mazzeo. "Micro-four-line Probe to Measure Electronic Conductivity and Contact Resistance of Thin-film Battery Electrodes." *J. Electrochem. Soc.* 162 (2015): A2145-A2151.
- Flygare, J.D., and A.A. Riet, B.A. Mazzeo, and D.R. Wheeler. "Mathematical Model of Four-line Probe to Determine Conductive Properties of Thin-film Battery Electrodes." *J. Electrochem. Soc.* 162 (2015): A2136-A2144.

TASK 7 – METALLIC LITHIUM AND SOLID ELECTROLYTES

Summary and Highlights

The use of a metallic lithium anode is required for advanced battery chemistries like Li-air and Li-S to realize dramatic improvements in energy density, vehicle range, cost economy, and safety.

However, the use of metallic Li with liquid and polymer electrolytes has been so far limited due to parasitic SEI reactions and dendrite formation. Adding excess lithium to compensate for such losses effectively negates the high energy density for lithium in the first place. For a long lifetime and safe anode, it is essential that no lithium capacity is lost to physical isolation from roughening, to dendrites or delamination processes, or to chemical isolation from side reactions. The key risk and current limitation for this technology is the gradual loss of lithium over the cycle life of the battery.

To date there are no examples of battery materials and architectures that realize such highly efficient cycling of metallic lithium anodes for a lifetime of 1,000 cycles due to degradation of the Li-electrolyte interface. A much deeper analysis of the degradation processes is needed, so that materials can be engineered to fulfill the target level of performance for electric vehicles (EVs), namely 1,000 cycles and a 15 year lifetime, with adequate pulse power. Projecting the performance required in terms of just the Li anode, this requires a high rate of lithium deposition and stripping reactions, specifically about 40μm Li per cycle, with pulse rates up to 10 and 20 nm/s charge and discharge, respectively. This is a conservative estimate, yet daunting in the total mass and rate of material transport. While such cycling has been achieved for state-of-the-art batteries using *molten* Na in Na-S and zebra cells, solid Na and Li anodes are proving more difficult.

The efficient and safe use of metallic lithium for rechargeable batteries is then a great challenge, and one that has eluded research and development efforts for many years. Task 7 takes a broad look at this challenge for both solid state batteries and batteries continuing to use liquid electrolytes. Four of the projects are new endeavors; two are ongoing. For the liquid electrolyte batteries, PNNL researchers are examining the use of cesium salts and organic additives to the typical organic carbonate electrolytes to impede dendrite formation at both the lithium and graphite anodes. If successful, this is the simplest approach to implement. At Stanford, novel coatings of carbon and boron nitride with a 3D structure are applied to the lithium surface and appear to suppress roughening and lengthen cycle life. A relatively new family of solid electrolytes with a garnet crystal structure shows superionic conductivity and good electrochemical stability. Four programs chose this family of solid electrolytes for investigation. Aspects of the processing of this ceramic garnet electrolyte are addressed at the University of Maryland and at the University of Michigan with attention to effect of flaws and composition. Computational models will complement their experiments to better understand interfaces and reduce the electrode area specific resistance (ASR). At Oak Ridge National Laboratory, composite electrolytes composed of ceramic and polymer phases are being investigated, anticipating that the mixed phase structures may provide additional means to adjust the mechanical and transport properties. The last project takes on the challenge to used nanoindentation methods to measure the mechanical properties of the solid electrolyte, the lithium metal anode, and the interface of an active electrode. Each of these projects involves a collaborative team of experts with the skills needed to address the challenging materials studies of this dynamic electrochemical system.

The highlights for this quarter include the following:

- **Task 7.1.** Pulse echo measured during the dc transport of Li ions is a new way to look for changes in the properties of a sintered LLZO solid electrolyte pellet; changes in the acoustic wave speed are seen prior to the onset of electrical shorting.
- **Task 7.2.** By careful surface preparation of the LLZO solid electrolyte pellet, the effective current density with lithium metal electrodes was increased by a factor of 6 to 0.3 mA/cm^2 without shorting the sample. This is approaching the goal of 1 mA/cm^2.

- **Task 7.3.** Polymer electrolyte composites with a high loading of the Ohara ceramic powder where prepared from several different slurry compositions. This has the potential for practical manufacturing if the interface with Li can be stabilized.
- **Task 7.4.** An LLZO solid electrolyte surface was prepared with an array of posts sintered to the surface. Such a structured surface has a lower interface resistance when coated with the LFMO cathode slurry.
- **Task 7.5.** Lithium metal was infused into mesh of ZnO coated polyimide nanofibers; the layer maintained a constant volume when completely stripped of lithium in the liquid electrolyte cell.
- **Task 7.6.** Stable cycling, to 500 deep cycles, was obtained for graphite//NMC coin cells by adding $CsPF_6$ and PC to the $LiPF_6$-EC/EMC electrolyte solution.

Task 7.1 – Mechanical Properties at the Protected Lithium Interface (Nancy Dudney, ORNL; Erik Herbert, Michigan Technological U.; Jeff Sakamoto, U. Michigan)

Project Objective. This project will develop the understanding of the Li metal-solid electrolyte interface through state-of-the-art mechanical nanoindentation methods coupled with solid electrolyte fabrication and electrochemical cycling. Our goal is to provide the critical information that will enable transformative insights into the complex coupling between the microstructure, its defects, and the mechanical behavior of Li metal anodes.

Project Impact. Instability and/or high resistance at the interface of lithium metal with various solid electrolytes limit the use of the metallic anode for batteries with high energy density batteries, such as Li-air and Li-S. The critical impact of this endeavor will be a much deeper analysis of the degradation, so that materials can be engineered to fulfill the target level of performance for EV batteries, namely 1000 cycles and a 15-year lifetime, with adequate pulse power.

Approach. Mechanical properties studies through state-of-the-art nanoindentation techniques will be used to probe the surface properties of the solid electrolyte and the changes to the lithium that result from prolonged electrodeposition and dissolution at the interface. An understanding of the degradation processes will guide future electrolyte and anode designs for robust performance. In the first year, the team will address the two critical and poorly understood aspects of the protected Li metal anode assembly: (1) the mechanical properties of the solid electrolyte and (2) the morphology of the cycled Li metal.

Out-Year Goals. Work will progress toward study of the electrode assembly during electrochemical cycling of the anode. We hope to capture the formation and annealing of vacancies and other defects in the lithium and correlate this with the properties of the solid electrolyte and the interface.

Collaborations. This project funds work at Oak Ridge National Laboratory, Michigan Technological University, and University of Michigan. Asma Sharafi (UM Ph. D. student), Dr. Robert Schmidt (UM) also contribute to the project. Steve Visco (PolyPlus) will serve as a technical advisor.

Milestones

1. Four nano-indentation maps showing grain boundary regions of the crystalline LLZO and the glass ceramic material from Ohara. (Q1 – Complete)
2. Two or three indentation studies with as-fabricated, air reacted and polished surfaces. (Q2 – Complete)
3. Demonstrate capability to transfer and then map viscoelastic properties of Li films and rolled lithium foils in vacuum system of sem. (Q3; go/no-go – Completed, using glove box rather than SEM)
4. Determine elastic properties of battery grade lithium from different sources and preparation, comparing to values from the reference literature. (Q4 – Initiated, delayed due to relocation and equipment installation.)

Progress Report

An acoustic impulse excitation (pulse echo) method was developed to provide a real-time, nondestructive indication of changes in the average elastic properties during lithium cycling. This test utilized a thick LLZO pellet with square cut walls. The acoustic transducers were positioned normal to the direction of the ion current. Figure 57 shows the sample between the Li contacts. The exposed faces were mated to the acoustic transducer.

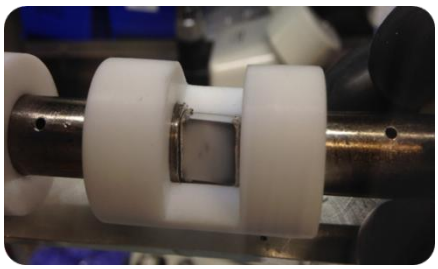

Figure 57. Sample between Li contacts.

After conditioning the lithium contacts at elevated temperature, current tests were conducted at room temperature. The current was applied in both directions, at 1 hour intervals, with an increase in current density at each step. Excursions and noise of the voltage indicate that the current has exceeded the critical limit, here about 0.3 mA/cm^2, where a short rapidly develops across the ceramic. These new results suggest that the onset of the short circuit is preceded by a change, generally a decrease in the wavespeed through the electrolyte. One result is shown as an example in figure 58.

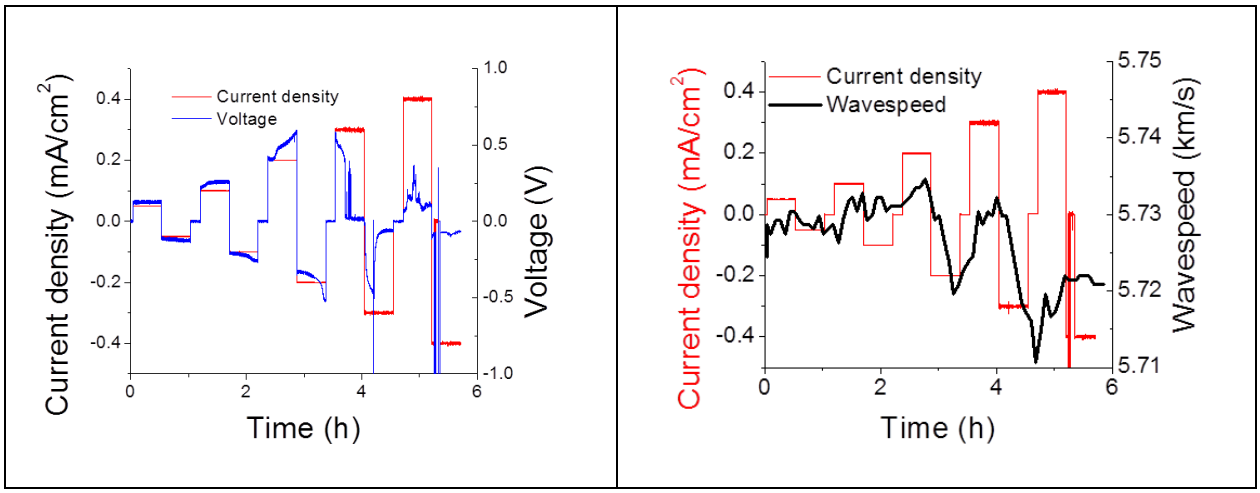

Figure 58. Cycling of Li through LLZO sample in both directions (left). Response of the impulse acoustic echo indicated as the wavespeed (right).

Nanoindentation of selected LLZO samples was repeated using the new surface preparation methods developed for the LLZO electrolyte surfaces (see Task 7.2). In the second quarter report, we showed a significant variation from indent to indent and also a strong variation with the depth of the indent. Now, with careful polishing of the LLZO surface, there is little deviation from point to point and little change with the depth of the indent. Values for the elastic properties by nanoindentation are in good agreement with those by acoustic pulse echo and from model calculations.

Patents/Publications/Presentations

Publication

- Yu, Seungho, and Robert D. Schmidt, Regina Garcia-Mendez, Erik Herbert, Nancy J. Dudney, Jeffrey B. Wolfenstine, Jeff Sakamoto, and Donald J. Siegel. "Elastic Properties of the Solid Electrolyte $Li_7La_3Zr_2O_{12}$ (LLZO)." *Chemistry of Materials* (Submitted).

Presentations

- The Battery Show in Novi, Michigan; Jeff Sakamoto moderated a session titled "The Solid-State Revolution," with speakers from Toyota, Google, Samsung, and Intel.
- Opening ceremony of the University of Michigan Energy Institute's Battery Lab (October 2, 2015); Jeff Sakamoto.

Task 7.2 – Solid Electrolytes for Solid-State and Lithium-Sulfur Batteries (Jeff Sakamoto, University of Michigan)

Project Objectives. Enable advanced Li-ion solid-state and lithium-sulfur EV batteries using LLZO solid-electrolyte membrane technology. Owing to its combination of fast ion conductivity, stability, and high elastic modulus, LLZO exhibits promise as an advanced solid- state electrolyte. To demonstrate relevance in electric vehicle (EV) battery technology, several objectives must be met. First, LLZO membranes must withstand current densities approaching ~1 mA/cm^2 (commensurate with EV battery charging and discharging rates). Second, low area specific resistance (ASR) between Li and LLZO must be achieved to achieve cell impedance comparable to conventional Li-ion technology (~10 Ohms/cm^2). Third, low ASR and stability between LLZO and sulfur cathodes must be demonstrated.

Project Impact. The expected outcomes will: (i) enable Li metal protection, (ii) augment DOE access to fast ion conductors and/or hybrid electrolytes, (iii) mitigate Li-polysulfide dissolution and deleterious passivation of Li metal anodes, and (iv) prevent dendrite formation. Demonstrating these aspects could enable Li-S batteries with unprecedented end-of-life, cell-level performance: > 500 Wh/kg, > 1080 Wh/l, >1000 cycles, lasting > 15 years.

Approach. Our effort will focus on the promising new electrolyte known as LLZO ($Li_7La_3Zr_2O_{12}$). LLZO is the first bulk-scale ceramic electrolyte to simultaneously exhibit the favorable combination of high conductivity (~1 mS/cm at 298K), high shear modulus (61 GPa) to suppress Li dendrite penetration, and apparent electrochemical stability (0-6V vs Li/Li+). While these attributes are encouraging, additional R&D is needed to demonstrate that LLZO can tolerate current densities *in excess of* 1mA/cm^2, thereby establishing its relevance for plug-in hybrid electric vehicle (PHEV)/EV applications. We hypothesize that defects and the polycrystalline nature of realistic LLZO membranes can limit the critical current density. However, the relative importance of the many possible defect types (porosity, grain boundaries, interfaces, surface & bulk impurities), and the mechanisms by which they impact current density, have not been identified. Using our experience with the synthesis and processing of LLZO (Sakamoto and Wolfenstine), combined with sophisticated materials characterization (Nanda), we will precisely control atomic and microstructural defects and correlate their concentration with the critical current density. These data will inform multi-scale computation models (Siegel and Monroe) which will isolate and quantify the role(s) that each defect plays in controlling the current density. By bridging the knowledge gap between composition, structure, and performance we will determine if LLZO can achieve the current densities required for vehicle applications.

Collaborations. This project collaborates with Don Siegel (UM atomistic modeling), Chuck Monroe (UM, continuum scale modeling), Jagjit Nanda (ORNL sulfur chemical and electrochemical spectroscopy), and Jeff Wolfenstine (ARL atomic force microscopy of Li-LLZO interfaces).

Milestones

The timeline for the milestones has been revised, with approval.

- M1.7 (changed from Q8): Demonstrate the ability to control surface cleanliness and surface roughness; Correlate the critical current density as a function of surface contamination and roughness. (Complete)

Progress Report

We successfully correlated the effect of surface contamination with the critical current density (CCD) (Figure 59). Using x-ray photoelectron spectroscopy (XPS), electrochemical impedance spectroscopy (EIS), and computation analysis, it was determined that a surface treatment must be used to reduce the Li-LLZO interfacial resistance to increase the CCD. The standard surface preparation, as described by Ren et al. [1] and Ishiguro, et al. [2], typically results in a CCD of ~ 0.05 mA/cm^2, comparable to the result in this work.

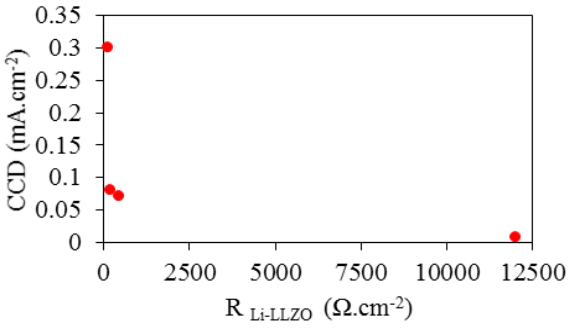

Figure 59. Critical current density as a function of the Li-LLZO interfacial resistance, which was controlled by the surface contamination.

Figure 60 shows the progress toward reducing $R_{Li\text{-}LLZO}$ at room temperature. The $R_{Li\text{-}LLZO}$ was measured using EIS on Li-LLZO-Li cells. The Nyquist plots compare the $R_{Li\text{-}LLZO}$ based on the surface preparation. Each of the plots consists of two distinct resistive components: one at relatively high frequency range (the Ohmic drop through the LLZO pellet), and a second in the lower frequency range (the Li-LLZO interface). The EIS spectrums were modeled using an equivalent circuit to determine the separate resistive phenomena for Ohmic drop through the LLZO pellet, and Li-LLZO interface. The Li-LLZO interface resistance was determined by dividing the low-frequency semicircle diameter by two since the cells employed two Li anodes. Using the typical surface treatment as described above, the $R_{Li\text{-}LLZO}$ is 514 Ohms cm^{-2}, which is in excellent agreement with previous result from Ohta et al. (530 Ω.cm^2) [3]. Using the new surface treatment in this work, the $R_{Li\text{-}LLZO}$ was determined to be 181 Ω.cm^2. By correlating the CCD with $R_{Li\text{-}LLZO}$, and achieving relatively low $R_{Li\text{-}LLZO}$ values, the project is now poised to further reduce $R_{Li\text{-}LLZO}$, thus increasing the CCD. By lowering $R_{Li\text{-}LLZO}$, it is also believed that the role that microstructural defects play in controlling the CCD can now be studied in earnest. Tracking progress toward the project goal of enabling a 1 mA/cm^2 Li-ion current density at 298 K, the CCD was increased from 0.05 to 0.3 mA/cm^2 after three quarters of work.

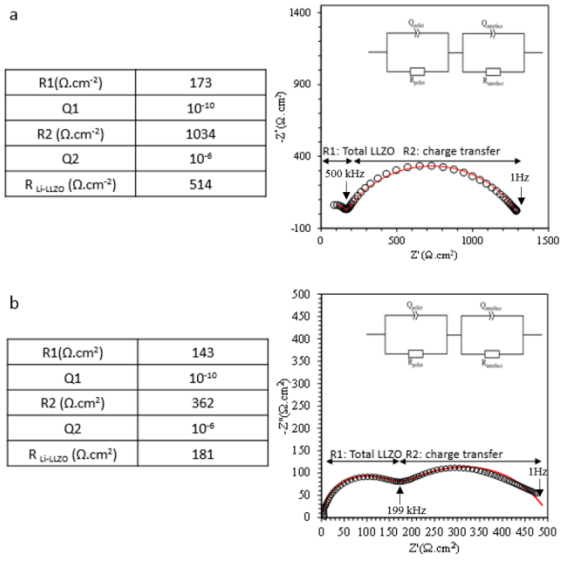

Figure 60. EIS data for Li-LLZO-Li cells using the standard surface preparation (a) and the new surface treatment (b).

This was the rationale for switching the period of performance for Tasks 1.7 (originally due Q8) and Task 1.1 (now due Q4). The change to the milestones was entered into the DOE Project Management System and approved on August 17, 2015.

[1] Ren, Y., and Y. Shen, Y. Lin, and C.-W. Nan. *Electrochemistry Communications* 57 (2015): 27-30.
[2] Ishiguro, K., et.al. *Journal of the Electrochemical Society* 160 (2013): A1690-A1693.
[3] Ohta, S., and T. Kobayashi, J. Seki, and T. Asaoka. *Journal of Power Sources* 202 (2012): 332-335.

Patents/Publications/Presentations

Publication

- Yu, Seungho, and Robert D. Schmidt, Regina Garcia-Mendez, Erik Herbert, Nancy J. Dudney, Jeffrey B. Wolfenstine, Jeff Sakamoto, and Donald J. Siegel. "Elastic Properties of the Solid Electrolyte $Li_7La_3Zr_2O_{12}$ (LLZO)." *Chemistry of Materials* (Submitted).

Presentations

- The Battery Show in Novi, Michigan; Jeff Sakamoto moderated a session titled "The Solid-State Revolution," with speakers from Toyota, Google, Samsung, and Intel.
- Opening ceremony of the University of Michigan Energy Institute's Battery Lab (October 2, 2015); Jeff Sakamoto.

Task 7.3 – Composite Electrolytes to Stabilize Metallic Lithium Anodes (Nancy Dudney and Frank Delnick, Oak Ridge National Laboratory)

Project Objective. Prepare composites of representative polymer and ceramic electrolyte materials to achieve thin membranes that have the unique combination of electrochemical and mechanical properties required to stabilize the metallic lithium anode while providing for good power performance and long cycle life. Understand the lithium ion transport at the interface between polymer and ceramic solid electrolytes, which is critical to the effective conductivity of the composite membrane. Identify key features of the composite composition, architecture, and fabrication that optimize the performance. Fabricate thin electrolyte membranes to use with a thin metallic lithium anode to provide good power performance and long cycle life.

Project Impact. A stable lithium anode is critical to achieve high energy density with excellent safety, lifetime, and cycling efficiency. This study will identify the key design strategies that should be used to prepare composite electrolytes to meet the challenging combination of physical and chemical and manufacturing requirements to protect and stabilize the lithium metal anode for advanced batteries. By utilizing well characterized and controlled component phases, the design rules developed for the composite structures will be generally applicable toward the substitution of alternative and improved solid electrolyte component phases as they become available. Success in this program will enable these specific DOE technical targets: 500-700Wh/kg, 3000-5000 deep discharge cycles, and robust operation.

Approach. This program seeks to develop practical solid electrolytes that will provide stable and long-lived protection for the lithium metal anode. Current electrolytes all have serious challenges when used alone: oxide ceramics are brittle, sulfide ceramics are air sensitive, polymers are too resistive and soft, and many electrolytes react with lithium. Composites provide a clear route to address these issues. This program does not seek discovery of new electrolytes; rather, the goal is to study combinations of current well known electrolytes. The program emphasizes the investigation of polymer-ceramic interfaces formed as bilayers and as simple composite mixtures where the effects of the interface properties can be readily isolated. In general, the ceramic phase is several orders of magnitude more conductive than the polymer electrolyte, and interfaces can contribute an additional source of resistance. Using finite element simulations as a guide, composites with promising compositions and architectures are fabricated and evaluated for lithium transport properties using ac impedance and dc cycling with lithium in symmetric or half cells. General design rules will be determined that can be widely applied to other combinations of solid electrolytes.

Out-Year Goal. Use advanced manufacturing processes where the architecture of the composite membrane can be developed and tailored to maximize performance and cost-effective manufacturing.

Collaborations. Electrolytes under investigation include a garnet electrolyte from Jeff Sakamoto (University of Michigan) and ceramic powder from Ohara. Staff at Corning Corporation will serve as our industrial consultant. Student intern, Cara Herwig, from Virginia Tech. University assisted this quarter.

Milestones

1. Compare the vapor absorption (rate and equilibrium) of small molecules in a single-phase polymer and a corresponding ceramic/polymer composite electrolyte. (Q1 – Complete)
2. Compare Li cycling, contacting Li with a buried Ni tab versus a surface metal contact. (Q2 – Complete)
3. By generating a database with at least 5 compositions, determine if the presence of trace solvent molecules that enhance the ionic conductivity are also detrimental to the stability and cyclability of a lithium metal electrode, and if the effect can be altered by adding an overlayer film. (Q3 – SMART, Ongoing)
4. Demonstrate a practical processing route to a thin, dense membrane 100μm x 50cm^2. (Q4 – Complete)

Progress Report

For milestone 4, we have produced a number of larger composite membranes, such as that shown in Figure 61. These are 50 vol.% Ohara glass particles dispersed in the polymer electrolyte matrix.

Most of the earlier work in this program has relied on melt-press methods for forming the composites in order to carefully control exposure to any volatile molecules that might contaminate the composite and influence the properties, even in trace concentrations. This made processing of large areas with large volume fraction of the ceramic component very difficult. The molten mixture with a large ceramic loading did not flow due to particle jamming, so it was necessary to evenly disperse the powder mixture across the heated plattens before pressing. The melt pressed membranes were smaller than desired and poorly uniform. No doubt there is extrusion processing equipment that could process such a composite mix, but instead we tried slurry methods that can be readily scaled to large areas.

Figure 61. An example of the scalable, composite membranes produced with 50 vol.% Ohara glass particles dispersed in polymer electrolyte matrix.

Slurry processing and coating methods proved much more practical, and surprisingly, the ion transport was found to be consistent with earlier melt processed materials. Two different carriers for the slurries have been investigated, along with several methods to form the membranes. The particular membrane in Figure 61 is 6 x 6 x 0.001 inch, but it could easily be scaled to much larger, thicker membranes.

Figure 62 compares the conductivity determined from the impedance scans of composites and the ceramic-free polymer electrolyte prepared by several different slurries. All are ≈ 50 vol% Ohara glass ceramic powder, and the results agree well with the melt cast materials. This shows that vacuum heating to remove the solvent was effective. The conductivity of the composite is very resistive due to a highly resistive interface for ions crossing the ceramic-polymer boundaries.

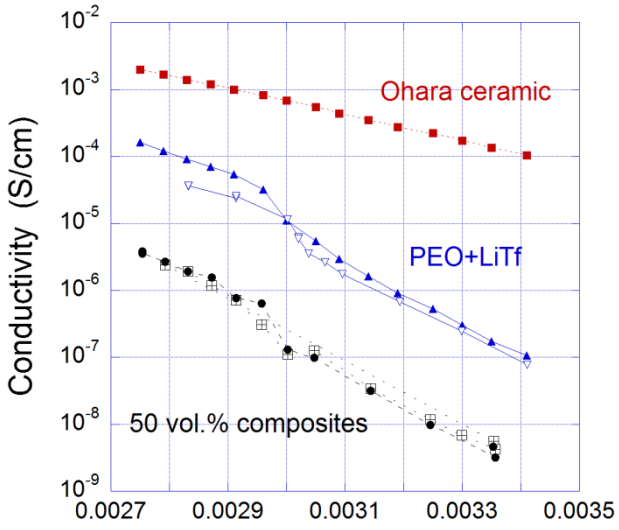

Figure 62. Comparison of conductivity determined from impedance scans of composites and ceramic-free polymer electrolyte prepared by different slurries.

For Milestone 3, the effect of solvent incorporation with melt-pressed composites is clear, but attempts to add a surface barrier coating to improve the stability have been inconclusive. With the new composite sheets, which appear to be both smoother and more homogeneous, this will be repeated.

Task 7.4 – Overcoming Interfacial Impedance in Solid-State Batteries (Eric Wachsman, University of Maryland – College Park)

Project Objective. The project objective is to develop a multifaceted and integrated (experimental and computational) approach to solve the key issue in solid-state Li-ion batteries (SSLiBs), interfacial impedance, with a focus on garnet-based solid-state electrolytes (SSEs), the knowledge of which can be applied to other SSE chemistries. The focus is to develop methods to decrease the impedance across interfaces with the solid electrolyte, and ultimately demonstrate a high power/energy density.

Project Impact. Garnet electrolytes have shown great promises for safer and high energy density batteries. The success of the proposed research can lead to dramatic progress on developing SSLiBs based on garnet electrolytes. Regarding fundamental science, our methodology by combining computations and experiments can lead to an understanding of the thermodynamics, kinetics, and structural stability and evolution of SSLiBs with the garnet electrolytes. Due to the ceramic nature of garnet electrolyte, being brittle and hard, garnet electrolyte particles intrinsically lead to poor contacts among themselves or with electrode materials. A fundamental understanding at the nanoscale and through computations, especially with interface layers, can guide improvements to their design and eventually lead to the commercial use of such technologies.

Approach. SSLiB interfaces are typically planar, resulting in high impedance due to low specific surface area; attempts to make 3D high surface area interfaces can also result in high impedance due to poor contact (for example, pores) at the electrode-electrolyte interface that hinder ion transport or degrade due to expansion/contraction with voltage cycling. We will experimentally and computationally determine the interfacial structure-impedance relationship in SSLiBs to obtain fundamental insight into design parameters to overcome this issue. Furthermore, we will investigate interfacial modification (layers between SSE and electrode) to see if we can extend these structure-property relationships to higher performance.

Collaborations. We are in collaboration with Dr. Venkataraman Thangadurai on garnet synthesis. We will collaborate with Dr. Leonid A. Bendersky (Leader, Materials for Energy Storage Program at NIST) and use neutron scattering to investigate the lithium profile across the bilayer interface with different charge-discharge rates. We are in collaboration with Dr. Kang Xu in U.S. Army Research Lab with preparation of PFPE electrolyte.

Milestones

1. Synthesize garnet and electrode materials. (Complete)
2. Determine frequency dependence of garnet and electrode impedances. (Complete)
3. Develop computation models for garnet-based interfaces. (Complete)
4. Identify gel or PFPE based electrolyte with a stable voltage window (0V-4.2 V). (Complete)

Progress Report

Structured Cathode/Electrolyte/Cathode interfaces. To make columnar structure on 150 µm garnet discs, thin garnet slurry was drop coated into polymer mesh template on disc surface. The coated sample was dried in oven and sintered at 800°C for 2 h. The white shining areas are the deposited column structures (Figure 63). Cathode/electrolyte/cathode symmetric cells were made by screen printing thick cathode slurry on the garnet discs. LFMO cathode was sintered at 500°C for 1 h. Silver paste was used as current collector. The thickness of the cathode was about 20µm. As Figure 64 shows, due to the larger contact area the structured garnet disc has lower interfacial resistance than that of as-polished garnet discs.

Figure 63. Structured garnet surface; white shiny areas are garnet columns.

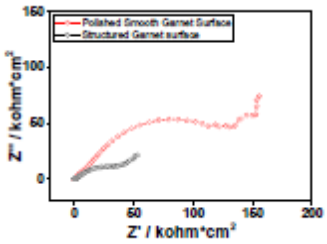

Figure 64. Impedance of cathode on smooth and structured garnet electrolyte interface.

Test of PFPE electrolyte electro-chemical stability. PFPE-DMC was prepared by the steps shown in Figure 65. Two types of PFPE-DMC were prepared using different salt solutions in the washing procedure, which makes type 1 yellow, and type 2 colorless. A Li/PFPE/Ti structure in a CR2025 coin cell was tested with cyclic voltammetry (CV). The CV results are shown in Figure 66. After the first few cycles, the CV curve becomes stable, indicating that the PFPE electrolyte is electrochemically stable between 0 V – 4.2 V. For the first type of PFPE, the peaks at about -0.3 V correspond to Li plating, while the peaks at about 4.2 V correspond to Li stripping. For the second type of PFPE electrolyte, no obvious peaks appear in the voltage region of -0.3 V – 4.2 V. The electrochemical stability of PFPE/LiTFSI in the voltage range of 0 V – 4.2 V ensures that this electrolyte is stable and can be used as the interfacial layer between LLCZN garnet and cathode for lithium ion batteries.

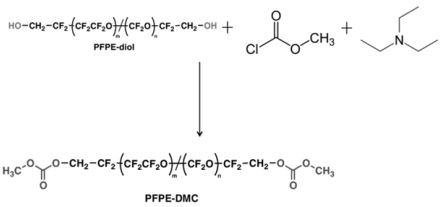

Figure 65. PFPE-DMC synthesis procedure.

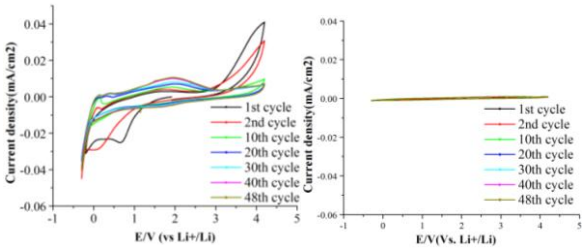

Figure 66. CV of two types of PFPE solvent in Li/PFPE+LiTFSI/Ti system (left, type 1; right, type 2).

Patents/Publications/Presentations

Publication

- Zhu, Yizhou, and Xingfeng He and Yifei Mo. "Origin of Outstanding Stability in the Lithium Solid Electrolyte Materials: Insights from Thermodynamic Analyses Based on First Principles Calculations." *ACS applied materials & interfaces* (Accepted).

Task 7.5 – Nanoscale Interfacial Engineering for Stable Lithium Metal Anodes (Yi Cui, Stanford University)

Project Objective. This study aims to render lithium metal anode with high capacity and reliability by developing chemically and mechanically stable interfacial layers between lithium metal and electrolytes, which is essential to couple with sulfur cathode for high-energy lithium-sulfur batteries. With the nanoscale interfacial engineering approach, various kinds of advanced thin films will be introduced to overcome the issues related to dendritic growth, reactive surface, and virtually "infinite" volume expansion of lithium metal anode.

Project Impact. The cycling life and stability of lithium metal anode will be dramatically increased. The success of this project, together with breakthroughs of sulfur cathode, will significantly increase the specific capacity of lithium batteries and decrease the cost as well, therefore stimulating the popularity of electric vehicles.

Out-Year Goals. Along with suppressing dendrite growth, the cycle life, Coulombic efficiency, as well as the current density of lithium metal anode will be greatly improved (no dendrite growth for current density up to 3.0 mA/cm^2, with Coulombic efficiency > 99.5%) by choosing the appropriate interfacial nanomaterial.

Milestones

1. Fabricate interconnected carbon hollow spheres with various sizes. (3/31/2015 – Complete)
2. Synthesize layered hexagonal boron nitride and graphene with different thicknesses and defect levels. (3/31/2015 – Complete)
3. Demonstrate the guiding effect of polymer nanofibers for improved lithium metal cycling performance. (6/30/2015 – Complete)
4. Demonstrate the improved cycling performance of lithium metal anode with different current density and areal capacity. (9/30/2015 – Complete)
5. Demonstrate the improved cycling stability and reduced volume change of lithium metal anode. (9/30/2015 – Complete)

Progress Report

In addition to the well known problems of lithium metal anode, such as dendrite formation and low cycling efficiency, virtually infinite volume change also prevents the practical use of lithium metal. Inspired from our previous work in which polymer fiber matrix was adapted as supporting matrix for lithium deposition (Liang, Z., et al. *Nano Letters* 15 (2015): 2910-2916), we developed an infusion method that creates nanoporous lithium with conformal lithium coating over polymer nanofibers (Figure 67). The chemically inert and thermally stable polyimide fiber served as stable framework for lithium metal anode, while the interface with lithium was compromised by a thin layer of zinc oxide, whose "lithiophilic" surface was essential for lithium infusion.

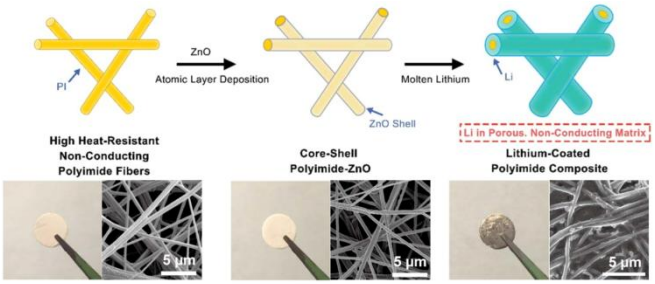

Figure 67. Schematic of the fabrication of the Li-coated PI matrix. Electrospun PI was coated with a layer of ZnO via ALD to form core-shell PI-ZnO. The existence of ZnO coating renders the matrix "lithiophilic" such that molten Li can steadily infuse into the matrix. The final structure of the electrode is Li coated onto a porous, non-conducting polymeric matrix.

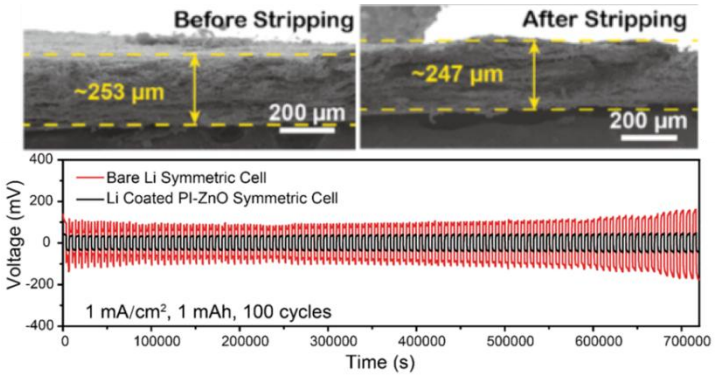

Figure 68. Electrochemical behaviors of the Li electrodes in EC/DEC electrolyte. (top) Cross-sectional scanning electron microscopy images of nanoporous lithium anode before and after complete lithium stripping. (bottom) Comparison of the cycling stability of the Li-coated PI matrix and the bare Li electrode at a current density of 1 mA/cm² with fixed capacity of 1mAh/cm².

As shown in Figure 68 (top), the lithium-infused polyimide fiber matrix largely retains its volume, even though all the lithium is completely electrochemically stripped, which is essential to minimize the mechanical fluctuation in a commercial cell. More importantly, the nanoporous lithium matrix exhibited well-confined electrochemical behavior during galvanostatic cycling. For the cell with symmetrically paired bare lithium, the overpotential increases gigantically over time, because of continuous morphology change and electrolyte consumption. On the contrary, lithium-infused polymer fiber matrix undergoes much lower and more stable overpotential overtime, resulting from larger surface area and the uniformly distributed morphology change, respectively.

Patents/Publications/Presentations

Publication

- Liu, Y., et al. "Lithium Coated Polymeric Matrix as Minimum Volume Change and Dendrite Free Lithium Metal Anode." Submitted.

Task 7.6 – Lithium Dendrite Suppression for Lithium-Ion Batteries (Wu Xu and Ji-Guang Zhang, Pacific Northwest National Laboratory)

Project Objective. The objective of this project is to prevent lithium (Li) dendrite formation on Li-metal anode used in Li-metal batteries and to prevent Li dendrite formation on carbon anodes used in Li-ion batteries during extreme charge conditions such as overcharge, fast charge and charge at low temperatures. We will further explore various factors that affect the morphology of Li deposition, especially at high current density conditions. These factors include solvent-cation reaction and Li-ion additive cation interaction. The long-term stability of these additives also will be investigated. Novel additives will be combined with common electrolytes used in state-of-the-art Li-ion batteries to prevent Li dendrite growth in these batteries, especially when they are operated under extreme conditions.

Project Impact. Li metal is an ideal anode material for rechargeable batteries. Unfortunately, uncontrollable dendritic Li growth and limited Coulombic efficiency during Li deposition/stripping inherent in these batteries have prevented their practical applications. This work will explore the new electrolyte additives that can lead to dendrite-free Li deposition with high Coulombic efficiency. The success of this work will increase energy density of Li and Li-ion batteries and accelerate market acceptance of electrical vehicles (EVs), especially for plug-in hybrid electrical vehicles (PHEVs) required by the EV Everywhere Grand Challenge proposed by the DOE Office of Energy Efficiency and Renewable Energy (EERE).

Out-Year Goals. The long-term goal of the work is to enable Li and Li-ion batteries with >120 Wh/kg (for PHEVs), 1000 deep-discharge cycles, a 10-year calendar life, improved abuse tolerance, and less than 20% capacity fade over a 10-year period.

Collaborations. This project engages in collaboration with the following:

- Bryant Polzin (ANL) – NCA, NMC and graphite electrodes
- Chongmin Wang (PNNL) – Characterization by transmission electron microscopy (TEM) and scanning electron microscopy (SEM)
- Kang Xu (ARL) – Electrospray ionisation mass spectrometry (ESI-MS) studies on cation-solvent interactions in electrolytes
- Vincent Battaglia (LBNL) – LFP electrode

Milestones

1. Develop electrolytes to suppress Li dendrite growth on Li metal and graphite anode and to maintain Li Coulombic efficiency over 98%. (12/31/2014 – Complete)
2. Protect graphite electrode in PC-EC-based carbonate electrolytes with electrolyte additives. (3/31/2015 – Complete)
3. Demonstrate over 300 cycles for 4-V Li-metal batteries without internal short circuiting, through optimized electrolyte formulation(6/30/2015 – Complete)
4. Achieve over 500 cycles for 4-V Li-metal batteries without internal short circuiting, through optimized electrolyte formulation. (9/30/2015 – Complete)

Progress Report

This quarter, the long-term cycling stability of Li||NMC-442 coin cells was investigated with various electrolytes including three controls based on 1.0 M $LiPF_6$ in EC/EMC at different ratios (E004, E256 and E448), four 1.0 M $LiPF_6$ + 0.05 M $CsPF_6$ in EC/PC/EMC at different ratios (E432, E440, E444 and E446), and three other salts-based electrolytes (E319, E319D and E456). NMC442 was used as the cathode due to its good structural stability and thermal stability, and the loading of NMC-442 was moderately high at 2.0 mAh/cm^2 so the results are more realistic. After two formation cycles at C/20 rate, the cells were charged at C/3 rate and discharged at 1C rate in the voltage range of 2.7 V to 4.3 V. Two new electrolytes (E446 and E448) show stable cycling for 500 cycles before the capacity retention reaches 80% (Figure 69).

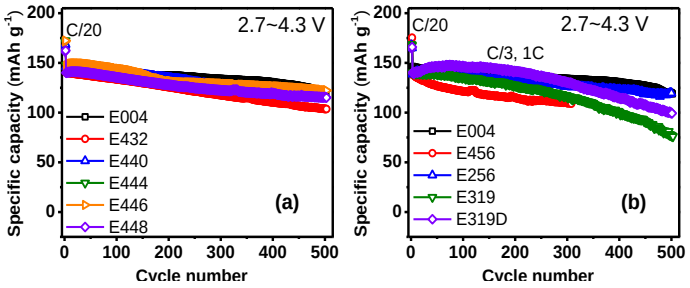

Figure 69. Long-term cycling stability of Li||NMC-442 coin cells with 10 electrolytes at RT.

It is well known that PC solvent can improve the low-temperature performance of the electrolyte, but a large portion of PC in electrolyte can lead to graphite degradation. The effect of $CsPF_6$ additive on the performance of graphite electrode was investigated using $LiPF_6$/EC-PC-EMC as base electrolytes. The role of PC content in the presence of $CsPF_6$ additive (0.05 M) on the performance of graphite electrode in Li||graphite half cells and graphite||NCA full cells has been systematically investigated. $CsPF_6$ additive has been demonstrated to effectively manipulate the formation of a robust, thin, and compact solid-electrolyte interphase (SEI) layer on graphite electrode surface, which then significantly suppresses PC co-intercalation and graphite exfoliation, thus improving the Coulombic efficiency of graphite electrode even in PC-rich electrolytes. As shown in Figure 70, the electrolyte with 20% PC in the solvent mixture shows the best cycling performance for 500 cycles at RT. This electrolyte also exhibits the same rate capability as the non-PC control electrolyte but better high-temperature cycling stability. The trend for Li dendrite formation on graphite anode during fast charge is also alleviated owing to the reduced kinetic barrier for Li^+ ion transportation through this ultrathin SEI layer. The synergistic effects of the desirable SEI layer formed on graphite electrode and the presence of low-melting-point PC solvent enable the sustainable operation of the graphite||NCA full cells under a wide spectrum of temperatures. The fundamental findings of this work also shed light on the importance of manipulating/maintaining the electrode/electrolyte interphasial stability in a variety of energy storage devices.

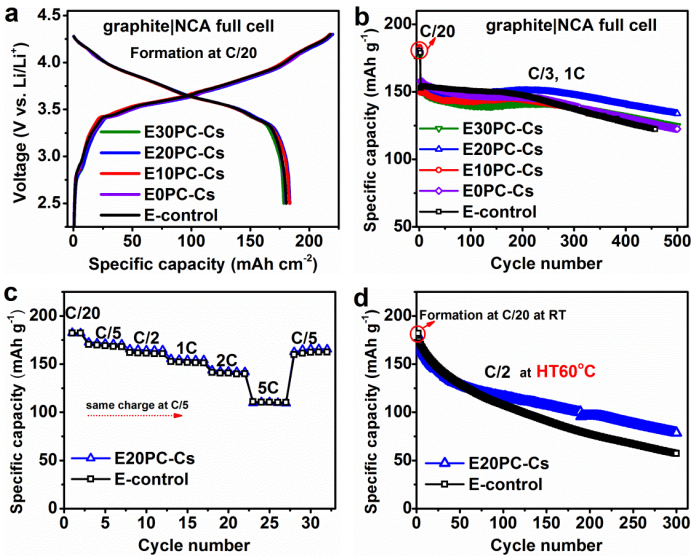

Figure 70. (a) Initial charge/discharge profiles at C/20 (1C = 1.5 mA cm^{-2}) and (b) long-term cycling performance of graphite||NCA full cells using electrolytes containing different amounts of PC at room temperature. (c) Rate capability at room temperature. (d) Long-term cycling stability (C/2 rate for charge and discharge) of graphite||NCA full cells using non-PC control and E20PC-Cs electrolytes at an elevated temperature of 60°C.

Patents/Publications/Presentations

Publications

- Xiao, Liang, and Xilin Chen, Ruiguo Cao, Jiangfeng Qian, Hongfa Xiang, Jianming Zheng, Ji-Guang Zhang*, and Wu Xu*. "Enhanced Performance of LijLiFePO_4 Cells Using $CsPF_6$ as an Electrolyte Additive." *Journal of Power Sources*, 293 (2015): 1062-1067.
- Xiang, Hongfa, and Donghai Mei, Pengfei Yan, Priyanka Bhattacharya, Sarah D. Burton, Arthur V. Cresce, Ruiguo Cao, Mark H. Engelhard, Mark E. Bowden, Zihua Zhu, Bryant J. Polzin, Chongmin Wang, Kang Xu, Ji-Guang Zhang, and Wu Xu."The Role of Cesium Cation in Directing Interphasial Chemistry on Graphite Anode in Propylene Carbonate-Rich Electrolytes." *ACS Applied Materials & Interfaces*, under review.

TASK 8 – LITHIUM SULFUR BATTERIES

Summary and Highlights

Advances in Li-ion technology thus far have been stymied by challenges facing the development of high reversible capacity cathodes and stable anodes. Hence, there is a critical need for the development of alternate battery technologies with superior energy densities and cycling capabilities. Lithium-sulfur (Li-S) batteries in this regard have been identified as the next flagship technology, holding much promise due to the attractive theoretical specific energy densities of 2,567 Wh/kg. Moreover, realization of the high theoretical specific capacity of 1,675 mAh/g corresponding to the formation of Li_2S utilizing earth-abundant sulfur renders the system highly promising compared to other hitherto available cathode systems. The current research focus has thus shifted toward the development of lithium sulfur (Li–S) batteries. This system, however, suffers from major drawbacks, as elucidated below.

- Limited inherent electronic conductivity of sulfur and sulfur compound based cathodes.
- Volumetric expansion and contraction of both the sulfur cathode and lithium anode.
- Soluble polysulfide formation/dissolution and sluggish kinetics of subsequent conversion of polysulfides to Li_2S resulting in poor cycling life.
- Particle fracture and delamination as a result of the repeated volumetric expansion and contraction.
- Irreversible loss of lithium at the sulfur cathode, resulting in poor Coulombic efficiency.
- High diffusivity of polysulfides in the electrolyte, resulting in plating at the anode and consequent loss of driving force (that is, drop in cell voltage).

These major issues cause sulfur loss from the cathode, leading to mechanical disintegration. Additionally, surface passivation of anode and cathode systems results in a decrease in the overall specific capacity and Coulombic efficiency (CE) upon cycling. As a result, the battery becomes inactive within the first few charge-discharge cycles. Achievement of stable high capacity in Li-S batteries requires execution of fundamental studies to understand the degradation mechanisms in conjunction with engineered solutions. Task 8 addresses both aspects with execution of esoteric, fundamental *in situ* x-ray spectroscopy (XAS) and *in situ* electron paramagnetic resonance (EPR) studies juxtaposed with applied research comprising use of suitable additives, coatings, and exploration of composite morphologies. Both ANL and LBNL use x-ray based techniques to study phase evolution and loss of CE in See_s during lithiation/delithiation, while understanding polysulfide formation in sulfur and polysulfides (PSL) in oligomeric polyethylene oxide (PEO) solvent, respectively. Work from PNNL, University of Pittsburg, and Stanford demonstrates high areal capacity electrodes in excess of 2 mAh/cm^2. Following loading studies reported in the first quarter, PNNL has performed *in situ* EPR to study reaction pathways mediated by sulfur radical formation. Coating/encapsulation approaches adopted by University of Pittsburgh and Stanford comprise flexible sulfur wire (FSW) electrodes coated with Li-ion conductors, and TiS_2 encapsulation of Li_2S in the latter, both ensuring polysulfide retention at sulfur cathodes. BNL work has focused on benchmarking of pouch cell testing by optimization of the voltage window and study of additives such as LiI and $LiNO_3$. *Ab initio* studies at Stanford and University of Pittsburg involving calculation of binding energies and reaction pathways, respectively, augment the experimental results. *Ab initio* molecular dynamics (AIMD) simulations performed at Texas A&M University reveal multiple details regarding electrolyte decomposition reactions and the role of soluble polysulfides (PS) on such reactions. Using Kinetic Monte-Carlo (KMC) simulations, electrode morphology evolution and mesostructured transport interaction studies were also executed. Each of these projects has a collaborative team of experts with the required skill set needed to address the EV Everywhere Grand Challenge of 350 Wh/kg and 750 Wh/l, and cycle life of at least 1000 cycles.

Highlights for this quarter include the following:

- Use of oxide based composite sulfur electrodes (Cui-Stanford) has been shown to result in improved cycling stability with lowest fade rate of ~0.034%/cycle reported over 300 cycles for MgO/C based composite electrodes.
- Sulfur CFM structures have been shown to have stable cycling over 180 cycles (~0.01%/cycle fade rate) subsequent to initial phase change (Kumta-U Pittsburgh).
- Using DFT and AIMD modeling (Balbuena-Texas A&M) outlined the mechanisms behind polysulfide fragmentation and Li_2S formation on the anode side of Li-S battery.

Task 8.1 – New Lamination and Doping Concepts for Enhanced Li – S Battery Performance (Prashant N. Kumta, University of Pittsburgh)

Project Objective. To successfully demonstrate generation of novel sulfur cathodes for Li-S batteries meeting the targeted gravimetric energy densities ≥ 350 Wh/kg and ≥ 750 Wh/l, with a cost target $125/kWh and cycle life of at least 1000 cycles for meeting the EV Everywhere blueprint. The proposed approach will yield sulfur cathodes with specific capacity ≥1400 mAh/g, at ≥ 2.2 V, generating ~460 Wh/kg energy density higher than the target. Full cells meeting the required deliverables will also be made.

Project Impact. Identification of new laminated sulfur cathode based systems displaying higher gravimetric and volumetric energy densities than conventional lithium ion batteries will likely result in new commercial battery systems that are more robust, capable of delivering better energy and power densities, and more lightweight than current Li-ion battery packs. Strategies and configurations based on new Li-ion conductor (LIC)-coated sulfur cathodes will also lead to more compact battery designs for the same energy and power density specifications as current Li-ion systems. Commercialization of the new sulfur cathode based Li-ion battery packs will represent, fundamentally, a hallmark contribution of the DOE Vehicle Technologies Office (VTO) and the battery community.

Out-Year Goals. This multi-year project comprises three major phases to be successfully completed in three years. Phase 1 (Year 1): Synthesis, Characterization, and Scale up of suitable LIC matrix materials and multilayer composite sulfur cathodes. This phase is completed. Phase 2 (Year 2): Development of LIC coated sulfur nanoparticles, scale up of high-capacity engineered LIC-coated multilayer composite electrodes, and doping strategies for improving electronic conductivity of sulfur. Phase 3 (Year 3): Advanced high energy density, high-rate, extremely cyclable cell development.

Collaborations. The project collaborates with the following members with the corresponding expertise:

- Dr. Spandan Maiti (University of Pittsburgh): for mechanical stability and multi-scale modeling
- Dr. A. Manivannan (NETL): for x-ray photoelectron spectroscopy (XPS) for surface characterization
- Dr. D. Krishnan Achary (University of Pittsburgh): for solid-state magic angle spinning nuclear magnetic resonance (MAS-NMR) characterization

Milestones

1. Develop novel lithium-ion conducting membrane systems using *ab initio* methods displaying impermeability to sulfur diffusion. (December 2014 – Complete)
2. Demonstrate capabilities for generation of novel sulfur 1D, 2D, and 3D morphologies exhibiting superior stability and capacity. (June 2015 – Complete)
3. Identification and synthesis of LIC materials for use as coatings for sulfur cathodes. (June 2015 – Complete)
4. Novel encapsulation and sheathing techniques, and exploration of unique architectures and generation of 3D composites displaying superior Li-ion conduction, reversible capacity, and stability. (June 2015 – Complete)
5. Identification of suitable dopants and dopant compositions to improve electronic conductivity of sulfur. (October 2015 – Complete)
6. Fundamental electrochemical study to understand the reaction kinetics, mechanism, and charge transfer kinetics. (October 2015 – On-going)
7. Go/No-Go decision will be based on the ability to demonstrate improvement in cycling upon use of the LIC coating. (October 2015 – Complete)

Progress Report

This quarter concludes Phase 1 of this project. The aim of Phase 1 was essentially to identify various materials that can act as lithium ion conductors (LICs) while preventing polysulfide transport and accompanying sulfur loss. The end of the fourth quarter has a Go/No-go point based on the ability to demonstrate that the working hypothesis is valid (that is, LICs improve Li-S battery cycle life). Previously identified strategies for achieving the same were the use of inorganic LICs in the form of pellet coatings (Q1, Q2), fabrication of flexible polymer-sulfur wires (Q2), as well as gel polymer electrolyte (GPE) used as an electrolyte medium containing a separator (Q3). All of these approaches resulted in improved cycling with scope for further optimization, an effort that will be undertaken in Phase 2 (Year 2). This quarter, the use of complex framework materials (CFM) as trapping agents for sulfur species was explored. The CFM materials containing nanopores are ideal for entrapping the soluble polysulfide species formed during lithiation of sulfur. Figure 71 depicts the morphology of certain nanoporous CFMs acting as sulfur-hosts. Significant improvement in initial capacity and cycling stability resulted from use of sulfur-containing CFMs as Li-S battery cathodes, and stable cycling has already been demonstrated for up to 200 cycles (further cycling is ongoing). The CFM electrodes exhibit a significantly low fade rate of ~0.01%/ cycle following initial phase change. A second effort and also a required deliverable this quarter was identifying strategies to improve the inherent electronic conductivity of sulfur. Toward this goal, first principles studies were conducted to understand the effect of dopants on the band-structure and density of electronic states (DOS) of sulfur (Figure 72). It can be seen that sulfur, which is inherently an insulator following introduction of dopants, exhibits semiconducting properties upon introduction of dopants into the sulfur lattice. Experimental synthesis of the doped sulfur followed by detailed evaluation will form part of the project's Phase-2 study to be initiated in Year 2.

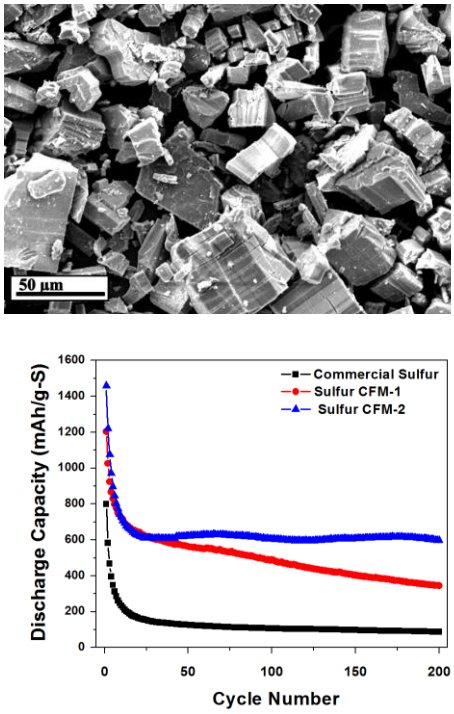

Figure 71. Morphology of sulfur-containing nanoporous CFMs and improvement in cycling stability as a result of the same.

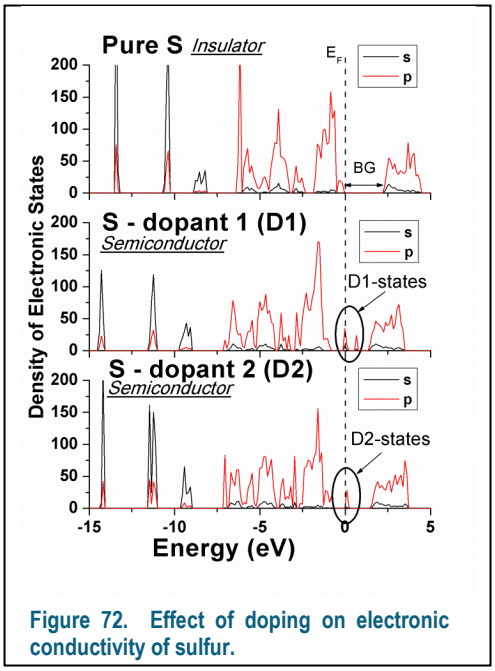

Figure 72. Effect of doping on electronic conductivity of sulfur.

Patents/Publications/Presentations

Publication

- Jampani, P.H., and B. Gattu, P.M. Shanthi, S.S. Damle, Z. Basson, R. Bandi, M.K. Datta, S.K. Park, and P.N. Kumta. "Flexible Sulfur Wires (Flex-SWs) – A Versatile Platform for Lithium-sulfur Batteries, *ChemElectrochem* (2015 – In press).

Task 8.2 – Simulations and X-ray Spectroscopy of Li-S Chemistry (Nitash Balsara, Lawrence Berkeley National Laboratory)

Project Objective. Lithium-sulfur cells are attractive targets for energy storage applications as their theoretical specific energy of 2600 Wh/kg is much greater than the theoretical specific energy of current lithium-ion batteries. Unfortunately, the cycle-life of lithium-sulfur cells is limited due to migration of species generated at the sulfur cathode. These species, collectively known as polysulfides, can transform spontaneously, depending on the environment, and it has thus proven difficult to determine the nature of redox reactions that occur at the sulfur electrode. The objective of this project is to use x-ray spectroscopy to track species formation and consumption during charge-discharge reactions in a lithium-sulfur cell. Molecular simulations will be used to obtain x-ray spectroscopy signatures of different polysulfide species, and to determine reaction pathways and diffusion in the sulfur cathode. The long-term objective of this project is to use the mechanistic information to build high specific energy lithium-sulfur cells.

Project Impact. Enabling rechargeable lithium-sulfur cells has the potential to change the landscape of rechargeable batteries for large-scale applications beyond personal electronics due to: (1) high specific energy, (2) simplicity and low cost of cathode (the most expensive component of current lithium-ion batteries), and (3) earth abundance of sulfur. The proposed diagnostic approach also has significant potential impact as it represents a new path for determining the species that form during charge-discharge reactions in a battery electrode

Out-Year Goals. Year 1: Simulations of sulfur and polysulfides (PSL) in oligomeric polyethylene oxide (PEO) solvent. Prediction of x-ray spectroscopy signatures of PSL/PEO mixtures. Measurement of x-ray spectroscopy signatures PSL/PEO mixtures. Year 2: Use comparisons between theory and experiment to refine simulation parameters. Determine speciation in PSL/PEO mixtures without resorting to adhoc assumptions. Year 3: Build an all-solid lithium-sulfur cell that enables measurement of x-ray spectra *in situ*. Conduct simulations of reduction of sulfur cathode. Year 4: Use comparisons between theory and experiment to determine the mechanism of sulfur reduction and Li_2S oxidation in all-solid lithium-sulfur cell. Use this information to build lithium-sulfur cells with improved life-time.

Collaborations. This project collaborates with Tsu-Chien Weng, Dimosthenis Sokaras, and Dennis Nordlund at Stanford Synchrotron Radiation Lightsource, Stanford Linear Accelerator Center in Stanford, California.

Milestones

1. Extend theoretical calculations of x-ray absorption spectroscopy (XAS) to finite polysulfide concentrations. (12/1/14 – Complete)
2. Experimental study of the effect of polysulfide concentration on XAS spectra. (2/15/15 – Complete)
3. Quantitative comparison of experimental and theoretical XAS spectra. (5/20/15 – On schedule)
4. Build and test cell for *in situ* XAS analysis. (8/23/15 – On Schedule)

Progress Report

Milestones 1 and 2 have been completed.

Milestone 3 is in progress. All theoretical XAS spectra for lithium polysulfide species dissolved in TEGDME have been calculated. Molecular dynamics simulations and spectra calculations of spectra for lithium polysulfide species in DMF continue. In particular, we are working to understand how the polysulfide/lithium ion/solvent molecule coordination environment differs between DMF (high electron pair donor number) and TEGDME (low electron pair donor number), and how differences affect XAS.

Milestone 4 is under way. We have performed *in situ* XAS studies on discharging Li-S cells. Li-S cells consisting of a lithium metal anode, a block copolymer electrolyte SEO containing $LiClO_4$, and a cathode containing carbon black, elemental sulfur, and SEO/$LiClO_4$ were discharged at the beamline while x-ray photons probed the battery. The resulting data is shown below. Analysis of the spectra is being done using our library of theoretically calculated spectra. Analysis is in progress.

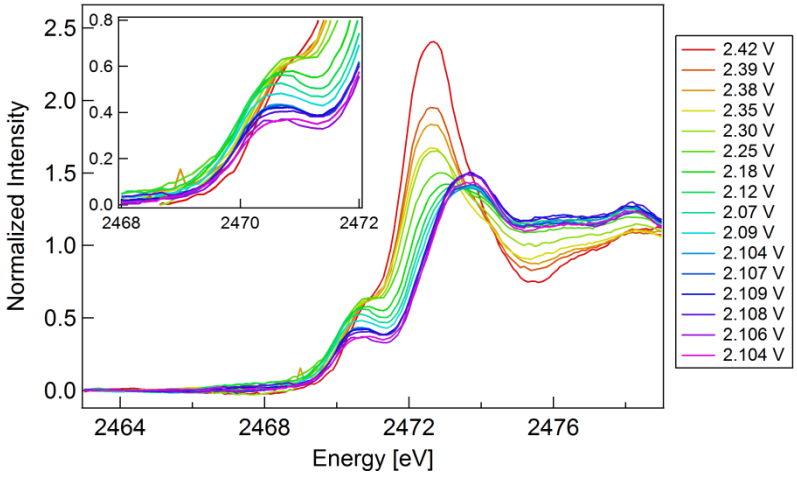

Figure 73. Sulfur K-edge XAS of discharging Li-S cell.

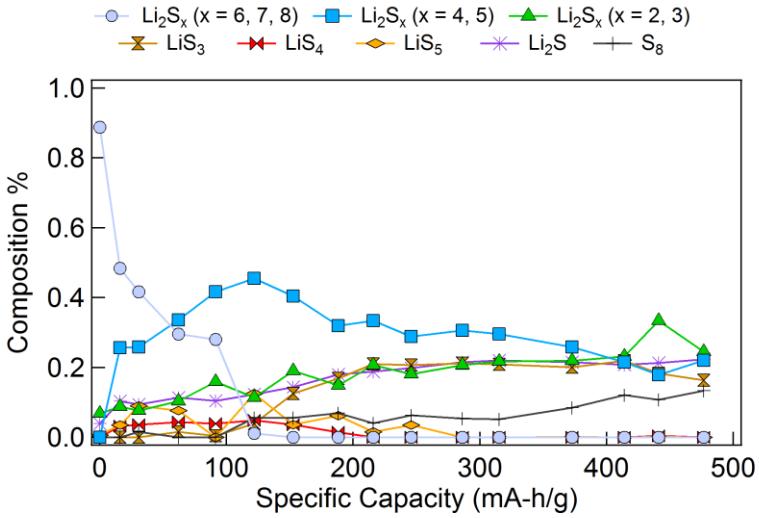

Figure 74. Spectral compositions determined using theoretical sulfur spectra.

Patents/Publications/Presentations

Publications

- Balsara, N.P. "Polysulfide Radicals Appearance in Partially Discharged Lithium-Sulfur Battery Analyzed By First-Principles Interpretations of X-ray Absorption Spectra." Meeting of the Electrochemical Society, Phoenix (October 14, 2015).
- Wang, D. R., et al. "Conductivity of Block Copolymer Electrolytes Containing Lithium Polysulfides." *Macromolecules* 48, no. 14 (2015): 4863-4873.

Presentations

- 2015 Advanced Light Source User Meeting, PICKLES [Prediction and Interpretation of Core-level (K-edge, L-edge, Etc.) Spectroscopy] Workshop, Lawrence Berkeley National Laboratory, Berkeley, California (October 5 – 2015): "Probing the Solution Structure and Electronic Charge State of Dissolved Sulfur Molecules using X-ray Spectroscopy"; T. Pascal.
- 2015 Advanced Light Source User Meeting, Lawrence Berkeley National Laboratory, Berkeley, California (October 6, 2015 – Invited): "Understanding Working Interfaces at the Nanoscale"; D. Prendergast.
- Sixth World Materials Research Institutes Forum, Lawrence Livermore National Laboratory, Livermore, California (September 15, 2015): "Exploring Details of Batteries from First Principles"; D. Prendergast.

Task 8.3 – Novel Chemistry: Lithium Selenium and Selenium Sulfur Couple (Khalil Amine, Argonne National Laboratory)

Project Objective: The objective of this project is to develop a novel SeS_x cathode material for rechargeable lithium batteries with high energy density, long life, low cost, and high safety.

Project Impact: Development of a new battery chemistry is promising to support the goal of plug-in hybrid electric vehicle (PHEV) and electric vehicle (EV) applications.

Approach: Embedding Se_xS_y in a porous carbon matrix to suppress the dissolution of lithium polysulfide and to enhance the life of batteries using such electrode. Impact of stoichiometric and the porous structure of carbon matrix will be investigated in detail.

Out-Year Goals: When this new cathode is optimized, the following result can be achieved:

- A cell with nominal voltage of 2 V and energy density of 600 Wh/kg.
- A battery capable of operating for 500 cycles with low capacity fade.

Collaborations: This project engages in collaboration with the following:

- Prof. Chunsheng Wang of University of Maryland
- Dr. Yang Ren and Dr. Chengjun Sun of Advanced Photon Source at ANL

Milestones

1. Synchrotron probe study of charge storage mechanism of Li/S batteries. (Q1 – Complete)
2. Study of stability of Li/Se batteries in carbonate-based electrolyte. (Q2 – Complete)
3. Investigation of the phase diagram of Se_xS_y system. (Q3 – Ongoing)
4. Encapsulating Se_2S_5 in nanoporous carbon (Q4 – Ongoing)

Progress Report

Last quarter, we explored the possible stable structures in S-Se binary phase diagram, and found that Se_2S_5 was stable in the amorphous state at the ambient condition, while both S and Se remained at crystalline state. Therefore, amorphous Se_2S_5 was investigated this quarter. Our *in situ* x-ray absorption spectroscopy study reported last quarter also showed a low utilization of Se when a carbonate-based electrolyte was used. This quarter, we tried to improve the utilization of Se_2S_5 by encapsulating the active material in a nanoporous carbon matrix. Figure 75 shows the scanning electron microscopy images of carbon materials investigated. Conventionally, Ketjenblack is widely used as the conducting agent for electrodes used in lithium-ion batteries, and it was investigated here as a control experiment. Figure 75a shows that Ketjenblack is composed of nanospheres with a diameter of about 50 nm; macropores are formed through the agglomeration of nano-balls. To further improve the electric conductivity of the electrode, multiwall carbon nanotubes were added as a complementary conductive agent to Ketjenblack. The active material was prepared by ball-milling a mixture of sulfur (25 wt%), selenium (25 wt%), Ketjenblack carbon black (45 wt%), and carbon nanotube (5 wt%) in Argon environment. The thermogravimetric analysis (TGA) confirmed the proper loading of Se_2S_5 active material in the carbon matrix (see Figure 76). The electrochemical testing shows that the composite material can deliver a stable capacity of about 400 mAh/g, which is substantially lower than its theoretical capacity (1389 mAh/g). Alternatively, we tried to encapsulate the active material in nanochannels of ordered microporous carbon (OMC) (see Figure 75c). For a fair comparison, 50 wt% of Se_2S_5 was loaded into OMC. However, no significant improvement on electrochemical performance was observed for Se_2S_5/OMC composite.

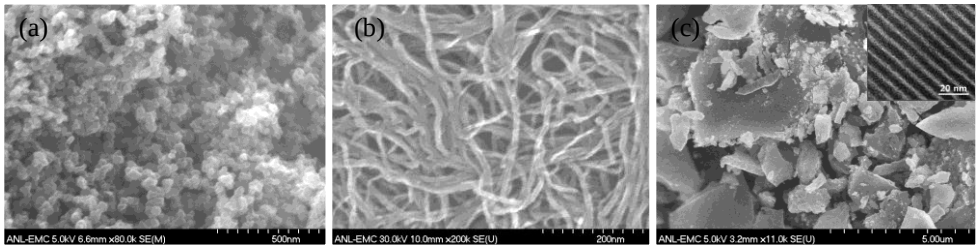

Figure 75. Scanning electron microscopy images of (a) Ketjenblack carbon black, (b) multiwall carbon nanotube, and (c) ordered microporous carbon (OMC). The insert in Figure 75c is a transmission electron microscopy image showing micron channels (about 5 nm in diameter) in OMC to host Se_2S_5.

It is also possible that the low reversible capacity can also originate from poor compatibility between the active material and the electrolyte. Our preliminary results shows that the reversible capacity can be improved up to 600 mAh/g by simply replacing the carbonate-based electrolyte with an ether-based one (see Figure 77).

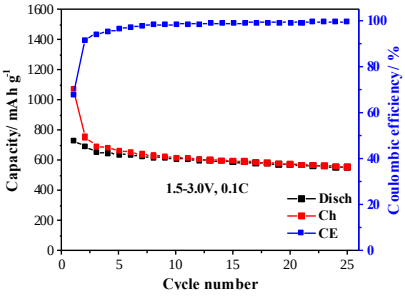

Figure 77. Charge/discharge capacity of a cell comprising Se_2S_5/ Ketjenblack-CNT. The electrolyte used was 1.0 M LiTFSI in DOL/TTE (1:1 by volume) with 0.1 M $LiNO_3$.

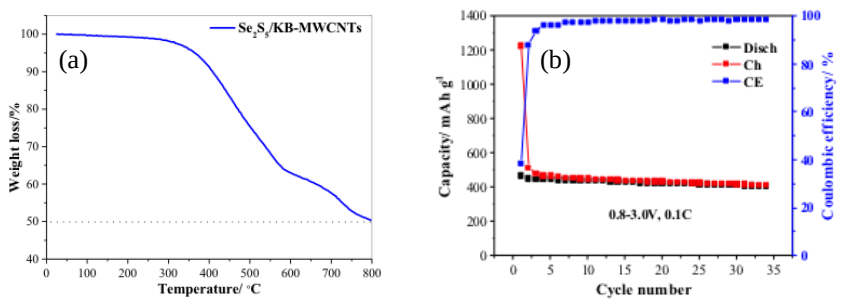

Figure 76. (a) Weight loss of a Se_2S_5/Ketjenblack-CNT composite during TGA analysis, confirming the proper loading of the active material in carbon matrix; and (b) charge/discharge capacity of cell using the prepared electrode using a carbonate-based electrolyte.

Task 8.4 – Multi-Functional Cathode Additives (MFCA) for Li-S Battery Technology (Hong Gan, Brookhaven National Laboratory; and Co-PI Esther Takeuchi, Brookhaven National Laboratory and Stony Brook University)

Project Objective. Develop a low-cost battery technology for plug-in electric vehicle (PEV) application utilizing Li-S electrochemical system by incorporating multifunctional cathode additives (MFCAs), consistent with the long-term goals of the DOE EV Everywhere blueprint.

Project Impact. The Li-S battery system has gained significant interest due to its low material cost potential (35% cathode cost reduction over Li-ion) and its attractive 2.8x (volumetric) to 6.4x (gravimetric) higher theoretical energy density compared to conventional Li-ion benchmark systems. Commercialization of this technology requires overcoming several technical challenges. This effort will focus on improving the cathode energy density, power capability and cycling stability by introducing MFCAs. The primary deliverable of this project is to identify and characterize the best MFCA for Li-S cell technology development.

Approach. Transition metal sulfides are evaluated as cathode additives in sulfur cathode due to their high electronic conductivity and chemical compatibility to the sulfur cell system. Electrochemically active additives will also be selected for this investigation to further improve the energy density of the sulfur cell system. In the first year, the team will evaluate the transition metal sulfide cathode cells and sulfur cathode cells individually to establish the baseline. Then the interaction between transition metal sulfide additives and the sulfur electrode will be investigated. In parallel, commercially unavailable selected additives will be synthesized for electrochemical cell interaction studies.

Out-Year Goals. This multi-year project comprises two major phases to be successfully completed in three years. Phase 1 includes cathode and MFCA investigation; Phase 2 will include cell component interaction studies and full cell optimization. The work scope for year 1 will focus on the cathode and cathode additive studies. The proof of concept and feasibility studies will be completed for the MFCAs. By year-end, multiple types of additives will be identified and prepared, including the synthesis of the non-commercially available additives. The electrochemical testing of all selected MFCAs will be initiated.

Collaborations. This project collaborates with Ke Sun, Dong Su, and Can Erdonmez at BNL, along with Amy Marschilok and Kenneth Takeuchi at Stony Brook University.

Milestones

1. Baseline Li/MFCA cell demonstration with selected transition metal sulfides. (Q1 – Complete)
2. Baseline Li/S cell demonstration with sulfur and/or Li_2S cathode. (Q2 – Complete)
3. Li/sulfur-MFCA concept cell demonstration for cathode-MFCA interaction. (Q3 – Complete)
4. Synthesis of selected non-commercial MFCA. (Q4 – Complete)

Progress Report

Synthesis of MFCA. The task objective is to synthesize cathode additive materials that have potential to enhance behavior of the cathode in the lithium/sulfur battery. Recent testing demonstrated that the CuS system did successfully enhance battery rate capability, but not cycle life (manuscript prepared and submitted). Thus, the synthetic efforts for this segment of research focused on two material targets: FeS_2 and TiS_2.

FeS_2 is commercially available as a highly crystalline material with crystallite sizes characteristic of bulk materials, on the order of 100 to 200 nm. For full integration in a composite electrode, nanocrystalline materials were targeted for preparation that would enable the nanocrystalline MFCA to disperse in the composite electrode providing improved opportunity for formation of a conductive percolation threshold.

The synthesis of nanocrystalline FeS_2 was designed using iron oxides as starting materials. Synthetic approaches using both Fe_3O_4 and Fe_2O_3 were developed. The iron oxide precursors were deliberately selected for the synthesis, as synthetic control of iron oxides has been studied in the laboratories of K. J. Takeuchi where the ability to prepare nanocrystalline samples using scalable aqueous based methodologies has been demonstrated. The first synthetic method for the preparation of FeS_2 used nanocrystalline Fe_3O_4, sulfur and sodium thiosulfate as reagents. Successful preparation of nanocrystalline FeS_2 was achieved with an average crystallite size of 45 nm. Using the method developed, gram scale quantities of nanocrystalline FeS_2 were prepared. A second approach utilized Fe_2O_3 as the precursor, where nanoscale Fe_2O_3 was first synthesized as the precursor. Spherical samples of FeS_2 were successfully prepared. Additionally, a novel cube-like morphology was targeted where the cube-like Fe_2O_3 precursor was prepared through control of the synthetic conditions (Figure 78). This precursor enabled preparation of nanoscale FeS_2 with cube-like morphology (Figure 79). Thus, the synthesis of FeS_2 was demonstrated enabling both size and morphology control. Several grams of both forms of nanocrystalline FeS_2 were synthesized.

The synthetic target for TiS_2 was based on a recent report where a core-shell type structure was prepared with a core of Li_2S and a TiS_2 shell (Z. W. She, et al. *Nature Commun*. DOI:10.1038/ncommS6017). The reaction utilized lithium sulfide (Li_2S) and titanium tetrachloride ($TiCl_4$) starting materials. The successful synthesis of crystalline Li_2S surrounded by an amorphous shell of TiS_2 was achieved. Additionally, prelithiated $LiTiS_2$ was prepared though an alternate scheme starting with TiS_2. All the materials prepared are available for integration with the sulfur-based cathodes.

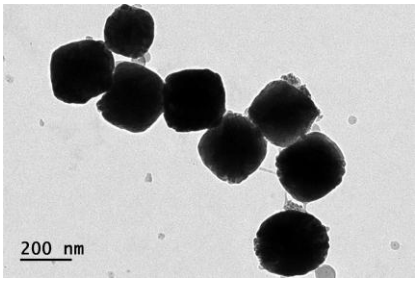

Figure 78. TEM of Nano-Fe_2O_3 precursor.

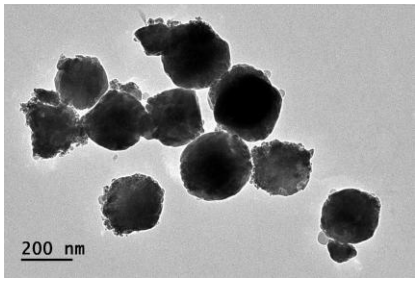

Figure 79. TEM of Nano-FeS_2.

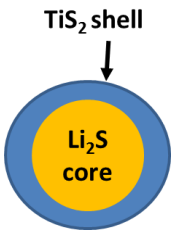

Figure 80. Schematic of Li_2S core with TiS_2 shell.

Patents/Publications/Presentations

Publication

- Sun, Ke, and Dong Su, Qing Zhang, David C. Bock, Amy C. Marschilok, Kenneth J. Takeuchi, Esther S. Takeuchi, and Hong Gan. "Interaction of CuS and Sulfur in Li-S Battery System.," Submitted.

Patents

- Gan, Hong, and Patrick J. Looney. "Multi Functional Cathode Additives for Battery Technologies." Filed USPTO, February 2015.
- Gan, Hong, and Ke Sun. "Hybrid Cathodes for Li-ion Battery Cells." Filed USPTO Provisional, April 2015.

Task 8.5 – Development of High-Energy Lithium-Sulfur Batteries (Jie Xiao and Jun Liu, Pacific Northwest National Laboratory)

Project Objective. The project objective is to develop high-energy, low-cost lithium sulfur (Li-S) batteries with long lifespan. All proposed work will employ thick sulfur cathode (≥2 mAh/cm^2 of sulfur) at a relevant scale for practical applications. The diffusion process of soluble polysulfide out of the thick cathode will be revisited to investigate the cell failure mechanism at different cycling. Alternative anode will be explored to address the lithium anode issue. The fundamental reaction mechanism of polysulfide under the electrical field will be explored by applying advanced characterization techniques to accelerate the development of Li-S battery technology.

Project Impact. The theoretical specific energy of Li-S batteries is ~2300 Wh/kg, which is almost three times higher than that of state-of-the-art Li-ion batteries. The major challenge for Li-S batteries is polysulfide shuttle reactions, which initiate a series of chain reactions that significantly shorten battery life. The proposed work will design novel approaches to enable Li-S battery technology and accelerate market acceptance of long-range electrical vehicles (EVs) required by the EV Everywhere Grand Challenge proposed by the DOE Office of Energy Efficiency and Renewable Energy (EERE).

Out-Year Goals. This project has the following out-year goals:

- Fabricate Li-S pouch cells with thick electrodes to understand sulfur chemistry/electrochemistry in the environments similar to the real application.
- Leverage the Li-metal protection project funded by DOE and PNNL advanced characterization facilities to accelerate development of Li-S battery technology.
- Develop Li-S batteries with a specific energy of 400 Wh/kg at cell level, 1000 deep-discharge cycles, improved abuse tolerance, and less than 20% capacity fade over a 10-year period to accelerate commercialization of electrical vehicles.

Collaborations. This project engages in collaboration with the following:

- Dr. Xiao-Qing Yang (LBNL) − *In situ* characterization
- Dr. Bryant Polzin (ANL) – Electrode fabrication
- Dr. Xingcheng Xiao (GM) – Materials testing

Milestones

1. Optimization of sulfur loading to reach 3-4 mAh/cm^2 areal specific capacity on the cathode. (12/31/2014 – Complete)
2. Complete the investigation on the fundamental reaction mechanism of Li-S batteries. (3/31/2015 – Complete).
3. Identify alternative anode to stabilize the interface reactions on the anode side (6/30/2014 – Complete).
4. Demonstrate the stable cycling of sulfur batteries (2-4 mAh/cm^2) with less than 20% degradation for 200 cycles. (9/30/2015 – Delayed)

Progress Report

In our recent work on the failure mechanism Li-S batteries, long-term cycling stability of Li-S batteries (with reasonably thick cathodes) not only depended on the stability of sulfur cathode, it was also strongly determined by the stability of Li metal anode when highly corrosive polysulfides and their derived sulfur radicals coexisted in the cell. To investigate the stability of sulfur cathode without the interference of Li anode corrosion problem, we revised the focus of our work last quarter and used graphite as an alternative anode in so called "Li-ion sulfur" batteries. Graphite was found to be stable in the 5M LITFSI-DOL electrolyte in the absence of EC in this novel prototype of Li-ion sulfur batteries. More effort was then focused on building a good platform to understand the electrochemical reactions and polysulfide redistribution occurring in the thick sulfur cathodes, especially in the enlarged testing vehicles.

This quarter, our patented S/C thick electrode preparation method was further validated by using the PNNL pouch cell assembly line. Pinhole-free and uniform sulfur electrode was successfully coated on continuous aluminum sheet (Figure 81a), confirming the effectiveness of this approach to prepare secondary S/KB particles for industry use. The sulfur loading was adjustable, and an example of double-side coated sulfur electrode is shown in Figure 81b with ca. 3.5 mg/cm^2 loading. As discussed in the earlier quarterly reports, the electrolyte wetting issue of thick sulfur cathode was still a concern, so the current sulfur loading was always fixed at 3-4 mg/cm^2 to exclude the wetting problem. Even so, the specific capacity of sulfur in the assembled Li-ion sulfur pouch cell (prelithiated graphite was used as the anode) was only around 450 mAh/g, although stable cycling was seen for the first few cycles. This indicates that, in addition to the wetting problems, other unexpected issues occurred in the large format testing of sulfur electrodes that need further systematic investigation.

The capability of making standard thick sulfur cathodes was important, and the samples were available for other BMR PIs for cross validation or testing of their own electrolytes/additives, etc. The prototype of Li-ion sulfur battery also provided a unique opportunity to study the issues associated with the thick sulfur electrodes when stepping from coin cells to pouch cells.

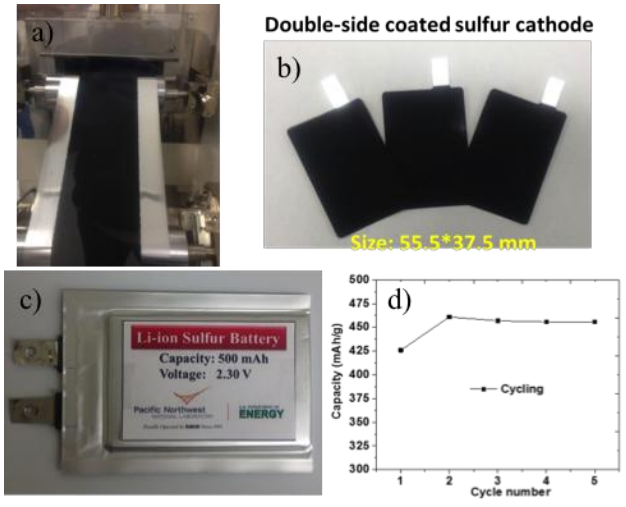

Figure 81. (a) Continuous coating of sulfur electrodes with adjustable loading. The S/C composite was prepared according to patented approach reported earlier. (b) An example of double-side coated sulfur electrodes. (c) Assembled pouch cell using thick sulfur cathodes and prelithiated graphite anodes. (d) Cycling of the Li-ion sulfur prototype cell that will be used to evaluate the electrochemical properties of thick sulfur electrodes.

.

Patents/Publications/Presentations

Publications

- Lu, D., and P. Yan, Y. Shao, Q. Li, S. Ferrara, H. Pan, G.L. Graff, B. Polzin, C. Wang, J.-G. Zhang, J. Liu, and J. Xiao. "High Performance Li-ion Sulfur Batteries Enabled by Intercalation Chemistry." *Chemical Communications*, 51 (2015): 13454.
- Xiao, J. "Understanding the Lithium Sulfur Battery System at Relevant Scales (Editorial)." *Advanced Energy Materials* 5 (2015): 1501102.

Task 8.6 – Nanostructured Design of Sulfur Cathodes for High Energy Lithium-Sulfur Batteries (Yi Cui, Stanford University)

Project Objective. The charge capacity limitations of conventional transition metal oxide cathodes are overcome by designing optimized nano-architectured sulfur cathodes.

This study aims to enable sulfur cathodes with high capacity and long cycle life by developing sulfur cathodes from the perspective of nanostructured materials design, which will be used to combine with lithium metal anodes to generate high-energy lithium-sulfur batteries. Novel sulfur nanostructures as well as multifunctional coatings will be designed and fabricated to overcome issues related to volume expansion, polysulfide dissolution, and the insulating nature of sulfur.

Project Impact. The capacity and the cycling stability of sulfur cathode will be dramatically increased. This project's success will make lithium-sulfur batteries to power electric vehicles and decrease the high cost of batteries.

Out-Year Goals. The cycle life, capacity retention, and capacity loading of sulfur cathodes will be greatly improved (200 cycles with 80% capacity retention, >0.3 mAh/cm^2 capacity loading) by optimizing material design, synthesis and electrode assembly.

Collaborations. This project engages in collaboration with the following:

- BMR program principal investigators
- Stanford Linear Accelerator Center (SLAC): *In situ* x-ray, Dr. Michael Toney
- Stanford: Prof. Nix, mechanics; Prof. Bao, materials

Milestones

1. Demonstrate synthesis to generate monodisperse sulfur nanoparticles with/without hollow space. (October 2013 – Complete)
2. Develop surface coating with one type of polymers and one type of inorganic materials. (January 2014 – Complete)
3. Develop surface coating with several types of polymers; Understand amphiphillic interaction of sulfur and sulfide species. (April 2014 – Complete)
4. Demonstrate sulfur cathodes with 200 cycles with 80% capacity retention and 0.3mAh/cm^2 capacity loading. (July 2014 – Complete)
5. Demonstrate Li_2S cathodes capped by layered metal disulfides. (December 2014 – Complete)
6. Identify the interaction mechanism between sulfur species and different types of sulfides/oxides/metals, and find the optimal material to improve the capacity and cycling of sulfur cathode. (July 2015 – Complete)

Progress Report

Previously, we demonstrated the absorption of lithium polysulfides on the surface of various non-conductive oxide materials, including CeO_2, Al_2O_3, La_2O_3, MgO, and CaO. Our DFT calculation and temperature swing adsorption experiments confirm that the monolayer chemisorption is dominant during the polysulphide capture. In addition, we evaluated the electrochemical performance of sulfur cathodes incorporated with non-conductive oxides.

Figure 82a shows the representative charge-discharge curves of the composite electrode based on different oxide/carbon nanostructures at a current rate of 0.1 C. No obvious difference can be found for the potential of the discharge plateaus. However, the CaO/C and C composite cathodes show higher charge over potentials than those of CeO_2/C, La_2O_3/C, Al_2O_3/C, and MgO/C composite electrodes (Figure 82a). The specific discharge capacities of Al_2O_3/C, CeO_2/C, La_2O_3/C, MgO/C, CaO/C and C at the 0.1C rate are measured to be 1330, 1388, 1345, 1368, 1246, and 1230 mAh g^{-1}, respectively (Figure 82a). It can be found that the CaO/C and C composite cathodes show relatively lower discharge capacity. The high over potential and low discharge capacity may result from the serious dissolution of polysulphide in electrolyte (shuttle effect), which causes the active material loss and the increase of electrolyte viscosity. Inductively coupled plasma optical emission spectrometry (ICP-OES) tests based on the same mass of Al_2O_3/C, CeO_2/C, La_2O_3/C, MgO/C, CaO/C and C samples reveal that both CaO/C and C have poorer polysulphide capture capability compared with other metal oxides/carbon. Figure 82b shows the discharge capacity and the corresponding Coulombic efficiency of the cathodes upon prolonged 300 cycles at 0.5 C. All the cathodes show high discharge capacities in the former several cycles. However, the Al_2O_3/C, CaO/C, and C cathodes exhibit obvious capacity fading especially in the first 100 cycles. Compared with Al_2O_3/C, CaO/C, and C cathodes, the electrode based on CeO_2/C, La_2O_3/C and MgO/C show better cycling performance; the MgO/C cathode is the best among all the samples. The capacity decay per cycle is 0.171%, 0.066%, 0.047%, 0.034%, 0.136%, and 0.170% for Al_2O_3/C, CeO_2/C, La_2O_3/C, MgO/C, CaO/C, and C, respectively. Considering that the serious capacity decay mainly happens in the first 50 cycles, the average Columbic efficiency in the first 100 cycles was calculated (Figure 82b). Al_2O_3/C, CeO_2/C, La_2O_3/C, MgO/C, CaO/C, and C cathodes show 99.6%, 99.1%, 98.7%, 99.4%, 98.3%, and 98.8% Coulombic efficiency. Lower Coulombic efficiency of Li-S batteries resulted from the significant lithium polysulphide dissolution, which causes the loss of S material and shuttle effect. This can be also supported by the ICP-OES results, revealing that Al_2O_3/C has the best capture capability and CaO/C and C have poorer capture capability for lithium polysulphide. Although Al_2O_3/C cathodes possess high initial discharge capacity and good Coulombic efficiency, the rate of capacity decay is higher than those of CeO_2/C, La_2O_3/C, and MgO/C cathodes.

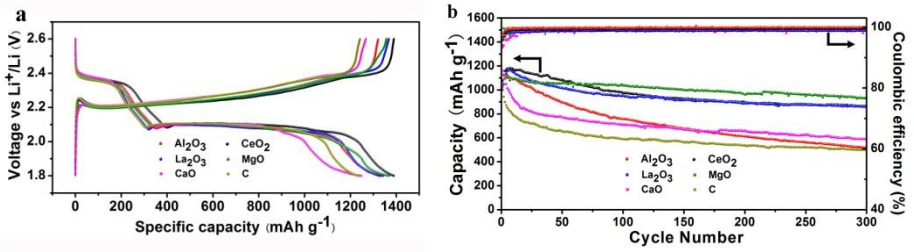

Figure 82. (a) Representative charge-discharge profiles of the composite electrodes at 0.1 C. (b) Specific capacity and the corresponding Coulombic efficiency of the composite electrodes upon prolonged 300 charge-discharge cycles at 0.5 C.

Task 8.7 – Addressing Internal "Shuttle" Effect: Electrolyte Design and Cathode Morphology Evolution in Li-S Batteries (Perla Balbuena, Texas A&M University)

Project Objective. The project objective is to overcome the lithium-metal anode deterioration issues through advanced Li-anode protection/stabilization strategies including (i) *in situ* chemical formation of a protective passivation layer and (ii) alleviation of the "aggressiveness" of the environment at the anode by minimizing the polysulfide shuttle with advanced cathode structure design.

Project Impact. Through formulation of alternative electrolyte chemistries as well as design, fabrication, and test of improved cathode architectures, it is expected that this project will deliver Li/S cells operating for 500 cycles at efficiency greater than 80%.

Approach. A mesoscale model including different realizations of electrode mesoporous structures generated based on a stochastic reconstruction method will allow virtual screening of the cathode microstructural features and the corresponding effects on electronic/ionic conductivity and morphological evolution. Interfacial reactions at the anode due to the presence of polysulfide species will be characterized with *ab initio* methods. For the cathode interfacial reactions, data and detailed structural and energetic information obtained from atomistic-level studies will be used in a mesoscopic-level analysis. A novel sonochemical fabrication method is expected to generate controlled cathode mesoporous structures that will be tested along with new electrolyte formulations based on the knowledge gained from the mesoscale and atomistic modeling efforts.

Out-Year Goals. By determining reasons for successes or failures of specific electrolyte chemistries, and assessing relative effects of composite cathode microstructure and internal shuttle chemistry vs. that of electrolyte chemistry on cell performance, expected results are : (1) develop an improved understanding of the Li/S chemistry and ways to control it; (2) develop electrolyte formulations able to stabilize the Li anode; (3) develop new composite cathode microstructures with enhanced cathode performance; and (4) develop a Li/S cell operating for 500 cycles at an efficiency > 80%.

Collaborations. This is a collaborative work combining first-principles modelling (Perla Balbuena, Texas A&M University), mesoscopic level modelling (Partha Mukherjee, Texas A&M University), and synthesis, fabrication, and test of Li/S materials and cells (Vilas Pol, Purdue University).

Milestones

1. Synthesis of the C/S cathode hybrid materials: Develop lab-scale Li-S composite. (December 2014 – Complete); Perform advanced characterization. (March 2015 – Complete)
2. Determination of the structure of the PS/Li Interface: Characterization of thermodynamics of nucleation and growth of PS deposits on the Li surface. (March 2015 – Complete)
3. Determination of the chemistry of the C/S composite cathode: Characterize dissolution, reduction, and lithiation of S in the composite cathode microstructure. (June 2015 – Complete)
4. Study of electrode morphology evolution and mesostructure transport interaction: Study cathode mesostructure impact on product formation and deposition. *Go/No-Go*: Comparative analysis of the mesoscale model and experimental characterization. (September 2015 – Complete)

.

Progress Report

Reactions at the anode/electrolyte surface. The extreme reactivity of the Li-anode surface in contact with the electrolyte solution in Li-S batteries has been investigated using DFT and *ab initio* molecular dynamics (AIMD) methods. From the electrolyte components used in Li-S batteries, the salt LiTFSI is much more reactive than typical solvents such as DOL and DME. Cleavage of the C-S or N-S bond was found as the starting point for all of the LiTFSI reduction pathways; the first is the most thermodynamically favorable. Eventually the salt becomes decomposed into multiple fragments. One of the products is LiF, but other charged radical anions are derived from C, SO_2, O, and CSN fragments that become adsorbed onto the metal surface. The primary method of Li_2S_8 fragmentation away from the anode surface does not involve delithiation; however, the most favorable pathway includes reaction of the lithiated PS with additional Li atoms in gas phase or in presence of the solvent, with four different fragmentation modes found having similar (very favorable) ΔGs of reaction. In contact with the anode surface, the long-chain PS species is highly decomposed despite the solvent used or the PS initial geometry (ring or linear), resulting in formation of a Li_2S layer characterized by analyses of bond distances and atomic charges. A manuscript has been submitted for publication.

Mesoscale modeling. A performance model with electrochemistry coupled charge and species transport has been developed for the Li-S cell sandwich. This formalism is hierarchically coupled with the coarse-grained model for Li_2S precipitation and with a pore-scale model for the cathode microstructure evolution due to the combined effects of precipitation and dissolution. This mesoscale model allows investigating the effect of the coupled electrochemical and transporting limiting mechanisms in the cathode. A kinetically limited formalism was developed to investigate the efficacy of different experimentally argued capacity loss mechanisms. Li_2S formation and sulfur isolation are found to be the predominant mechanisms determining the discharge capacity and performance. The new interfacial growth model explicitly describes dynamics of the Li_2S molecule on the carbon surface, including adsorption, desorption, diffusion, and nucleation (stabilization). The effect of temperature on coverage growth rate indicated that the surface coverage grows faster at lower temperatures, which can reduce the Li_2S desorption rate and diffusion rate. This condition may facilitate the formation of small Li_2S nanoislands, which can supply sufficient lateral clustering sites to stabilize free Li_2S molecules (Figure 83). A poro-mechanics based modeling formalism studies the influence of Li_2S precipitation induced stress evolution at the pore-scale. The analysis of volume expansion during discharge is conducted by applying the Green-Lagrange strain to capture the large deformation. Maximum stress concentration is observed at sharp corners, and these act as crack initiation sites for mesoporous carbon-based cathode architectures. Thin walls are also prone to rupture during the discharge process.

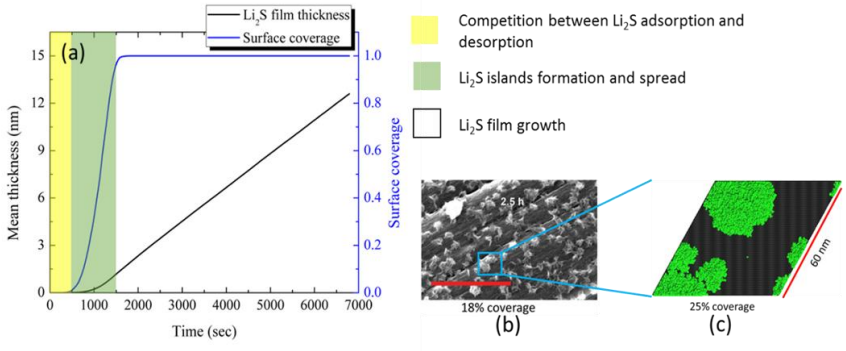

Figure 83. (a) Li_2S film thickness and coverage variation versus time. (b) Scanning electron microscopy image of Li_2S nanoislands formation on carbon substrate from F.Y. Fan, et al. *Advanced Materials*, 27 (2015): 5203-5209. (c) Snapshot of Li_2S nanoislands formation on carbon substrate from coarse-grained KMC simulation.

Experimental. To understand the polysulfide shuttle reduction effect of various dopant compounds, various representative materials were chosen as dopants for graphene. The materials chosen in conjunction with the computational analysis are molybdenum disulfide, elemental molybdenum, and iron (III) oxide. Raman spectroscopy and electrochemical analysis showed preliminary encouraging results.

Patents/Publications/Presentations

Publications

- Liu, Z., and D. Hubble, P.B. Balbuena, and P.P. Mukherjee. "Adsorption of Insoluble Polysulfides Li_2S_x (x = 1, 2) on Li_2S Surfaces." *Phys. Chem. Chem. Phys.* 17 (2015): 9032-9039.
- Camacho-Forero, Luis E., and Taylor W. Smith, Samuel Bertolini, and Perla B. Balbuena. "Reactivity at the Lithium-Metal Anode Surface of Lithium-Sulfur Batteries." *J. Phys. Chem. C* (under review).
- Dysart, Arthur A., and Juan C. Burgos, Aashutosh Mistry, Chien-Fan Chen, Zhixiao Liu, Perla B. Balbuena, Partha P. Mukherjee, and Vilas G. Pol. "Towards Next Generation Lithium-Sulfur Batteries: Non-Conventional Carbon Compartments/Sulfur Electrodes and Multi-scale Analysis." Submitted.

Presentation

- BMR meeting, Lawrence Berkeley National Laboratory (January 22, 2015): "Addressing Internal 'Shuttle' Effect: Electrolyte Design and Cathode Morphology Evolution in Li-S Batteries DE-EE-0006832"; P.B. Balbuena.

TASK 9 – LI-AIR BATTERIES

Summary and Highlights

High-density energy storage systems are critical for electric vehicles (EVs) required by the EV Everywhere Grand Challenge proposed by the DOE Office of Energy Efficiency and Renewable Energy (EERE). Conventional Li-ion batteries still cannot fully satisfy the ever-increasing needs because of their limited energy density, high cost, and safety concerns. As an alternative, the rechargeable Li-O_2 battery has the potential to be used for long range EVs. The practical energy density of a Li-O_2 battery is expected to be ~ 800 Wh kg-1. The advantages of Li-O_2 batteries come from their open structure; that is, they can absorb the active cathode material (oxygen) from the surrounding environment instead of carrying it within the batteries. However, the open structure of Li-O_2 batteries also leads to several disadvantages. The energy density of Li-O_2 batteries will be much lower if oxygen has to be provided by an onboard container. Although significant progress has been made in recent years on the fundamental properties of Li-O_2 batteries, the research in this field is still in an early stage and many barriers must be overcome before practical applications. The main barriers include:

- Instability of electrolytes. Superoxide species generated during discharge or O_2 reduction process is highly reactive with electrolyte and other components in the battery. Electrolyte decomposition during charge or O_2 evolution process is also significant due to high over-potentials.
- Instability of air electrode (dominated by carbonaceous materials) and other battery components (such as separators and binders) during charge/discharge processes in an oxygen-rich environment.
- Limited cyclability of the battery associated with instability of the electrolyte and other components of the batteries.
- Low energy efficiency associated with large over-potential and poor cyclability of Li-O_2 batteries.
- Low power rate capability due to electrode blocking by the reaction products.
- Absence of a low-cost, high-efficiency oxygen supply system (such as oxygen selective membrane).

The main goal of the PNNL Task is to provide a better understanding on the fundamental reaction mechanisms of Li-O_2 batteries and identify the required components (especially electrolytes and electrodes) for stable operation of Li-O_2 batteries. The PNNL researchers will investigate stable electrolytes and oxygen evolution reaction (OER) catalysts to reduce the charging overvoltage of Li-O_2 batteries and improve their cycling stability. New electrolytes will be combined with stable air electrodes to ensure their stability during Li-O_2 reaction. Considering the difficulties in maintaining the stability of conventional liquid electrolyte, the Liox team will explore the use of a nonvolatile, inorganic molten salt comprising nitrate anions and operating Li-O_2 cells at elevated temperature (> 80°C). It is expected that these Li-O_2 cells will have a long cycle life, low over potential, and improved robustness under ambient air compared to current Li-air batteries. At Argonne National Laboratory, new cathode materials and electrolytes for lithium-air batteries will be developed for Li-O_2 batteries with long cycle life, high capacity, and high efficiency. The state-of-the-art characterization techniques and computational methodologies will be used to understand the charge and discharge chemistries. UMass/BNL team will investigate the root causes of the major obstacles of the air cathode in the Li-air batteries. Special attention will be paid to optimizing high-surface carbon material used in the gas diffusion electrode, catalysts, electrolyte, and additives stable in Li-air system and with capability to dissolve Li oxide and peroxide. Success of this project will establish a solid foundation for further development of Li-O_2 batteries toward practical applications for long-range EVs. The fundamental understanding and breakthrough in Li-O_2 batteries may also provide insight on improving the performance of Li-S batteries and other energy storage systems based on chemical conversion processes.

The highlights for this quarter include:

- **Giordani (Liox).** Investigated the solubility of possible ORR products LiOH and Li_2CO_3 as well as the electrochemical performance of non-carbonaceous cathode materials such as gold and transition metal nanopowders.
- **Qu (UWM).** Boron containing Lewis acid can not only catalyze superoxide disproportionation, but also improve the round-trip efficiency by reducing recharge overpotential.

Task 9.1 – Rechargeable Lithium-Air Batteries (Ji-Guang Zhang and Wu Xu, PNNL)

Project Objective. The objective of this work is to develop stable electrolyte and oxygen evolution reaction (OER) catalysts to reduce the charging overvoltage of lithium (Li)-air batteries and improve the cycling stability of rechargeable Li-air batteries. New catalysts will be synthesized to improve the capacity and cycling stability of Li-O_2 batteries. New electrolytes will be investigated to ensure their oxygen-stability during Li-O_2 reaction.

Project Impact. Li-air batteries have a theoretical specific energy that is more than five times that of state-of-the-art Li-ion batteries and are potential candidates for use in next-generation, long-range electric vehicles (EV). Unfortunately, the poor cycling stability and low Coulombic efficiency of Li-air batteries have prevented practical application to date. This work will explore a new electrolyte and electrode that could lead to long cyclability and high Coulombic efficiencies in Li-air batteries that can be used in the next generation EVs required by the EV Everywhere Grand Challenge proposed by the DOE Office of Energy Efficiency and Renewable Energy (EERE).

Out-Year Goals. The long-term goal of the proposed work is to enable rechargeable Li-air batteries with a specific energy of 800 Wh/kg at cell level, 1000 deep-discharge cycles, improved abuse tolerance, and less than 20% capacity fade over a 10-year period to accelerate commercialization of long-range EVs.

Collaborations. This project engages in collaboration with the following:

- Yangchuan (Chad) Xing (University of Missouri) – Metal oxide coated glassy carbon electrode
- Chunmei Ben (NREL) – Metal oxide coated glassy carbon electrode
- Chongmin Wang (PNNL) – Characterization of cycled air electrodes by transmission electron microscopy (TEM) and scanning electron microscopy (SEM).

Milestones

1. Synthesize and characterize the modified glyme solvent and the dual transition metal oxide catalyst. (12/31/2014 – Complete)
2. Improve the stability of solvent using conventional carbon air electrode. (3/31/2015 – Complete)
3. Identify the solvent to be stable for at least 50 cycles on modified air electrode. (6/30/2015 – Complete)
4. Integrate the new electrolyte and modified air electrode to assemble Li-O_2 batteries with at least 120 cycles stable operation. (9/30/2015 – Complete)

Progress Report

This quarter, we studied the effects of concentrated LiTFSI-electrolytes with acetonitrile (AN) and dimethyl sulfoxide (DMSO) on the cycling performance of Li-O_2 batteries with CNTs/PVDF/carbon paper air electrodes. Three LiTFSI/solvent mole ratios of 1:4, 1:3, and 1:2 were used for each solvent-based electrolyte. The test protocol was the capacity limitation at 1000 mAh g^{-1}. Unlike the concentrated LiTFSI-DME electrolytes tested in Q3, three concentrated LiTFS-AN electrolytes and the LiTFSI-2DMSO electrolyte cannot be cycled. According to Bruce et al., the discharge in AN-electrolytes is the surface chemistry due to the low donor number of AN; thus, the air electrode surface is quickly passivated by the insulating Li_2O_2, and low discharge capacity is yielded. The LiTFSI-2DMSO probably has too low an oxygen solubility and high viscosity, so the discharge cannot be completed before the 1000 mAh g^{-1} limit is reached. The electrolytes of LiTFSI-3DMSO and LiTFSI-4DMSO would be discharged and charged for 36 and 32 cycles, respectively (see Figure 84a-b), but the charging process is not reversible. When the two electrolytes were cycled at a lower capacity limitation (that is, 600 mAh g^{-1}), their cycle lives could be extended to about 80 and 71 cycles, respectively (Figure 84c-d). The reasons may include the instability of DMSO against reduced oxygen species and Li metal, and the low oxidation voltage of DMSO.

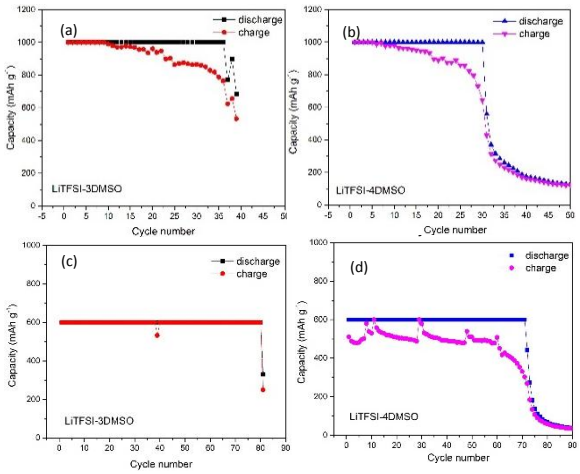

Figure 84. Cycling stability of electrolytes, LiTFSI-3DMSO (a, c) and LiTFSI-4DMSO (b, d), in Li-O_2 coin cells at two different capacity limitations at 1000 mAh g^{-1} (a, b) and 600 mAh g^{-1} (c, d).

We also synthesized a binder-free air electrode based on metal oxide catalyst on carbon cloth (CC). The obtained binder-free catalytic air electrode was pre-treated before testing in Li-O_2 coin cells with 1 M LiTf-tetraglyme electrolyte under full discharge/charge (2.0~4.5 V) protocol, and compared with the pristine catalyst/CC and pure CC air electrodes. The treated catalyst/CC electrode showed extremely high discharge and charge capacities at the first cycle (Figure 85a). Although the capacities at the second cycle were significantly reduced, the treated catalyst/CC electrode still showed stable cycling at a capacity above 1200 mAh g^{-1} for 120 cycles and 1000 mAh g^{-1} for 140 cycles. As a comparison, the pristine catalyst/CC electrode showed a stable cycling at a capacity around 300 mAh g^{-1}, much lower than the treated catalyst/CC air electrode. More work will be done to understand the extremely high first cycle capacity and good cycling stability for the pre-treated catalyst/CC air electrode.

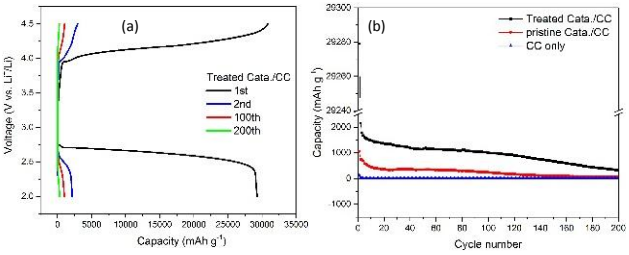

Figure 85. (a) Voltage profiles of treated catalyst/carbon cloth air electrode in Li-O_2 coin cells at selected cycles. (b) Cycling stability of Li-O_2 coin cells with air electrodes of treated catalyst/carbon cloth, pristine catalyst/carbon cloth, and pure carbon cloth under full discharge/charge (2.0~4.5 V) cycling.

Patents/Publications/Presentations

Publication

- Liu, B., and W. Xu,* P. Yan, P. Bhattacharya, R. Cao, M.E. Bowden, M.H. Engelhard, C.-M. Wang, and J.-G. Zhang*. "*In Situ* Grown $ZnCo_2O_4$ on Single Walled Carbon Nanotubes as Air Electrode Materials for Rechargeable Lithium-Oxygen Batteries." *ChemSusChem* (2015). DOI: 10.1002/cssc.201500636.

Task 9.2 – Efficient Rechargeable Li/O_2 Batteries Utilizing Stable Inorganic Molten Salt Electrolytes (Vincent Giordani, Liox)

Project Objective. The project objective is to develop high specific energy, rechargeable Li-air batteries having lower overpotential and improved robustness under ambient air compared to current Li-air batteries. The technical approach involves replacing traditional organic and aqueous electrolytes with a nonvolatile, inorganic molten salt comprising nitrate anions and operating the cell at elevated temperature (> 80°C). The research methodology includes powerful *in situ* spectroscopic techniques coupled to electrochemical measurements (for example, electrochemical mass spectrometry) designed to provide quantitative information about the nature of chemical and electrochemical reactions occurring in the air electrode.

Project Impact. If successful, this project will solve particularly intractable problems relating to air electrode efficiency, stability and tolerance to the ambient environment. Furthermore, these solutions may translate into reduced complexity in the design of a Li-air stack and system, which in turn may improve prospects for use of Li-air batteries in electric vehicles (EVs). Additionally, the project will provide materials and technical concepts relevant for development of other medium temperature molten salt Li battery systems of high specific energy, which may also have attractive features for EVs.

Out-Year Goals. The long-term goal of this project is to develop Li-air batteries comprising inorganic molten salt electrolytes and protected Li anodes that demonstrate high (>500 Wh/kg) specific energy and efficient cyclability in ambient air. By the end of the project, it is anticipated that problems hindering use of both the Li anode and air electrode will be overcome due to materials advances and strategies enabled within the intermediate (>80 °C) operating temperature range of the system under development.

Collaborations. This project engages in collaboration with the following:

- Bryan McCloskey (LBNL): Analysis of air electrode and electrolyte
- Julia Greer (Caltech): Design of air electrode materials and structures

Milestones

1. Demonstrate eutectic compositions having eutectic points below 120°C. (December 2014 – Complete)
2. Measure ionic conductivity and Li^+ transference number in eutectic compositions. (December 2014 – Complete)
3. Measure diffusion coefficients and solubilities of O_2, Li_2O_2, and Li_2O. (March 2015 – Complete)
4. Synthesize oxidation-resistant carbons. (March 2015 – Complete)
5. *Go/No-Go*: Demonstrate suitability of analytical approach for elevated temperature molten salt metal-O_2 cells. Criteria: Quantify e^-/O_2 yield, e^-/O_2, and OER/ORR ratios for baseline carbon air electrodes. (June 2015 – Complete)
6. Quantify e^-/O_2 and OER/ORR ratios for oxidation-resistant carbon air electrodes. (June 2015 – Complete)
7. Measure diffusion coefficients and solubilities of H_2O, CO_2, LiOH, and Li_2CO_3. (September 2015 – Complete)
8. Synthesize metals and metal alloys of high air electrode stability and/or catalytic activity. (September 2015 – Complete)

Progress Report

This quarter, we measured diffusivity and bulk concentration of LiOH and Li_2CO_3 in $LiNO_3$-KNO_3 eutectic at 150 °C. We found that LiOH and Li_2CO_3, expected oxygen reduction reaction (ORR) discharge products under ambient air, can be electrochemically oxidized near equilibrium potentials (3.4 and 3.6 V, respectively). We also found that LiOH forms eutectic compositions with alkali metal nitrates (for example, $LiNO_3$/LiOH/KNO_3 43/11/46 mol. %, M_P = 118.8°C). High LiOH solubility in (Li, K)NO_3 (4.3 M) may enable high capacity for cells operating in ambient air. Diffusivity and bulk concentration of LiOH and Li_2CO_3 were determined by Rotating Disk Electrode measurements at a Pt disk electrode (Table 4).

Table 4. Bulk concentration and diffusion coefficient of LiOH and Li_2CO_3 in molten nitrate electrolyte $LiNO_3$-KNO_3 at 150°C.

	LiOH	Li_2CO_3
C (mM)	4300	9.9
D (cm^2/s)	$9x10^{-7}$	$8.2x10^{-9}$

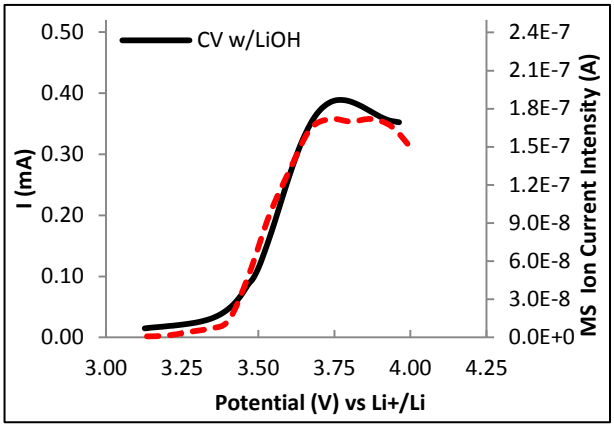

Figure 86. LSV/*in situ* gas analysis performed on Ir wire working electrode in LiOH-saturated (Li,K)NO_3 electrolyte at 150°C. *v* = 5 mV/s.

We reported before that the amorphous carbon air electrode was unstable in the molten salt Li/O_2 cell and responsible for limited cycle life (~30 cycles). Our objective is to identify non-carbonaceous air electrode materials. This quarter, we investigated the electrochemical behavior of commercially available metal nanopowders, namely, Fe, Ni, Co, and Pt, as well as nanoporous Au, in molten salt Li/O_2 cells. 1 cm^2 projected area gold cathode was obtained from white gold leaf with Ag etched away in HNO_3 at 80°C. Nanoporous Au was presoaked in aqueous solution of nitrate eutectic mixture before careful drying at 200°C overnight. *In situ* pressure analysis coupled to mass spectrometry was used to determine e^-/O_2 and oxygen evolution reaction (OER)/ORR molar ratios. Preliminary results indicate $e^-/O_2 \neq 2$, for both discharge and charge, and OER/ORR equals to 0.77, suggesting gold tends to decompose during cycling. Additional experiments are ongoing to fully evaluate the chemical/electrochemical stability of Au. Results obtained using

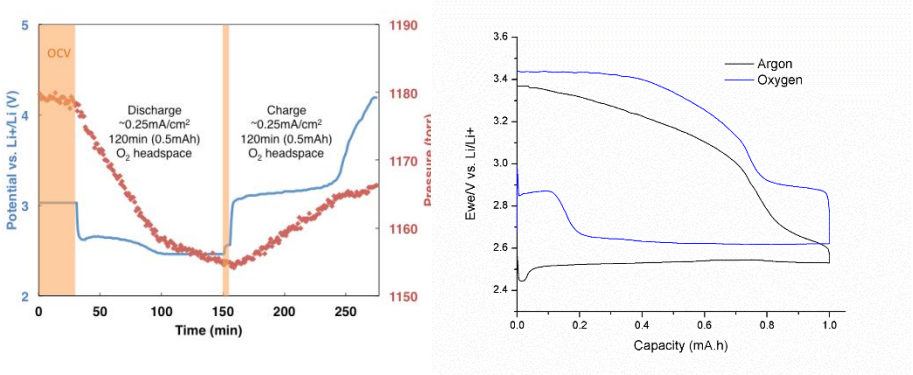

Figure 87. Li/O_2 cell galvanostatic cycling at 0.25 mA/cm^2 in $LiNO_3$-KNO_3 eutectic at 150°C. *Left plot:* nanoporous Au cathode. *Right plot:* Ni nanopowder cathode both under Ar and O_2 gas.

transition metal nanopowder cathodes (Ni, Fe and Co) showed somewhat limited O_2 activity. Electrode wettability in molten nitrates as well as possible metal surface oxidation to a less conductive (or blocking) oxide layer when brought in contact with the melt at 150°C might prevent the electrochemical reduction of O_2. Further investigation is needed to understand the behavior of these cathode materials in molten nitrates.

Task 9.3 – Li-Air Batteries (Khalil Amine, ANL)

Project Objective. The project objectives are as follows:

- Develop new cathode materials and electrolytes for lithium-air batteries for long cycle life, high capacity, and high efficiency.
- Use state-of-the-art characterization techniques to understand the charge and discharge chemistries.
- Use state-of-the-art computational methodologies to understand and design new materials and electrolytes for Li-air batteries.

Project Impact. This project anticipates the following impacts:

- New electrolytes that are stable and increase cycle life.
- New cathode materials that increase cycle life and reduce overpotentials.
- Increased cycle life.

Approach. We are using a joint theoretical/experimental approach for design and discovery of new electrolytic additives that react in a preferential manner to prevent detrimental decomposition of cell components. We use quantum chemical screening based on density functional theory (DFT) and wave-function based methods to predict accurate oxidation and reduction potentials and decomposition pathways that form desirable coatings and to find stable additives for overcharge protection. Synthesis of the new additives and testing of them is done to determine the cycle life of the batteries followed by characterization.

Out-Year Goals. The out-year goals of this work are to find catalysts that promote discharge product morphologies that reduce charge potentials and to find electrolytes for long cycle life through testing and design.

Collaborations. This project engages in collaboration with Professor Yang-Kook Sun at Hanyang University, Professor Yiying Wu at Ohio State University, and Dr. Dengyun Zhai.

Milestones

1. Characterize stability of the LiO_2 component of the activated carbon cathode using Raman techniques. Use DFT calculations to model the stability of the LiO_2 component of the activated carbon cathode to explain the Raman results. (12/31/2014 – Complete)
2. Investigate the role of impurities in the performance of activated carbon and how they can promote the formation and stability of LiO_2 and reduce charge overpotentials. Use (DFT) calculations to help understand how the impurities affect the morphologies. (3/31/2015 – Complete)
3. Investigate addition of metal nanoparticle catalysts to high surface area carbons such as reduced graphene oxides to promote growth of morphologies with higher LiO_2 contents to reduce charge overpotentials. Use DFT calculations to model the nanoparticle catalysts. (6/30/2015 – Ongoing)
4. Use one of the metal catalyst/carbon systems with good performance to start investigations of how electrolytes can be used to improve the performance (cycle life) of the Li-air battery. Use DFT calculations to help design new electrolytes for the Li-air batteries. (9/30/2015 – Ongoing)

Progress Report

Although lithium-oxygen batteries are attracting considerable attention because of potential for extremely high energy density, their practical use has been restricted due to a low energy efficiency and poor cycle life compared to lithium-ion batteries. The cycle life of a Li-air cell will depend on the stability of the electrolyte, which can be affected by several sources including reactions with the carbon surface, the discharge product surface, the anode surface, and reduction products in the electrolyte. To some extent, decomposition reactions, such as on carbon surfaces, can be limited by reducing the charge potentials. However, even at low charge potentials, decomposition at the anode and on the discharge product is likely to be a problem. Another source of poor cycle life is electrocatalyst poisoning. Finally, increasing capacity requires understanding of the oxygen reduction process and how to engineer cathode architectures to effectively increase oxygen reduction.

This quarter, we started investigating characterization techniques for determining decomposition products in the electrolyte from the new catalyst we are developing Li-O_2 cells. This will be used in subsequent work to find improved electrolytes. The methods investigated include nuclear magnetic resonance (NMR), Raman, and Fourier transform infrared (FT-IR). NMR spectra were collected on a Bruker spectrometer in deuterated tetrahydrofuran (THF-d8) or deuterium oxide (D_2O). Battery samples were cycled a specific number of times before disassembly and rinsing with a deuterated solvent. NMR of washings from 20th cycles for TEGDME electrolytes showed the presence of some formate and acetate known to be the decomposition products from ethers in Li-O_2 cells. This is also observed in FT-IR peaks shown in Figure 88; the FT-IR technique is especially sensitive to these decomposition products.

These two techniques are being used in studies of decomposition products in Li-O_2 batteries using our new cathode materials and will be used to help find better electrolytes. We have also started DFT studies of the stability of ethers to reactive intermediates such as superoxide anion, lithium superoxide, and others, as well as models for the discharge product surface; this includes hydrogen abstraction and C-O bond breaking. These calculations are being used to help find functional groups on ethers and other possible base molecules such as amides.

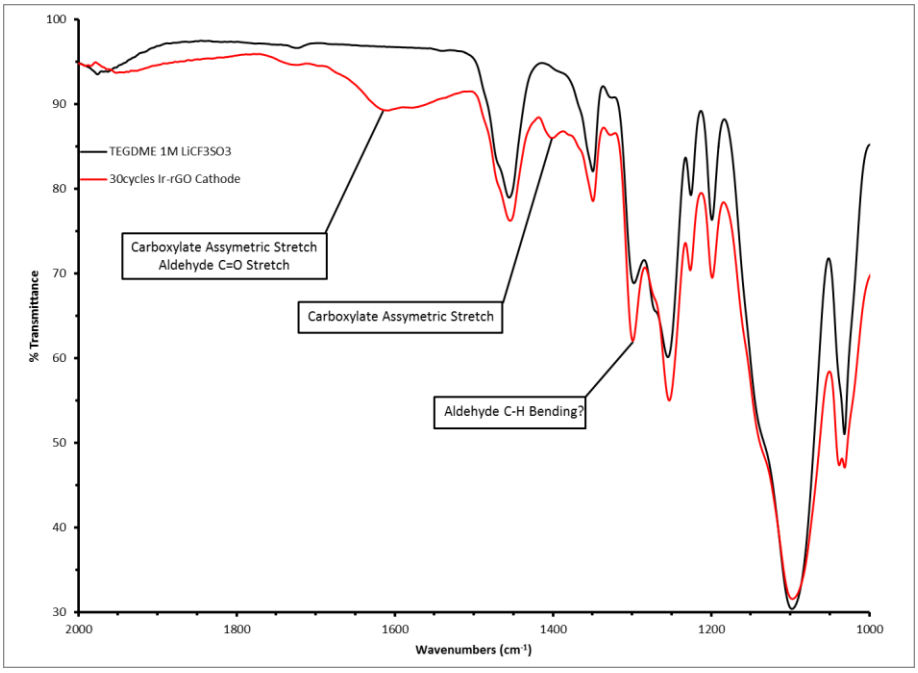

Figure 88. FT-IR spectra showing sensitivity of this method to carboxlylate groups (red curve) from TEGDME decomposition after cycling in a Li-O_2 cell.

Patents/Publications/Presentations

Publication

- Zhai, D., and K.C. Lau, H.-H. Wang, J. Wen, D.J. Miller, J. Lu, F. Kang, B. Li, W. Yang, J. Gao, E. Indacochea, L.A. Curtiss, and K. Amine. "Interfacial Effects on Lithium Superoxide Disproportionation in Li-O^2 Batteries." *Nano Lett*. 15, no. 2 (2015): 1041–1046.

Task 9.4 – Overcome the Obstacles for the Rechargeable Li-air Batteries (Deyang Qu, University of Wisconsin – Milwaukee; and Xiao-Qing Yang, Brookhaven National Laboratory)

Project Objective. The primary objective is to investigate the root causes of the major obstacles of the air cathode in the Li-air batteries, which impede the realization of high energy, high power, long cycle life Li-air batteries, and understand the mechanisms of such barriers and eventually overcome those obstacles. In this objective, special attention will be paid to the investigation of high surface carbon material use in the gas diffusion electrode (GDE), establishment of 2-phase interface on the GDE, catalysts, electrolyte and additives stable in Li-air system and with capability to dissolve Li oxide and peroxide. The electrolyte investigation and development will involve close collaboration with Brookhaven National Laboratory. The secondary objective is to engineer design of a Li-air battery with high energy, high rate, long cycle life, and high round-trip efficiency; special attention will be paid to Li-air flow cell.

Project Impact. Li-air chemistry represents the highest energy density among chemical energy systems. The successful implementation of the technology in the electric vehicles would not only reduce the cost of electrochemical energy storage system, but also provide long driving distance per charge by significantly increasing energy density. The attributes would enable cost effective market entry of electric vehicles for U.S. automakers.

One-Year Goals. The project research will focus on fundamental mechanisms of oxygen reduction in nonaqueous electrolytes and the re-oxidization of the soluble boron-peroxide complex; multiple boron complexes will be synthesized and tested. The impact of carbon surface structure on the O_2 reduction will be investigated. The unique flow-cell design will be further optimized by means of the inclusion of boron additives.

Collaborations. Principal investigator Deyang Qu is the Johnson Control Endowed Chair Professor; the UWM and BNL team closely collaborates with Johnson Control scientists and engineers. The collaboration enables the team to validate outcomes of fundamental research in pilot-scale cells. This team has been working closely with top scientists on new material synthesis at ANL, LBNL, and PNNL, with U.S. industrial collaborators at General Motors, Duracell, and Johnson Control. The team also works with international collaborators in Japan and South Korea. These collaborations will be strengthened and expanded to give this project a vision on both today's state-of-the-art technology and tomorrow's technology, with feedback from the material designer and synthesizers upstream as well as industrial end users downstream.

Milestones

1. Complete the studies of the impact of carbon surface structure on the O_2 reduction. (December 2014 – Complete)
2. Complete the kinetics studies of catalytic disproportionation of superoxide (determination of reaction order and reaction constant). (March 2015 – Complete)
3. Complete the test of the Li-air flow cell. (June 15 – Complete)
4. Complete *in situ* electrochemical study for the oxygen reduction in various boron additives. (September 2015 – Complete)

Progress Report

This quarter, all milestones have been achieved. Multiple boron-containing Lewis acid compounds were synthesized. Both analytical and electrochemical analyses were done. The chemical stability and capability of dissolving Li_2O_2 were determined. The electrochemical oxidation of B-O_2^{2-} was tested.

Table 5. Examples of the synthesized B-compound (left) and their properties (right).

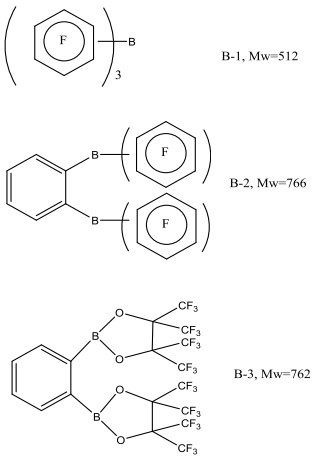

B-compound in DMSO	Conc. (mM)	solubility Li_2O (mM)	solubility Li_2O_2 (mM)	Solubility Li_2CO_3 (mM)	Stability
B1	21.6	6.5	4.0	2.4	Y
B2	20.1	14.3	18.6		N
B3	21.2	36.6	24.0		Y
N1	27.9	19.6	31.6		y
N2	31.3	33.9	39.9		y
N3	43.6	42.1	46.7		N
N4	17.1	25.0	34.2		y
N5	19.6	28.2	36.0		y
N6	19.8	38.6	31.0		y
Background	0.0	0.9	0.7	036	
DMSO				0.11	

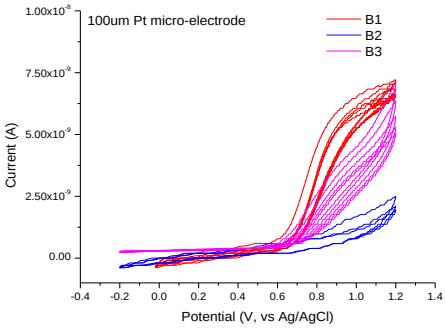

Figure 89. The oxidation of B1, B2 and B3-O_2^{2-}.

The electrochemical oxidation of B-O_2^{2-} with different anion coordinators is different. As shown in Figure 89, the maximum oxidation current for B1-O_2^{2-} is the highest; however, the solubility of Li_2O_2 in the B1 solution is the lowest among the three compounds (Table 5).

The stability of the boron compounds is closely related to the molecule structure. Some of them can chemically react with either Li_2O_2 or Li_2O. The stability of the compound was investigated by the MS spectrum before and after the exposure to Li_2O_2 or Li_2O in a solution. The two HPLC/ESI(-) MS results are shown in Figure 90.

Examples are shown in Figure 90. B3 compound did not experience any changes after dissolving in the Li_2O and Li_2O_2 solutions; however, more compounds were shown after reacting B2 with Li_2O and Li_2O_2.

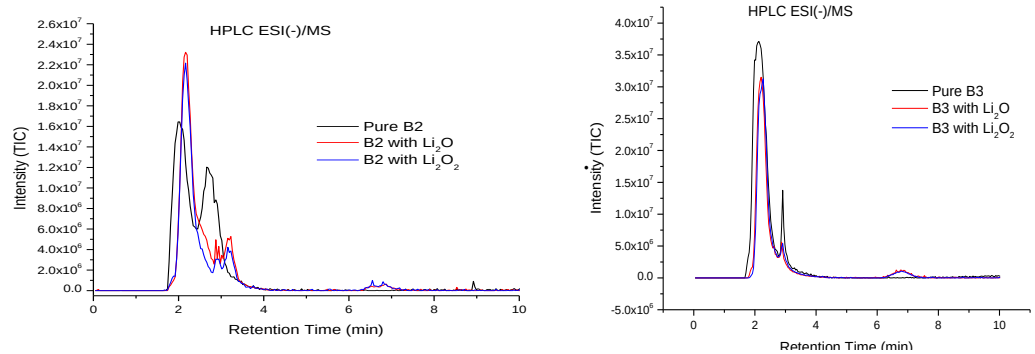

Figure 90. HPLC-MS analysis for the stability of B2 (left) and B3 (right) after reacting with Li_2O and L_2O_2.

Patents/Publications/Presentations

Publication

- Zheng, Dong, and Xuran Zhang, Deyu Qu, Xiao-Qing Yang, Hung-Sui Lee, and Deyang Qu. "Investigation of the Electrocatalytic Oxygen Reduction and Evolution Reactions in Lithium-Oxygen Batteries." *J. Power Sources* 288 (2015): 9-12.

.

TASK 10 – NA-ION BATTERIES

Summary and Highlights

To meet the challenges of powering the plug-in hybrid electric vehicle (PHEV), the next generation of rechargeable battery systems with higher energy and power density, lower cost, better safety characteristics, and longer calendar and cycle life (beyond lithium-ion batteries, which represent today's state-of-the-art technology) must be developed. Recently, Na-ion battery systems have attracted increasing attention due to the more abundant and less expensive nature of the Na resource. The issue is not insufficient lithium on a global scale, but what fraction can be used in an economically effective manner. Most untapped lithium reserves occur in remote or politically sensitive areas. Scale-up will require a long lead time, involve heavy capital investment in mining, and may require the extraction and processing of lower quality resources, which could drive extraction costs higher. Currently, high costs remain a critical barrier to the widespread scale-up of battery energy storage. Recent computational studies on voltage, stability, and diffusion barriers of Na-ion and Li-ion materials indicate that Na-ion systems can be competitive with Li-ion systems.

The primary barriers and limitations of current state-of-the-art of Na-ion systems are as follows:

- Building a sodium battery requires redesigning battery technology to accommodate the chemical reactivity and larger size of sodium ions.
- Lithium batteries pack more energy than sodium batteries per unit mass. Therefore, for sodium batteries to reach energy densities similar to lithium batteries, the positive electrodes in the sodium battery need to hold more ions.
- Since Na-ion batteries are an emerging technology, new materials to enable Na electrochemistry and the discovery of new redox couples along with the diagnostic studies of these new materials and redox couples are quite important.
- In sodium electrochemical systems, the greatest technical hurdles to overcome are the lack of high-performance electrode and electrolyte materials that are easy to synthesize, safe, and non-toxic, with long calendar and cycling life and low cost.
- Furthermore, fundamental scientific questions need to be elucidated, including (1) the difference in transport and kinetic behaviors between Na and Li in analogous electrodes; (2) Na insertion/extraction mechanism; (3) solid electrolyte interphase (SEI) layer on the electrodes from different electrolyte systems; and (4) charge transfer in the electrolyte–electrode interface and Na^+ ion transport through the SEI layer.

This task will use the synchrotron based *in situ* x-ray techniques and other diagnostic tools to evaluate new materials and redox couples, to explore fundamental understanding of the mechanisms governing the performance of these materials and provide guidance for new material developments. This task will also be focused on developing advanced diagnostic characterization techniques to investigate these issues, providing solutions and guidance for the problems. The synchrotron based *in situ* x-ray techniques (x-ray diffraction and hard and soft x-ray absorption) will be combined with other imaging and spectroscopic tools such as high resolution transmission electron microscopy (HRTEM), mass spectroscopy (MS), and transmission x-ray microscopy (TXM).

Task 10.1 – Exploratory Studies of Novel Sodium-Ion Battery Systems (Xiao-Qing Yang and Xiqian Yu, Brookhaven National Laboratory)

Project Objective: The primary objective of this proposed project is to develop new advanced *in situ* material characterization techniques and to apply these techniques to explore the potentials, challenges, and feasibility of new rechargeable battery systems beyond the lithium-ion batteries (LiBs), namely the sodium-ion battery systems for plug-in hybrid electric vehicles (PHEV). To meet the challenges of powering the PHEV, new rechargeable battery systems with high energy and power density, low cost, good abuse tolerance, and long calendar and cycle life must be developed. This project will use the synchrotron based *in situ* x-ray diagnostic tools developed at BNL to evaluate the new materials and redox couples, exploring the fundamental understanding of the mechanisms governing the performance of these materials.

Project Impact. The Multi Year Program Plan of the DOE Vehicle Technologies Office (VTO) describes the goals for battery: "Specifically, lower-cost, abuse-tolerant batteries with higher energy density, higher power, better low-temperature operation, and longer lifetimes are needed for the development of the next-generation of HEVs, PHEVs, and EVs." If this project succeeds, the knowledge gained from diagnostic studies and collaborations with U.S. industries and international research institutions will help U.S. industries develop new materials and processes for a new generation of rechargeable battery systems beyond lithium-ion batteries, such as Na-ion battery systems in their efforts to reach these VTO goals.

Approach. This project will use the synchrotron based *in situ* x-ray diagnostic tools developed at BNL to evaluate the new materials and redox couples to enable a fundamental understanding of the mechanisms governing the performance of these materials and to provide guidance for new material and new technology development regarding Na-ion battery systems.

Out-Year Goals. Complete the *in situ* x-ray diffraction (XRD) and absorption studies of sodium iron ferrocyanide (Prussian Blue Analogous) as cathode materials for Na-ion batteries during charge-discharge cycling.

Collaborations. The BNL team has been working closely with top scientists on new material synthesis at ANL, LBNL, and PNNL, with U.S. industrial collaborators at General Motors, Duracell, and Johnson Control along with international collaborators in Japan and South Korea. These collaborations will be strengthened and expanded to give this project a vision on both today's state-of-the-art technology and tomorrow's technology being developed, with feedback from the material designer and synthesizers upstream and from industrial end users downstream.

Milestones

1. Complete the particle size effects on kinetic properties of $Li_4Ti_5O_{12}$ as anode materials for Na-ion batteries using synchrotron based *in situ* x-ray diffraction. (December 2014 – Complete)
2. Complete the *in situ* x-ray diffraction studies of sodium iron ferrocyanide (Prussian Blue Analogous) as cathode materials for Na-ion batteries during charge-discharge cycling. (March 2015 – Complete)
3. Complete the *in situ* x-ray absorption near edge structure (XANES) studies of sodium iron ferrocyanide (Prussian Blue Analogous) at Fe k-edge as cathode materials for Na-ion batteries during charge-discharge cycling. (June 2015 – Complete)
4. Complete the *in situ* extended x-ray absorption fine structure (EXAFS) studies of sodium iron ferrocyanide (Prussian Blue Analogous) at Fe k-edge as cathode materials for Na-ion batteries during charge-discharge cycling. (Complete)

Progress Report

This quarter, the fourth milestone for FY 2015 was completed, as BNL focused on the studies of a new cathode material for sodium-ion batteries. Structure evolution of sodium iron ferrocyanide (Prussian Blue Analogous) as cathode materials for Na-ion batteries was studied using *ex situ* extended X-ray absorption fine structure spectroscopy (EXAFS) at different charge or discharge states at the Fe k-edge. Fourier transformed magnitudes of the Fe K-edge EXAFS spectra of the pristine, fully charged and discharged samples are shown in Figure 91. Three dominant peaks are observed in all the spectra; the peaks at 1.5, 2.5, and 4.4 – 4.8 Å can be ascribed to the Fe–C, Fe–N, and Fe–Fe shells, respectively. The significant splitting of the Fe–C and Fe–N peaks for the pristine and discharged samples reveals an irregular or distorted iron octahedral environment due to lower symmetry of the rhombohedral structure, which agrees well with XRD results. The intensities of these peaks increased for the fully sodium-extracted sample (4.4 V), which agrees well with the XRD observation of the phase transformation from rhombohedral to a higher symmetry cubic phase upon Na^+ extraction. An obvious change of the peak attributed to the Fe–Na shell (3.0 Å) can also be observed for the pristine and fully discharged electrodes in which sufficient Na^+ ions occupy the interstitial sites in the lattice.

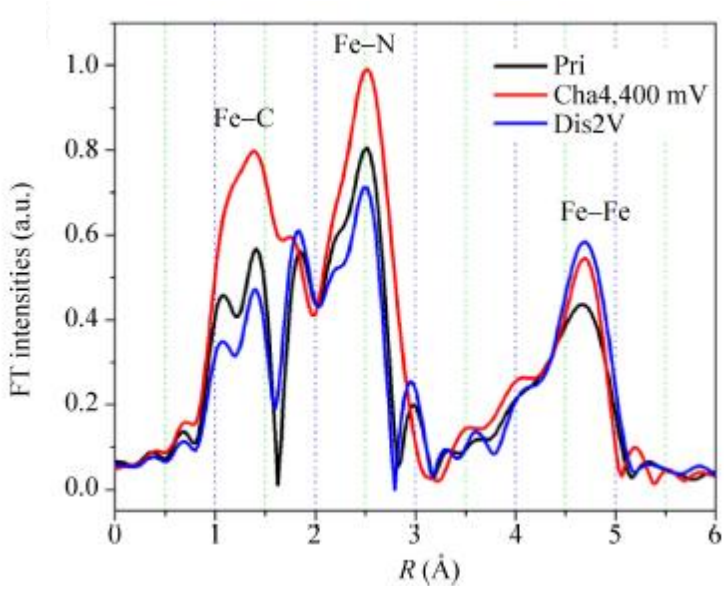

Figure 91. ***Ex situ*** **Fourier transformed magnitude of Fe K-edge EXAFS spectra of the NaFe(1.63) electrode collected at different charge and discharge states.**

Patents/Publications/Presentations

Publication

- He, Kai, and Feng Lin, Yizhou Zhu, Xiqian Yu, Jing Li, Ruoqian Lin, Dennis Nordlund, Tsu-Chien Weng, Ryan M. Richards, Xiao-Qing Yang, Marca M. Doeff, Eric A. Stach, Yifei Mo, Huolin Xin, and Dong Su*. "Sodiation Kinetics of Metal Oxide Conversion Electrodes: A Comparative Study with Lithiation." *Nano Lett.* 15, no. 9 (2015): 5755–5763. DOI: 10.1021/acs.nanolett.5b01709 (Web Publication Date: August 19, 2015)